WOODHEAD PUBLISHING SERIES IN BIOMEDICINE

MONOCLONAL ANTIBODIES

MEETING THE CHALLENGES IN MANUFACTURING, FORMULATION, DELIVERY AND STABILITY OF FINAL DRUG PRODUCT

STEVEN J. SHIRE

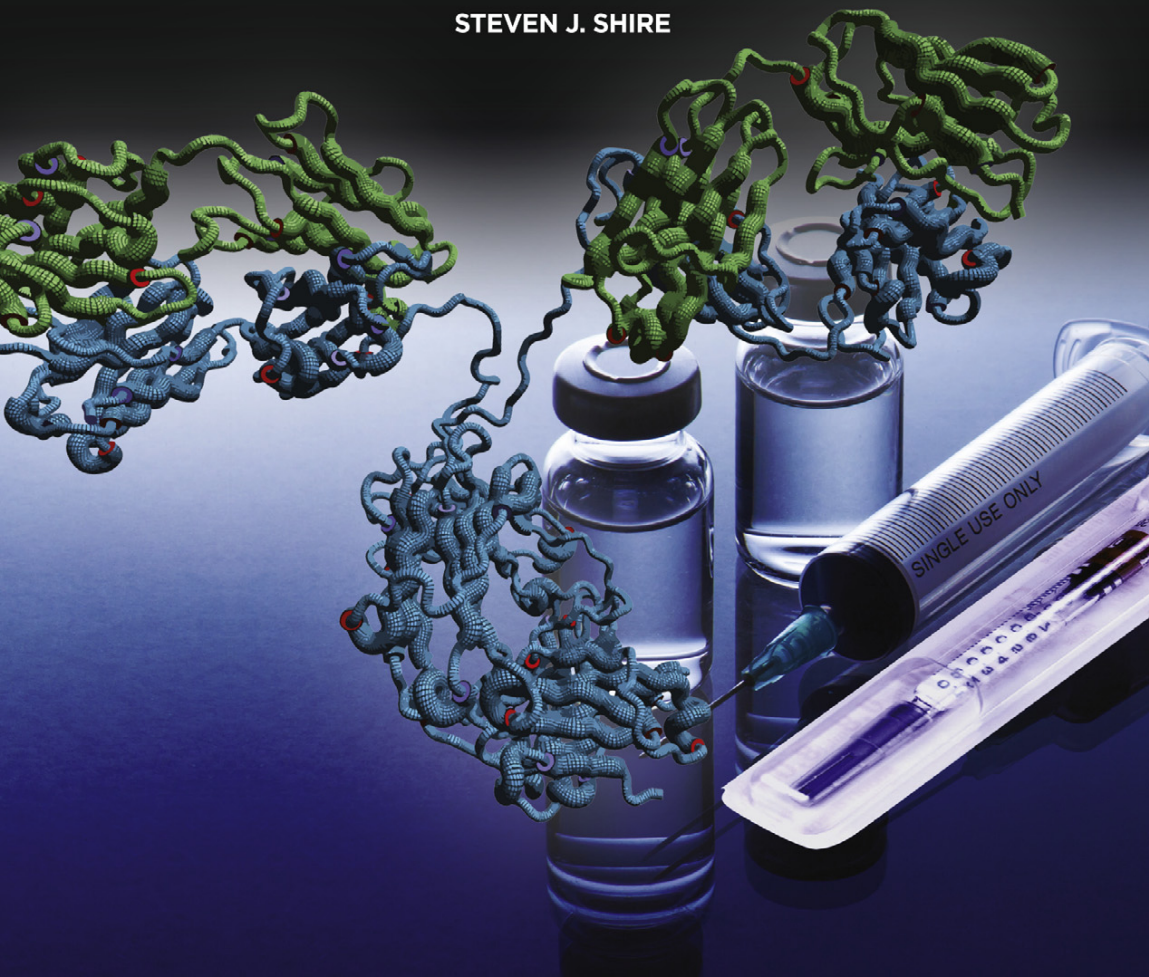

Monoclonal Antibodies

Related titles

Ossipow and Fischer, *Monoclonal Antibodies: Methods and Protocols (Methods in Molecular Biology)*, Second edition, Humana Press, 2014, 9781627039918, $108.64

Goding, *Monoclonal Antibodies: Principles and Practice*, Third edition, Academic Press, 1996, 9780122870231, $104.14

Woodhead Publishing Series in Biomedicine: Number 77

Monoclonal Antibodies

Meeting the Challenges in Manufacturing, Formulation, Delivery and Stability of Final Drug Product

Steven J. Shire

AMSTERDAM • BOSTON • CAMBRIDGE • HEIDELBERG
LONDON • NEW YORK • OXFORD • PARIS • SAN DIEGO
SAN FRANCISCO • SINGAPORE • SYDNEY • TOKYO
Woodhead Publishing is an imprint of Elsevier

Woodhead Publishing is an imprint of Elsevier
80 High Street, Sawston, Cambridge, CB22 3HJ, UK
225 Wyman Street, Waltham, MA 02451, USA
Langford Lane, Kidlington, OX5 1GB, UK

British Library Cataloguing-in-Publication Data
A catalogue record for this book is available from the British Library

Library of Congress Control Number: 2015932042

ISBN: 978-0-08-100296-4 (print)
ISBN: 978-0-08-100297-1 (online)

Contents

This page intentionally left blank

List of figures

This page intentionally left blank

List of tables

This page intentionally left blank

About the author

Dr Shire has over 30 years experience in the pharmaceutical biotechnology industry. He received his PhD from Indiana University Chemistry Department and after postdoctoral training at the University of Connecticut began his career at Genentech as research scientist in the Department of Protein Chemistry. He was involved in the early work to isolate heterologous recombinant proteins expressed in bacterial systems. This work led to the granting of a patent and served as the basis for further product development of proteins expressed in bacterial systems. During his tenure in the Protein Chemistry Department, he used numerous physicochemical techniques to characterize Genentech proteins at various stages of development. Shortly after the creation of the Pharmaceutical Research and Development Department at Genentech, he joined the department where he made numerous contributions to development of protein formulation and delivery. In addition, he set up one of the first analytical ultracentrifugation laboratories in the biotechnology industry. He had been responsible for directing research and development of formulations for a variety of recombinant human proteins including Pulmozyme® and Xolair®. After 32 years at Genentech, Inc. he retired from his position as a staff scientist in the Late Stage Pharmaceutical Development Department at Genentech. Currently he is an adjunct faculty member of the USC School of Pharmacy and University of Connecticut School of Pharmaceutical Sciences, and serves as a consultant for the biotechnology industry. Dr Shire has served as the chair of the American Association of Pharmaceutical Scientists (AAPS) Biotechnology Section, and was elected as a fellow of AAPS in 1998 and member at large to the AAPS Executive Council in 2001. He has published over 90 reviews and papers dealing with various aspects of formulation and pharmaceutical development of therapeutic proteins.

This page intentionally left blank

Preface

When Glynn Jones from Elsevier publishing contacted me about writing a book on monoclonal antibodies, I looked at several excellent books on development of antibodies, which covered all aspects of therapeutic antibody development. Most of the books did have some excellent short reviews on the development of the drug product, but concentrated mainly on the challenges and solutions to manufacture the drug substance, i.e., from the research and design of the mAb, host cells used for expression, cell culture techniques, and recovery and purification. Since I had just retired after 32 years at Genentech, I thought that writing of a book devoted to the challenging aspects of development of drug product would be appropriate, and that this would be a good project to undertake to help ease my way into retirement.

The second issue I faced was whether the book should be created for the researcher and developer working on mAbs or should I include many of the R & D people who were just getting acquainted with mAb development. In many of the conferences I attended, I met many people who were just getting into this challenging field and so I decided to put in some background material to help them in their initial foray into the development of an mAb into a pharmaceutical.

My goal was to organize this book in a straightforward fashion. The first chapter discusses what is meant by pharmaceutical development. I originally submitted a proposed book title: "Pharmaceutical Development of Monoclonal Antibodies: Meeting the challenges in manufacturing, formulation, delivery and stability of final drug product," but I was advised to drop the term "pharmaceutical development," I suspect because no one was sure what that meant. I recall shortly, after the "Pharmaceutical Research and Development" department was created at Genentech the name was abbreviated as "Pharm R & D," and apparently this was interpreted to mean Pharmacology Research and Development, even though everyone thought of us as the formulation department! This demonstrated to me that many of my Genentech colleagues truly did not understand what pharmaceutics was and what we did as a department. At any rate I felt the book should begin with what pharmaceutical development means and what is required to succeed in this "late-stage" development phase. I also included a brief summary of mAb structure to be sure that ensuing discussion of assays and stability would be easier to follow. The second chapter reviews the analytical and potency assay formats used to investigate stability and formulation of proteins and mAbs. I unabashedly started with Andrew Jones' excellent review of analytics and tried to add discussions of new techniques. In the third chapter, the chemical and physical degradation pathways for proteins and mAbs are discussed. I tried to provide many references discussing mechanisms for the degradation routes since an understanding

of the chemistry and structural stability of mAbs can lead to better, more rational formulation development. The fourth chapter discusses various aspects of formulation development including choice of solid vs. liquid dosage forms, strategies for development of the formulation, and excipients commonly used to stabilize the protein or mAb. In the fifth chapter, the key challenges in delivery of mAbs by the intravenous route are discussed, and how those challenges are addressed. The sixth chapter reviews the requirements for a subcutaneous (SC) formulation for a mAb, and the key issues of formulation design, manufacturing, and delivery of the mAb for SC administration. The strategies for dealing with the SC challenges are discussed in Chapter 7, especially the strategies that can be used to handle the high viscosities encountered during SC development. The development of delivery device technology for delivery of viscous high concentration SC mAb formulations is reviewed in Chapter 8. Chapter 9 reviews the work from my lab and several other groups on what we know about the molecular basis for the high viscosity and the protein–protein interactions that dictate solubility and viscosity, where the ultimate goal is to develop rational formulations based on these basic scientific inquiries. Finally, Chapter 10 discusses the future of mAbs as protein therapeutics. The new developments include bispecifics, single chain mAbs, and antibody drug conjugates (ADC), which undoubtedly will have their own set of challenges. The ADC format is currently a major development focus area and probably would require a separate book on its own so I did not discuss the development of final ADC drug product, but did discuss the key differences between development of an ADC versus mAb.

I am indebted to many of my colleagues at Genentech and at other institutions for the many productive discussions about this exciting field, especially knowing the great successes already attained in helping us to provide new hope for patients with severe diseases. It is virtually impossible for me to list everyone, so please do not feel slighted, because I do value all the wonderful interactions I have had during my career. In particular, I would like to thank John Wang, Sreedhara Alavattam, and Sandeep Yadav for reviewing parts of the book and providing valuable constructive criticism. I also highly valued the stimulating discussions with Tom Patapoff who also contributed to many of the ideas for the research of monoclonal antibody viscosity. Thomas Laue at the University of New Hampshire who organized the National Science Foundation (NSF) industry/academic consortium known as the Biomolecular Interaction Technology Center (BITC) has also provided great discussions and collaborations that greatly enhanced the research into the role of charge and viscosity in proteins and mAbs. I had many great collaborations with key people outside of Genentech and one of the most productive and active collaborations was with Devendra Kalonia and his student Sandeep Yadav at the University of Connecticut. Sandeep eventually joined my lab group as a post doc and is now fully employed as a scientist at Genentech. I also had two other post docs, Sonoko Kanai and Jun Liu who also contributed greatly to our understanding of mAbs. Sonoko is currently working at Roche/Basil and Jun is a principal scientist at Genentech. His main focus is on ADC development so perhaps he should write the next book on ADCs.

I especially need to thank Genentech for giving me the opportunity to travel the road of biotechnology. Genentech is well respected for its culture where everyone

is interested in what others are doing and wants to help in solving technically challenging problems. That is certainly the way to encourage innovation and progress. I think much of this has to do with the founders of Genentech, Bob Swanson and Herb Boyer, but I also believe a great deal of this should be credited to Art Levinson, VP of Research and eventually CEO of Genentech. Art certainly carried out his administrative and corporate duties but always had an interest in the basic science, even attending the research and review committee meetings of projects.

Finally, I want to thank my long-time friend and colleague William Henzel for unbridled enthusiasm for science and the great discussions we had over the last few years. I also want to thank my wife Maria, daughter Katie, and son Joseph for putting up with the long hours I spent writing this book. Overall my family supported me emotionally, and I appreciated this very much.

Steven J. Shire
November 2014

This page intentionally left blank

Introduction

1

Pharmaceutical development

Pharmaceutical development departments are often labeled as "Formulation," and while this is certainly an important part of creating a pharmaceutical, in reality it is only part of the whole process where the active pharmaceutical ingredient often referred to as the "API" is made into a pharmaceutical. Creation of a robust formulation is critical for the ultimate success of the product. This generally means that the API is formulated in the presence of buffers, excipients, and stabilizers to ensure its physical, chemical, and biological stability over its entire shelf life. However, if the formulation process is done just to achieve the greatest stability possible that may not lead to a successful development of the API into a pharmaceutical. Essentially the formulation, in addition to being stable and maintaining product quality, must be safe, easy to administer, easy and economical to manufacture, convenient for the end users, and ultimately marketable. Development to attain all these qualities requires an interface of many disciplines as well as focus areas. Thus, pharmaceutical development can be envisioned as a Venn diagram (Figure 1.1) where within each focus area there are many possibilities that can lead to a successful outcome for that particular attribute. The challenge is to interface all of these attributes to lead to a pharmaceutical target whereby the key elements from all of the areas meet the needs for the pharmaceutical. In order to successfully "hit" such a target requires a clear understanding of the needs for the pharmaceutical for the chosen indication by all the relevant functional areas in development. Such a document or agreement is often referred to as the target product profile (TPP).

The role of the TPP is to create a clear set of target goals that require input from all functional groups that contribute to the development of an API into the final drug product. Often the TPP is considered a document that meets directly the clinical and marketing needs, but it is important to also include manufacturing requirements. Development of a laboratory-derived successful formulation that is stable, safe, and easy to deliver can become very problematic if an efficient, easy, and economical manufacturing scale-up is not possible. Some of the key challenges in each of the development areas highlighted in Figure 1.1 will be discussed in the following subsections. Although the TPP applies to goals in general for pharmaceutics, much of the discussion will concentrate on the development of biotherapeutics manufactured by recombinant DNA technology, and in particular monoclonal antibodies.

Monoclonal Antibodies. http://dx.doi.org/10.1016/B978-0-08-100296-4.00001-4

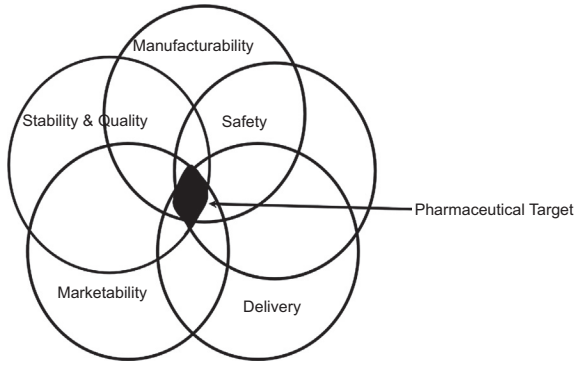

Figure 1.1 Major contributors to successful pharmaceutical development.

Development of the API

Traditional small-molecule pharmaceutical process development begins with a medicinal chemist who generates a synthetic approach for making the small-molecule drug. The purified API, usually a solid phase preparation, is then handed off to the formulation chemist for development of a final dosage form for administration. This overall process is very different for rDNA-derived protein drugs, and the manufacturing of rDNA-derived API, generally referred to as drug substance (DS), has been extensively reviewed and discussed in several books. In particular, DS is manufactured using organisms transformed with the appropriate gene coding for the protein along with genetic control elements to allow for manipulation of protein synthesis during fermentation or cell-culture processing. Although many different host cells have been used, the most frequently used systems have been *Escherichia coli* and Chinese hamster ovary cells. After centrifugal harvesting of the cells, the expressed protein is recovered and purified from either the centrifuged cells (if expressed intracellularly) or the supernatant (if secreted into the harvest fluid). The resulting purified protein therapeutic DS at this point is in a solution after exchange that consists of all the excipients required for the final liquid chromatography step. Thus, unlike a small-molecule pharmaceutical the development of a formulation manufacturing process that can be efficient and economical resides with the recovery and purification scientists. However, this step cannot be developed until the pharmaceutical scientist creates an appropriate formulation that confers the required stability and compatibility with the administration route. Moreover, the DS also needs to be formulated to allow for long-term storage of bulk DS since several final drug product (DP) lots may come from one manufactured DS lot.

Generally the DS formulation will be similar to the final DP, but there are several challenges that have to be addressed. Often the final dosing required is not known, and thus it is difficult to choose one final volume and concentration of the protein therapeutic for the formulation. Thus, "preformulation" studies to determine a range of concentrations and excipients are required. These studies are facilitated by designing

experiments to investigate the impact of external conditions such as pH, temperature, and ionic strength on the solubility and stability of the molecule. It is also important to determine early on in development what route of administration is required for the particular indication. As an example development of formulations for subcutaneous (SC) versus intravenous (IV) routes will have different challenges and will be discussed in later chapters. One important aspect in the development of the DP formulation is whether the biopharmaceutical requires low dosing, such as erythropoietin for generation of red blood cells (μg/kg), or high dosing such as human growth hormone (mg/kg). This book will focus on development and the challenges to address the requirements of the TPP of a class of protein therapeutics, monoclonal antibodies (mAbs), that although are very selective for targets, generally require high dosing for efficacy. The term mAb as used in this book encompasses full length and fragments of mAb as well as radiolabeled and drug-conjugated forms. Antibody drug conjugates have their own set of challenges, which will be briefly discussed in the last chapter, but are not within the scope of this book.

mAbs as protein therapeutics

With the advent of recombinant DNA technology it became possible to express human or designed proteins in a variety of microbial, plant, and mammalian systems. Over the years the development of mAbs as drugs has increased at a large rate. As of 2014 there have been 64 mAbs approved (4 of these mAbs have been voluntarily withdrawn from the market) or in review in Europe and the United States or pending (Table 1.1). Of the 64 mAbs, 8 are radioisotope-labeled imaging agents and 1 a radioisotope-labeled mAb for treatment. A majority of the approved mAbs (40) are delivered by IV and the remainder by SC (9), intramuscular (IM) (2) (Amevive is given either IV or IM), and intravitreal (2). In addition, there are more than 200 mAbs in clinical studies with more than 600 in preclinical development (Reuters, 2014). The market forecast for mAbs in 2014 is $35 billion in the United States alone (Frost & Sullivan, 2008).

There are several reasons why mAbs have become increasingly popular for commercial development. mAbs are highly specific, binding to a single antigen target, which leads to fewer side effects than conventional small-molecule drugs. Although mAbs have been created to bind to specific targets on cells or ligands that bind to targets that mediate disease, one of the exciting prospects is the development of mAbs as specific drug delivery molecules, which deliver conjugated toxins or radioisotopes to specific cellular targets (Wankanker, 2010). For conjugated drug toxins, appropriate design of linkers for the drug conjugate minimizes the exposure of nontarget cells to the toxin during circulation resulting in a reduction of harmful side effects (Junutula, Raab, Clark, & Sunil, 2008). Radioisotope-labeled mAbs can also be used as both therapeutic and imaging agents. The latter greatly increases the ability to excise tumors during surgical procedures. Overall these attributes have led to the emergence of mAb therapeutics as a dominant class of biotherapeutics.

Table 1.1 Therapeutic monoclonal antibodies, Fc fusion and Fab conjugates approved or in review in the European Union or United States[a]

Brand name	Molecule	Type of mAb	Year approved	Company	Indication	Administration route
Abthrax	Raxibacumab	Anti-B; anthrasis PA; human IgG1	(2012)	Human Genome Sciences/Glaxo Smith Kline	Anthrax	SC
Actemra	Tocilizumab	Anti-ILER; humanized IgG1	2009 (2010)	Genentech/Roche	Rheumatoid arthritis	IV infusion
Adcetris	Brentuximab vedotin	Anti-CD30; chimeric IgG1 immunoconjugate	2012 (2011)	Seattle Genetics	Hodgkin's lymphoma	IV infusion
Amevive	Alefacept	Fusion protein that consists of the extracellular CD2-binding portion of the human leukocyte function antigen-3 (LFA-3) linked to a human IgG1 Fc	(2003) withdrawn from the market in 2011	Astellas Pharma US, Inc.	Moderate to severe psoriasis with plaque formation, where it interferes with lymphocyte activation	IV or IM
Arcalyst	Rilonacept	Fusion protein consisting of the ligand-binding domains of the extracellular portions of the human interleukin-1 receptor component (IL-1R1) and IL-1 receptor accessory protein (IL-1RAcP) linked in-line to an Fc human IgG1 that binds and neutralizes IL-1	(2008)	Regeneron	Cryopyrin-associated periodic syndromes (CAPS), including familial cold autoinflammatory syndrome, Muckle–Wells syndrome, and neonatal onset multisystem inflammatory disease (not approved in the US on this indication)	SC
Arzerra	Ofatumumab	Anti-CD20; human IgG1	2010 (2009)	Glaxo Smith Kline	Chronic lymphocyte leukemia	IV infusion

Avastin	Bevacizumab	Anti-VEGF; humanized IgG1	2005 (2004)	Genentech	Metastatic carcinoma of colon or rectum, binds VEGF	IV infusion
Benlysta	Belimumab	Anti-BLy8; human IgG1	2011 (2011)	Human Genome Sciences/Glaxo Smith Kline	Systemic lupus erythematosis	IV infusion
Bexxar	Tositumomab and I-131 tositumomab	Anti-CD21; murine IgG2λ	NA/(2003)	Corixa and GSK	CD20 positive follicular non-Hodgkin's lymphoma	IV infusion
Blincyto	Blinatumomab	Bispecific CD19-directed CD3 target and produced in CHO	2014	Amgen	BLINCYTO is a bispecific CD19-directed CD3 T-cell engager indicated for the treatment of Philadelphia chromosome-negative relapsed or refractory B-cell precursor acute lymphoblastic leukemia (ALL)	IV infusion
Campath	Alemtuzumab	Anti-CD52; humanized IgG1κ	2001 (2001)	Ilex Oncology; Millenium and Berlex	B-cell chronic lymphocytic leukemia	IV infusion
CEA-Scan	Arcitumomab	Anti-CEA (carcinoembryonic antigen); murine fab	1996 (1996)	Immunomedics	Imaging agent for colorectal cancer	IV infusion
Cimzia	Certolizumab pegol	Anti-TNFα; humanized fab′ fragment bound to PEG	2009 (2008)	UCB Pharma	Crohn's disease	SC
Cyramza	Ramucirumab	Anti-VEGFR2; human IgG1	In review	–	Gastric cancer	–

Continued

Table 1.1 Therapeutic monoclonal antibodies, Fc fusion and Fab conjugates approved or in review in the European Union or United States[a]—cont'd

Brand name	Molecule	Type of mAb	Year approved	Company	Indication	Administration route
Enbrel	Etanercept	Anti-tumor necrosis factor (TNF) dimeric fusion protein consisting of the extracellular ligand-binding portion of the human tumor necrosis factor receptor (TNFR) linked to the Fc portion of a human IgG1	First approved in 1999	Amgen	Moderate to severe rheumatoid arthritis (RA), adult chronic moderate to severe plaque psoriasis in patients who are candidates for systemic therapy or phototherapy, psoriatic arthritis, moderate to severe juvenile idiopathic arthritis (JIA), and ankylosing spondylitis (AS)	SC
Entyvio	Vedolizumab	Anti-$\alpha_4\beta_7$ (LPAM-1), lymphocyte Peyer's patch adhesion molecule; humanized IgG1	In review (2013)	Takeda	Ulcerative colitis; Crohn's disease	IV infusion
Erbitux	Cetuximab	Anti-EGFR; chimeric IgG1κ	2004 (2004)	ImClone and BMS	Treatment of EGFR-expressing colorectal carcinoma	IV infusion
Eylea	Aflibercept	Fc fusion consisting of portions of human VEGF receptors 1 and 2 extracellular domains fused to the Fc portion of human IgG1	2012 (2011)	Regeneron	Age-related wet macular degeneration	Intravitreal injection
Gazyva	Obinutuzumab	Anti-CD20; humanized IgG1; glycoengineered	In review	–	Chronic lymphocytic leukemia	–

Herceptin	Trastuzumab	Anti-HER2; humanized IgG1κ	2000 (1998)	Genentech	Metastatic breast cancer with tumor overexpression of HER2 protein	IV infusion
Humaspect	Votumumab	Anti-cytokeratin tumor associated antigen; human mAb	1998, withdrawn in 2003	Organon Teknika	Detection of carcinoma of the colon or rectum	IV infusion
Humira	Adalimumab	Anti TNF; human IgG1κ	2003 (2002)	CAT and Abbott	RA patients not responding to DMARDs. Blocks TNF-alpha	SC
Ilaris	Canakinumab	Anti-IL1β; human IgG1	2009 (2009)	Novartis	Muckle–Wells syndrome	SC
Indimacis 125	Igovomab	Anti-tumor associated antigen CA 125; murine Fab_2	1996, withdrawn in 2009	CIS Bio	Diagnosis of cutaneous melanoma lesions	IV infusion
Kadcyla	Trastuzumab emtansine	Anti-Her2; humanized IgG1; immunoconjugate	In review (2013)	Genentech/Roche	Breast cancer	IV infusion
Keytruda	Pembrolizumab	Anti-PD1b, humanized mAb	2014	Merck	Advanced melanoma	IV
Lucentis	Ranibizumab	Anti-VEGF; humanized IgG1κ Fab fragment	2007 (2006)	Genentech	Age-related wet macular degeneration	Intravitreal injection
LeukoScan	Sulesomab	Anti-NCA 90, a surface granulocyte nonspecific cross-reacting antigen; murine mAb labeled with 99m technetium	1997	Immunomedics	Diagnostic imaging for infection and inflammation in bone of patients with osteomyelitis	IV
Mylotarg	Gemtuzumab ozogamicin	Anti-CD33; humanized IgG4κ conjugated to calicheamicin	NA (2000)	Celltech and Wyeth	Treatment of CD33 positive acute myeloid leukemia	IV infusion

Continued

Table 1.1 Therapeutic monoclonal antibodies, Fc fusion and Fab conjugates approved or in review in the European Union or United States[a]—cont'd

Brand name	Molecule	Type of mAb	Year approved	Company	Indication	Administration route
MyoScint	Imciromab pentetate	Anti-human cardiac myosin; murine mAb fragment labeled with indium-111	(1996)	Centocor	Myocardial infarction imaging agent	IV
Nplate	Romiplostim	Fc peptide fusion. This molecule contains two identical single-chain subunits, each consisting of human immunoglobulin IgG1 Fc domain, covalently linked at the C-terminus to a peptide containing two thrombopoietin receptor-binding domains	(2008)	Amgen	Chronic idiopathic (immune) thrombocytopenic purpura (ITP)	SC
NeutroSpec	Fanolesomab	Anti-CD15; murine mAb labeled with technetium-99	(2004)	Palatin-Technologies	Imaging of equivocal appendicitis	IV
OncoScint	Satumomab pendetide	Anti-TAG72 (tumor-associated glycoprotein; murine IgG1κ conjugated to GYK-DTPA	1992 (1992)	Cytogen	Imaging agent for colorectal and ovarian cancer	IV injection
Opdivo	Nivolumab	Anti-PD1 antibody. The molecule is a human IgG4 κ immunoglobulin	2014	Bristol-Myers Squibb	Treatment for patients with unrespectable (cannot be removed by surgery) or metastatic (advanced) melanoma who no longer respond to other drugs	IV

Orencia	Abatacept	Fusion protein composed of the Fc region of an IgG1 fused to the extracellular domain of CTLA-4	(2005)	Bristol-Meyers Squib	Rheumatoid arthritis	IV
Orthoclone OKT-3	Muromonab-CD3	Anti-CD23; murine IgG2a	1986 (1986)	Ortho Biotech	Reversal of acute kidney transplant rejection (anti-CD3-antigen)	IV injection
Pending	Dinutuximab	Anti-GD2; chimeric IgG1	In review	–	Neuroblastoma	–
Pending	Pembrolizumab	Anti-PD1; humanized IgG4	In review	–	Melanoma	–
Pending	Nivolumab	Anti-PD1; human IgG4	Approved in Japan	–	Melanoma	–
Pending	Secukinumab	Ant-IL-17a; human IgG1	In review	–	Immunosuppression	–
Perjeta	Pertuzumab	Anti-HER2 humanized IgG1	2013 (2012)	Genentech/Roche	Breast cancer	IV infusion
Prolia	Denosumab	Anti-RANK-L; human IgG2	2010 (2010)	Amgen	Bone loss	SC
ProstaScint	Indium-111 capromab pendetide	Anti-PSMA (prostate specific membrane antigen); murine IgG1κ conjugated to GYK-DTPA	1996	Cytogen	Imaging for prostate cancer	IV injection
Raptiva	Efalizumab	Anti-CD11a; humanized IgG1κ	2004 (2003) withdrawn voluntarily from the market in 2009	Xoma and Genentech	Chronic moderate to severe plaque psoriasis	SC
Remicade	Infliximab	Anti-TNFα; chimeric, 70% corresponds to human IgG1 heavy chain and human κ light chain constant region	1999 (1998)	Centocor	RA and Crohn's disease	IV infusion

Continued

Table 1.1 Therapeutic monoclonal antibodies, Fc fusion and Fab conjugates approved or in review in the European Union or United States[a]—cont'd

Brand name	Molecule	Type of mAb	Year approved	Company	Indication	Administration route
Removab	Catumaxomab	Anti-EPCAM/CD3; rat/murine bispecific mAb	2009 (NA)	Trion Pharma	Malignant ascites	IV infusion
ReoPro	Abciximab	Anti-glycoprotein IIb/IIIa receptor; chimeric Fab	1995 (1994)	Centocor and Lilly	Reduction of acute blood clot-related complications	IV injection and infusion
Rituxan	Rituximab	Anti-CD20; chimeric IgG1κ	1998 (1997)	IDEC and Genentech	Non-Hodgkin's lymphoma	IV infusion
Scintimun	Besilesomab	Anti-NCA-95 found on surface of granulocytes; murine mAb	2010	CIS Bio International	In vivo diagnosis/investigation of sites of inflammation/infection via scintigraphic imaging	IV
Simponi	Golimumab	Anti-TNFα; human IgG1	2009 (2009)	Centocor	Rheumatoid and psoriatic arthritis, ankylosing spondylitis	SC
Simulect	Basiliximab	Anti-IL2; chimeric IgG1κ	1998 (1998)	Novartis	Prevention of acute kidney transplant rejection	IV injection and infusion
Soliris	Eculizumab	Humanized IgG2/IgG4	2007 (2007)	Alexion	Treatment of paroxysmal nocturnal hemoglobinuria (PNH)	IV infusion
Stelara	Ustekinumab	Anti-IL2/23; human IgG1	2009 (2009)	Janssen Biotech/Centocor	Psoriasis	SC
Sylvant	Siltuximab	Anti-IL-6; chimeric IgG1	2014	Janssen Biotech, Inc.	Castleman disease	IV
Synagis	Palivizumab	Anti-protein F of RSV; humanized IgG1κ	1999 (1998)	Medimmune	Respiratory tract disease caused by respiratory syncytial virus (RSV)	IM

Technemab	MoAb 225.28S	Anti-HMW; murine mAb Fab'_2	(1996)	Sorin Biomedica	Diagnosis of cutaneous melanoma lesions	IV
Tysabri	Natalizumab	Anti-α4 integrin; humanized IgG4κ	2006 (2004)	Biogen IDEC	MS relapse	IV infusion
Vectibix	Panitumumab	Anti-EGFr; human IgG2κ	2007 (2006)	Amgen	Treatment of patients with EGFr-expressing metastatic colorectal cancer	IV injection
Verluma	Nofetumomab	Anti-tumor antigen (40 kDa glycoprotein); murine fab	1996	Boehringer Ingelheim and Dupont Merck	Imaging agent for lung cancer	IV injection
Xgeva	Denosumab	Human IgG2 monoclonal antibody that binds to human RANKL	(2010)	Amgen	Osteoporosis, treatment-induced bone loss, bone metastases, multiple myeloma, and giant cell tumor of bone	SC
Xolair	Omalizumab	Anti-IgE; humanized IgG1κ	2005 (2003)	Genentech with Novartis and Tanox	IgE-mediated allergic asthma	SC
Yervoy	Ipilimumab	Anti-CTLA-4; human IgG1	2011 (2011)	Bristol-Myers Squibb	Metastatic melanoma	IV infusion
Zenapax	Daclizumab	Anti-IL2; humanized IgG1	1999 (1997)	Roche	Prophylaxis of acute organ rejection in patients receiving renal transplants	IV infusion
Zevalin	Ibritumomab-tiuxetan	Anti-CD20; murine IgG1κ covalently linked to tiuxetan; radioimmunotherapy	2004 (2002)	IDEC	Non-Hodgkin's lymphoma, binds to CD20 antigen and irradiates cells with yttrium-90	IV infusion

IM, intramuscular; IV, intravenous; SC, subcutaneous.
[a]US approval dates in parentheses.

Brief review of mAb structure

There are several reviews on mAb structure (Davies & Metzger, 1983; Presta, 2003; Wang, Singh, Zeng, King, & Nema, 2007), and here we briefly summarize the main structural components. mAbs are highly complex macromolecules where the monomeric unit has a molecular mass of 150–180 kDa and an overall Y shape (Figure 1.2(a)). The secondary and tertiary structural features of antibodies have been reviewed (Janeway, Travers, Walport, & Shlomchik, 2001; Woof & Burton, 2004). Essentially, the polypeptide chains form antiparallel β sheets which comprise ~70% of the secondary structure as shown by Fourier Transform Infrared Spectroscopy (FTIR) and Circular Dichroism (CD) analysis (Cathou, Kulczycki, Jr. Haber, 1968; Chen et al., 2003). These β sheets are organized into

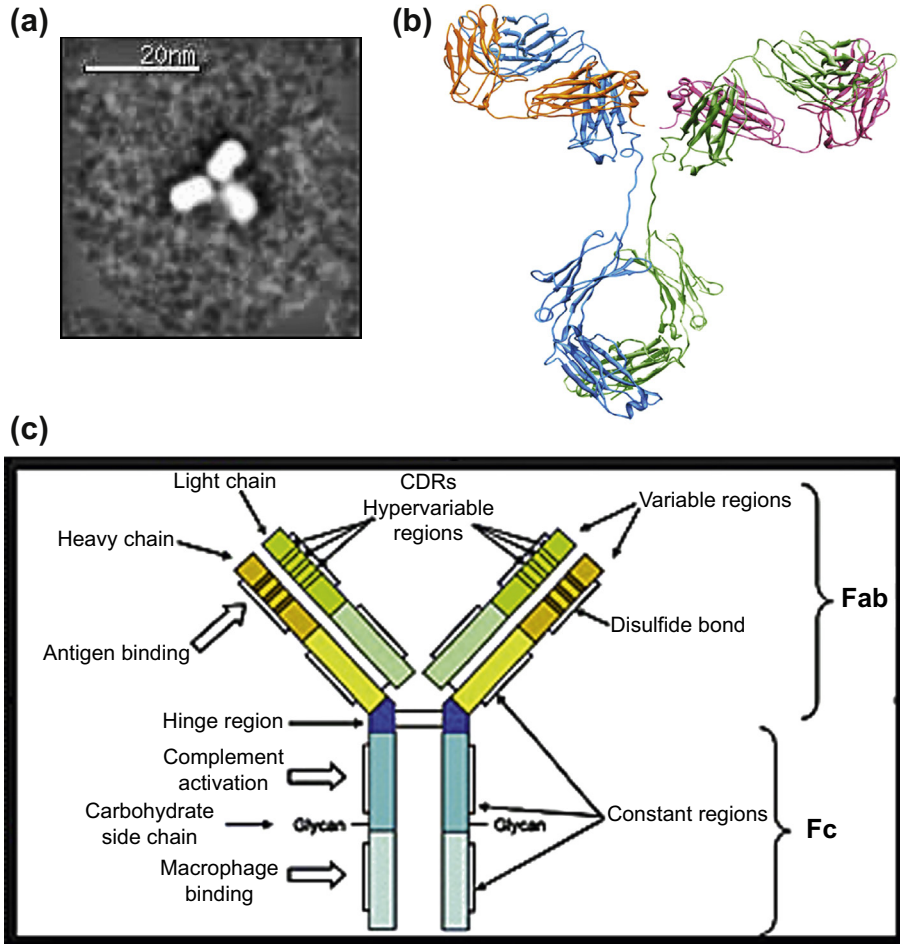

Figure 1.2 (a) Electron microscope photo of an IgG1 mAb. (b) Ribbon diagram of an antibody showing main, secondary, and tertiary structural folding (directional arrows are β sheet structures). (c) Schematic of an IgG mAb showing key structural features.

β barrels in separate domain regions, each about 110 amino acids long, which are found in two identical light chains (LC with two domains) and two identical heavy chains (HC with four domains) (Furtado et al., 2004). These domains interact with each other and fold into three lobes linked by a flexible hinge region (Figure 1.2(b)) forming the overall Y shape of the molecule.

The basic primary structure of antibodies consists of two regions: a variable (V) region and a constant (C) region connected by the flexible hinge region (Figure 1.2(c)). The V region is contained in two identical structures that are at the top of the Y structure called Fabs and contains the target-binding (antigen) region. The C region is essentially the stem of the Y structure and consists of regions that interact with cellular receptors and molecules that modulate the immune system, often referred to as "cell effector function." These chains are linked by noncovalent as well as several covalent disulfide bonds. There are four intrachain disulfide bonds in the H and L chain domains of each Fab arm, which stabilize those domains, as well as two intrachain disulfide bonds in each of the heavy chains that make up the Fc regions. Four interchain disulfide bonds link the heavy chains to the LC (Figure 1.2(c)).

The immunoglobulins can be classified as five different classes: IgA, IgD, IgE, IgM, and IgG, which are based on the composition of their C regions which can contain one of five heavy-chain classes designated as α, δ, ε, μ, and γ (Wang et al., 2007). Although most immunoglobulins are monomeric, IgA and IgM are dimers and pentamers, respectively. Commercially the most used class of immunoglobulin is the IgG class which has a molecular mass of ~150 kDa and will be the focus of all further discussions.

The IgGs are further classified into subclasses, IgG1, IgG2, and IgG4 consisting of different heavy chains designated as γ1, γ2, γ3, and γ4, respectively. The number and location of the interchain disulfide bonds are different in these subtypes. The LC are of two types, λ and κ. Approximately, the first 110 amino acid residues of both the heavy and light chains make up the antigen-binding site of the Fab regions, whereas the remaining sequences are constant regions that form the Fc region.

The variable regions in an IgG consist of three hypervariable sequences also called complementarity-determining regions (CDRs) (HV1, HV2, and HV3) on both heavy and light chains which are flanked by sequences termed framework regions. These framework residues form β sheets with the hypervariable regions displayed as three loops at the end of a β barrel. The C regions can also be subdivided into three domains termed CH_1, CH_2, and CH_3. The interactions with immune cells appear to reside mainly in the CH_2 region in the Fc (Tao & Morrison, 1989).

The IgG molecules also have a flexible hinge region that connects the two arms of the Fabs to the Fc region. This hinge region, which imparts flexibility to these molecules, varies in length as well as flexibility (Oda, 2004) between the subtypes. It has also been suggested that the flexibility of the hinge region may impact stability as shown by increased fragmentation around the hinge region during storage (Cordoba, Shyong, Breen, & Harris, 2005).

mAbs are also glycosylated proteins where for IgGs one N-linked oligosaccharide chain is attached to the conserved Asn-297 in each of the CH_2 Fc domains. These carbohydrate chains of the IgG are sequestered in the interior between the CH_2 domains

(Figure 1.2(c)). Although these chains are buried within the mAb Fc structure they can be removed using PNGase F (Weitzhandler, Hardy, Co, & Avdalovic, 1994), and this is likely due to the flexibility and mobility between the Fc heavy chains. The carbohydrates play a huge role in governing the so-called "cell effector function" (Jefferis, Lund, & Pound, 1998; Mattu et al., 1998; Mimura et al., 2001). In particular, if the oligosaccharides are removed from the IgGs they no longer can bind to C1q, the first component of the complement cascade, as well as cellular receptors such as $F_c\gamma$RI, II, and III, which are used to activate immune cells (Wang et al., 2007). In addition to modulating immune function the carbohydrates impact conformation, stability, and immunogenicity of the IgGs (Tao & Morrison, 1989; Wang et al., 2007; Wen, Jiang, & Nahri, 2008). Although aglycosylated mouse/human chimera IgGs are still able to bind to target antigens as well as protein A, and appear to be properly assembled, they are generally more sensitive to protease than their corresponding IgG1 with oligosaccharides (Tao & Morrison, 1989).

Although mAbs are monoclonal, having been derived from one cell line, the manufactured DS can be very heterogeneous due to differences in glycosylation, errors in transcription or translation during cellular protein synthesis resulting in misincorporation of amino acid residues, and posttranslational processing (Guo et al., 2010; Liu, Gaza-Bulseco, Faldu, Chumsae, & Sun, 2008). The glycosylation in mAbs is a result of an enzymatic reaction, which occurs in cells, and differences in glycosylation occur during protein synthesis. Differences in glycosylation pattern are also dependent on the species used for expression of the mAb (Raju , Briggs, Borge, & Jones 2000). The most common posttranslational processes leading to heterogeneity include incomplete disulfide formation as well as C-terminal processing whereby lysine residues are removed (Liu et al., 2008).

Overall, IgG mAbs are complex molecular machines capable of selectively binding to targets. The hinge region, especially in IgG1 mAbs, confers substantial flexibility to the molecule and can impact stability and function of these therapeutic agents. The next chapter will discuss stability of this important class of biotherapeutics.

References

Cathou, R. E., Kulczycki, A., Jr., & Haber, E. (1968). Structural features of gamma-immunoglobulin, antibody, and their fragments. Circular dichroism studies. *Biochemistry*, *7*(11), 3958–3964.

Chen, B., Bautista, R., Yu, K., Zapata, G. A., Mulkerrin, M. G., & Chamow, S. M. (2003). Influence of histidine on the stability and physical properties of a fully human antibody in aqueous and solid forms. *Pharmaceutical Research*, *20*(12), 1952–1960.

Cordoba, A. J., Shyong, B. J., Breen, D., & Harris, R. J. (2005). Non-enzymatic hinge region fragmentation of antibodies in solution. *Journal of Chromatography B: Analytical Technologies in the Biomedical and Life Science*, *818*(2), 115–121.

Davies, D. R., & Metzger, H. (1983). Structural basis of antibody function. *Annual Review of Immunology*, *1*, 87–117.

Frost and Sullivan. (2008). *Frost & Sullivan technical report #N167–52 U.S. Biotechnology – Therapeutic monoclonal antibodies market*. From http://www.marketresearch.com/Frost.

Furtado, P. B., Whitty, P. W., Robertson, A., Eaton, J. T., Almogren, A., Kerr, M. A., et al. (2004). Solution structure determination of monomeric human IgA2 by x-ray and neutron scattering, analytical ultracentrifugation and constrained modelling: a comparison with monomeric human IgA1. *Journal of Molecular Biology*, *338*(5), 921–941.

Guo, D. L., Gao, A., Michels, D. A., Feeney, L., Eng, M., Chan, B., et al. (2010). Mechanisms of unintended amino acid sequence changes in recombinant monoclonal antibodies expressed in Chinese hamster ovary (CHO) cells. *Biotechnology and Bioengineering*, *107*(1), 163–171.

Janeway, C. A., Travers, P. A., Walport, M., & Shlomchik, M. J. (2001). *Immunobiology*. New York: Garland Press.

Jefferis, R., Lund, J., & Pound, J. D. (1998). IgG-Fc-mediated effector functions: molecular definition of interaction sites for effector ligands and the role of glycosylation. *Immunological Reviews*, *163*, 59–76.

Junutula, J. R., Raab, H., Clark, S., & Sunil, B. (2008). Site-specific conjugation of a cytotoxic drug to an antibody improves the therapeutic index. *Nature Biotechnology*, *26*(8), 8.

Liu, H. C., Gaza-Bulseco, G., Faldu, D., Chumsae, C., & Sun, J. (2008). Heterogeneity of monoclonal antibodies. *Journal of Pharmaceutical Sciences*, *97*(7), 2426–2447.

Mattu, T. S., Pleass, R. J., Willis, A. C., Kilian, M., Wormald, M. R., Lellouch, A. C., et al. (1998). The glycosylation and structure of human serum IgA1, Fab, and Fc regions and the role of N-glycosylation on Fc alpha receptor interactions. *Journal of Biological Chemistry*, *273*(4), 2260–2272.

Mimura, Y., Sondermann, P., Ghirlando, R., Lund, J., Young, S. P., Goodall, M., et al. (2001). Role of oligosaccharide residues of IgG1-Fc in Fc gamma RIIb binding. *Journal of Biological Chemistry*, *276*(49), 45539–45547.

Oda, M. (2004). Antibody flexibility observed in antigen binding and its subsequent signaling. *Journal of Biological Macromolecules*, *4*(2), 45–56.

Presta, L. (2003). Antibody engineering for therapeutics. *Current Opinion in Structural Biology*, *13*(4), 519–525.

Raju, T. S., Briggs, J. B., Borge, S. M., & Jones, A. J. S. (2000). Species-specific variation in glycosylation of IgG: evidence for the species-specific sialylation and branch-specific galactosylation and importance for engineering recombinant glycoprotein therapeutics. *Glycobiology*, *10*(5), 477–486.

Reuters. (2014). *Research and markets: Global and Chinese monoclonal antibody industry report, 2013–2017*. From http://www.reuters.com/article/2014/01/07/research-and-markets-idUSnBw075871a+100+BSW20140107.

Tao, M., & Morrison, S. (1989). Studies of aglycosylated chimeric mouse-human IgG. Role of carbohydrate in the structure and effector functions mediated by the human IgG constant region. *Journal of Immunology*, *143*, 2595–2601.

Wang, W., Singh, S., Zeng, D. L., King, K., & Nema, S., et al. (2007). Antibody structure, instability, and formulation. *Journal of Pharmaceutical Sciences*, *96*(1), 1–26.

Wankanker, A. (May 2010). *Antibody drug conjugates: The next wave of monoclonal antibody-mediated chemotherapeutics*. AAPS News Magazine.

Weitzhandler, M., Hardy, M., Co, M. S., & Avdalovic, N. (1994). Analysis of carbohydrates on IgG preparations. *Journal of Pharmaceutical Sciences*, *83*(12), 1670–1675.

Wen, J., Jiang, Y., & Nahri, L. (2008). Effect of carbohydrate on thermal stability of antibodies. *American Pharmaceutical Review*.

Woof, J. M., & Burton, D. R. (2004). Human antibody-Fc receptor interactions illuminated by crystal structures. *Nature Reviews Immunology*, *4*(2), 89–99.

This page intentionally left blank

Analytical tools used in the formulation and assessment of stability of monoclonal antibodies (mAbs)

2

Analytical methods for evaluation of monoclonal antibody stability

As will be discussed in Chapter 3 there are several degradation pathways for proteins and monoclonal antibodies (mAbs). The mAb DP requires formulations that are sufficient to meet the specific TPP for the specific mAb. However, in order to do this several analytical methods are used to determine the stability of the mAb and set a shelf life for the product. There are many excellent reviews of analytics used to assess protein/mAb stability (Chang & Hershenson, 2002; Jones, 1993; Reubsaet et al., 1998a,b). Many of the analytics are used in characterization of the mAb DS that is produced. Also mass spectrometry techniques coupled with chromatography have been used to identify the alterations that occur in the mAb primary structure. Development of mAb DP formulations requires high-throughput assays since many formulations may need to be evaluated over many time points during storage. Thus, here we limit our discussion to briefly discuss the different methods used to assess stability and aid in choosing appropriate formulation excipients.

Chromatographic methods

High-performance liquid chromatography (HPLC) and recently ultra high-performance liquid chromatography have been the main workhorses for analysis of mAb chemical degradation. HPLC methods used to assess chemical degradation in proteins are usually based on change in polarity or charge of the protein. Physical degradation that results in aggregate formation is usually assessed by sizing chromatography. Some of the most common methods used for mAb analysis are as follows.

Size exclusion chromatography

Size exclusion chromatography (SEC) has been the main chromatographic method used to determine the size of proteins, and in particular the distribution of aggregates in final DP. The chromatographic matrix consists of beads with pores of a defined size, which allows for penetration of protein molecules. The greater the penetration into the pores, the greater is the residence time on the column, resulting in greater elution times. The apparent molecular weight of the applied protein sample is defined by running a set of protein molecular weight standards (Andrews, 1970; Whitaker, 1963). However, the elution of the protein is dependent only on the hydrodynamic volume so that shape plays a large

Monoclonal Antibodies. http://dx.doi.org/10.1016/B978-0-08-100296-4.00002-6

role in determining the molecular weight from the reference standards (Andrews, 1970). Thus, molecular weight determinations of highly asymmetric molecules will be in error when using typical calibrated globular protein molecular weight standards. Development of light scattering detection systems has mitigated this problem since actual molecular weight determinations are made on the separated peaks (Wen, Arakawa, & Philo, 1996). Despite this improvement, there remain several difficulties due to nonspecific adsorption of protein molecules onto the column gel matrix. The use of solvents such as isopropyl alcohol (IPA) or salts can decrease these interactions, but may alter the molecular weight distribution that occurs in the aqueous buffer systems (Philo, 2009). Ricker and Sandoval analyzed a number of mAbs at varying ionic strengths (Ricker & Sandoval, 1996). It was shown that the results varied among the antibodies, and that some mAbs showed retention time shifts and poor peak resolution at low ionic strength.

Another complication is that the protein sample dilutes during the chromatography, and if the protein reversibly self-associates as a function of concentration, it may be difficult to determine the actual molecular weight distribution of the original formulated protein at higher concentration (Shire, 1994). Large molecular weight aggregates may also be filtered out during the chromatography, resulting in loss of protein which leads to erroneous determinations of percent aggregate in the protein sample (Philo, 2009). For all of these reasons regulatory agencies have requested the use of other molecular weight determination methods to verify that SEC is measuring the correct molecular weight distribution of the formulated DP. This aspect will be discussed in more detail in descriptions of biophysical assays.

Despite all these disadvantages for actual molecular weight determination, SEC can be a very useful high throughput assay to explore conformational changes in a protein. Thus an independent measurement of molecular weight can lead to determination of effective hydrodynamic radius by SEC (Martenson, 1978). The use of light scattering detectors online facilitates such a determination, and can be useful in assessing conformational changes as a function of formulation conditions (Wen et al., 1996).

Ion exchange chromatography

Ion exchange chromatography (IEX) is a chromatographic separation method essentially based on the net charge of the protein, and is generally used to follow deamidation and succinimide formation. Positive (cationic) or negative (anionic) charge moieties are directly linked to the chromatographic matrix. At any specific pH the protein or mAb will have a net charge that is governed by the different amino acid residues that are capable of hydrogen ion ionization. Acidic residues such as Asp or Glu contribute negative charge when deionized, whereas basic residues such as His, Lys, and Arg contribute positive charge when unionized. The net charge of a protein can be computed from the amino acid composition by summing up the individual side chain ionizations assuming that there are no electrostatic interactions or impact of conformation (Tanford, 1962). The chromatography is usually run at low ionic strength so that the protein can bind to the charged residues on the ion exchange matrix. After binding they can be eluted using either a pH or a salt gradient. Theoretically at any pH value, proteins should elute in order of their net charge, i.e., on an anion exchange

column the net negatively charged protein would elute after the positively charged protein. However, localized concentrated regions of net negative or positive charge may influence the order of elution. In addition to this, protein surfaces are irregular resulting in different exposures of charged groups to solvent. Thus, the flexibility of the protein will also dictate the order of elution since in some cases a fair amount of structural distortion must occur to maximize charge–charge interactions at a substantial cost of free energy. Ion exchangers using extended linkers to place charges on the matrix have been developed (Figure 2.1; Muller, 1990). The extended linkers were generated by chemical modification where polymerized acrylamide derivatives were grafted onto hydrophilic supports. Chromatography using these types of matrices has been termed tentacle ion exchange chromatography and theoretically will enable the protein-charged residues to interact with the matrix without large distortion of protein

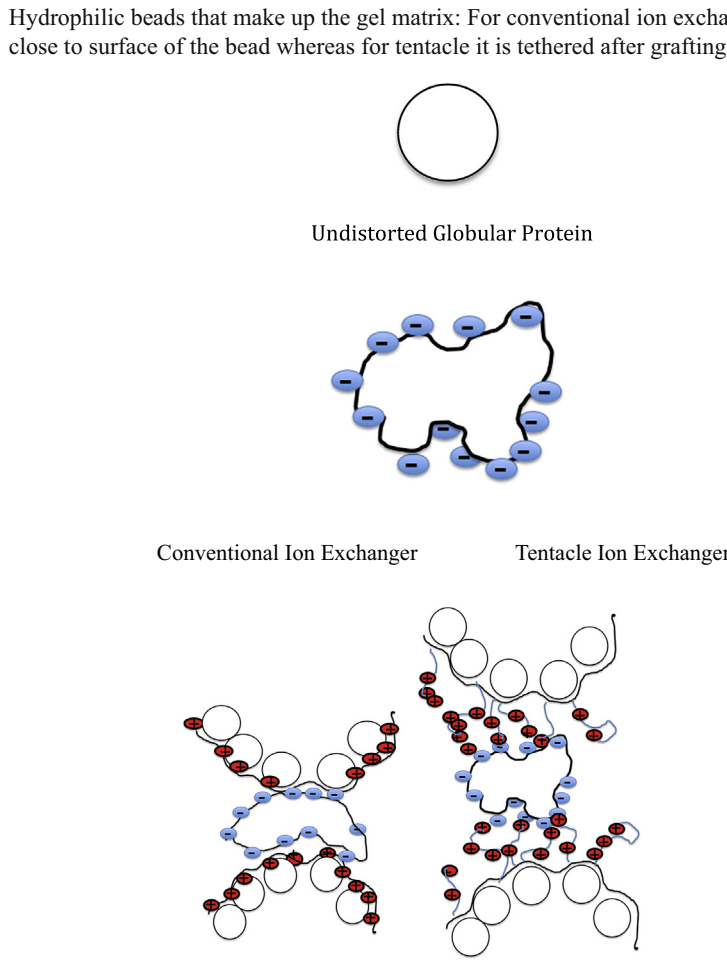

Figure 2.1 Schematic of tentacle ion exchangers compared to conventional ion exchangers (shown for an anion exchange resin).

structure (Donovan, Rabel, & Zahran, 1991; Weitzhandler et al., 1998). Antibodies with flexibility at the hinge region may accommodate some of the distortion, and essentially the mAb structure can distort to maximize the interaction of the surface charged moieties on conventional ion exchangers with the mAb charges. Several studies using tentacle ion exchange resins for mAb purification have been published and involve exploring different resins, which have different support matrices and density of tethered charges. The main point of these investigations was to increase recovery capacity when compared to conventional protein-A chromatographic media. Tentacle cation ion exchange chromatography was used during development of Pulmozyme® (an inhaled recombinant derived human DNase for treatment of cystic fibrosis) to attempt to improve the ion exchange resolution (Cacia, Quan, Vasser, Sliwkowski, & Frenz, 1993). Surprisingly, only two peaks were resolved and it was then determined that the tethered negative charges mimicked the poly PO_4 backbone of DNA which bound specifically to a site with an exposed Asn residue. Deamidation of the residue weakened this interaction resulting in two peaks, one the deamidated and the other the non-deamidated form of Pulmozyme®. This was nicely shown using isoelectric focusing (see details for this technique below) where each resolved peak had several charged species of either the deamidated or non-deamidated Pulmozyme® (see Figure 7 of Cacia et al., 1993).

Hydrophobic interaction chromatography

Hydrophobic interaction chromatography (HIC) separates proteins based on the hydrophobicity of the protein (Queiroz, Tomaz, & Cabral, 2001), and has been used to follow oxidation and Asp isomerization. Hydrophobic interactions tend to be strongest at high salt concentrations. Small hydrophobic residues such as phenyl or propyl groups are coupled to the chromatographic matrix. After loading in high salt the protein is eluted using a decreasing salt gradient. In this manner the more hydrophobic proteins elute later during the chromatography. This type of chromatography was successfully used to separate four different forms of tissue plasminogen activator (tPA) (Wu, 1992). It has been very useful in analyzing mAbs for Asp isomerization and oxidation of Trp and Met (Boyd, Kaschak, & Yan, 2011; Valliere-Douglass, Wallace, & Balland, 2008). Asp isomerization in the complementarity region of a mAb that binds to IgE was further elucidated on HIC by using either pepsin to generate $F(ab)'_2$ fragments or papain to generate Fab and Fc fragments via cleavage at the mAb hinge region (Cacia, Keck, Presta, & Frenz, 1996).

Reversed phase chromatography

Reversed phase chromatography (RP-HPLC) uses resins with small hydrophobic groups attached. Instead of using salt gradients to elute hydrophobic species, organic modifiers such as acetonitrile or propanol are added to the elution buffer to decrease the water concentration in the mobile phase. This in turn weakens the hydrophobic attraction of the hydrophobic groups on the chromatography matrix for the protein. This is akin to what happens in the folding of proteins in aqueous media. The hydrophobic forces are due to structuring of water around the hydrophobic residue resulting

in a decrease in total system entropy. In order to maximize the system entropy, the hydrophobic residues orient away from the water resulting in an increase in bulk water entropy and hence an increase in system entropy. Thus, removing the water in the reversed phase elution buffer weakens the entropic driving forces for the so-called hydrophobic bond (Tanford, 1980), and the stronger hydrophobic interactions will require higher concentrations of organic modifiers. Therefore a gradient of organic solvent will release proteins from the column matrix in the order of their hydrophobic interaction strengths.

Initially this method was used to separate small organic molecules, and has been successfully used to separate peptides that are generated after specific proteolysis using enzymes such as trypsin (Fullmer & Wasserman, 1979). This chromatography coupled with mass spectrometry has enabled peptide mapping whereby residues in large proteins that are chemically modified can be identified. Although RP-HPLC has been used successfully to analyze small proteins such as insulin (Seino, Funakoshi, Fu, & Vinik, 1985), growth hormone (Kohr, Keck, & Harkins, 1982), and human relaxin (Cipolla & Shire, 1991), especially for Met oxidation products, the resolution of larger intact proteins is limited. Specifically, in larger proteins the effect of the chemical alterations on the elution profile is smaller than for peptides and small proteins, and thus this chromatographic assay has limited utility in analyzing degradation in large proteins. Although this is generally the case, appropriate optimization of the RP-HPLC can be done to investigate chemical changes such as Trp oxidation in mAbs (Yang, Wang, Liu, & Raghani, 2007). The use of RP-HPLC for analysis of small rDNA-derived proteins has been reviewed (Frenz, Hancock, Henzel, & Horvath, 1990).

Electrophoretic methods

Reduced and nonreduced sodium dodecyl sulfate electrophoresis

In this method, an electric field is applied over a gel-based matrix, usually consisting of a polyacrylamide slab gel, and this assay is termed sodium dodecyl sulfate polyacrylamide gel electrophoresis (SDS PAGE). The buffer system of this gel matrix contains SDS and samples are incubated at higher temperature in a loading buffer solution that also contains SDS. Proteins will unfold in the typical SDS concentrations used, and thus will migrate as simple linear polypeptide chains (with disulfide cross-linking in the absence of reducing agent). After loading samples, usually with an added dye to visualize the transport into the gel, an electric field is applied. The pore size of the matrix, which is generated during the polymerization process, dictates the rate at which the unfolded protein molecules transport during electrophoresis. Charge is not a predominant factor because most proteins bind a constant ~1.4 g of SDS/g of protein resulting in SDS complexes with similar mass to negative charge ratio, and thus the protein samples separate on the basis of their size. The SDS binds to the protein through its hydrophobic portion, and thus membrane-bound proteins that have large hydrophobic regions may bind greater amounts of SDS resulting in incorrect determination of size. The use of reducing agents readily shows if protein covalent aggregates

are disulfide linked, and thus is a reflection of alterations in oxidation of Cys residues. This method is also useful in quickly ascertaining if there are noncovalent linkages such as those caused by di-Tyr generation as a result of Tyr oxidation. Although apparent molecular sizes can be determined using SDS PAGE with appropriate protein size markers, the actual molecular weight in solution may be dramatically different, as we will show in the physical assay section.

Native PAGE

This method is similar to SDS PAGE but analyzes protein transport in an electric field without the presence of SDS. As might be expected the protein molecules will separate on the basis of both their size and charge. Thus, this can be used as a quick complementary assay for comparison with IEX chromatography.

Isoelectric focusing

As previously mentioned proteins as well as mAbs are multicharged macromolecules. The net charge of the protein is a function of the hydrogen ion equilibria as well as binding of ions. The protein net charge will vary with the pH, whereby the maximum net positive charge is at acidic pH values and the protein progressively becomes less positively charged as the pH increases. At some pH value termed the isoelectric point, pI, the number of positive charges equals the number of negative charges and the protein has a net zero charge. Electrophoresis in an electric field with a pH gradient results in the protein migrating to the pH where the net charge is zero, and the protein no longer migrates in the field. The generation of a pH gradient in the applied electric field results from the use of "carrier ampholytes" of appropriate pI and buffer capacity. When a mixture of these ampholytes is subjected to an electric field they each migrate to a zone determined by their pI resulting in a stable pH gradient. Protein samples run under this gradient then migrate and essentially "focus" at the pI value. Commercially available markers are used to determine the pI for the applied sample. When isoelectric focusing (IEF) is run using large-pore gel systems such as agarose or polyacrylamide (Righetti & Drysdale, 1974) a resolution of as little as 0.02 pH units can be attained (Vesterberg & Svensson, 1966). Although IEF has high resolving power, a significant problem is that many proteins have minimum solubility at their pI and thus surfactants or urea may be required to keep the protein in solution. In this case the determined pI values will not be for the native protein, but for the unfolded protein due to the use of surfactants or a denaturing molecule such as urea. Despite this disadvantage the high resolution that is attained can actually distinguish one single charge difference between proteins. An example of this is shown in Figure 2.2 where the coat protein from a plant virus (TMVP), tobacco mosaic virus, was expressed by rDNA technology in *Escherichia coli* and compared to the wild-type protein from virus isolated from tobacco plant (Shire et al., 1990). In the plant the TMVP is acetylated on the N-terminus, whereas in *E. coli* no such processing occurs resulting in a free amino terminal group. Thus the rDNA-produced TMVP has only one charge difference, and can be resolved by IEF. Another issue when using IEF is that the pH gradient may degenerate over time resulting in a substantial decrease in resolution. This has been overcome by

Figure 2.2 Isoelectric focusing of TMVP and r-TMVP in 8 M urea. Lanes 1–3 correspond to r-TMVP, pl markers (Pharmacia), and wild-type TMVP, respectively. The marker proteins (with the respective pI values) from top to bottom are human carbonic anhydrase B (6.55), bovine carbonic anhydrase B (5.85), β-lactoglobulin A (5.20), soybean trypsin inhibitor (4.59), glucose oxidase (4.19), and amyloglucosidase (3.50). pI values are not corrected for urea.
Reproduced from Shire et al. (1990) Biochemistry.

preparing a gradient of acrylamide that contains acrylamide moieties with buffer groups (Righetti, Gelfi, & Chiari, 1996). After the acrylamide is polymerized the gel network has covalently attached buffer groups leading to a highly stable pH gradient. Such an immobilized pH gradient IEF leads to resolution as low as 0.001 pH units (Bjellqvist et al., 1982).

Capillary electrophoresis

In capillary electrophoresis (CE) the electrophoresis is done in small capillary tubes, usually on the order of 50 μm in diameter to avoid overheating of samples when using high voltages (Rabel & Stobaugh, 1993). High voltages are used since the analysis can be done faster with higher resolution as the voltage increases (proportionately with the square of the voltage). Additional advantages over standard electrophoretic techniques are the decrease in convective flow in the narrow capillaries, the use

of HPLC detectors to analyze the eluents during the electrophoresis, and the high throughput-rapid turnover for the assay. The capillaries are made from fused silica, and the predominance of negative charges can interfere with electrophoresis of protein samples. Fortunately, appropriate coatings have been developed to mask these charge groups and permit analysis of large protein molecules. CE has been used in several formats including non-gel sieving (Hunt & Nashabeh, 1999) and IEF (Hunt, Hotaling, & Chen, 1998; Hunt, Moorhouse, & Chen, 1996). SDS PAGE analysis of proteins and mAbs with and without reducing agents is very useful for determination of disulfide-linked species. Hunt and Nashabeh (1999) showed that CE non-gel sieving yields similar results to SDS PAGE with silver staining.

Membrane-confined electrophoresis

Many of the charge-based assays such as IEX chromatography and native PAGE do not provide a direct measurement of the effective charge on the protein. Usually the net charge as a function of pH is estimated from a summation of the ionization of the side chain residues in proteins (Shire, 1983; Tanford, 1962). Improvements have been made in such computations by incorporating electrostatic interactions and steric environments of a protein (Olsson, Sondergaard, Rostkowski, & Jensen, 2011). The actual net charge on a protein or mAb can be determined by measuring electrophoretic mobility coupled with an independent determination of the frictional coefficient. Determining the frictional coefficient in an electric field can be difficult. A more direct determination involves electrophoresis in the absence of any sieving mechanism. An apparatus for such a measurement has been developed and described by Laue et al. (Ridgeway et al., 1998). Comparison of charge determined by MCE with predicted theoretical charge using T4 lysozyme charge mutants showed very good agreement (Durant, Chen, Laue, Moody, & Allison, 2002). However, it has been shown that often the determined charge of mAbs is significantly different from the computed values. Some of this difference may be due to selective binding of anions by mAbs (T. Laue, personal communication).

Spectroscopic methods

Spectroscopic assays have been used mainly for analysis of protein conformation and higher order structure. Many of these methods are rapid and can provide valuable stability data to enable formulation development. The most commonly used methods in therapeutic protein formulation development include ultraviolet absorption, circular dichroism, fluorescence, and infrared spectroscopy.

Ultraviolet absorption spectroscopy

Ultraviolet absorption spectra from 240 to 320 nm are due to the aromatic amino acid residues, Tyr, Phe, and Trp, and a spectral scan from 240 to 320 nm provides a fast and reliable way to determine concentration of proteins in solution. Often an independent method such as quantitative amino acid composition is used to obtain concentration of the protein in order to determine absorptivity values. Once

the value of the absorptivity for a protein in a particular solvent is determined, the concentration can be readily assessed from the UV spectra using Beer's law. UV spectra of known concentrations of N and C terminal-blocked Phe, Tyr, and Trp peptides have also been used to determine the absorptivity contributions from the aromatic side chains in a protein, and then computing the absorptivity value for the protein by summing up the individual contributions from the aromatic amino acid residues. However these computations do not take into account the effect of environment on the UV absorption of the contributing residues due to the folded structure, and therefore usually give concentrations within 10% of the actual value. Difference (Donovan, 1973) and derivative spectroscopy (Balestrieri, Colonna, Giovane, Irace, & Servillo, 1978) can explore the impact of environment due to protein folding. The change from a hydrophobic to a more hydrophilic environment that occurs when a protein unfolds results in a change in polarizability which generally results in a red shift of the UV spectra and an increase in the absorptivity of 10–15% (Donovan, 1973). It has been shown that comparing natively folded protein to enzymatically digested protein using second-derivative UV spectroscopy can assess the magnitude of these effects (Bewley, 1982). Comparison of the second-derivative UV spectra with that computed from blocked Phe, Tyr, and Trp compounds confirms that the protein is fully denatured and the computed absorptivity for unfolded protein is used to determine the absorptivity for native protein (Gray, Stern, Bewley, & Shire, 1995).

Since the UV spectra of a protein are highly dependent on the exposure of the residues during unfolding, this method can be used to assess the impact of formulation and storage conditions on the physical stability of a protein or mAb. For example, stability of the tertiary structure of the mAb Rituxan stored at 0.4 mg/mL for 1 and 6 months at 40 °C was assessed by second-derivative UV spectroscopy (Paul, Vieillard, Jaccoulet, & Astier, 2012). The results showed little change after 1 month but measurable alteration after 6 months.

Circular dichroism

Circular dichroism (CD) measures the difference between right and left circularly polarized light, which provides an indication of the chiral environment around amino acid residues in proteins. CD in the far UV region (~190 to 240 nm) provides information on the secondary structure of a protein due to the arrangement of peptide bonds into well-defined constrained structures. Polylysine was used to show that the main class of structures, i.e., α-helix, β-sheet, and "random" coil, has distinct spectra (Davidson & Fasman, 1967) which can be deconvoluted from the total CD spectra to obtain estimates of secondary structure content (Chen, Yang, & Chau, 1974). Improvements in fitting algorithms coupled with the CD of proteins with known structure determined by NMR or X-ray crystallography have refined the determination of secondary structure by CD (Perczel & Fasman, 1992; Provencher & Glockner, 1981). The modification of CD instruments to allow for reliable CD measurements in a vacuum results in CD spectra as low as 180 nm. As discussed by Johnson (1990) such measurements provide more robust analysis of secondary structure since there are

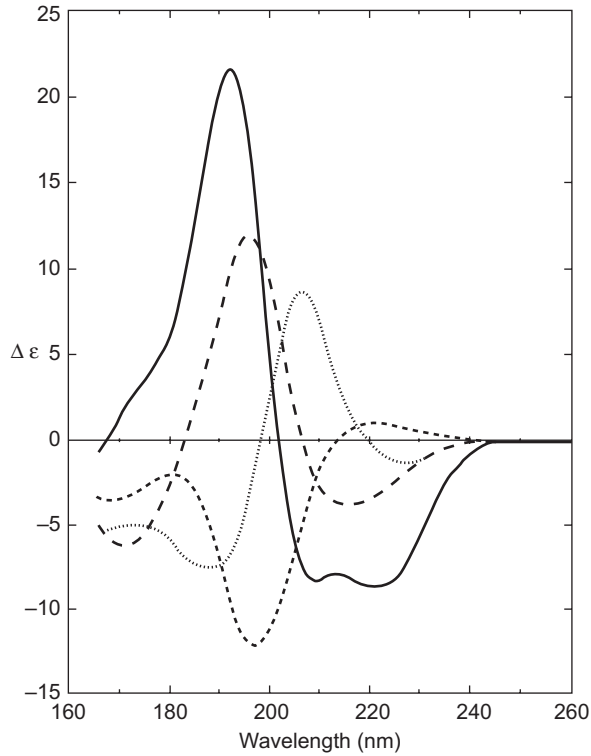

Figure 2.3 The circular dichroism (CD) for various secondary structures: α-helix (solid line), antiparallel (β-sheet (bold dashed line), (β-turn (dotted line), and random coil (dashed line). From Johnson (1990).

two additional CD bands between 200 and 178 nm (Figure 2.3). Although the CD of the α-helix dominates with an intense positive band at 192 nm, the β-sheet has an intense positive band and the random coil has an intense negative band at 198 nm. Thus, extending the CD spectra to below 200 nm makes it easy to discern random coil from β sheet and β turn structures.

The near UV CD spectral (region) (240–350 nm) reflects the chiral environment around the aromatic amino acid residues, Phe, Tyr, and Trp, and also around disulfide linkages. Changes with solution conditions such as pH, ionic strength, and temperature are usually interpreted in terms of changes in the tertiary structure of the protein. However, this should be done with caution since any change in the aromatic amino acid environment will lead to a change in the near UV CD spectra. As an example, the near UV CD concentration difference spectra of human relaxin is actually a reflection of the sequestering of a Tyr residue upon dimerization of the protein, rather than a tertiary structural change (Shire, Holladay, & Rinderknecht, 1991).

Assessing structural changes as a function of formulation conditions is a main attribute of CD spectroscopy. It often is used to follow denaturation of the protein as a function of solution conditions such as temperature and pH. An example of the use

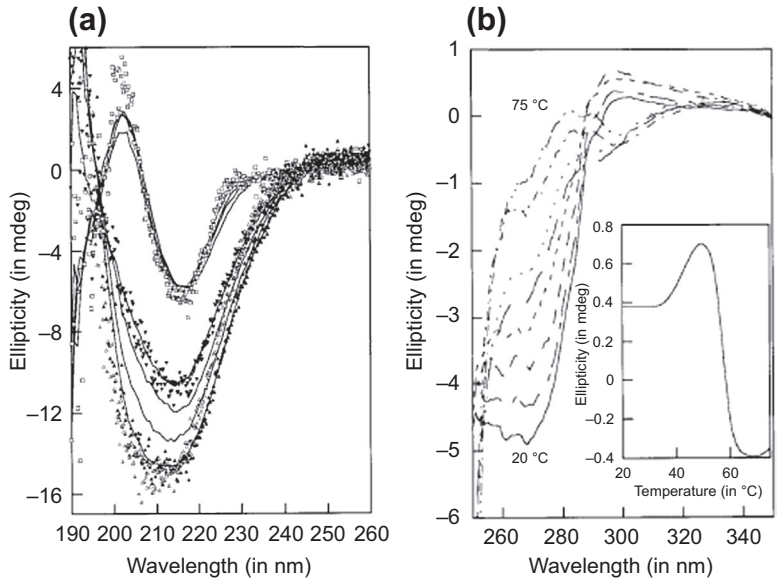

Figure 2.4 Far UV (a) and near UV (b) CD spectra of an IgG (0.2 mg/ml) in a 10 mM phosphate buffer, pH 8.1. The experimental data points in panel A are shown for three temperature values, (open squares) 20 °C, (solid inverted triangles) 60 °C, and (solid triangles) 75 °C. IgG_2 heated to 75 °C and cooled prior to measurement is shown as open triangles. For clarity, symbols for individual data points for other temperatures are omitted and the solid curves are smoothed through the experimental data measured at 20, 35, 50, 55, 60, 65, 70, and 75 °C, decreasing respectively. The solid curves in panel B are smoothed through the experimental data measured at 20, 35, 50, 55, 60, 65, 70, and 75 °C, respectively. The inset shows a circular dichroism temperature scan of IgG measured at 300 nm.
From Vermeer and Norde (2000) *Biophysical Journal*, 78, 394–404.

of CD to assess mAb IgG_2 stability as a function of temperature is shown in Figure 2.4(a). The CD undergoes little change up to temperatures of 55 °C showing that this IgG2 secondary structure is stable from 20 to 55 °C. The far UV CD spectra in this temperature range are typical of mAbs and show a high amount of β-sheet structure, in good agreement from structural analysis by X-ray crystallography (Figure 2.2(b)). At higher temperatures spectral changes occur where the minimum at 217 nm broadens and shifts to a lower wavelength with appearance of a shoulder band at ~208 nm. This shift reflects the generation of random coil with concurrent losses of β-sheet and β-turn at the higher temperature. The secondary structural content was analyzed using polylysine CD spectra for α-helix, β-sheet, β-turn, and random coil essentially using deconvolution methods described by Chen et al. (1974), and clearly shows the increase of random coil as the mAb unfolds at the higher temperatures (Table 2.1). The resulting unfolding was also irreversible as shown in the CD spectra of the IgG2 heated to 75 °C and cooled prior to the measurement (Figure 2.4(a)). The near UV CD spectrum for this IgG_2 as a function of temperature shows that the negative CD band at 270 nm decreases (becomes more positive) as the temperature increases (Figure 2.4(b)). This reflects

Table 2.1 Secondary structure of an IgG2 determined by far UV circular dichroism measurements as a function of temperature

Temperature (°C)	α-Helix	β-Sheet	β-Turn	Random coil	RMS error
50	0	66	22	12	8.5
55	0	59	16	25	8.8
60	4	44	8	44	4.5
65	7	43	6	44	6.7
70	9	39	6	46	7.3
75	9	38	6	47	7.2

Medium, 10 mM phosphate buffer, pH 8.1.
From Vermeer and Norde (2000).

the exposure of the aromatic residues to solvent and increased motion of these residues as the protein unfolds. The inset of Figure 2.4(b) shows the change in CD signal at ~300 nm as a function of temperature, and as can be seen, there is a large decrease in the signal at about 55 °C, which corresponds nicely to the observed secondary structure changes by far UV CD measurements. Although this IgG2 is highly unfolded at 75 °C there still is a significant amount of folded secondary structural elements since 50% of this mAb still has β-sheet, β-turn, and α-helix (Table 2.1). This is in stark contrast to the denaturation of a murine IgG_1 at 6 M guanidinium hydrochloride where only random coil was observed (Buchner et al., 1991).

Fluorescence spectroscopy

The aromatic amino acid residues of proteins have fluorescence in the 300–400 nm range when excited at 250–300 nm. The environment of these residues dictates the fluorescence spectra and therefore this spectroscopy can complement UV and CD spectroscopy for analysis of tertiary structure of proteins. There are several reviews and books on this spectroscopic technique (Eftink, 1998; Lakowicz, 1984, 2002). Examples of application to the study of immunoglobulin structure by fluorescence measurements include investigation of stability of murine antibodies as a function of pH and temperature (Jiskoot et al., 1991; Jiskoot, Beuvery, Dekoning, Herron, & Crommelin, 1990), characterization of a murine mAb at low pH (Buchner et al., 1991), and studies on conformational changes of goat polyclonal anti-human serum albumin antibodies denaturation at low pH (Lin, Andrade, & Chang, 1989).

Infrared spectroscopy

The bending and stretching of bonds in proteins result in characteristic infrared (IR) bands. Application of Fourier techniques to IR spectra has led to Fourier transform infrared (FTIR) spectroscopy which allows for enhanced resolution of the spectra from amide vibrations. Deconvolution of the absorption envelope of the amide vibrations is related to the secondary structure of the amide group in peptide linkages.

The major advantage of FTIR is that it can be used in analysis of solid dosage forms. Examples of use of FTIR to investigate storage conditions and formulation variables of mAbs include studies on an anti-IgE mAb after freeze drying (Andya, Hsu, & Shire, 2003) and spray drying (Costantino, Andya, Shire, & Hsu, 1997).

Additional biophysical methods

Mass spectrometry

In early development of a formulation of proteins and mAbs various high-throughput assays such as chromatographic-based assays are evaluated over time of storage at different formulation conditions at different temperatures. Although changes in the assay are easily determined, the use of mass spectrometry coupled with peptide mapping has enabled identification of the actual sites and chemical route of degradation. There are some excellent reviews and discussions on mass spectrometry, which essentially can determine with high precision the mass of peptides altered in the protein structure due to chemical degradation (Biemann, 1995; Bourell, Clauser, Kelley, Carter, & Stults, 1994; Lanucara, Holman, Gray, & Eyers, 2014; Papac & Shahrokh, 2001).

Surface plasmon resonance

Surface plasmon resonance (SPR) technology has been used to obtain kinetics and equilibrium data without the requirement of having to label any of the interacting molecules (Hodgson, 1994), and has been extremely useful in obtaining binding data with high affinity (Day, Capili, Borysenko, Zafari, & Whitty, 2013). The basic principle is the behavior of light at boundaries with different refractive indices. At the interface of a higher refractive index surface (the sensor) and a lower refractive index solution, light internally reflects beyond a critical angle. The internal reflection creates an electromagnetic field, the evanescent wave, that tranverses from the interface into the solution. The angle at which this wave is greatly enhanced is the resonance angle and is extremely sensitive to the refractive index changes at the sensor surface. These changes are related to the mass of binding molecules to the target molecule that is captured on a dextran-coated gold surface of the sensor. Since one of the binding molecules must be immobilized onto the sensor surface a caveat of this technology is the dependence of the determined binding affinity constants on the orientation, method of binding, and which of the binding molecules are immobilized on the surface (O'Shannessy, 1994; Trilling, Harmsen, Ruigrok, Zuilhof, & Beekwilder, 2013).

Analytical ultracentrifugation

Analytical ultracentrifugation (AUC) is probably one of the best methods for quantitative studies of protein interactions (Schachman, 1989). There are many reviews and books that discuss this biophysical method (Harding, Rowe, & Horton, 1992; Schachman, 1959; Schuster & Laue, 1994; Teller, 1973).

Protein solutions are analyzed while centrifuging in a well-defined centrifugal field. Current commercially available analytical centrifuges consist of a centrifuge

equipped with optical systems, temperature control, and interfacing with computer control and data acquisition systems. The AUC experiment can be performed in essentially two modes, sedimentation equilibrium and sedimentation velocity. In sedimentation equilibrium the centrifuge is run at sufficiently low speeds so that the sedimentation of the protein is equivalent to the diffusion, resulting in a time-invariant concentration versus radial position profile. Analysis of the concentration gradient yields molecular weight distributions. The use of specific models, such as monomer to dimer, etc., allows for the determination of association equilibrium constants for reversibly self-associating protein systems. Sedimentation velocity is conducted at higher centrifugal fields so that different sized protein molecules migrate to the bottom of the centrifuge cell. The migration of the sedimentation boundaries is dependent on both the molecular weight of the species and the shape as reflected in the frictional coefficient. Although sedimentation equilibrium is useful for obtaining actual molecular weight, sedimentation velocity has become the main use of the analytical ultracentrifuge in development of protein and mAb therapeutics. This analysis has been facilitated with the development of computer software, which fits the sedimentation data to the Lamm equation (Schuck, 2000). The data are generally displayed as a distribution function yielding peaks that are representative of the individual sedimenting species providing the species do not self-associate. Regulatory agencies are now aware of the deficiencies of SEC for determination of protein aggregates (see the discussion on SEC) and are requesting the use of alternative biophysical methods, preferably AUC, to confirm the veracity of the SEC results. The argument for using an alternative method to confirm SEC results has been presented (Carpenter et al., 2010). The quantitation of aggregates and the limits of precision and accuracy in AUC measurements have been explored using three mAbs of unspecified origin (Pekar & Sukumar, 2007). This study showed a precision of ±0.3% over a measured range of 0.6–67% aggregate. Good accuracy, as ascertained by aggregate spiking experiments, could be achieved down to aggregate levels as low as 1.5%. Examples of the use of AUC to confirm SEC results for mAbs include studies on two humanized mAbs stored at −70 °C and 40 °C (Liu, Andya, & Shire, 2006) and a study of aggregates of a humanized mAb (Andya, Liu, & Shire, 2010). In this later study, SEC and AUC were used to determine percent of aggregates in the same mAb sample. Although SEC showed a single monomer peak at 99.6% with a small amount of aggregated species the AUC analysis showed a significant aggregate peak (Figure 2.5(a)). This amount of aggregate was concentration dependent as shown by sedimentation analysis at different loading concentrations (Figure 2.5(b)) as well as a determination of weight average molecular weight by sedimentation equilibrium (Figure 2.5(c)). This again illustrates what can be missed by SEC analysis due to dilution during the chromatography.

AUC has also been used to help confirm SPR determinations. A recent publication used AUC in a competitive binding mode to determine if published SPR data comparing the binding of three inhibitors of vascular endothelial growth factor A (VEGF-A) were correct (Yang et al., 2014). Essentially, the solution-based AUC method showed that the SPR results were not correct. This was also demonstrated by using different SPR formats, which gave different results.

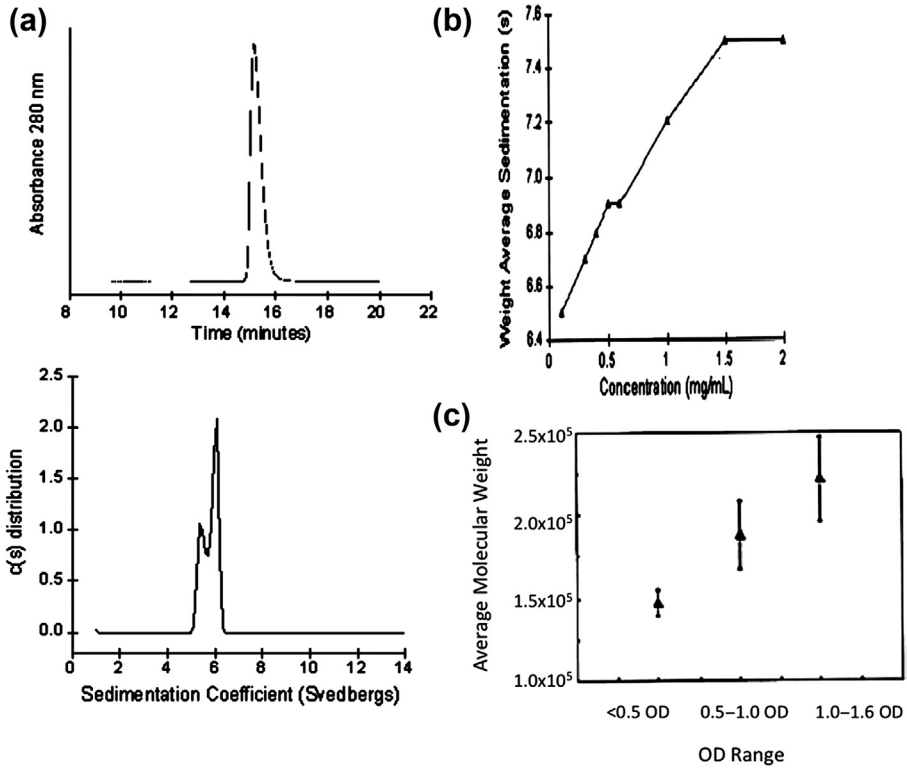

Figure 2.5 Panel A: Size distribution of a full-length mAb determined by (a) size exclusion chromatography and (b) analytical ultracentrifugation (AUC) sedimentation velocity. Panel B: Weight average sedimentation coefficient versus protein concentration observed during AUC sedimentation velocity analysis of the mAb in PBS. Panel C: Weight average molecular weight determined by AUC sedimentation equilibrium of the mAb in PBS.
Reproduced from Andya et al. (2010).

Light scattering

Light scattering is an alternative biophysical method to determine molecular weight, size, and information of protein interactions. When used as a time-averaged method, referred to as static light scattering, SLS, the main information is weight average molecular weight and shape information. Characterization of protein–protein interactions can also be done using determined second and third virial coefficients. This is obtained by measuring the scattering intensity as a function of angular dependence at a series of concentrations. When extrapolated to infinite dilution (zero concentration), the molecular weight and shape of the protein can be determined using a Zimm plot (Zimm, 1948). Since many proteins and aggregates are smaller than the wavelength of light used for the scattering measurement, usually scattering at 90° can provide molecular weight information. Although scattering can provide information on aggregates, even large mAbs that are not aggregating will have detectable scattering due to the size of the molecules (Sukumar, Doyle, Combs, & Pekar,

2004). When performing a concentration dependence measurement using UV absorption at ~280 nm, the scattering must be taken into account. If the scattering is sufficiently low a simple subtraction of absorbance at 320 nm will suffice, but larger contributions may need to be corrected using methods such as outlined by Englander (Englander & Epstein, 1957).

Dynamic light scattering can also be performed using the time course of the light scattering signal, which is used to determine the diffusion coefficient by autocorrelation methods (Lorber, Fischer, Bailly, Roy, & Kem, 2012). Independent measurements of shape or approximation of spherical geometry can be used to obtain molecular weights from the diffusion coefficient using the Stokes–Einstein equations. With the advent of computer interfacing and plate readers, DLS has become a higher throughput assay. In addition DLS experiments as a function of concentration can yield an interaction parameter, which is useful in investigations of protein–protein interactions. Much of this will be discussed in a later chapter on high-concentration formulations for subcutaneous delivery of mAbs.

Differential Scanning Calorimetry (DSC)

Microcalorimetry has been used to study thermal transitions in biomolecules and the application of this method in biotechnology has been reviewed (Chowdhry & Cole, 1989). Differential scanning calorimetry (DSC) has been used to aid in formulation development and to characterize the glass transition temperature in freeze-dried solid dosage forms. Although DSC has been used to aid in formulation development, it should not be used in the absence of other assays, especially those that monitor chemical changes. As will be discussed and shown, chemical alterations can occur in natively folded protein, and thus choosing formulation excipients and conditions that show stabilization by DSC does not guarantee a robust formulation. When used in conjunction with other methods to evaluate stability, DSC can be extremely useful. In particular, DSC can give valuable information on which region of a mAb is stabilized by excipients or which regions are prone to physical stability issues (Mehta, Bee, Randolph, & Carpenter, 2014; Oganesyan, Damschroder, Leach, Wu, & Dall'Acqua, 2008).

Also determination of the unfolding temperature for a protein can aid in designing appropriate high-temperature studies where the protein remains essentially in a folded state. A good example of this is a stability study of Pulmozyme where several temperatures were used below the DSC measured unfolding transition (Shire, 1966). This coupled with the use of tentacle ion exchange chromatography as a biomemetic assay (discussed earlier) that specifically monitors the deamidation of an Asn in the binding pocket for the target DNA allowed for successful use of Arrhenius kinetics. This study showed that the extrapolated rate constant from an Arrhenius plot was in very good agreement with that measured in real time (Table 2.2).

DSC has also been used to determine the glass transition temperature, Tg′, for freeze-dried formulations where the matrix becomes more fluid resulting in less stability than when stored at temperatures below Tg′. Formulations that have high sugar content require a modified form of DSC called modulated DSC. In traditional DSC experiments the difference in the heat flow between a sample and a reference (usually the buffer system of the sample) is measured as a result of a linear change in temperature. The heat capacity can also be determined by subjecting two different samples

Table 2.2 Comparison of rate constants for Pulmozyme deamidation at 5 °C obtained from Arrhenius kinetics and real-time stability data after 88 days at 2–8 °C storage

Formulation[a]	k88 days ($days^{-1}$)	Karrhenius ($days^{-1}$)	ΔE≠ (kcal/mol)
Tris, pH 8	$1.1 \pm 0.1 \times 10^{-2}$	9.3×10^{-3}	14
Tris, pH 7	$1.9 \pm 0.5 \times 10^{-3}$	2.5×10^{-3}	13.4
Succinate, pH 6	+	7.3×10^{-6}	28
Maleate, pH 6	+	3.6×10^{-5}	29.9
Histidine, pH 6	$3 \pm 3 \times 10^{-4}$	3.8×10^{-4}	19.0
Succinate, pH 5	$3.7 \pm 10 \times 10^{-5}$	3.6×10^{-5}	29.3
Citrate, pH 5	+	3.1×10^{-5}	26.0
Acetate, pH 5	+	3.2×10^{-5}	25.5

ΔE≠, energy of activation. Succinate at pH 6 and 5 was evaluated without the 15 °C data because of the large error in the values at 15 °C.
+, indicates that slope was positive. The origin and significance of such a result is discussed in the text.
[a]Buffers consist of 5 mM buffer salt, 150 mM NaCl, and 1 mM $CaCl_2$.
From Shire (1996).

to different linear heating rates. In modulated DSC the heat flow and heat capacity are measured in a single experiment by superimposing a changing heat rate (modulated) on top of a linear heating rate (Gill, Sauerbrunn, & Reading, 1993). Application of modulated DSC for characterization of a mAb freeze-dried formulation with high sugar content has been reported (Breen, Curley, Overcashier, Hsu, & Shire, 2001).

Field flow fractionation

This method originally invented by Giddings (1993, 2000) is useful for analyzing aggregates (Liu et al., 2006; Rambaldi, Reschiglian, & Zattoni, 2011) and also large particles, which are difficult to separate using standard chromatographic and electrophoretic techniques (Williams, Runyon, & Ashames, 2011). Thus, this method allows for characterization of aggregates over a wide size range, from 0.001 to 50 mm (Giddings, 2000). The separation of biomolecules is done within a buffer-filled channel without any column matrix (Rambaldi et al., 2011). The separation occurs by applying an external field that is perpendicular to the laminar flow. This field can be gravitational, centrifugal, magnetic, electrical, temperature, or flow-based (Giddings, 2000). The effluent from the channel can be monitored using UV, refractive index, and light scattering detection. In particular, online UV, RI, and LS detectors allow for protein characterization and determination of the molecular weight of each species.

The most commonly used configuration of field flow fractionation (FFF) used for therapeutic proteins is asymmetrical field flow FFF (AF4), where the orthogonal external field is a cross flow. Larger protein species remain in the center of the laminar flow, whereas the smaller species are driven to the bottom of the channel which is equipped with a membrane to allow for the cross flow to exit. Although the technique does not use a column matrix, interaction of protein molecules with the bottom membrane can

have a profound effect on the elution profiles. Thus, a fair amount of research has been done to use membrane materials that do not have significant interaction with the biomolecules. For protein species that are well below 1 mm in size the elution is highly dependent on the diffusion coefficient. Assuming a spherical shape for all species the molecular weight can then be estimated from the retention times, which are related to the external field strength and diffusion coefficients by a well-defined equation. The precision and accuracy of AF4 for protein and mAb characterization have been explored, and resolution compared to that obtained by SV-AUC and SEC (Liu et al., 2006; Liu, Zhu, Shire, & Demeule, 2012). The conclusion of these studies was that AF4 is a useful orthogonal method to determine the size distribution of protein aggregates and fragments. However, appropriate procedures and careful optimization are required to provide reliable quantitative information. Since this separation method is very different from that of SEC, AF4 may be useful as another orthogonal method to confirm results from SEC.

Methods to evaluate particulates in protein formulations

Large visible particulates can be assessed by visual inspection where the inspection conditions are well defined. However, human visual inspection can be problematic and often instruments designed for visual inspection are used (Borchert et al., 1986), and brief reviews have been presented (Das, 2012; Das & Nema, 2008). Subvisible particulates are analyzed using the US Pharmacopeia (USP) microscopy method. However, this method can be tedious and time-consuming. A more automated and common analysis is done using the light obscuration method with instruments such as the HIAC-Royco particle counter (Borchert et al., 1986; Demeule, Messick, Shire, & Liu, 2010, USP XXII, 1990). In this assay the sample is flowed past a small window where light is focused through for measurement with a photomultiplier tube. Particles as they traverse the light beam reduce the intensity of the light, which is proportional to the cross-sectional area of the particle. Pulses are then counted within the different amplitude ranges resulting in a particle size distribution. Both the microscopy and HIAC assays are official tests in the USP. The USP requirements for HIAC determination are that there should be at or below 6000 particles at >10 mm size and 600 particles at >25 mm size per container (USP XXII, 1990). There have been many alternative methods developed, some of which are discussed in an AAPS themed issue (Shire & Laue, 2010). Recently a device called the Archimedes device that determines particle sizes by buoyancy measurements has been compared to standard techniques for particle size determination using a mAb sample (Panchal, Kotarek, Marszal, & Topp, 2014; Patel, Lau, & Liu, 2012).

Another technology that is being used more frequently is microflow digital imaging (MDI) where photo microscopy is used to analyze distribution and overall morphology of particulates and includes instruments such as those manufactured by Occhio, Brightwell, and Flow Cam (Wuchner, Buchler, Spycher, Dalmonte, & Volkin, 2010). A comparison of four different instruments has recently been published (Zolls et al., 2013). These types of measurements may prove very useful in discerning irregularly shaped protein particulates from more spherical silicone oil droplets that are often found in prefilled syringes. This will be discussed in more detail in later chapters.

Potency assays

Regulatory agencies require that the final formulated drug product be safe and efficacious when administered to patients over the recommended lifetime storage of the drug. Thus, an important part of a stability program is the demonstration that for the specific approved drug the drug maintains its activity over the intended shelf life. This assessment requires the development of biologically relevant assays. Many protein therapeutics are pleotropic and may be used for treatment of different diseases. As an example, human growth hormone (hGH) can be used to treat burn victims as well as hypopituitary children requiring hormone for natural growth. Thus it would not be correct to develop a biological assay that assesses healing in burn victims if the hGH is being developed for treatment of growth inhibition due to lack of the hormone.

Development of potency assays can be categorized as in vivo animal-based, ex vivo cell- or tissue-based, or in vitro analytical-based assays. These types of assays and the advantages and disadvantages of each are herein discussed.

In vivo animal based

When the mechanism of action is not fully understood the use of a whole animal model is the preferred assay for assessing potency. One issue with this approach is how equivalent is the animal biochemistry to that of humans. Correlating responses in the animal model with that in humans can mitigate some of this. These assays are often difficult because of the variability in animal responses as well as the expense and time needed to perform such assays. As an example, the weight gain assay for hGH (Marx, Simpson, & Evans, 1942) results in coefficient of variability as high as 30–50% even when more than 10 animals are used in the assay (Jones, 1993). Although measuring weight gain for longer treatment times may attain an increased precision, this is generally not possible since the animal has immune responses to the exposure of the foreign human protein.

Ex vivo cell or tissue based

Cell-based assays are greatly preferred over the animal-based models since greater precision may be attained and the expense and time for obtaining results may be reduced. However, the choice of cell line may be crucial in the type of response, and the mechanism of action needs to be better understood. As an example, elucidation of the molecular interactions of hGH with the hGH receptor (Devos, Ultsch, & Kossiakoff, 1992) suggests that generation of a cell line that expresses the hGH receptor and proliferates in response to exposure to hGH may be a suitable replacement for the whole animal bioassay. Alternative approaches may use specific animal tissue that is responding to exposure to the protein drug. In vitro assays for human relaxin have been developed where the whole animal mouse pubic symphysis assay (Ferraiolo, Cronin, Bakhit, Chesnut, & Lyon, 1989) has been replaced by a uterine smooth cell contractility assay (Norstrom, Bryman, Wiquist, Sahni, & Lindblom, 1984) and a histamine release assay from rat mast cells transfected with the alpha subunit of FcεRI (Lowe, Jardieu, Van Gorp, & Fei, 1995).

In vitro analytical based

This type of assay is probably the hardest to develop and justify to regulatory agencies as replacements for in vivo assays. The mechanism of action needs to be fully understood to ensure that the in vitro assay mimics what occurs biologically. For this reason regulatory agencies frown upon purely analytical techniques such as chromatographic analysis since it may not be possible to ensure that the measured changes always coincide with the biological response. As an example although it has been proposed to replace the bioassay with a chromatographic assay for evaluation of hGH potency, this approach has not been accepted by regulatory agencies.

If the mechanism of action of the protein drugs is well understood, it may be possible to develop an in vitro assay, which mimics the biological response. This may require development of specific reagents that are actually components of the biological pathway. As an example the tissue-based and whole animal model bioassays for human relaxin have been replaced with a cell-based assay that uses endometrial cells, which produce cAMP upon stimulation with relaxin (Fei, Gross, Lofgren, Mora-Worms, & Chen, 1990).

A common target for mAbs are transmembrane proteins on cell surfaces which act as receptors that result in cellular responses that are linked to a disease. The region of the transmembrane protein that is exposed on the surface is termed the cytoplasmic domain. This cytoplasmic domain, which is soluble, can be used to develop a binding assay to determine the effectiveness of binding of a mAb to the exposed receptor. However, even though the binding may not be altered, the biological response may be changed using a degraded form of the protein drug.

Development of a potency assay for a mAb

The potential problem using a simple binding assay is demonstrated by studies using murine monoclonal IgG1 antibody that binds to the growth receptor p185HER2. This mAb was heated at 40 °C, which resulted in the generation of irreversible aggregates. Mixtures of heated samples with one that was not heated resulted in mAb solutions with different percent of irreversible aggregate. The expected percent of aggregate and that determined by SEC were similar. These samples were then assayed using two binding assays to the soluble cell target receptor. One of the assays used an enzyme-linked immunosorbent assay (ELISA) and the other a radioimmunoassay approach using radionuclide-labeled reagents to determine binding to the extracellular domain (ECD) of the p185HER2 target. The samples were also assayed using an ex vivo cell-based assay that assesses the ability of the mAb to inhibit growth of human SK-BR-3 breast carcinoma cells. Although both binding assays are in good agreement, the decrease in determined concentration for the response ("active concentration") as a function of irreversible aggregate is less than measured by the ex vivo antiproliferation cell-based assay (Figure 2.6). This example clearly shows that a determination of binding to target may not be sufficient to assess the potency of a mAb.

Although binding to an ECD of a target may not be useful as a potency assay, it is possible to develop such an assay if the mechanism of action is well understood. In the case of a mAb that binds to IgE for the treatment of asthma the mechanism of action is fairly well understood. On exposure to an antigen, B-lymphocytes transform to plasma cells that produce an IgE specific to that allergen, i.e., the Fab regions interact with the

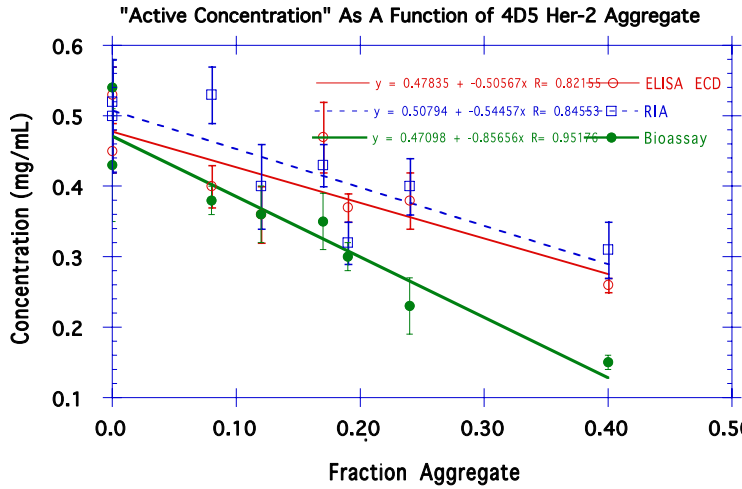

Figure 2.6 Active concentration of 4D5 HER2 murine mAb determined by ELISA binding to the extracellular domain (ECD) of p185HER2, RIA binding to ECD, and the bioassay as a function of aggregate content.

allergen. The IgE binds via its Fc region to high-affinity receptors on basophils and mast cells. These cells are then primed and upon a second exposure to the allergen results in cross-linking of the IgE bound to the high-affinity Fc receptors. The cross-linking then signals the mast cell or basophil to release histamine and leukotrienes that result in asthmatic symptoms. An anti-IgE mAb that binds to essentially the same site on the IgE as the high-affinity receptor prevents the initial priming of the cell. An in vitro assay that mimics this mechanism of action was done using ELISA. In this assay a 96-well plate is coated with an FcεRIα–IgG chimeric receptor. The chimeric receptor essentially is an IgG Fc fused with two soluble forms of the FcεRIα extracellular domains. A mixture of IgE and biotin-labeled IgE is added with different amounts of the anti-IgE mAb (Figure 2.7(a)). The binding to the FcεRIα–IgG chimeric was then assessed using avidin conjugated to horseradish peroxidase (HRP) followed by detection using a substrate that, when oxidized by HRP using hydrogen peroxide as the oxidizing agent, yields a characteristic change that is detectable by spectrophotometric methods. In another assay the amount of biotin-labeled IgE bound to the FcεRIα–IgG chimeric was determined. A bioassay that uses allergen-induced histamine release from mast cells transfected with the α-subunits of FcεRI was also developed as an ex vivo potency assay (Lowe, Jardieu, VanGorp, & Fei, 1995). These three assays were used to analyze percent specific activity (the effective concentration from the assay divided by the concentration determined spectrophotometrically) of anti-IgE mAb stored at −70 °C, 2–8 °C, 25 °C, and 40 °C over 36 weeks of storage. The correlation of the receptor binding inhibition assay with the bioassay was much better than that of the IgE plate binding assay (Figure 2.7(b)). While this example again shows the danger of using a straight binding assay it also shows that formatting the assay in a competitive binding mode can result in development of an in vitro surrogate assay for the bioassay. This approach worked since the mechanism of action biologically is replicated with the in vitro receptor binding inhibition assay.

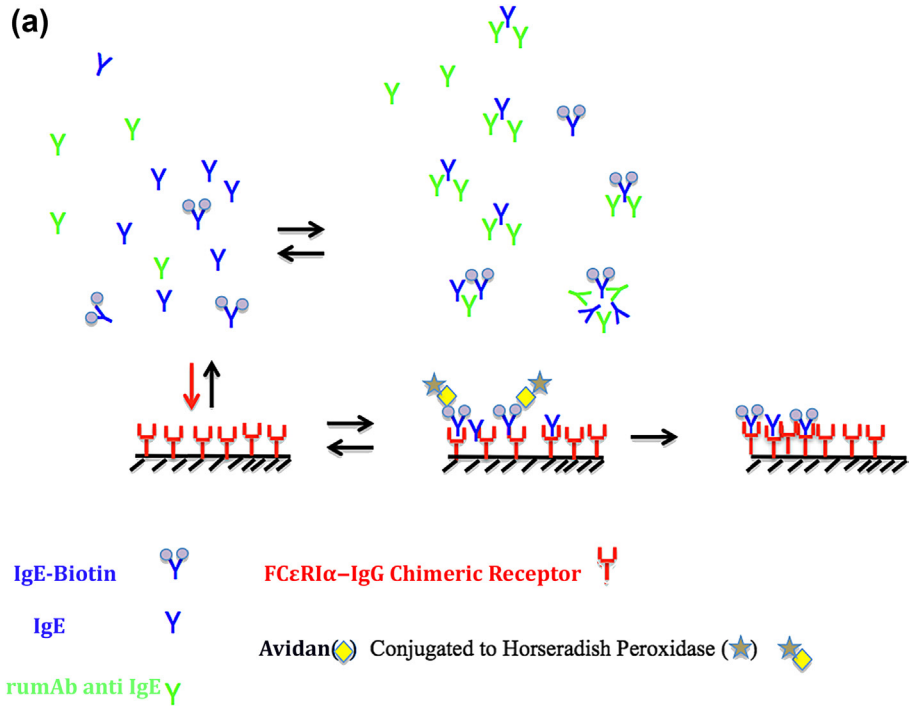

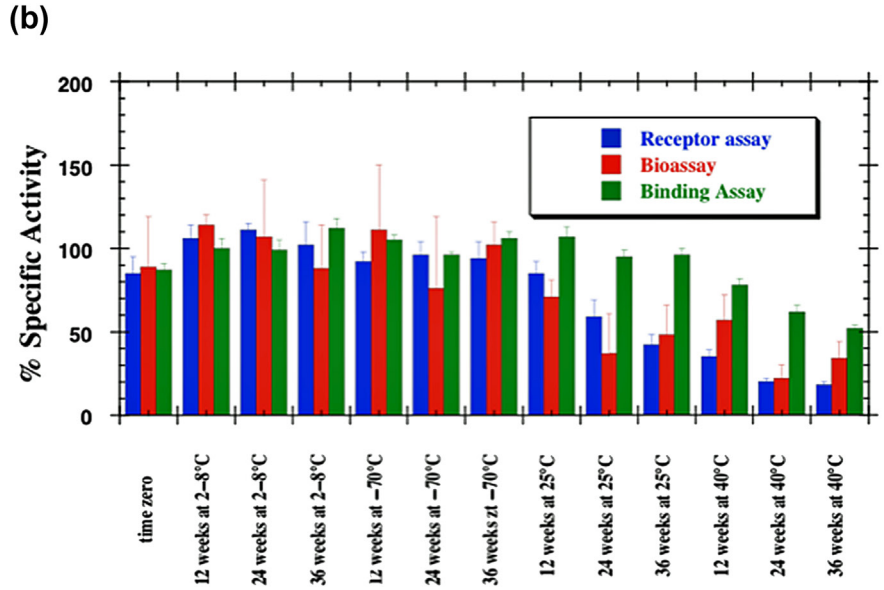

Figure 2.7 (a) Format of the ELISA-based receptor inhibition assay for anti-IgE mAb. (b) Correlation of the determined potencies using the plate binding assay, receptor inhibition assay, and the rat mast cell bioassay of stability samples of rhu anti-IgE mAb.

References

Andrews, P. (1970). Estimation of molecular size and molecular weights of biological compounds by gel filtration. *Methods of Biochemical Analysis*, *18*, 1–53.

Andya, J. D., Hsu, C. C., & Shire, S. J. (2003). Mechanisms of aggregate formation and carbohydrate excipient stabilization of lyophilized humanized monoclonal antibody formulations. *AAPS PharmSciTech*, *5*(2), 32–38.

Andya, J. D., Liu, J., & Shire, S. J. (2010). Analysis of irreversible aggregation, reversible self-association, and fragmentation of monoclonal antibodies by analytical ultracentrifugation. In S. J. Shire, W. G. Gombotz, K. Bechtold-Peters, & J. Andya (Eds.), *Current trends in monoclonal antibody development and manufacturing* (Vol. XI) (pp. 207–227). New York: AAPS Press/Springer.

Balestrieri, C., Colonna, G., Giovane, A., Irace, G., & Servillo, L. (1978). Second-derivative spectroscopy of proteins. A method for the quantitative determination of aromatic amino acids in proteins. *European Journal of Biochemistry*, *90*(3), 433–440.

Bewley, T. A. (1982). A novel procedure for determining protein concentrations from absorption spectra of enzyme digests. *Analytical Biochemistry*, *123*(1), 55–65.

Biemann, K. (1995). The coming of age of mass-spectrometry in peptide and protein chemistry. *Protein Science*, *4*(9), 1920–1927.

Bjellqvist, B., Ek, K., Righetti, P. G., Gianazza, E., Gorg, A., Westermeier, R., et al. (1982). Isoelectric-focusing in immobilized pH gradients – principle, methodology and some applications. *Journal of Biochemical and Biophysical Methods*, *6*(4), 317–339.

Borchert, S. J., Abe, A., Aldrich, D. S., Fox, L. E., Freeman, J. E., & White, R. D. (1986). Particulate matter in parenteral products: a review. *Journal of Parenteral Science and Technology*, *40*(5), 212–241.

Bourell, J. H., Clauser, K. P., Kelley, R., Carter, P., & Stults, J. T. (1994). Electrospray ionization mass spectrometry of recombinantly engineered antibody fragments. *Analytical Chemistry*, *66*(13), 2088–2095.

Boyd, D., Kaschak, T., & Yan, B. X. (2011). HIC resolution of an IgG1 with an oxidized trp in a complementarity determining region. *Journal of Chromatography B-Analytical Technologies in the Biomedical and Life Sciences*, *879*(13–14), 955–960.

Breen, E. D., Curley, J. G., Overcashier, D. E., Hsu, C. C., & Shire, S. J. (2001). Effect of moisture on the stability of a lyophilized humanized monoclonal antibody formulation. *Pharmaceutical Research*, *18*(9), 1345–1353.

Buchner, J., Renner, M., Lilie, H., Hinz, H. J., Jaenicke, R., Kiefhaber, T., et al. (1991). Alternatively folded states of an immunoglobulin. *Biochemistry*, *30*(28), 6922–6929.

Cacia, J., Keck, R., Presta, L. G., & Frenz, J. (1996). Isomerization of an aspartic acid residue in the complementarity-determining regions of a recombinant antibody to human IgE: identification and effect on binding affinity. *Biochemistry*, *35*(6), 1897–1903.

Cacia, J., Quan, C. P., Vasser, M., Sliwkowski, M. B., & Frenz, J. (1993). Protein sorting by high-performance liquid-chromatography. 1. Biomimetic interaction chromatography of recombinant human deoxyribonuclease-I on polyionic stationary phases. *Journal of Chromatography*, *634*(2), 229–239.

Carpenter, J. F., Randolph, T. W., Jiskoot, W., Crommelin, D. J. A., Middaugh, C. R., & Winter, G. (2010). Potential inaccurate quantitation and sizing of protein aggregates by size exclusion chromatography: essential need to use orthogonal methods to assure the quality of therapeutic protein products. *Journal of Pharmaceutical Sciences*, *99*(5), 2200–2208.

Chang, B. S., & Hershenson, S. (2002). Practical approaches to protein formulation development. *Pharmaceutical Biotechnology*, *13*, 1–25.

Chen, Y. H., Yang, J. T., & Chau, K. H. (1974). Determination of the helix and beta form of proteins in aqueous solution by circular dichroism. *Biochemistry*, *13*(16), 3350–3359.

Chowdhry, B. Z., & Cole, S. C. (1989). Differential Scanning Calorimetry: applications in Biotechnology. *Trends in Biotechnology*, *7*, 11–18.

Cipolla, D. C., & Shire, S. J. (1991). Analysis of oxidized human relaxin by reverse phase HPLC, mass-spectrometry and bioassays. In J. J. Villafranca (Ed.), *Techniques in protein chemistry II* (pp. 543–555). San Diego: Academic Press.

Costantino, H. R., Andya, J. D., Shire, S. J., & Hsu, C. C. (1997). Fourier-transform infrared spectroscopic analysis of the secondary structure of recombinant humanized immunoglobulin G. *Pharmaceutical Sciences*, *3*, 121–128.

Das, T. K. (2012). Protein particulate detection issues in biotherapeutics development—current status. *AAPS PharmSciTech*, *13*(2), 732–746.

Das, T. K., & Nema, S. (2008). Protein particulate issues in biologics development. *American Pharmaceutical Review*, *11*, 52–57.

Davidson, B., & Fasman, G. D. (1967). The conformational transitions of uncharged poly-L-lysine. Alpha helix-random coil-beta structure. *Biochemistry*, *6*(6), 1616–1629.

Day, E. S., Capili, A. D., Borysenko, C. W., Zafari, M., & Whitty, A. (2013). Determining the affinity and stoichiometry of interactions between unmodified proteins in solution using biacore. *Analytical Biochemistry*, *440*(1), 96–107.

Demeule, B., Messick, S., Shire, S. J., & Liu, J. (2010). Characterization of particles in protein solutions: reaching the limits of current technologies. *AAPS Journal*, *12*(4), 708–715.

Devos, A. M., Ultsch, M., & Kossiakoff, A. A. (1992). Human growth-hormone and extracellular domain of its receptor – crystal-structure of the complex. *Science*, *255*(5042), 306–312.

Donovan, J. W. (1973). Ultraviolet difference spectroscopy–new techniques and applications. *Methods in Enzymology*, *27*, 497–525.

Donovan, J., Rabel, F., & Zahran, J. (1991). Protein separations on tentacle ion exchangers. *American Biotechnology Laboratory*, *9*(5), 20–22.

Durant, J. A., Chen, C. Y., Laue, T. M., Moody, T. P., & Allison, S. A. (2002). Use of T4 lysozyme charge mutants to examine electrophoretic models. *Biophysical Chemistry*, *101*, 593–609.

Eftink, M. R. (1998). The use of fluorescence methods to monitor unfolding transitions in proteins. *Biochemistry-Moscow*, *63*(3), 276–284.

Englander, S. W., & Epstein, H. T. (1957). Optical methods for measuring nucleoprotein and nucleic acid concentrations. *Archives of Biochemistry and Biophysics*, *68*(1), 144–149.

Fei, D. T. W., Gross, M. C., Lofgren, J. L., Mora-Worms, M., & Chen, A. B. (1990). Cyclic AMP response to recombinant human relaxin by cultured human endometrial cells—a specific and high throughput in vitro bioassay. *Biochemical Biophysical Research Communications*, *170*, 214–222.

Ferraiolo, B. L., Cronin, M., Bakhit, C. R. M., Chesnut, M., & Lyon, R. (1989). The pharmacokinetics and pharmacodynamics of a human relaxin in the mouse pubic symphysis bioassay. *Endocrinology*, *125*, 2922–2926.

Frenz, J., Hancock, W. S., Henzel, W. J., & Horvath, C. S. (1990). Reversed phase chromatography in analytical biotechnology of proteins. In K. M. Gooding, & F. E. Regnier (Eds.), *HPLC of biological macromolecules* (pp. 145–177). New York: Dekker.

Fullmer, C. S., & Wasserman, R. H. (1979). High-performance liquid-chromatography (HPLC) – analytical peptide mapping and preparative separation of peptides for sequence-analysis. *Federation Proceedings*, *38*(3), 326.

Giddings, J. C. (1993). Field-flow fractionation: analysis of macromolecular, colloidal, and particulate materials. *Science*, *260*(5113), 1456–1465.

Giddings, J. C. (2000). The field-flow fractionation family: underlying principles. In M. E. Schimpf, K. D. Caldwell, & J. C. Giddings (Eds.), *Field flow fractionation handbook*. New York: Wiley.

Gill, P. S., Sauerbrunn, S. R., & Reading, M. (1993). Modulated differential scanning calorimetry. *Journal of Thermal Analysis*, *40*(3), 931–939.

Gray, R. A., Stern, A., Bewley, T. A., & Shire, S. J. (1995). *Rapid determination of spectrophotometric absorptivity by analytical ultracentrifugation*. Palo Alto: Beckman, Applications Information Note A-18157A.

Harding, S. E., Rowe, A. J., & Horton, J. C. (Eds.). (1992). *Analytical ultracentrifugation in biochemistry and polymer science*. Cambridge, England: The Royal Society of Chemistry.

Hodgson, J. (1994). Light, angles, action. *Bio-Technology*, *12*(1), 31.

Hunt, G., Hotaling, T., & Chen, A. B. (1998). Validation of a capillary isoelectric focusing method for the recombinant monoclonal antibody C2B8. *Journal of Chromatography A*, *800*(2), 355–367.

Hunt, G., Moorhouse, K. G., & Chen, A. B. (1996). Capillary isoelectric focusing and sodium dodecyl sulfate capillary gel electrophoresis of recombinant humanized monoclonal antibody HER2. *Journal of Chromatography A*, *744*(1–2), 295–301.

Hunt, G., & Nashabeh, W. (1999). Capillary electrophoresis sodium dodecyl sulfate nongel sieving analysis of a therapeutic recombinant monoclonal antibody: a biotechnology perspective. *Analytical Chemistry*, *71*(13), 2390–2397.

Jiskoot, W., Beuvery, E. C., Dekoning, A. A. M., Herron, J. N., & Crommelin, D. J. A. (1990). Analytical approaches to the study of monoclonal-antibody stability. *Pharmaceutical Research*, *7*(12), 1234–1241.

Jiskoot, W., Bloemendal, M., Vanhaeringen, B., Vangrondelle, R., Beuvery, E. C., Herron, J. N., et al. (1991). Nonrandom conformation of a mouse IgG2a monoclonal-antibody at low pH. *European Journal of Biochemistry*, *201*(1), 223–232.

Johnson, W. C. (1990). Protein secondary structure and circular-dichroism – a practical guide. *Proteins-Structure Function and Bioinformatics*, *7*(3), 205–214.

Jones, A. J. S. (1993). Analysis of polypeptides and proteins. *Advanced Drug Delivery Reviews*, *10*(1), 29–90.

Kohr, W. J., Keck, R., & Harkins, R. N. (1982). Characterization of intact and trypsin-digested biosynthetic human growth-hormone by high-pressure liquid-chromatography. *Analytical Biochemistry*, *122*(2), 348–359.

Lakowicz, J. R. (1984). *Principles of fluorescence spectroscopy*. New York: Plenum Press.

Lakowicz, J. R. (Ed.). (2002). *Topics in fluorescence spectroscopy-protein fluorescence*. New York: Kluwer Academic Publishers.

Lanucara, F., Holman, S. W., Gray, C. J., & Eyers, C. E. (2014). The power of ion mobility-mass spectrometry for structural characterization and the study of conformational dynamics. *Nature Chemistry*, *6*(4), 281–294.

Lin, J. N., Andrade, J. D., & Chang, I. N. (1989). The influence of adsorption of native and modified antibodies on their activity. *Journal of Immunological Methods*, *125*(1–2), 67–77.

Liu, J., Andya, J. D., & Shire, S. J. (2006). A critical review of analytical ultracentrifugation and field flow fractionation methods for measuring protein aggregation. *AAPS Journal*, *8*(3), E580–E589.

Liu, J., Zhu, Q., Shire, S. J., & Demeule, B. (2012). Assessing and improving asymmetric flow field flow fractionation of therapeutic proteins. In S. K. R. Williams, & K. D. Caldwell (Eds.), *Field-flow fractionation in biopolymer analysis*. Vienna: Springer-Verlag.

Lorber, B., Fischer, F., Bailly, M., Roy, H., & Kem, D. (2012). Protein analysis by dynamic light scattering: methods and techniques for students. *Biochemistry and Molecular Biology Education*, *40*, 372–382.

Lowe, J., Jardieu, P., VanGorp, K., & Fei, D. T. W. (1995). Allergen-induced histamine release in rat mast cells transfected with the a subunits of FceRI. *Journal of Immunological Methods*, *184*, 113–122.

Martenson, R. E. (1978). The use of gel filtration to follow conformational changes in proteins: conformational flexibility of bovine myelin basic protein. *The Journal of Biological Chemistry*, *253*(24), 8887–8893.

Marx, W., Simpson, M. E., & Evans, H. M. (1942). Bioassay of the growth hormone of the anterior pituitary. *Endocrinology*, *30*, 1–10.

Mehta, S. B., Bee, J. S., Randolph, T. W., & Carpenter, J. F. (2014). Partial unfolding of a monoclonal antibody: role of a single domain in driving protein aggregation. *Biochemistry*, *53*(20), 3367–3377.

Muller, W. (1990). New ion-exchangers for the chromatography of biopolymers. *Journal of Chromatography*, *510*, 133–140.

Norstrom, A., Bryman, I., Wiquist, N., Sahni, S., & Lindblom, B. (1984). Inhibiting action of relaxin on human cervical smooth muscle. *J. Clin. Endocrinol. Metab*, *59*, 379–382.

O'Shannessy, D. J. (1994). Determination of kinetic rate and equilibrium binding constants for macromolecular interactions: a critique of the surface plasmon resonance literature. *Current Opinion in Biotechnology*, *5*(1), 65–71.

Oganesyan, V., Damschroder, M. M., Leach, W., Wu, H., & Dall'Acqua, W. F. (2008). Structural characterization of a mutated, ADCC-enhanced human Fc fragment. *Molecular Immunology*, *45*(7), 1872–1882.

Olsson, M. H. M., Sondergaard, C. R., Rostkowski, M., & Jensen, J. H. (2011). PROPKA3: consistent treatment of internal and surface residues in empirical pKa predictions. *Journal of Chemical Theory and Computation*, *7*(2), 525–537.

Panchal, J., Kotarek, J., Marszal, E., & Topp, E. M. (2014). Analyzing subvisible particles in protein drug products: a comparison of dynamic light scattering (DLS) and resonant mass measurement (RMM). *AAPS Journal*, *16*(3), 440–451.

Papac, D. I., & Shahrokh, Z. (2001). Mass spectrometry innovations in drug discovery and development. *Pharmaceutical Research*, *18*(2), 131–145.

Patel, A. R., Lau, D., & Liu, J. (2012). Quantification and characterization of micrometer and submicrometer subvisible particles in protein therapeutics by use of a suspended microchannel resonator. *Analytical Chemistry*, *84*(15), 6833–6840.

Paul, M., Vieillard, V., Jaccoulet, E., & Astier, A. (2012). Long-term stability of diluted solutions of the monoclonal antibody rituximab. *International Journal of Pharmaceutics*, *436*(1–2), 282–290.

Pekar, A., & Sukumar, M. (2007). Quantitation of aggregates in therapeutic proteins using sedimentation velocity analytical ultracentrifugation: practical considerations that affect precision and accuracy. *Analytical Biochemistry*, *367*(2), 225–237.

Perczel, A., & Fasman, G. D. (1992). Quantitative-analysis of cyclic beta-turn models. *Protein Science*, *1*(3), 378–395.

Philo, J. S. (2009). A critical review of methods for size characterization of non-particulate protein aggregates. *Current Pharmaceutical Biotechnology*, *10*(4), 359–372.

Provencher, S. W., & Glockner, J. (1981). Estimation of globular protein secondary structure from circular-dichroism. *Biochemistry*, *20*(1), 33–37.

Queiroz, J. A., Tomaz, C. T., & Cabral, J. M. (2001). Hydrophobic interaction chromatography of proteins. *Journal of Biotechnology*, *87*(2), 143–159.

Rabel, S. R., & Stobaugh, J. F. (1993). Applications of capillary electrophoresis in pharmaceutical analysis. *Pharmaceutical Research*, *10*(2), 171–186.

Rambaldi, D. C., Reschiglian, P., & Zattoni, A. (2011). Flow field-flow fractionation: recent trends in protein analysis. *Analytical and Bioanalytical Chemistry*, *399*(4), 1439–1447.

Reubsaet, J. L. E., Beijnen, J. H., Bult, A., van Maanen, R. J., Marchal, J. A. D., & Underberg, W. J. M. (1998). Analytical techniques used to study the degradation of proteins and peptides: chemical instability. *Journal of Pharmaceutical and Biomedical Analysis*, *17*(6–7), 955–978.

Reubsaet, J. L. E., Beijnen, J. H., Bult, A., van Maanen, R. J., Marchal, J. A. D., & Underberg, W. J. R. (1998). Analytical techniques used to study the degradation of proteins and peptides: physical instability. *Journal of Pharmaceutical and Biomedical Analysis*, *17*(6–7), 979–984.

Ricker, R. D., & Sandoval, L. A. (1996). Fast, reproducible size-exclusion chromatography of biological macromolecules. *Journal of Chromatography A*, *743*(1), 43–50.

Ridgeway, T. M., Hayes, D. B., Moody, T. P., Wilson, T. J., Anderson, A. L., Lavasseur, J. H., et al. (1998). An apparatus for membrane-confined analytical electrophoresis. *Electrophoresis*, *19*(10), 1611–1619.

Righetti, P. G., & Drysdale, J. W. (1974). Isoelectric focusing in gels. *Journal of Chromatography*, *98*(2), 271–321.

Righetti, P. G., Gelfi, C., & Chiari, M. (1996). Isoelectric focusing in immobilized pH gradients. *Methods in Enzymology*, *270*, 235–255.

Schachman, H. K. (1959). *Ultracentrifugation in biochemistry*. New York: Academic Press.

Schachman, H. K. (1989). Analytical ultracentrifugation reborn. *Nature*, *341*(6239), 259–260.

Schuck, P. (2000). Size-distribution analysis of macromolecules by sedimentation velocity ultracentrifugation and lamm equation modeling. *Biophysical Journal*, *78*(3), 1606–1619.

Schuster, T. M. & Laue, T. M. (Eds.), (1994). Modern analytical ultracentrifugation. *Emerging biochemical and biophysical techniques*. Boston: Birkhauser.

Seino, S., Funakoshi, A., Fu, Z. Z., & Vinik, A. (1985). Identification of insulin variants in patients with hyperinsulinemia by reversed-phase, high-performance liquid-chromatography. *Diabetes*, *34*(1), 1–7.

Shire, S. J. (1983). pH-dependent polymerization of a human-leukocyte interferon produced by recombinant deoxyribonucleic-acid technology. *Biochemistry*, *22*(11), 2664–2671.

Shire, S. J. (1994). Analytical ultracentrifugation and its use in biotechnology. In T. M. Schuster, & T. M. Laue (Eds.), *Modern analytical ultracentrifugation* (pp. 261–291). Boston: Birrkhauser.

Shire, S. J., Holladay, L. A., & Rinderknecht, E. (1991). Self-association of human and porcine relaxin as assessed by analytical ultracentrifugation and circular-dichroism. *Biochemistry*, *30*(31), 7703–7711.

Shire, S. J., & Laue, T. (Eds.). (2010). *Methods for Detetcting and Characterizing Sub-Visible Particulates*. The AAPS Themed Issue, published on-line 2010.

Shire, S. J., Mckay, P., Leung, D. W., Cachianes, G. J., Jackson, E., Wood, W. I., et al. (1990). Preparation and properties of recombinant-DNA derived tobacco mosaic-virus coat protein. *Biochemistry*, *29*(21), 5119–5126.

Shire, S. J. (1996). Stability characterization and formulation development of recombinant human deoxyribonuclease I [Pulmozyme, (dornase alpha)]. In R. Pearlman, & J. Wang (Eds.), *Formulation, characterization and stability of protein drugs* (pp. 393–426). New York: Plenum Publishing.

Sukumar, M., Doyle, B. L., Combs, J. L., & Pekar, A. H. (2004). Opalescent appearance of an IgG1 antibody at high concentrations and its relationship to noncovalent association. *Pharmaceutical Research*, *21*(7), 1087–1093.

Tanford, C. (1962). The interpretation of hydrogen ion titration curves of proteins. *Advances in Protein Chemistry*, *17*, 69–165.

Tanford, C. (1980). *The hydrophobic effect: Formation of micelles and biological membranes*. USA: John Wiley & Sons.

Teller, D. C. (1973). Characterization of proteins by sedimentation equilibrium in the analytical ultracentrifuge. *Methods in Enzymology*, *27*, 346–441.

Trilling, A. K., Harmsen, M. M., Ruigrok, V. J. B., Zuilhof, H., & Beekwilder, J. (2013). The effect of uniform capture molecule orientation on biosensor sensitivity: dependence on analyte properties. *Biosensors and Bioelectronics*, *40*(1), 219–226.

Valliere-Douglass, J., Wallace, A., & Balland, A. (2008). Separation of populations of antibody variants by fine tuning of hydrophobic-interaction chromatography operating conditions. *Journal of Chromatography A*, *1214*(1–2), 81–89.

Vesterberg, O., & Svensson, H. (1966). Isoelectric fractionation, analysis, and characterization of ampholytes in natural pH gradients. IV. Further studies on the resolving power in connection with separation of myoglobins. *Acta Chemica Scandinavica*, *20*, 820–834.

Weitzhandler, M., Farnan, D., Horvath, J., Rohrer, J. S., Slingsby, R. W., Avdalovic, N., et al. (1998). Protein variant separations by cation-exchange chromatography on tentacle-type polymeric stationary phases. *Journal of Chromatography A*, *828*(1–2), 365–372.

Wen, J., Arakawa, T., & Philo, J. S. (1996). Size-exclusion chromatography with on-line light-scattering, absorbance, and refractive index detectors for studying proteins and their interactions. *Analytical Biochemistry*, *240*(2), 155–166.

Whitaker, J. R. (1963). Determination of molecular-weights of proteins by gel-filtration on sephadex. *Analytical Chemistry*, *12*, 1950–1953.

Williams, S. K. R., Runyon, J. R., & Ashames, A. A. (2011). Field-flow fractionation: addressing the nano challenge. *Analytical Chemistry*, *83*(3), 634–642.

Wu, S. L. (1992). Rapid Hplc and capillary electrophoresis – a perspective of protein-analysis from analytical biotechnology. *LC GC-Magazine of Separation Science*, *10*(6), 430.

Wuchner, K., Buchler, J., Spycher, R., Dalmonte, P., & Volkin, D. B. (2010). Development of a microflow digital imaging assay to characterize protein particulates during storage of a high concentration IgG1 monoclonal antibody formulation. *Journal of Pharmaceutical Sciences*, *99*(8), 3343–3361.

USP XXII (1990). *<788> particulate matter in injections*. 1596–1598.

Yang, J., Wang, X., Fuh, G., Yu, L., Wakshull, E., Khosraviani, M., et al. (2014). Comparison of binding characteristics and in vitro activities of three inhibitors of vascular endothelial growth factor A. *Molecular Pharmaceutics*, *11*, 3421–3430.

Yang, J., Wang, S., Liu, J., & Raghani, A. (2007). Determination of tryptophan oxidation of monoclonal antibody by reversed phase high performance liquid chromatography. *Journal of Chromatography A*, *1156*(1–2), 174–182.

Zimm, B. H. (1948). Development of Zimm's methods for analysis of angular dependence. *Journal of Chemical Physics*, *16*, 1093–1099.

Zolls, S., Weinbuch, D., Wiggenhorn, M., Winter, G., Friess, W., Jiskoot, W., et al. (2013). Flow imaging microscopy for protein particle analysis–a comparative evaluation of four different analytical instruments. *AAPS Journal*, *15*(4), 1200–1211.

Stability of monoclonal antibodies (mAbs)

3

Degradation routes in monoclonal antibodies

Many of the degradation reactions and routes that govern monoclonal antibody (mAb) stability are essentially the same as found in proteins. Some important differences between the general class of proteins and mAbs are due to the greater flexibility of mAbs related to the hinge region between Fab and Fc domains. An overall schematic of protein degradation routes shows that protein can degrade via alterations in physical as well as chemical attributes (Figure 3.1). Although chemical and physical degradation routes are often depicted as separate events they, in fact, can correlate in their impact on stability. As an example, chemical degradation routes can alter conformation, which in turn may result in formation of protein aggregates. Likewise a local conformational change may impact environments around chemically susceptible amino acid residues resulting in enhancement of degradation kinetics. There are many reviews on protein stability (Cleland, Powell, & Shire, 1993; Jaenicke, 2000; Manning, Chou, Murphy, Payne, & Katayama, 2010; Manning, Patel, & Borchardt, 1989; Oliyai, Schoneich, Wilson, & Borchart, 1992; Wang & Hanson, 1988) and a mini review on mAb stability (Wang, Singh, Zeng, King, & Nema, 2007). Here we summarize the main degradation routes for proteins, and specifically mAbs.

Chemical degradation

Chemical degradation involves alterations in amino acid residues, which are covalent in nature. The most common chemical degradation routes are oxidation, deamidation, Asp isomerization, and cross-linking. The chemical changes that occur may or may not impact the activity of the protein since it depends on the site of the chemical change. The alteration of a residue in an active site or binding pocket for ligand may result in a local change such as a conformational or charge change, which impacts the function of the specific site. Examples of such specific changes that result in loss of binding include an Asp isomerization in Xolair®, a mAb used for treatment of asthma (Cacia, Keck, Presta, & Frenz, 1996), and an Asn deamidation in Pulmozyme®, a protein used in the treatment of cystic fibrosis (Shire, 1996). A chemical change can also result in a change in function or activity due to aggregation promoted by an amino acid residue alteration, such as in loss of solubility and hence activity of human relaxin due to oxidation (Li, Nguyen, Schoneich, & Borchardt, 1995; Khossravi, Shire, & Borchardt, 2000).

Monoclonal Antibodies. http://dx.doi.org/10.1016/B978-0-08-100296-4.00003-8

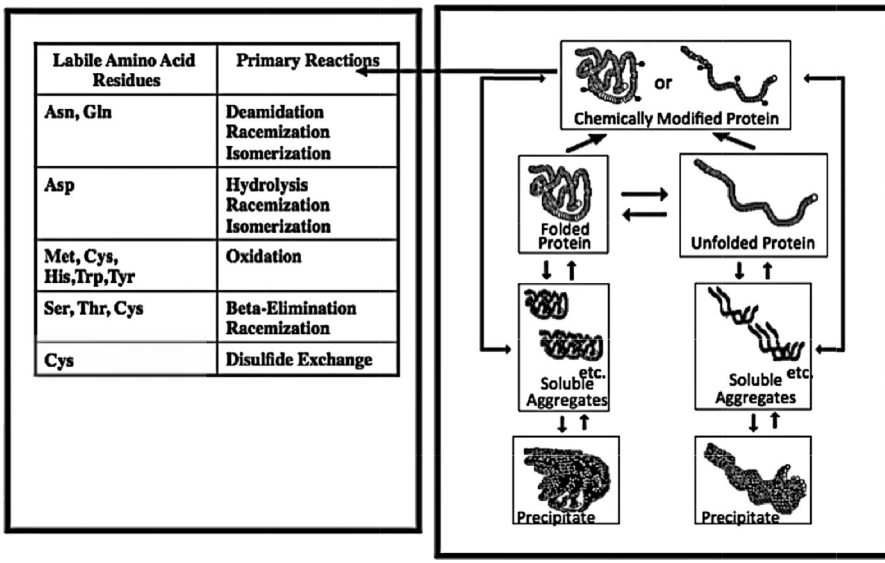

Figure 3.1 Schematic of chemical and physical protein degradation.

Deamidation and aspartic acid isomerization

Deamidation is a very common degradation route in proteins and is dependent on the amino acids that flank the amide residue. Initial studies by Robinson et al. using 42 pentapeptides of the form GlyXxxAsnXxxGly or GlyXxxGlnXxxGly show that in general Asn residues deamidate much more rapidly than Gln residues (Robinson, Scotchler, & McKerrow, 1973). It was also shown that a Gly residue nearest neighbor at the C-terminal side results in some of the fastest rates of reaction. Eventually these types of studies were expanded on by several researchers (Bhatt, Patel, & Borchardt, 1990; Oliyai & Borchardt, 1993; Patel & Borchardt 1990a, 1990b; Robinson & Robinson, 2001a; Tyler-Cross & Schirch, 1991) and some general rules regarding the impact of amino acid sequence evolved. In particular, Robinson and Robinson determined the deamidation rates for 306 Asn-containing peptides of the form GlyXxxAsnYyyGly at pH 7.4, 37.0 °C, 0.15 M Tris-HCl, and found first-order half-times that ranged from 1 day to 455 days (Robinson & Robinson, 2001a). From these studies it was apparent that deamidation rates increased with Ser or His as nearest neighbors and bulky side chains decreased deamidation rates. Moreover, the residue on the C-terminus side of the Asn residue had a greater effect than the residue on the N-terminus side. In general the increased size and branching of the amino acid on the C-terminus side resulted in ~70-fold lower rates compared with the AsnGly sequence. The key goal for these studies was to enable prediction of deamidation hot spots in a protein using the polypeptide sequence. Although sequence was an effective predictor for amides near the flexible end of the protein chain such as in cytochrome *C* and aldolase (McKerrow & Robinson, 1971; Robinson, McKerrow, & Legaz, 1974; Robinson & Robinson, 2004), it became apparent that primary structure

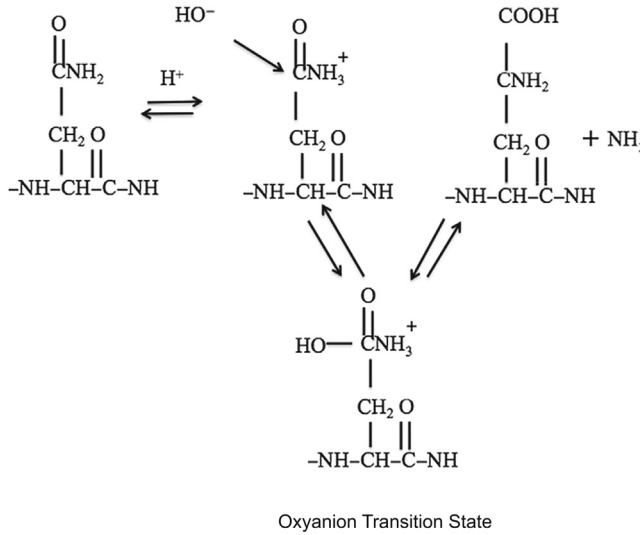

Figure 3.2 General acid and base catalysis of deamidation. The tetrahedral oxyanion intermediate is inferred to be the transition state. Stabilization of this structure by proton donors increases the rate of the deamidation reaction.

in itself was not an accurate predictor of sites of increased deamidation, and that protein conformation and flexibility were also determinants (Kossiakoff, 1988; Lura & Schirch, 1988; Robinson & Robinson, 2001b). An elucidation of the mechanisms for deamidation in proteins led to a further understanding on the role of primary, secondary, and tertiary protein structures.

Mechanism of deamidation

Deamidation of Asn and Gln residues is an acid–base-catalyzed reaction where the acid-catalyzed step involves protonation of the amide leaving group and the base-catalyzed reaction involves a nucleophilic attack of the amide carbonyl by hydroxide or a conjugate base. The transition state appears to be an oxyanion tetrahedral intermediate that can be stabilized by proton donors leading to increased rates of deamidation (Figure 3.2). Since deamidation is both acid- and base-catalyzed, one would expect a pH dependency of deamidation where there is a particular pH where the reaction rate is minimized (Scochler & Robinson, 1974; Wright, 1991a) as seen for the half-lives and deamidation rates for two Gln-containing pentapeptides (Figure 3.3). Some of the general rules for impact of amino acid sequence can be interpreted using this general acid/base-catalyzed mechanism (Wright, 1991a). Amino acid residues adjacent to the Asn or Gln residue, such as Thr or Ser, can function as general acid groups that provide a proton in the acid-catalyzed step. Other amino acids such as Asp, Glu, and His at neutral pH act as nucleophiles by attacking the amide carbonyl carbon. Amino acids such as Thr, Ser, and protonated Lys and Arg residues are proton donors that stabilize the oxyanion transition state, which accelerates the deamidation reaction.

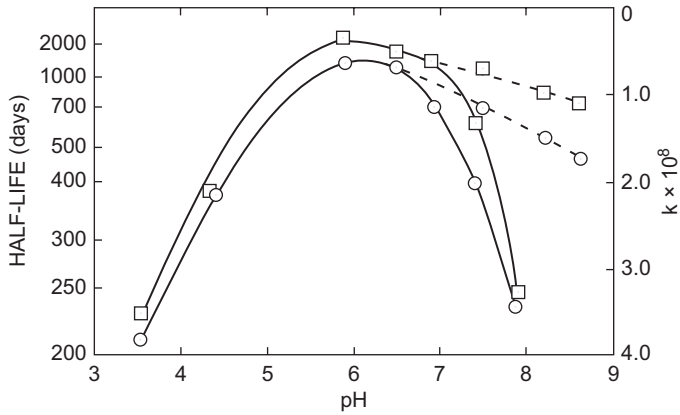

Figure 3.3 The half-lives and first-order rate constants of deamidation for GlyLeuGln AlaGly (□) and Gly ArgGlnAlaGly (○) as a function of pH.
Reproduced with permission from Scochler and Robinson (1974).

Although an understanding of the general acid–base mechanism could explain many of the observations based on amino acid sequence, there were many instances where using primary sequence leads to incorrect predictions of deamidation hotspots. This suggested that protein conformation and flexibility of the peptide chain can play an important role in dictating the rates that have been observed in proteins. The further elucidation of the deamidation mechanism involved the discovery that in addition to the direct deamidation of Asn and Gln, whereby ammonia was released, the deamidation could proceed via a succinimide intermediate where the α-amino group of the C-terminus carboxyl amino acid residue attacks the side chain carbonyl carbon of the adjacent Asn residue. The additional methylene group in the Gln side chain makes the formation of this intermediate more difficult. This mechanism has been extensively discussed (Capasso, Mazzarella, Sica, & Zagari, 1989; Capasso, Mazzerella, Sica, Zagari, & Salvadori, 1993; Capasso & Salvadori, 1999; Robinson & Robinson, 2004; Wright, 1991b) and the overall reaction is summarized in Figure 3.4. Depending on which of the carbonyl bonds hydrolyze the resulting deamidation leads to either an Asp residue or an isoAsp residue where the Asp side chain is incorporated into the polypeptide backbone resulting in an insertion of an additional methylene group in to the polypeptide backbone (Figure 3.4). The ratio of isoAsp to Asp has been found to usually be 3:1 (Capasso et al., 1989). At low pH the direct deamidation of Asn predominates with little succinimide intermediate observed as shown by the marked decrease in the observed isoAsp:Asp ratio (Meinwald, Stimson, & Scheraga, 1986). At neutral and basic conditions the deamidation usually occurs via the cyclic succinimide intermediate. At around pH 5 the intermediate may be stable and has been detected in various proteins (Teshima, Stults, Ling, & Canovadavis, 1991; Tomizawa, Yamada, Ueda, & Imoto, 1994; Violand et al., 1992). Although base catalysis still occurs at high pH, the increased rate of formation and subsequent hydrolysis of the imide usually obscures the accumulation of the imide intermediate. In addition to generation of

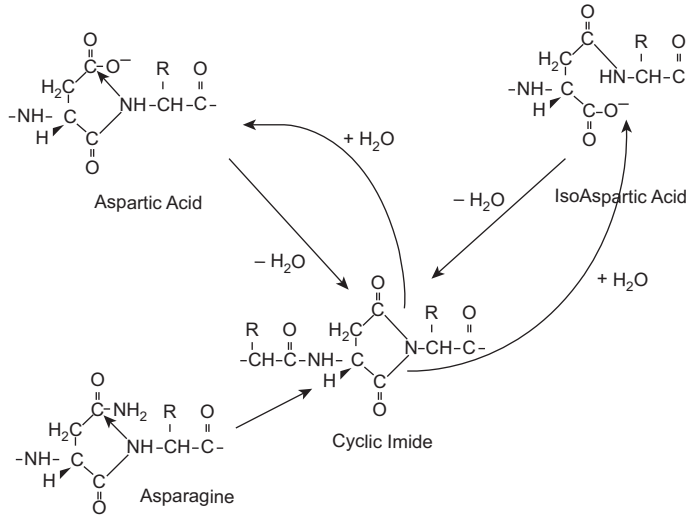

Figure 3.4 Formation of a cyclic imide as a result of nucleophilic attack by main chain amide nitrogen on the carboxyl carbon of either the side chain amide or carboxylic acid groups and formation of either Asp or isoAsp as a result of hydrolysis of either of the carbonyl nitrogen bonds in the cyclic imide.

Asp and isoAsp the cyclic imide mechanism also allows for racemization resulting in D and L isomers (Radkiewicz, Zipse, Clarke, & Houk, 1996).

The generation of a cyclic succinimide intermediate suggests that flexibility of the polypeptide as well as conformation of the polypeptide chain may impact the rate of deamidation and isomerization. As an example Clarke used crystal structures of proteins to examine if the stereochemistry may inhibit the cyclic imide formation. (Clarke, 1987). He concluded from his studies that there were restrictions of the polypeptide chain conformation such as exclusion of conformations with a ψ angle of 120° whereby the succinimide intermediate could not form, thus resulting in reduced deamidation and isomerization rates. Another way that conformation can impact deamidation rates is to bring distant residues (in terms of sequence) into close proximity to the deamidation/isomerization site where they may catalyze or decrease the deamidation reaction. As an example two closely related mAbs (mAb I and mAb II), which bound to the same target, showed different isomerization rates for two AspGly sites that are close to each other in sequence position (Wakankar et al., 2007; Figure 3.5(a)). It was shown that the differences in the Asp isomerization rates between the two mAbs could be attributed to structural factors including the conformational flexibility and the extent of solvent exposure of the labile Asp residue. Isomerization rates for the two mAbs as well as pentapeptide models, which included the labile Asp residues and their neighboring amino acid residues, are shown in Figure 3.5(b). Based on this pH-rate profile, the Asp isomerization rates in mAb I were faster than those in its peptide model VDYDG under neutral-to-basic conditions (pHs >6). This was attributed to residues that hydrogen bonded to the labile Asp, which could catalyze its reactivity to isomerization (Brennan & Clarke, 1993).

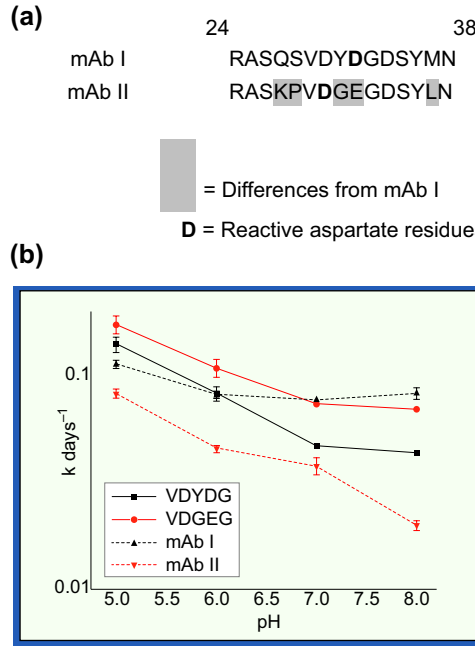

Figure 3.5 (a) The differences between the primary sequences of two closely related mAbs (mAbI and mAbII), (b) pH rate of Asp isomerization in two closely related mAbs and respective model peptides.
Adapted from Wakankar et al. (2007), kindly provided by A. Wakankar.

An X-ray crystal structure for mAb I Fab showed there was a Tyr residue located within H-bonding distance of the labile Asp residue due to the structural folding of the polypeptide chain. An H-bond-donating residue such as Tyr could potentially catalyze Asp reactivity, especially under pH conditions where the Asp is ionized, that is, at pH>pKa of the Asp (pH>4). The lack of a similar catalytic effect in the peptide model VDYDG could be attributed to the flexibility of the peptide which does not favor a stable H-bond formation between the Asp and the Tyr.

Deamidation and Asp isomerization in mAbs

As in most proteins deamidation of mAbs is prevalent, as has been reported in the literature (Chelius, Rehder, & Bondarenko, 2005; Daugherty & Mrsny, 2006; Gaza-Bulseco, Li, Bulseco, & Liu, 2008; Harris et al., 2001; Kroon, Baldwinferro, & Lalan, 1992; Liu, Gaza-Bulseco, Faldu, Chumsae, & Sun, 2008; Paborji, Pochopin, Coppola, & Bogardus, 1994; Timm, Gruber, Wasiliu, Lindhofer, & Chelius, 2010; Vlasak & Ionescu, 2008; Zheng & Janis, 2006). Isomerization also can occur, proceeding through the cyclic succinimide intermediate. The isomerization can occur at Asn sites where deamidation occurs or at Asp residues. Again there have been many literature reports on Asp isomerization in mAbs (Cacia et al., 1996; Harris et al., 2001; Huang, Li, Wroblewski, Beals, & Riggin, 2005; Liu et al., 2008; Pace, Wong, Zhang, Kao, & Wang, 2013; Sreedhara, Cordoba, Zhu, Kwong, & Liu, 2012; Vlasak & Ionescu, 2008; Wakankar et al., 2007; Zheng & Janis, 2006; Zhang, Yip, & Katta, 2011). Asp isomerization may have an impact on the activity of the mAb, especially if the degradation occurs in one of the

complementarity determining regions (CDRs) where binding to the target occurs. Examples of this are Herceptin® where an isomerization of Asp H102 in the CDR results in an 80–90% decrease in activity and an anti-IgE mAb where an isomerization of Asp L32 on one chain results in a decrease of 60% activity and on both chains a reduction in activity of 85% relative to the mAb with unaltered Asp residues.

Oxidation

Oxidation of proteins is the next most common degradation pathway where amino acid residues in proteins susceptible to oxidation include Met, Tyr, His, Trp, and Cys. Oxidation may be mediated by oxidants such as peroxides, exposure to light, metals, and ionizing radiation. Oxidation can also occur in the absence of oxidants, a process referred to as auto-oxidation. However, the direct reaction between ground-state molecular oxygen and proteins is extremely slow and does require the presence of catalysts. In particular, exposure to light and transition metal ions may accelerate the oxidation process and be the major factors responsible for apparent auto-oxidation.

As shown for deamidation/isomerization several factors such as solvent exposure, conformation, and primary sequence can impact the rate of oxidation for the same residue at different positions in the polypeptide chain. As an example, in human relaxin, a small protein pregnancy hormone closely related to human insulin, the rate of oxidation of the two Met residues in the B chain appears to be sequential where one Met oxidizes before the other during photooxidation (Cipolla & Shire, 1991). This was also shown for oxidation by hydrogen peroxide where the determined rate of oxidation at Met 25 was faster than at Met 4 (Nguyen, Burnier, & Meng, 1993). However, in the case of metal-catalyzed oxidation the rate of oxidation at Met 4 was faster than at Met 25 (Li et al., 1995). Inspection of the crystallographic structure for human relaxin shows that this observation may be explained by the close proximity of the Met 4 to potential metal-binding sites (Asp and Lys).

The oxidation of the different amino acid residues results in the generation of different species. The common degradation products include Met sulfoxide from Met, 2-oximidazoline, Asp and Asn from His, *N*-formyl kynurenine and kynurenine from Trp, Tyr–Tyr cross-links and DOPA from Tyr, and sulfenic acid, sulfinic acid, and disulfide scrambling from Cys (Li, Schoneich, et al., 1995a). Since the different susceptible residues yield different reaction products it is worthwhile to discuss mechanisms of oxidation for the different residues.

Mechanisms of oxidation

The various mechanisms for oxidation have been reviewed extensively (Berges, Trouillas, & Houee-Levin, 2011; Chu et al., 2004; Cleland et al., 1993; Hiller, Masloch, Gobl, & Asmus, 1981; Li, Schoneich, et al., 1995a; McDermott, Chiesa, Roberts, & Dillon, 1991; Pattison, Rahmanto, & Davies, 2012; Sharma, 2013; Sharma & Graham, 2010; Stadtman, 1990; Stadtman & Berlett, 1998; Stadtman & Levine, 2000; Swallow, 1960) and a brief summary of mechanism for each oxidizing residue in proteins follows.

Met oxidation

Formation of Met sulfoxide has frequently been observed in proteins and is the most common oxidation reaction in proteins. Generally three mediators of oxidation, chemical oxidants such as peroxides, light, and metals, convert Met to Met sulfoxide. The mechanism for chemically induced oxidation is believed to involve the transfer of oxygen from the oxidant peroxide via a nucleophilic substitution reaction where the sulfur on the Met residue interacts with the oxygen atom of the peroxide. This reaction, which is acid catalyzed, proceeds through an intermediate as shown in Figure 3.6(a). The formation of Met sulfoxide by exposure to light proceeds by interaction with singlet oxygen forming an unstable intermediate persulfoxide, which then oxidizes a second Met to form Met sulfoxide (Figure 3.6; Sysak, Foote, & Ching, 1977). Oxidation of Met by metals is very complex and involves catalysis by the metal ion to produce reactive oxygen species such as O_2^-, H_2O_2, $^1O_2$, and OH (Stadtman, 1990). Schöneich et al. identified the main reactive oxygen intermediates that were responsible for Met oxidation as peroxides at pH < 7 and other intermediates such as iron-bound hydroperoxide or site-specifically generated reactive oxygen species at pH > 7 (Li, Schoneich, et al., 1995b). The latter likely goes via a mechanism whereby the reactive oxygen species are formed near metal-binding sites on the protein and react with residues that are in close proximity. This observation is supported by the fact that oxygen radical scavengers have little effect on metal-catalyzed oxidation in proteins.

Met oxidation in mAbs

As in most proteins oxidation of Met in mAbs occurs frequently. In one of the first mAbs to be commercialized, OKT3 (an IgG_2), the major degradation route was oxidation of Met residues during storage at 5 °C (Kroon et al., 1992). Light exposure at 27 °C of another mAb, Herceptin®, formulated as a liquid, had oxidation at Met 255 and 431 in the Fc region after storage at 30 and 40 °C (Lam, Yang, & Cleland, 1997).

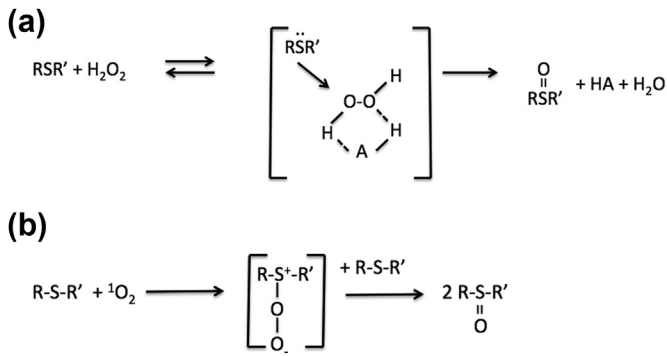

Figure 3.6 (a) Acid–base catalysis of Met to Met sulfoxide by hydrogen peroxide (HA = acid). (b) Photooxidation of Met to Met sulfoxide by singlet oxygen. Reproduced with permission from Li, Schoneich, and Borchardt (1995a).

The Fc region of IgGs is highly conserved with up to four conserved methionine residues (Edelman et al., 1969). Oxidation of Met residues in the Fc region has been reported in other IgG antibodies and may result in altered binding to proteins A and G, which is used in affinity columns for recovery by chromatography (Gaza-Bulseco, Faldu, Hurkmans, Chumsae, & Liu, 2008), and Fc γ and FcRn receptors (Bertolotti-Ciarlet et al., 2009). The latter may have consequences for the circulating half-time of the antibody which could affect potency (Wang et al., 2011). Met oxidation in the Fc region also can alter the conformation of the mAb as shown by destabilization of the native helical structure of residues 247–253 after hydrogen peroxide oxidation of Met residues (Burkitt, Domann, & O'Connor, 2010).

Histidine oxidation

Oxidation of His in peptides and proteins proceeds mainly by photooxidation and metal-catalyzed reactions. Asp and Asn can be formed as a result of exposure to light or metal catalysis. Studies of photooxidation suggest there is a formation of 2,5-endoperoxides through electrophilic addition of singlet oxygen to the electron-rich imidazole ring of histidine (Tomita, Irie, & Ukita, 1969). The resulting cycloperoxide ring may further degrade to produce hydroxyl compounds that subsequently form other intermediate compounds, which are eventually converted to aspartic acid and asparagine. It has been proposed that the metal-catalyzed reaction proceeds through an oxometallacyclic intermediate resulting in conversion to Asp and Asn residues (Uchida, 2003). Later studies showed that the metal-catalyzed reaction also resulted in generation of 2-oxo-His (Lewisch & Levine, 1995; Uchida, 2003). Oxidation of His to 2-oxo-histidine by a metal-catalyzed oxidation using ascorbate/Cu(II)/O_2 (Zhao et al., 1997) and metal-catalyzed photooxidation (Chang, Teshima, Milby, GilleceCastro, & CanovaDavis, 1997) was detected in human growth hormone (hGH), and several mechanistic pathways for formation of 2-oxo-His have been proposed (Schoneich, 2000).

An important concept that distinguishes metal-catalyzed reactions from chemically induced oxidation using oxidants such as hydrogen peroxide is "non-site-specific oxidation" versus "site-specific oxidation" as discussed by Borchardt and coworkers (Li, Schoneich et al., 1995a). Generally, in "non-site-specific" oxidation the accessibility of the oxidized amino acid residue dictates the speed of the reaction. As an example, in hGH the rate of oxidation of three Met residues by hydrogen peroxide appears to be directly correlated with their solvent accessibility (Houghten, Glaser, & Li, 1977; Teh et al., 1987). It was also suggested by Nguyen et al. that solvent exposure was responsible for the faster oxidation rate for Met B25 versus Met B4 in human relaxin (Nguyen et al., 1993). For metal-catalyzed reactions, especially for histidine, a "site-specific oxidation" occurs, where the close proximity of the oxidized amino acid residue to a metal-binding site can result in faster oxidation rates. Thus, for human relaxin greater solvent exposure of Met B25 compared to Met B4 results in faster oxidation by hydrogen peroxide (Nguyen et al., 1993), whereas the proximity of Met B4 to potential metal-binding sites resulted in faster oxidation rates for Met B4 compared to Met B25 (Li, Nguyen, et al., 1995). It was also observed that the sole His residue in relaxin undergoes a metal-catalyzed oxidation even though this residue is only partially accessible to solvent (~57% of the surface area is

exposed to solvent). This is not surprising, since His is known to have a high affinity for binding of metals. Interestingly, it was also observed that the ability of His to bind metals can affect the oxidation of other oxidizable residues in close proximity to the His residue whereby the His serves as an intramolecular catalyst (Li, Nguyen, et al., 1995).

His oxidation in mAbs

Although oxidation of His, primarily by metal-catalyzed oxidation, has been shown for several proteins and peptides (Chang et al., 1997; Ji, Zhang, Cheng, & Wang, 2009; Khossravi et al., 2000; Li, Nguyen, et al., 1995; Levine, 1983; Rippa & Pontremoli, 1968; Torosantucci et al., 2013; Uchida & Kawakishi, 1990; Yamagata, Takahashi, & Egami, 1962; Zhao et al., 1997), the literature is sparse on examples of oxidation of histidine in mAbs. Recently it was shown in the copper-catalyzed oxidation of an IgG2 mAb that His residues in the Fc portion of the antibody were oxidized (Luo et al., 2011), and it was suggested that this oxidation may be linked to the production of immunogenic aggregates (Joubert, Luo, Nashed-Samuel, Wypych, & Narhi, 2011). The potential impact of histidine oxidation on safety and physical properties has also been established in some of the studies of proteins. Specifically, the oxidation of histidine in human relaxin results in aggregation and precipitation (Li, Nguyen, et al., 1995; Khossravi et al., 2000), whereas for RNase T1 (Yamagata et al., 1962) and glutamine synthetase (Levine, 1983) it results in a loss of catalytic activity.

Trp oxidation

The oxidation of Trp occurs mainly after exposure to light and metal-catalyzed reactions resulting in the generation of a variety of oxidation products, including *N*-formal kynurenine, knyurenine, and hydroxy Trps (Dyer, Bringans, & Bryson, 2006; Figure 3.7(a)). A suggested mechanistic route is the interaction of singlet oxygen with the Trp indole group resulting in a dioxetane intermediate, which can thermally decompose to kynurenine and *N*-formyl kynurenine (Adam, Ahrweiler, Sauter, & Schmiedeskamp, 1993). The detection of some of these oxidation products in proteins is aided by the changes in the UV absorption spectrum (Kasson & Barry, 2012). In addition, generation of kynurenine and *N*-formyl kynurenine can result in yellow-colored solutions due to red shifts in the absorption spectrum (Figure 3.7(b)). Examples of Trp oxidation in proteins include human serum albumin, human erythrocyte superoxide dismutase (Dubinina et al., 2002), and bovine lens α-crystallin (Finley, Dillon, Crouch, & Schey, 1998). It has been suggested that the oxidation of Trp in α-crystallin leads to increased pigmentation of the lens in eyes due to the formation of *N*-formyl kynurenine and kynurenine (Finley et al., 1998; Pirie, 1971; Sen, Ueno, & Chakrabarti, 1992). Thus, Trp oxidation can lead to modification of proteins that impact function.

Trp oxidation in mAbs

There have been several reports of oxidation of Trp residues in mAbs (Hensel et al., 2011; Lam, Lai, Chan, Ling, & Hsu, 2011; Qi et al., 2009; Sreedhara et al., 2013; Wei

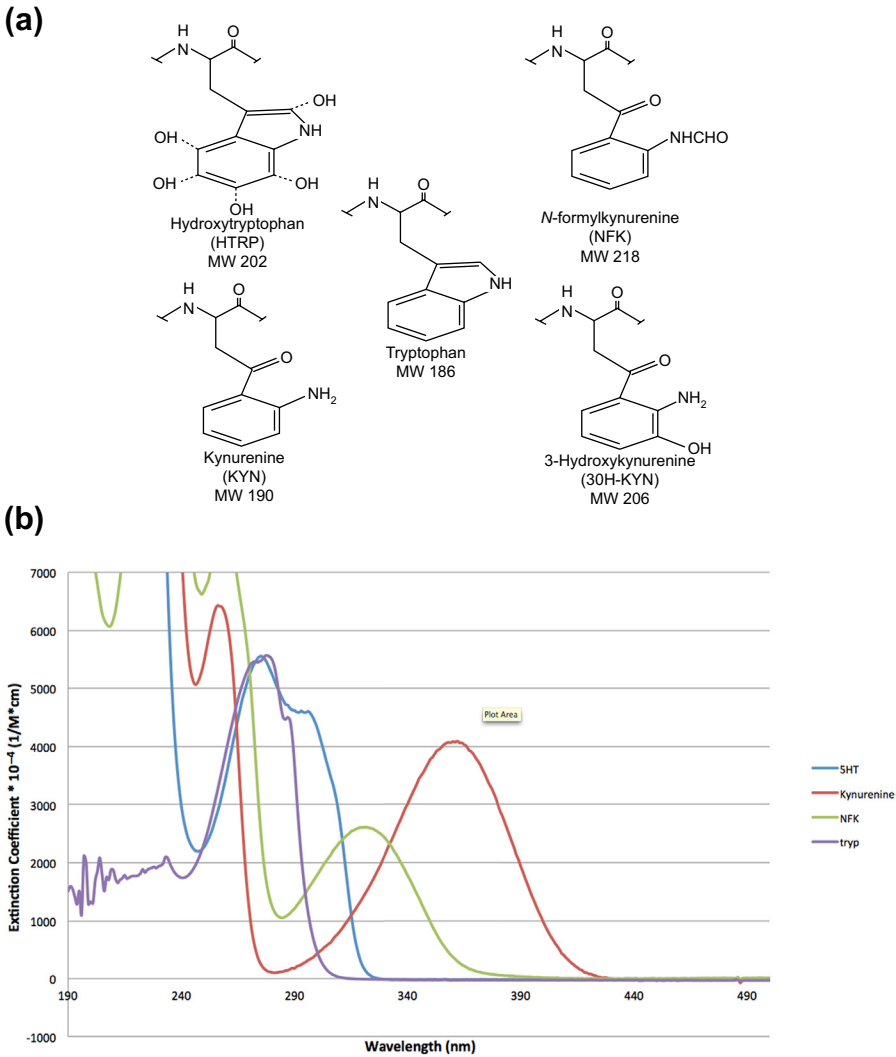

Figure 3.7 (a) The structures of Trp, hydroxyTrp, kynurenine, *N*-formyl kynurenine, and 3-hydroxy kynurenine (*Reproduced from Finley et al. (1998)*). (b) Absorption spectrum of the major oxidation products of Trp *(Kindly provided by Felix Jiang, Genentech)*.

et al., 2007; Wong, Strachan-Mills, & Burman, 2012). A single Trp residue in a solvent-exposed position of the heavy chain of one of the CDRs of palivizumab, a humanized IgG_1 mAb, oxidized when exposed to UV light irradiation. This particular Trp 105 was critical for the biological activity of this antibody (Wei et al., 2007). Recently it was shown that under real-time storage and elevated temperatures a solvent-exposed Trp (Trp 32) residue in the light chain of one of the CDRs of an IgG_1 was susceptible to oxidation (Hensel et al., 2011). *tert*-Butylhydroperoxide (TBHP) was used in order to

generate rapidly a sufficient amount of oxidized Trp in this mAb to develop a quantitative liquid chromatography–mass spectrometry method. Previous studies had shown that Met residues oxidized readily when exposed to TBHP, but not Trp residues. However, when the mAb was treated with TBHP for 3 months at 35 °C, it was shown that Trp 32 was oxidized. The extent of this oxidation was significantly higher than that of Met 107 and the heavy chain Met 429 (highly conserved in IgG_1 sequences) of Herceptin®, an IgG_1 mAb, both of which are very sensitive to chemical oxidation. TBHP oxidation of the Trp 32 also enabled studies of activity of the mAb. Real-time storage for 9 months at 4 °C and for 3 months at 35 °C resulted in ~3–8% Trp 32 oxidation, whereas treatment with TBHP for 7 days resulted in 13% Trp 32 oxidation. The oxidation of this Trp residue by TBHP led to a significant decrease (~68% of control) on the binding to the mAb target. It was also shown that this Trp residue occurs in the same sequence position in about 50% of the patented CDRs of IgG1s so the oxidation of this particular residue may be of significant interest when assessing stability of IgG1 mAbs. In another study, Trp was oxidized in a humanized Fab via an autocatalytic reaction of polysorbate 20 (PS20) in the formulation. PS20 is known to have peroxides depending on how the PS20 was stored (Lam et al., 2011). Formulation with PS20 containing increasing levels of peroxide resulted in a specific oxidation at Trp 50. Oxidation of Trp by peroxides does not occur readily but can be accelerated in the presence of metals, that is, a metal-catalyzed oxidation. Although high concentrations of H_2O_2 or TBHP did not oxidize the Trp, after adjusting the H_2O_2 concentration to 3000 ppm and adding 500 ppm ferric chloride there was detectable oxidation of the Trp residue. It was hypothesized that His 31, which is in close proximity to the Trp 50 in the tertiary structure, may serve as a localized binding site for metals which then catalyzes the oxidation of the Trp residue by generating free radicals from the H_2O_2. This hypnotized mechanism was supported by use of a mutant where the His 31 was replaced with Asn, which did not show any Trp oxidation.

Another recent publication focuses on the role of exposed Trps on the surface of antibodies that results in the generation of reactive oxygen species such as singlet oxygen and superoxides upon exposure to light (Sreedhara et al., 2013). In particular, antibodies are capable of catalyzing a water oxidation pathway termed the antibody-catalyzed water oxidation pathway (Wentworth et al., 2001), and surface-exposed Trps in the antibody during exposure to light catalyze this process (Figure 3.8(a)). This was confirmed by investigating a mutant where the surface-generated exposed Trp 53 is replaced with an Ala residue. This mutant results in a 50% reduction in H_2O_2, which strongly suggests the involvement of the Trp 53 in the catalytic reaction. Most importantly this example shows that in mAbs an exposed Trp residue not only undergoes an oxidation but can also help generate oxidative species, which can oxidize other non-Trp residues (Figure 3.8(b)). This interesting oxidation reaction mechanism is due to the mAbs' ability to generate H_2O_2 from molecular oxygen at much greater efficiency than nonimmunoglobulin proteins, and should be considered a potential oxidation degradation pathway in mAbs.

Tyr oxidation

Tyr oxidizes primarily by exposure to light and the main oxidation degradation for Tyr results in generation of 3,4-dihydroxyphenylalanine (DOPA) and dityrosine

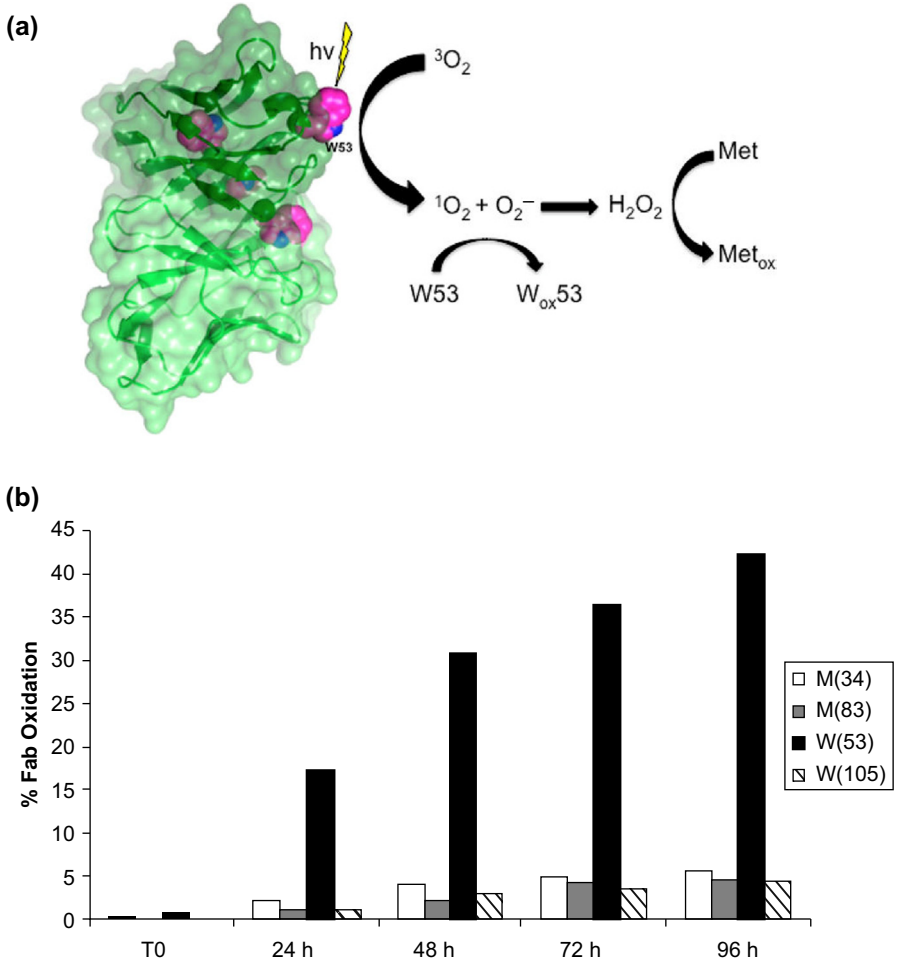

Figure 3.8 (a) Photooxidation of surface-exposed Trp in a mAb, which catalyzes the generation of H_2O_2. The H_2O_2 produced can in turn oxidize other susceptible residues such as Met. (b) Liquid chromatography–mass spectrometry/mass spectrometry tryptic peptide map analysis of a mAb at 50 mg/mL in formulation buffer exposed to light. Samples: 1 = T0; 2 = 24 h; 3 = 48 h; 4 = 72 h; and 5 = 96 h light exposure under ICH guidelines.
Reproduced from Sreedhara et al. (2013).

(Figure 3.9). Dityrosine was first described by Gross and Sizer after oxidation of Tyr with peroxidase and H_2O_2 (Gross & Sizer, 1959). There is evidence that an excited state complex can form between phenols and water (Creed, 1984), and that the tyrosyl radicals can form cross-links between polypeptide chains by generation of Dityrosine. Tyr photooxidation in most proteins is not as common as Trp mainly due to the greater absorbance of light energy by Trp than Tyr (the extinction coefficient of Trp is 45 times greater than Tyr at 290 nm). However, the extinction coefficient for the anionic ionized Tyr residues is greater at 290 nm than the nonionized

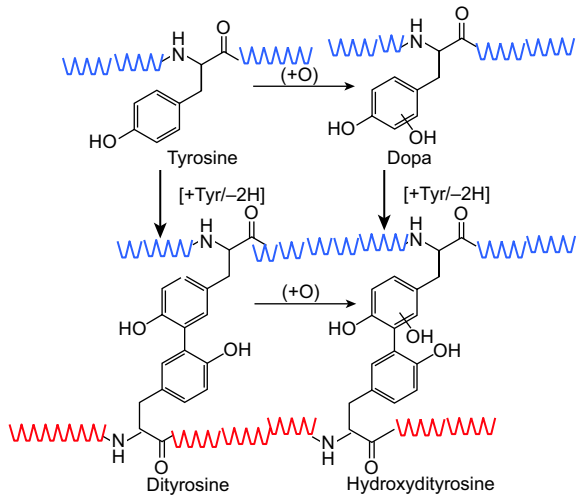

Figure 3.9 Main degradation products resulting from oxidation of Tyr. Blue and red helices represent the main polypeptide chains.

form and only half of that of Trp at 290 nm so that photooxidation of Tyr appears to proceed mainly by the ionized Tyr. Most Tyr residues have pKa values above 10, and since many therapeutic protein formulations are well below pH 10 the Tyr photooxidation is less common than other photosensitive amino acid residues. Thus, the rates of photooxidation in proteins are generally His > Trp > Met > Tyr (Matheson & Lee, 1979), and examples of Tyr oxidation of proteins are much more sparse than for the other susceptible amino acid residues. Tyr residues can also be oxidized with chemical oxidants or metal-catalyzed reactions. One example is the oxidation of Tyr in superoxide dismutase and human serum albumin via the well-known Fenton reaction where Fe^{2+} is oxidized to Fe^{3+} in the presence of H_2O_2 generating free radical $OH^{\cdot}$ (Dubinina et al., 2002). The subsequent one-electron oxidation of Tyr results in long-lived Tyr radicals, which can then form dityrosine cross-links that may disrupt secondary and tertiary structure of the proteins. In another study, several proteins (horseradish peroxidase, crystalline insulin, bovine pancreatic insulin, bovine serum albumin, and collagen) and L-tyrosine are shown to form dityrosine cross-links after oxidation with peroxidase and H_2O_2 at pH 9.5 (Aeschbach, Amado, & Neukom, 1976).

Tyr oxidation in mAbs

The literature has some examples of Tyr oxidation of proteins but there are few, if any, reports of oxidation of Tyr in mAbs. Although many of the product inserts for therapeutic mAbs state that exposure to light should be avoided, generally there are no data available that show whether Tyr residues are oxidized. This is not surprising since photooxidation proceeds mainly via the ionized Tyr, and as

stated previously Tyr pKa values are ~10, whereas mAbs are formulated at pH values <10.

Oxidation of Cys

Cys can be readily oxidized, where the main degradation products are mixed disulfides within one molecule, disulfide cross-links between molecules, and sulfenic, sulfinic, and cysteic acid (Figure 3.10(a); Li, Schoneich, et al., 1995a). Transition metals such as Cu^{2+} and Fe^{3+} can catalyze the formation of disulfide bonds (Stadtman, 1993; Figure 3.10(b)). As an example, human fibroblast growth factor (FGF-1) forms dimers as the result of intermolecular disulfides by copper-catalyzed oxidation (Engleka & Maciag, 1992). These metal-catalyzed reactions generally can occur without a neighboring thiol group. In the absence of transition metals the formation of new intramolecular or intermolecular disulfide bridges generally requires a nearby free thiol group that breaks apart the existing native disulfide bridge and then the free thiol can reoxidize to form the disulfide bridge (Figure 3.11(a) and (b)). Since this reaction requires a free thiol anion (pKa is ~9) an increase in the solution pH will result in an increase in formation of mixed disulfide. However, the pKa values for Cys can vary depending on the proximity of other ionizing groups in the tertiary structure. These interactions are primarily electrostatic in nature and since the ionization of these neighboring groups changes with the pH (Antosiewicz, McCammon, & Gilson, 1996; Yang, Gunner, Sampogna, Sharp, & Honig, 1993) the pKa values of the Cys residues will be a function of pH. As an example, the thiol pKa in papain for the active site Cys 25 has been estimated to be 4.1 at pH 6 and 8.4 at pH 9 (Shaked, Szajewski, & Whitesides, 1980). This observation suggests that at pH 6 there is a His residue with positive charge in close proximity to Cys 25, whereas at pH 9 the electrostatic interactions are dominated by close negatively charged residues such as Asp or Glu residues. The effects of local electrostatic environments on thiol pKa values and disulfide exchange have been discussed by Snyder, Cennerazzo, Karalis, and Field (1981). Ion pairing with His residues has also been proposed for the decrease in the Cys pKa values (Lo Bello et al., 1993; Mellor, Thomas, Topham, & Brocklehurst, 1993; Plou, 1996).

It is also possible to have disulfide shuffling without the presence of a free thiol. This was shown for studies on a protein, Thaumatin, isolated from the berry of a West African plant, that has eight disulfides but no free Cys residues. However, after heating at pH 7 above 70 °C aggregates were generated, which were shown to be the result of intermolecular disulfide bridging. This was ascribed to a β-elimination reaction whereby Cys was generated from disulfide bonds (Kaneko & Kitabatake, 1999). This reaction summarized in Figure 3.12 leads to generation of a persulfide and dehydroalanine, and a free thiol that can be formed from the persulfide (Florence, 1980).

Oxidation of the Cys residue in proteins does not necessarily result in disulfide exchange as shown in the case of α1-antitrypsin inhibitor (Griffiths, King, & Cooney, 2002) where nonreducing SDS PAGE did not show the presence of any disulfide cross-links after oxidation for 20 min at pH 10 by 0.2 mM H_2O_2. The resulting oxidation product in this case was sulfenic acid. As previously discussed a free thiolate anion is usually required to generate mixed disulfide and this would be expected to be the case at pH 10, especially since

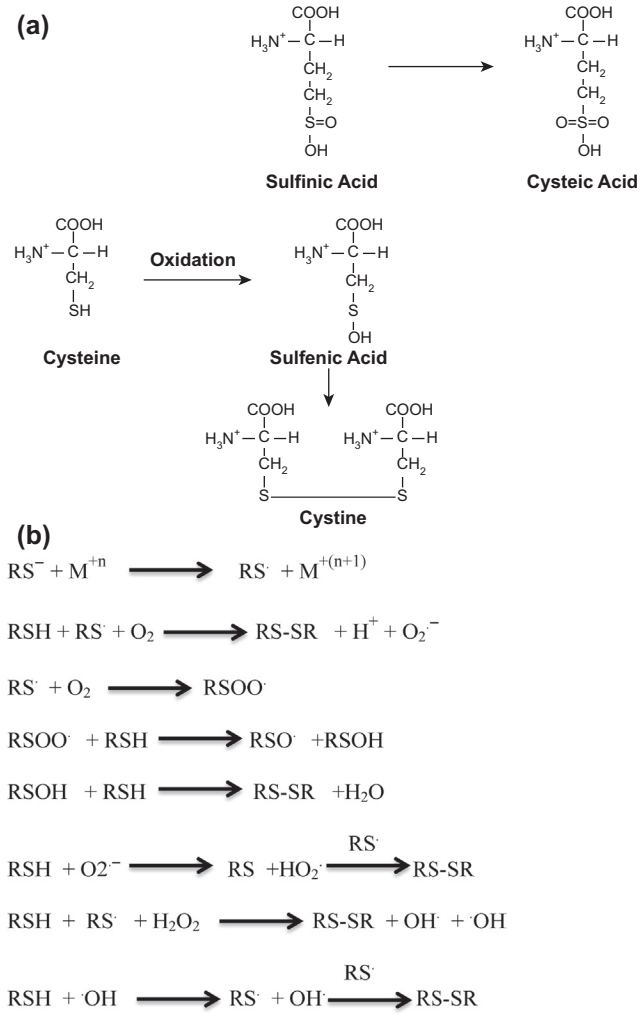

Figure 3.10 (a) Generation of disulfide cross-links (cysteine), sulfenic, sulfonic, and cysteic acids from H_2O_2 oxidation of Cys. (b) Proposed mechanism for metal-catalyzed oxidation of Cys.
Reproduced from Li, Schoneich, and Borchardt (1995a).

the pKa for the Cys residue appears to be decreased substantially, mainly by electrostatic interactions with surrounding Lys residues (Griffiths et al., 2002).

Cys oxidation and mixed disulfides in mAbs

Intermolecular disulfide cross-linking has been shown to occur in several mAbs. At first glance this is surprising since a free Cys residue is generally required for formation of mixed disulfides, and all Cys residues in a mAb are paired (Figure 1.2 (c)) so that there should not be any free thiol. However, it has been shown that recombinantly produced

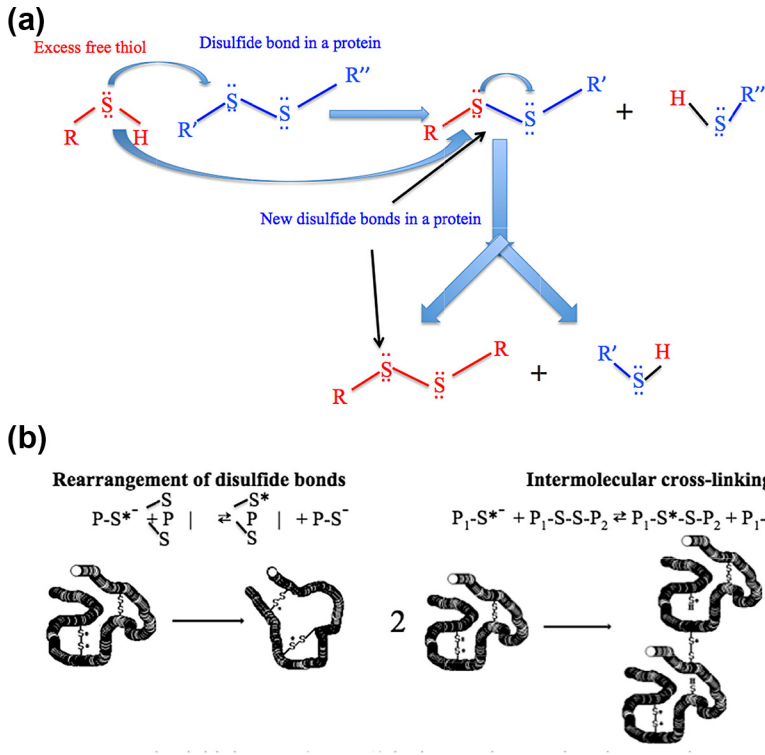

Figure 3.11 (a) Generation of new disulfide bonds in the presence of free thiol. (b) Altered intramolecular and intermolecular disulfides in a protein as a result of disulfide reduction and reoxidation.

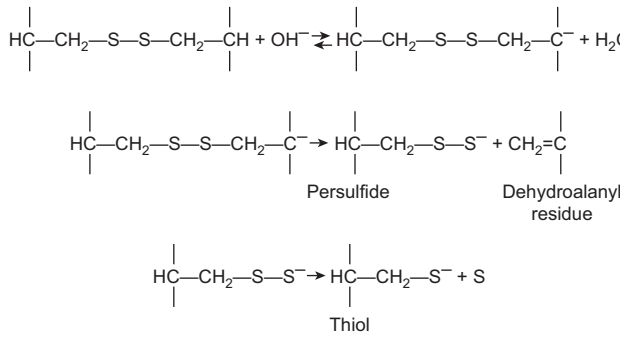

Figure 3.12 Generation of a free thiol from a β-elimination reaction of a disulfide bond. From Florence (1980).

mAbs often have a small amount of unpaired Cys residues (Zhang & Czupryn, 2002; Zhang et al., 2012), and thus there may be sufficient free thiol that participates in the mixed disulfide formation. During formulation development for an antifibrin monoclonal antibody the percent dimer formation increased as a function of pH suggesting the

formation of disulfide cross-links since there would be an increased amount of ionized thiol at the higher pH values (Kamat, Tolman, & Brown, 1996). A mAb that was freeze-dried without any lyoprotectants had about 35% aggregate after storage as a freeze-dried preparation for 1 year at 30 °C (Andya, Hsu, & Shire, 2003). Separation of the aggregates by sizing chromatography and determination of weight average molecular weights with an online light scattering detector resulted in determined molecular weights consistent with monomers, dimers, and trimers (Figure 3.13(a)). Reduced versus nonreduced sodium dodecyl sulfate polyacrylamide gel electrophoresis (SDS PAGE) conclusively proved that these aggregates were the result of formation of intermolecular disulfide bonds (Figure 3.13(b)). In another study, spray drying of an anti-IgE IgG1 mAb resulted in formation of disulfide cross-links (Andya et al., 1999). Often solid-state formulations using drying technology such as freeze-drying or spray drying without sufficient protective excipients can result in disulfide exchange since the average distance between the mAbs is greatly reduced compared to aqueous formulations. Since the reaction requires two Cys residues the rate of disulfide formation generally is inversely related to the distance between the residues. It has been demonstrated that the oxidation of Cys to cystine (disulfide link) decreases as the distance between the residues increases (Barron, Miller, & Kalnitsky, 1947; Overberger & Ferraro, 1962).

Nonenzymatic peptide fragmentation

The peptide bond generally is very stable requiring highly acidic conditions and high temperature to fragment. Under mild acidic conditions, where Asp residues are not ionized, cleavage of the Asp peptide bonds occurs at ~100× the rate of other peptide bonds (Schultz, 1967), and occurs more frequently at Asp–Gly and Asp–Pro sites in proteins (Powell, 1996). Possible pathways for cleavage at Asp peptide bonds have been proposed (Inglis, 1983). It has also been reported that fragmentation at Asn and Asp occurs through the succinimide intermediate that is formed during deamidation of proteins (Geiger & Clarke, 1987; Klotz & Thomas, 1993; Voorter, Dehaardhoekman, Vandenoetelaar, Bloemendal, & Dejong, 1988). The cleavage of peptide chains at an Asp residue via a succinimide intermediate has been studied using theoretical computations (Catak, Monard, Aviyente, & Ruiz-Lopez, 2008). Although deamidation of the Asn predominates cleavage at Asp sites, it was proposed that if deamidation via the succinimide intermediate is prevented by protein tertiary structure, fragmentation may be a competing pathway. It was also shown that the activation barrier for cleavage at Asp residues is ~10 kcal/mol lower than for Asn, suggesting that fragmentation usually occurs after the Asn residue has deamidated into an Asp residue. Based on the theoretical computations a mechanism for fragmentation at Asp through a succinimide intermediate was proposed (Figure 3.14).

Fragmentation in mAbs

Fragmentation of peptide chains has been reported for several mAbs. Fragments were observed after an antibody against human cytomegalovirus was stored for 14 days at 37 °C at pH 4 and pH 10. These fragments were detected using reducing and

(a)

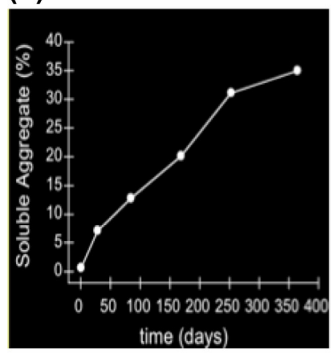

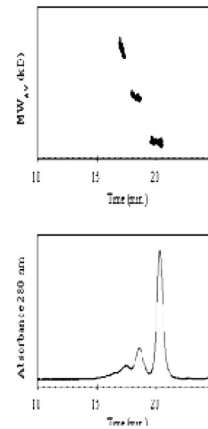

Formulation	SEC Peak[†]	MW_{AV}[†] (kd)	Identification[‡]
Excipient-free	1	151 ± 20	Monomer
	2	297 ± 33	Dimer
	3	469 ± 49	Trimer

(b)

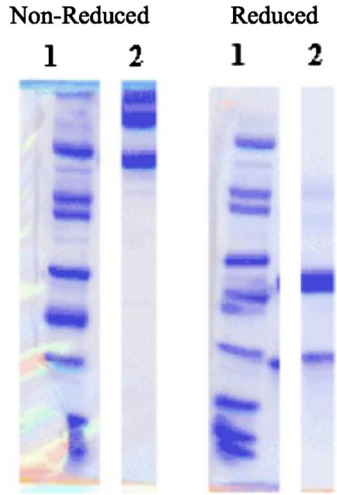

Figure 3.13 (a) Pseudo first-order reaction kinetics for formation of aggregate in freeze-dried mAb (left panel). Size exclusion chromatograph (SEC) after storage at 30 °C for 1 year (lower right panel). Online weight average molecular weight (MW) using light scattering detection (upper right panel) and lower table. (b) Nonreduced and reduced SDS PAGE (using β-mercaptoethanol). Lane 1: MW standards; lane 2: mAb freeze-dried without excipients after 1 year at 30 °C.

Adapted from Andya, Hsu, and Shire (2003).

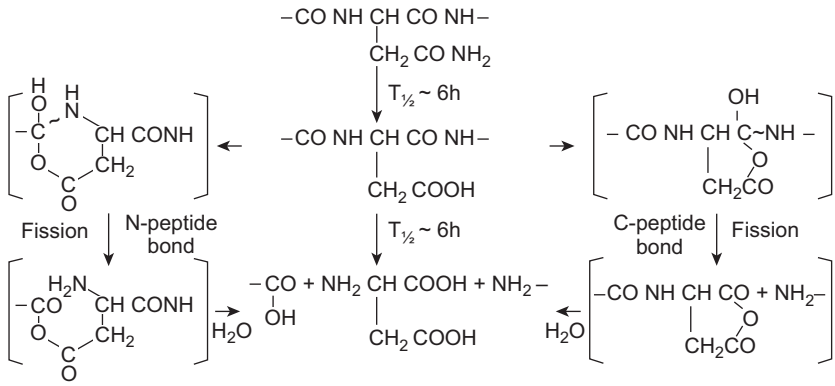

Figure 3.14 Possible pathways for cleavage of peptide bonds at Asp sites. Reproduced from Inglis (1983).

nonreducing SDS PAGE, but no further characterization of the fragments was reported (Usami, Ohtsu, Takahama, & Fujii, 1996). Thermal stress (4 days at 60 °C at pH 7) also resulted in generation of fragments in a mouse chimera mAb (Paborji et al., 1994). In another study after storage for 166 h at pH 8.5 at 60 °C fragments were observed in a murine chimera mAb by matrix-assisted laser desorption measurements (Alexander & Hughes, 1995). Mass characterization suggested that the fragments consisted of a mAb missing one light chain, a mAb with only one Fab arm, and separate light and heavy chains. This observation shows that mAb fragmentation can result from the disruption of disulfide bonds in the mAbs. In addition to these types of fragments, species with lower mass than common antibody domains were also observed, indicating that peptide bond cleavage also occurred (Alexander & Hughes, 1995). The generation of mAb fragments after storage at elevated temperatures often results in generation of fragments. Additional examples include a study on a murine mAb at 37 °C storage where Fab-sized fragments were observed (Jiskoot, Beuvery, Dekoning, Herron, & Crommelin, 1990), and fragmentation of a humanized mAb (subtype not specified) was shown to be dependent on pH as well as temperature of storage (Zheng & Janis, 2006).

Fragmentation into isolated mAb domains may also result from cleavage of peptide bonds near the hinge region. The hinge region in IgG1 mAbs has considerable flexibility (Jefferis & Lund, 2002; Oda, 2004) that may be susceptible to cleavage at higher temperature of storage. As an example, incubation of four humanized IgG1s at pH 5.2 for 1 month at 40 °C resulted in generation of small amounts of fragment detected by sizing chromatography (Cordoba, Shyong, Breen, & Harris, 2005; Figure 3.15), and these were identified as a mAb with one Fab and a Fab fragment by electrospray mass spectroscopy. A summary of the cleavage sites, all near the flexible hinge region of the IgG1 mAbs, is given in Table 3.1. The fragmentation at these sites near the hinge region may be due to kinetic processes where the activation energy for hydrolytic fragmentation is lowered. Moreover, these sites are adjacent to Asp and His residues, and it has been hypothesized that this results in a local environment that is more acidic or basic accelerating hydrolysis at those sites (Cordoba et al., 2005).

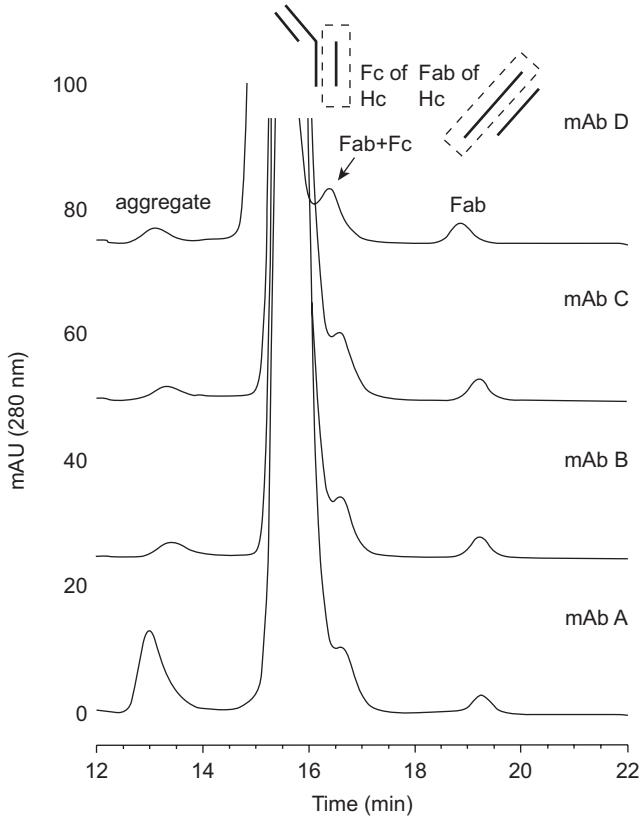

Figure 3.15 Size exclusion chromatography of four humanized IgG1 mAbs after incubation at pH 5.2 for 1 month at 40 °C.
From Cordoba et al. (2005).

An alternative mechanism may involve contaminating host cell proteases, which cleave at accelerated rates at higher temperature. Using a variety of protease inhibitors no change in fragmentation was detected at higher temperature suggesting that a nonenzymatic process was responsible for the fragmentation (Cordoba et al., 2005).

Another common fragmentation in mAbs occurs at the C-terminus of the heavy chains where C-terminus Lys and Arg residues are clipped. Examples include a chimeric IgG1 mAb (Harris, 1995), Herceptin® (Harris et al., 2001), and an anti-IgE mAb (Cacia et al., 1996). This particular degradation route generally occurs during the expression of the mAb in the host cell, usually Chinese hamster ovary (CHO) cells, and has been ascribed to carboxypeptidases from the host cell (Harris, 1995). Generally not all the mAb molecules have the C-terminal Lys or Arg removed, thus contributing to the heterogeneity of a mAb drug substance. This is not considered a safety or regulatory concern since plasma-derived proteins are often similarly processed.

Table 3.1 Electrospray fragments of mAb B (Figure 3.8) collected from size exclusion chromatography

Residues[a]	Expected mass	Observed mass	Cleavage site
HC: 1–222	23,619.5	23,617.3	Ser–Cys
HC: 1–223	23,722.6	23,721.0	Cys–Asp
HC: 1–224 (−18 Da)	23,837.7	23,818.1	Asp–Lys
HC: 1–224	23,837.7	23,836.5	Asp–Lys
HC: 1–225	23,965.9	23,964.6	Lys–Thr
HC: 1–227	24,204.1	24,203.1	His–Thr
HC:228–449 w/G0	26,415.7	26,414.6	His–Thr
HC:227–449 w/G0	26,552.9	26,556.5	Thr–His
HC:225–449 w/G0	26,782.2	26,782.0	Asp–Lys
HC:225–449 w/G1	26,944.2	26,942.1	Asp–Lys
HC:225–449 w/G2	27,106.2	27,105.9	Asp–Lys
HC:224–449 w/G0	26,897.2	26,897.0	Cys–Asp
HC:224–449 w/G1	27,059.3	27,059.2	Cys–Asp

[a]G0, G1, and G2 refer to Fc oligosaccharides with 0, 1, or 2 galactose residues, respectively.
From Cordoba et al. (2005)

Nonreducible cross-linking in mAbs

The most common types of cross-linking in mAbs are disulfide bonds and dityrosine formation, both as a result of oxidation. The disulfide bonds can usually be broken by use of reductants such as β-mercaptoethanol, whereas the dityrosine cross-links tend to be nonreducible. Other nonreducible cross-links have been observed. Usami et al. observed nonreducible SDS PAGE bands above the light chains in a human mAb that formed after incubation at pH 4 or 10 for 14 days at 37 °C (Usami et al., 1996). Jiskoot et al. detected a nonreducible SDS PAGE band at 88 kDa in two murine mAbs after incubation at pH 10 for 32 days at 37 °C (Jiskoot et al., 1990). A major nonreducible SDS PAGE band at 88 kDa was also observed after incubation at ~37 °C of the mAb OKT3 in phosphate-buffered saline with polysorbate 80 at pH 7. This band was also detected following incubation for 3 years at 5 °C. Peptide mapping showed that the cross-links were between heavy and light chains specifically between L46-52 and H99-121 (Kroon et al., 1992). No further characterization was done so the exact chemical mechanism for formation on the nonreducible cross-links was not determined. However, it appeared likely due to an oxidative degradation pathway since samples incubated with an argon overlay or that contained thiosulfate resulted in a delay of formation of the 88 kDa band (Rao & Kroon, 1993). A nonreducible species was detected by reducing SDS PAGE and reducing capillary electrophoresis in several humanized mAbs and found to be the result of a thioether bond between Cys 223 of the heavy chain and the C-terminal Cys residue of the light chain (Tous et al., 2005; Figure 3.16). This bond was found in samples before incubation at high temperature, and increased with duration of incubation at 40 °C, approximately 14% for 40 °C storage versus 0.4% at 5 °C

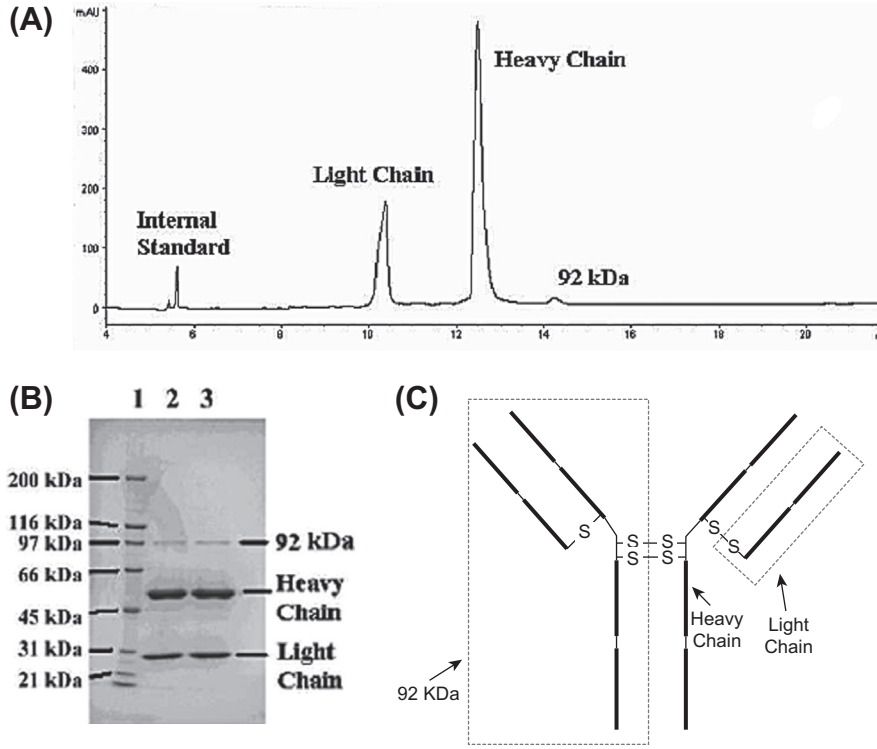

Figure 3.16 Generation of a 92 kDa thioester cross-link between the heavy and light chain in a humanized mAb. (A) Reducing capillary gel electrophoresis, (B) SDS PAGE, lane 1—molecular weight standards, lanes 2 and 3 reduced. (C) Schematic of the heavy chain, light chain, and 92 kDa cross-linked species.
Reproduced from Tous et al. (2005).

storage. Nonreducible thioether cross-links were also observed in several antibodies by size exclusion chromatography coupled with a mass spectrometer detector (Liu, Gaza-Bulseco, & Chumsae, 2009). It has been proposed that the β-elimination mechanism for a disulfide bond creates a cross-link of Cys with dehydroalanine that leads to the generation of a thioester linkage (Galande, Trent, & Spatola, 2003; Liu & May, 2012).

Physical degradation

Many chemical degradation pathways can lead to physical alterations of a protein and this has been discussed in the previous section. Here we consider physical degradation that is not driven by covalent modifications of primary structure. There are essentially three areas of interest: conformational changes, aggregation, and surface adsorption. This will now be discussed in general for protein biotherapeutics with an emphasis on mAbs.

Conformational changes, that is, protein denaturation

Proteins in general have what is referred to as "higher order structure." The amino acid sequence is termed the primary structure, and the polypeptide chain can fold into segments that are helical, β sheet, and random coil, termed secondary structure. The topological folding of the secondary structure into an organized folded structure is referred to as tertiary structure, and the spatial orientation of single folded polypeptide chains is the quaternary structure. An overall drawing showing these levels of structure for a protein is shown in Figure 3.17. Denaturation or unfolding of proteins has been

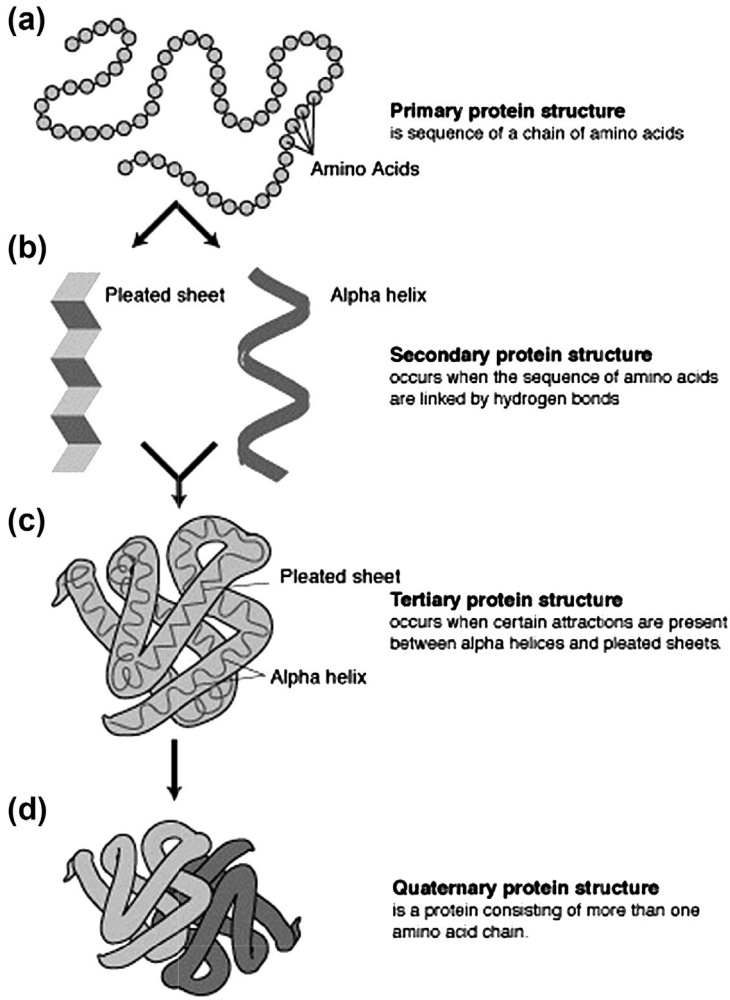

Figure 3.17 Levels of structural organization in proteins: (a) primary structure, (b) secondary structure showing α helix and β sheet structures, (c) tertiary structure (folding of the polypeptide chains with secondary structure into an organized spatial structure), and (d) quaternary, association of different tertiary structures.

Courtesy of the National Genome Research Institute as part of the public domain.

well discussed in the literature (Chan & Dill, 1993; Cleland, 1993, Dill, Chan, & Yue, 1995; Dill, Ozkan, Shell, & Weikl, 2008; Dill, Ozkan, Weikl, Chodera, & Voelz, 2007; Dill & MacCallum, 2012). Early investigations based on unfolding of small globular proteins, such as RNase, led to the development of two-state models for protein unfolding. The early classic experiments by Anfinsen (for which he was awarded a Nobel Prize) on RNase showed that when solution conditions were changed that favored the unfolded state the protein lost its overall structure, but could be refolded after changing solution conditions back to initial conditions (Anfinsen, 1973). These studies led to the conclusion that all the information for maintaining the structure/conformation of the protein resided in the amino acid sequence, known as primary structure. Although the two-state model could account for the concerted unfolding process as monitored by spectroscopy such as circular dichroism, later kinetic measurements of the process suggested that there were intermediates present (Tsong, Baldwin, & Elson, 1971).

Solution variables that may determine conformational stability include temperature changes, shear forces, ice formation as a result of freezing and thawing, changes in ionic strength, and changes in protein–solvent interactions. Recent work investigating the response of mAb to typical shear forces encountered during processing suggests that shear forces are less of a contributor to protein/mAb aggregation (Bee et al., 2009).

Although most proteins undergo unfolding at temperatures below 70 °C, mAbs in general do not unfold completely until the temperature exceeds 70 °C. The unfolding process can be monitored by spectroscopic assays, such as fluorescence, UV absorption, circular dichroism, and Fourier transform infrared (FTIR) spectroscopy.

A nice example of the impact of processing conditions on protein conformation is the process of creating a sustained delivery formulation for recombinant human growth hormone (rhGH). In this process polymer microspheres containing rhGH were created by spray freeze-drying rhGH formulated with or without Zn in an organic solvent that contains poly(lactic-*co*-glycolic acid) copolymer (Johnson et al., 1996). Addition of Zn generates precipitates of rhGH and it was found that the precipitation did not alter rhGH secondary structure (Yang et al., 2000). However, after extraction from the microspheres it was shown that without Zn addition the rhGH underwent conformational changes as assessed by FTIR measurements, whereas precipitation of rhGH with Zn resulted in protection of the protein conformation (Yang et al., 1999). Apparently the exposure to organic solvents in the process perturbed the rhGH secondary structure, and generation of precipitates with Zn prior to the microencapsulation prevented the solvent-induced conformational change.

As previously discussed, one distinguishing feature of IgG1 mAbs is the large amount of flexibility in the hinge region, which connects up the two Fab domains with the Fc domain. Conformational changes in the hinge region could conceivably impact the flexibility of the mAb which may impact the binding to the antigen target. This appears to be the case in a study by Taschner et al. (2001) where a mAb (subtype not mentioned) lost its ability to bind to a targeted carbohydrate on a cancer cell after freeze-drying. Standard biochemical assays, such as SDS PAGE, gel sizing chromatography, and capillary zone electrophoresis, did not show any alterations compared to mAb before freeze-drying. Scanning transmission electron microscopy was used to compute the distribution of angles between Fab domains of the mAb before and after lyophilization. The results suggested that the nonlyophilized mAb had a wider

range of shapes, and hence angles between the Fabs than after reconstitution of the freeze-dried mAb. It was hypothesized that the difference in angle distribution was due to loss of flexibility in the hinge region, which then impacted ability to bind target antigen.

A systematic study of the impact of excipients on conformational stability of two IgG1 monoclonal antibodies using a variety of biophysical techniques has been reported recently (Thakkar et al., 2012). The unfolding profile, aggregation behavior, and predenaturation transitions in response to solution conditions such as pH and temperature were different for the two IgG1 mAbs. The mAbs also showed different effective concentrations and effects from two stabilizing excipients as determined by differential scanning calorimetry (DSC), high-resolution ultrasonic spectroscopy, and fluorescent measurements. The main conclusion from these studies is that stabilizing excipients can have different effects on conformation and flexibility of mAbs of the same IgG1 class. The authors discuss in detail the differences in response to the solution condition and excipients between the two mAbs, and mention that the molecular origin of these differences still needs to be elucidated. These differences may be accounted for by differences in amino acid sequence that determine higher order structure. Alternatively the stressed conditions applied, such as extremes in pH or temperature, may result in covalent changes via chemical degradation routes, which in turn led to conformational changes. The latter was not investigated in these studies since no analysis of chemical alterations was done.

Usually conformational changes in proteins, especially when under storage at higher temperatures (>40 °C), result in protein aggregation so discussions that relate conformational changes to aggregation will be covered in the next section. In addition processing of mAbs to create freeze-dried formulations can result in conformational changes (Tian et al., 2007), and will be discussed in more detail in the chapter on formulation development.

Aggregation

Protein aggregation is one of the most common physical degradation routes, and has been summarized in several review articles and books (Mahler & Jiskoot 2012; Manning et al., 2010; Wang & Roberts, 2010). As previously discussed, aggregation can be induced by covalent chemical degradation routes. Although chemical degradation can result in aggregation, conformational changes can also lead to aggregation, very often as a result of exposure of interior hydrophobic amino acid residues.

As shown in Figure 3.1 these aggregates may be comprised of proteins mainly in their native conformation or denatured protein. The aggregates are considered "soluble aggregates" if there are no visible particulates in solution and the aggregates cannot be removed easily by filtration, which again may consist of either natively folded or denatured protein molecules. Issues have been raised regarding the lack of monitoring and quantification of subvisible aggregates that can exceed the solubility of the protein in solution resulting in particulates in the range of 0.1–10 mm. A big concern is that these particulates may be potentially immunogenic (Carpenter et al., 2009). However, it has been suggested that the link between the presence of these

particulates and immunogenicity has not been established unequivocally (Singh et al., 2010). In particular, such particulates are present in marketed products that are safe and efficacious despite a lack of monitoring. It has been emphasized that there are limitations currently in the assays available for particulate detection, and variability due to container/closure contacts, viscosity, concentration, and batch heterogeneity that make such measurements unsuitable as specifications for release and stability. However such measurements may be used to guide product development. Assays used to analyze for particulates have been discussed in Chapter 2.

If the aggregates cannot be resolubilized easily such as by temperature change or solvent conditions without denaturants such as GndHCl they are referred to as irreversible aggregates that can be separated on a gel sizing column. The aggregates may also be reversible, especially by dilution, and this type of aggregation is often referred to as self-association (Esfandiary et al., 2013). This may not be regarded as a problem since upon administration the concentration of protein is often decreased which results in loss of aggregate. However, as we will see in a later chapter on subcutaneous (SC) delivery of mAbs, self-association may have huge consequences for delivery as well as manufacture of SC formulations.

Protein aggregation is undesirable because it can lead to a reduction in activity and altered pharmacokinetics (Klotz & Thomas, 1993; Maggio, 2010; Shao, Li, Krishnamoorthy, Chermak, & Mitra, 1993). Aggregates have also been implicated in a heightened immune response (Moore & Leppert, 1980; Ratner, Phillips, & Steiner, 1990; Ring, Stephan, & Brendel, 1979; Underwood, Voina, & Van Wyk, 1974), and adverse events due to antibody aggregates have also been reported (Demeule, Gurny, & Arvinte, 2006; Ryan, Webster, & Statler, 1996). The concern over mAb aggregates especially for IV dosing has resulted in a limitation by the World Health Organization (WHO) of less than 5% aggregate in commercialized mAb therapeutics.

Protein aggregation occurs as the result of protein–protein interactions, which can increase as a function of concentration whereby the average distances between protein molecules decrease. If the aggregation is reversible it may be difficult to detect by sizing chromatography since the protein solution becomes more dilute as it separates on the column. As an example human relaxin has been shown to undergo reversible dimerization (Shire, Holladay, & Rinderknecht, 1991). When analyzed by size exclusion chromatography, essentially one peak is detected with a molecular weight at ~6 kDa which is close to the expected monomer molecular weight of 6.5 kDa as determined by amino acid composition (Figure 3.18(a); Canovadavis, Baldonado, & Teshima, 1990). The weight average molecular weight is concentration dependent as shown by analytical ultracentrifugation (Figure 3.18(b)) with an extrapolated molecular weight near zero concentration of protein to that expected of a monomer. It has been reported that increasing the loading concentration to 2 mg/mL results in relaxin eluting on sizing chromatography as a dimer (Canovadavis et al., 1990). Thus, if one is not aware that reversible self-association is occurring, sizing chromatography may not detect association due to dilution on the column.

Aggregation of proteins produced using recombinant DNA technology can occur as a result of different processing steps, usually referred to as unit operations. An

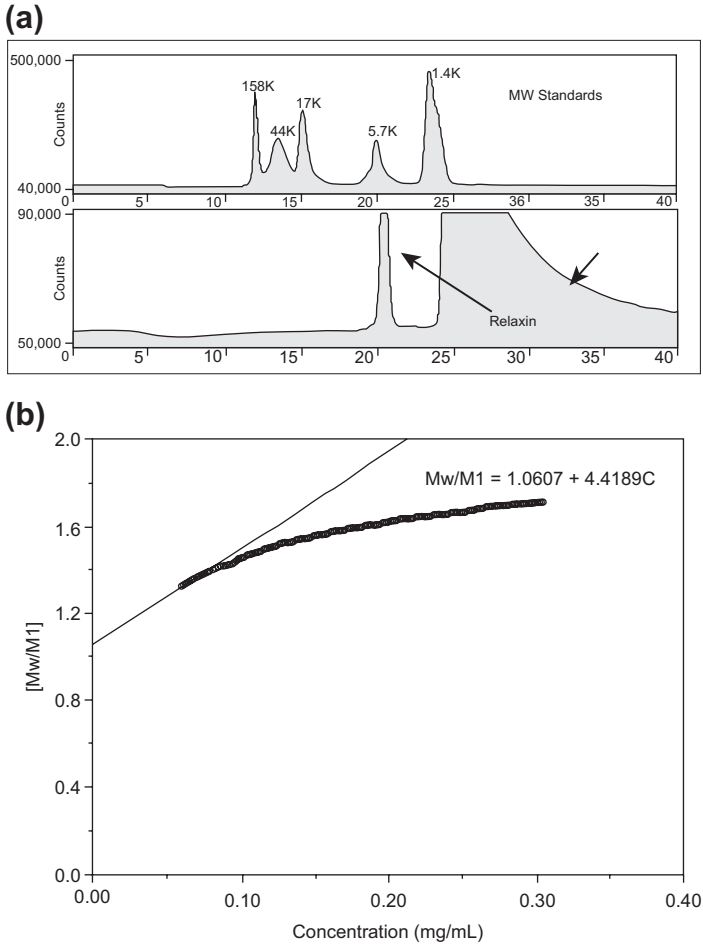

Figure 3.18 (a) Sizing chromatography of human relaxin. 50 µL at x mg/mL loaded onto a TSK G2000 SWXL column (300 × 7.5 mm I.D.) equilibrated with 10 mM sodium citrate, pH 5.0 in 0.25 M sodium chloride. Flow rate at 0.5 mL/min with detection at 214 nm. (b) Weight average molecular weight (Mw) determined by sedimentation equilibrium analytical ultracentrifugation divided by the monomer molecular weight (M1) determined from amino acid composition of human relaxin. Human relaxin at concentrations ranging from 0.05 to 0.2 mg/mL in 10 mM sodium citrate, 0.15 M sodium chloride at pH 5.0 was centrifuged at 22 or 32 k rpm at 19–21 °C for 18 h and concentration gradients detected at 280 nm.

overview of protein production by recombinant DNA technology is shown in Figure 3.19. As can be seen there are many opportunities for generation of protein aggregates. The aggregates that form during upstream processing can often be removed by a final chromatographic purification step. Although insoluble aggregates may be removed by filtration, soluble aggregates generated during downstream processing may be more difficult to remove since there are no chromatographic purification

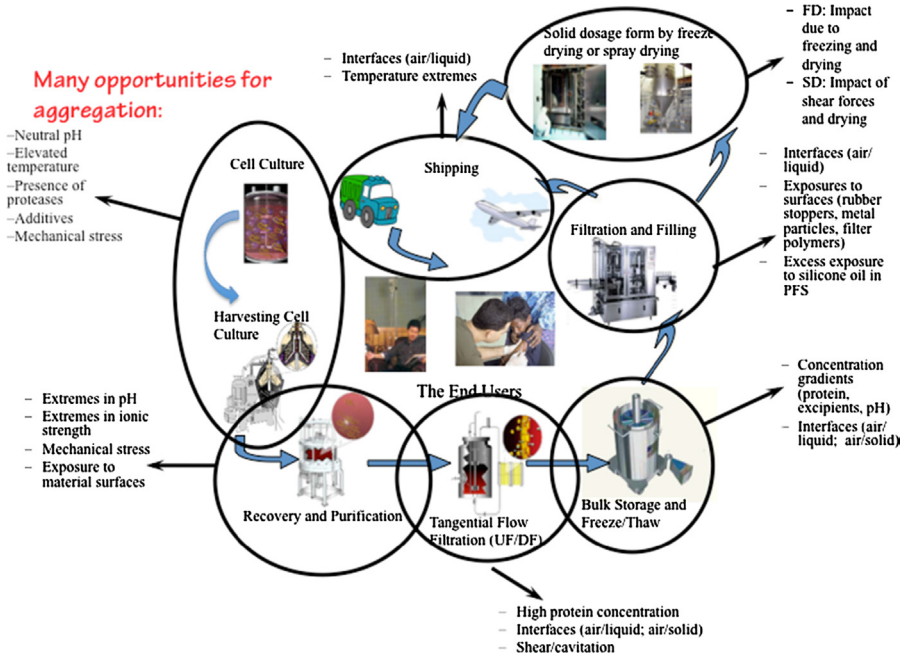

Figure 3.19 Generation of aggregates during bioprocessing.

processes used during preparation of DP. During production of the bulk DS exposure to shear and stress during agitation as well as different solution conditions that include pH, ionic strength, and temperature can lead to aggregate formation. Preparation of DP from bulk DS involves several unit operations such as tangential flow filtration for concentration and buffer exchange, freeze-thawing in cryogenic vessels for bulk storage, filtration and filling into final DP containers, and solid dosage form processes such as freeze-drying and spray drying. Aggregates can form during these unit operations. The resulting DP may also aggregate as a result of long-term storage conditions such as pH, ionic strength, and temperature (Schreiber, 2002). In addition, agitation and exposure to temperature excursions during shipping can lead to protein aggregation. Once shipped, aggregates can also be generated during handling of the final DP for administration to the patient, and this aspect will be discussed further in a later chapter.

Specific examples of mAb aggregation

Aggregation of a mAb during long-term storage

As discussed previously, altered conformation of proteins can lead to aggregation. An interesting example of this is for an IgG_2 mAb where it was shown that disulfide isoforms, which contribute to conformational changes, can govern the aggregation behavior of this antibody (Perico, Purtell, Dillon, & Ricci, 2009). Three disulfide

isoforms (IgG_2-A, IgG_2-B, and IgG_2-A/B) involving different disulfide linkages with the hinge region have been proposed based on peptide mapping (Dillon et al., 2008; Wypych et al., 2008) and are shown in Figure 8 of Wypych et al. (2008). This IgG_2 mAb produced and purified out of CHO cells was investigated at either 30 or 100 mg/mL at the target storage temperature of 4 °C as well as at 29 and 37 °C from pH 5 to 5.5 for 1 year (Perico et al., 2009). The higher storage temperatures are often used since the rate of degradation at the target 2–8 °C for long-term storage may be so slow that it is difficult to detect changes in stability in a reasonable amount of time. The rate of aggregation was determined at each pH and storage temperature by size exclusion chromatography. Arrhenius plots were generated from these data that showed nonlinearity that increased with decreasing pH. Interestingly, the trend in the rates at 4 °C was opposite to that seen at 37 °C. Essentially the rate of aggregation at 5 °C was lowest at pH 5, whereas at 37° it was highest at pH 5. This trend was not observed at 30 mg/mL mAb, but was observed at 100 mg/mL mAb. DSC measurements also suggested that this mAb did not undergo thermal unfolding until well beyond 50 °C, and thus the amount of unfolded proteins at 37 °C was very small. These observations could be mainly explained by the aggregation and fragmentation tendencies of the IgG_2 disulfide isoforms. Redox treatment of the IgG2 mAb with and without 1 M GuHCl allowed for the enrichment of the disulfide isoforms. Isoforms IgG2-A and IgG_2-B were shown to have different temperature-dependent aggregation profiles when formulated at pH 5 and stored for 1 year at 4, 29, and 37 °C. The inverse pH dependency as well as the temperature and concentration dependency could be explained by the different fragmentation behavior of the two isoforms. These fragments are able to aggregate and thus at lower temperatures of 2–8° at acidic pH the IgG_2 mAb undergoes minimal aggregation, whereas at the higher temperature the increase in fragmentation leads to increased aggregation. The aggregation of the fragments was also shown to be concentration dependent. In the pH range of 5.2–5.5 at 30 mg/mL aggregation was pH independent. The IgG_2 investigated by Perico et al. had a mixture of disulfide isoforms A and B, and thus the complex kinetics of aggregation for the IgG_2 was due to the net sum of the fragmentation and aggregation properties of the component A and B isoforms. It was also shown that the main difference in high-temperature clipping between the isoforms was due to fragmentation in the flexible CH1 region even though both regions have the same amino acid sequence. Therefore, the differences in conformation of the A and B isoform hinge region due to differences in disulfide connectivity impact the fragmentation and hence the aggregation rate of the two isoforms.

These studies show that accelerated storage conditions may have very different aggregation rates than at the lower temperature storage conditions. In addition conformational changes were not observed for either isoform between 29 and 37 °C which has implications for the mechanism of protein and mAb aggregation.

Many of the early studies of small globular proteins led to a two-state model whereby the native state is in equilibrium with the denatured state (Lumry & Biltonen, 1966), and this was refined by depicting the native and denatured states that have an ensemble of structures that are in dynamic equilibrium. The two-state model was supported by differential calorimetry measurements. A pure two-state model was

expected to have no significant amount of intermediates and it was shown that a calorimetric measurement of enthalpy for the denaturation process should be equal to that determined indirectly by the temperature dependence of the denaturation equilibrium constant, which yields the van't Hoff enthalpy (Tanford, 1968). Privalov showed that this was the case for several small globular proteins (Privalov & Khechinashvili, 1974). However, it was shown by rapid temperature jump studies that kinetic intermediates could be present and that a small globular protein such as ribonuclease A undergoes denaturation via a sequential unfolding mechanism (Tsong et al., 1971). The proposed two-state model also suggested that large unfolding of the overall protein structures often drives protein aggregation, but in fact even small localized unfolding may result in protein aggregation as shown by the IgG_2 studies where large denaturation transitions were not observed by DSC until after 37 °C.

Aggregation of mAb during unit processing operations

Freezing and Thawing

Manufacturing lots of protein DP are often stored as bulk in freeze tanks and portions thawed as needed for final fill and finishing. During this freezing process the water component of the DP starts freezing and excludes formulation excipients and protein from its environment, resulting in regions where the protein molecules and excipients are concentrated (Kolhe, Holding, Lary, Chico, & Singh, 2010). This "cryoconcentration" leads to extreme changes in solution conditions such as pH, osmolality, ionic strength, etc., which may impact protein conformation and promote aggregation. During the thawing of large frozen bulk solutions concentration gradients are also generated, which may promote aggregation. Using specially designed cryovessels, where the thawed solution is circulated during the thawing process, can mitigate some of this (Wisniewski & Wu, 1996). In addition, during the freezing process ice crystal formation can promote aggregation (Strambini & Gabellieri, 1996). Measurement of Trp intrinsic phosphorescence emission lifetime, τ, correlates with rigidity of the protein core and was used to show that perturbation of protein conformation results from the direct interaction of the protein with the ice crystal surface. The number and size of the ice crystals will determine the ice surface area available for interaction with the protein. Slow cooling rate and long-term storage can promote the formation of fewer and larger crystals resulting in decreased surface area for protein interaction with ice surfaces (Franks, 1985). The decreased surface area should also lead to smaller conformational changes of the protein resulting in less aggregation. This was demonstrated by comparing changes in τ for protein solutions seeded with an ice crystal and cooled either at 200 or at 1 °C/min. The protein solutions that were tested overall showed smaller perturbations of structure at the slower cooling rate. Frozen solutions left to anneal for 10 h at −6 °C resulted in some reversal of τ showing that maturation of the ice structure into fewer and larger crystals results in less structural perturbation.

A systematic study on the freeze-thawing of an IgG_2 mAb as a function of pH, with and without 150 mM KCl, mAb concentration, cooling and warming rates, and container type and material showed that although all the parameters studied had an impact

on soluble aggregate formation, the type and composition of the freeze container was most pronounced (Kueltzo, Wang, Randolph, & Carpenter, 2008). The mAb tertiary structure was also investigated as a function of pH and KCl using second-derivative UV spectroscopy. Overall, aggregation was most prevalent at pH 3 and 4 and was impacted most by the cooling and thawing rates. In general, <10% monomer loss occurred at pH 5 and 8, regardless of salt percentage, with the exception of rapid cooling conditions, where up to 15% loss was observed. The correlation between faster warming rate and loss of monomer was greatest at pH 3, and this effect was enhanced at 150 mM KCl. The mAb aggregation was also affected by the presence of air–water interfaces and container surface interactions. The impact of container was evaluated for five different types, polypropylene, polyethylene, glass, Teflon, and Flexboy™ freezing bags. After freezing, the containers were thawed at 25 °C for 30 min. Although less soluble aggregate was formed in the Flexboy and Teflon containers at pH 3 and 4, there was significant loss of mAb, up to 55% in the Flexboy bags. These studies suggested that adsorption of protein to the surface of the bags as well as Teflon may be responsible for the overall loss of protein. These observations are consistent with the reported adsorption of proteins onto hydrophobic Teflon surfaces (Sluzky, Tamada, Klibanov, & Langer, 1991; Vermeer, Bremer, & Norde, 1998; Vermeer, Giacomelli, & Norde, 2001). Conformational changes also occurred as a result of the surface adsorption as assessed by second-derivative UV absorption spectroscopy. Thus, not only solution conditions, and rates of cooling and thawing may impact aggregate formation, but also the choice of freeze container is important.

Another important consideration for freezing of mAbs is the choice of buffer components. Several buffer systems such as Tris-HCl and sodium phosphate have large dpKa/dT, which can result in change in pH during cooling and freezing. Recent studies have suggested that pH changes due to buffer during cooling and freezing can be ruled out as a factor in aggregation behavior (Kolhe, Amend, & Singh, 2010). However, buffer systems where the pH changes due to crystallization of a buffer salt upon freezing can impact protein conformation as shown by studies on the freeze-drying of γ interferon (Lam, Costantino, Overcashier, Nguyen, & Hsu, 1996). These studies show that γ interferon loses its native structure at lower pH and it was postulated that prior to drying a decrease in pH upon freezing leads to increased instability for the product. This was further demonstrated by freeze-drying at pH 5 in two different buffer systems, glycolate and succinate. It was suggested that the freezing step prior to the drying step may induce a pH drop in the succinate buffer system in contrast to the glycolate system. Then as a result of this pH decrease the γ IFN unfolds in the freeze-concentrated phase. From these results it is not inconceivable that a mAb that is aggregation prone at lower pH may aggregate as a result of such pH decreases during freezing.

Crystallization of other excipients such as trehalose has also been shown to increase the aggregation of an IgG_2 mAb when stored at −20 °C, but not at −10 or −40 °C (Singh et al., 2011). The main cause for the increased aggregation rate at −20 °C was the crystallization of the freeze-concentrated trehalose when the temperature of the frozen solute exceeds the glass transition temperature of the frozen matrix. It was hypothesized that even though trehalose crystallization occurred at −10 °C there was still sufficient mobility of the mAb in the frozen matrix so that mAb that unfolded at

the ice interface on freezing was able to refold before significant aggregation occurred. At −40 °C there was no evidence for crystallization and aggregation, which was attributable to the lack of mobility.

Exposure to air/water interfaces due to agitation

During mAb production, homogeneity of the mAb solution is achieved by agitation using mixing and solution flow. The agitation of the solutions generates air/water interfaces which promotes mAb aggregation. Proteins are amphipathic molecules consisting of hydrophilic and nonpolar hydrophobic regions. These nonpolar sections tend to migrate to the more hydrophobic air section, whereas the hydrophilic regions stay in the aqueous environment (Andrade et al., 1992 and Figure 3.20). Over time the proteins may unfold at the interface generating more separation between the hydrophobic and hydrophilic regions. The unfolded protein may then aggregate and eventually release insoluble aggregates into the solution. Generation of insoluble aggregates of mAbs as a result of exposure to air–water during agitation has been reported (Fesinmeyer et al., 2009; Mahler, Muller, Friess, Delille, & Matheus, 2005). In particular it was shown that interaction of anions with IgG_2 mAbs could enhance portioning at the air–water interface resulting in mAb insoluble aggregate formation (Fesinmeyer et al., 2009).

Protein aggregation is generally a second or higher order concentration process since bimolecular and higher order collisions of molecules are involved. Thus protein and mAb aggregation is expected to increase with protein concentration. However, it has been shown that agitation-induced aggregation decreases with an increase in protein concentration (Treuheit, Kosky, & Brems, 2002). In essence, less of the protein in solution is exposed to the air–water interface surface resulting

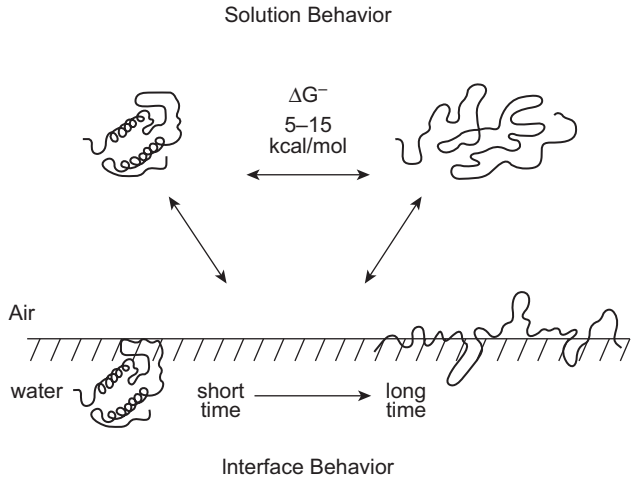

Figure 3.20 Protein unfolding at air–water interfaces.
From Andrade et al. (1992).

in an overall smaller percentage of total protein that can unfold as the total protein concentration increases, that is, the ratio of available air–water surface area to total protein decreases.

The method used to generate the air–water interface dictates the types of aggregates that are formed. Aggregation of an IgG_1 mAb was studied at 5 and 25 °C using two agitation methods, either shaking or stirring (Kiese, Papppenberger, Friess, & Mahler, 2008). In addition, the impact of different air headspaces on mAb aggregation was also investigated. There was a large difference between horizontal shaking with a headspace and stirring in terms of the number and size of protein aggregates. In particular, shaking the solution resulted in generation of visible particulates, smaller subvisible particles (<2 mM), and soluble aggregates, whereas stirring resulted in an increase in solution turbidity attributable to generation of subvisible particles, but without production of soluble aggregates. It was suggested that these differences are due to the different stresses exerted on the solution by shaking compared to stirring. Shaking results in replenishment of the air–water interface and migration of aggregated protein into solution. Decrease of headspace by increasing the volume of agitated solution in a container decreases the amount of aggregated protein, which can be explained by the suppression of liquid movement within the closed container. Stirring results in different mechanical stresses such as local heating by friction of the stirrer and bottom of the container, and solid–water interface interactions between the hydrophobic surface of the stirrer and protein.

Use of large-scale pumps in DP unit operations

Large-scale pumps are often used to transfer DP into holding tanks or used for the actual processing step such as ultrafiltration/diafiltration and filling operations. These pumping operations can expose the mAb to mechanical stresses, which include shear and cavitation. These stresses may result in conformational changes in the mAb creating opportunities for aggregation. Although the shear itself may not impact aggregation of mAbs, the generation of air/water interfaces, exposure to solid surfaces, and pump cavitation that are associated with shear forces can be major factors in generation of aggregates. The types of pumps used have also been shown to impact aggregation processes. The following sections discuss in more detail DP unit operations that use pumps and the impact of these operations on mAb aggregation.

Filtration

Ultrafiltration/diafiltration unit operations are used as a manufacturing step to concentrate and formulate the mAb DS (Figure 3.19). In addition whenever the mAb DP is stored prior to filling the product it needs to be sterile filtered, usually through a 0.2 μm filter cassette. A common problem in these types of operations is the fouling

of the membranes which results in unacceptably long times for filtration. Membrane fouling may be due to several factors, and the presence of protein aggregates may be a significant factor. The aggregates may be present prior to the filling, having been generated by previous unit operations such as freeze–thaw, or actually may be generated during the filtration process. Examination of the fouling deposits of albumin after filtration using field emission scanning electron microscopy (FESEM) showed two different types of fouling deposits on membrane surfaces described as cakes and aggregates (Kim, Fane, Fell, & Joy, 1992). Filtration using higher initial ultrafiltration (UF) flux showed protein aggregates whereas filtrations at lower initial UF flux showed cake formation. The "cake formation" is believed to consist of protein aggregates. These aggregates may have been generated by a rapid increase of protein concentration at the membrane surface due to the high initial convective flows. Although the FESEM was unable to detect protein deposits in the membrane pores, it was concluded that even one or two layers of protein deposits could explain the decline in flux. Such limited quantities of protein deposit are not detectable by the FESEM technique.

Cromwell et al. have discussed a nice example of the impact of UF/DF processing on a mAb (Cromwell, Hilario, & Jacobson, 2006). It was observed that the recovered sample from UF/DF processing had a significantly greater turbidity as measured at 350 nm. This increase in turbidity was hypothesized to be the result of mechanical stresses from the continuous pumping operations used during the UF/DF processing.

Filling

During filling mAb DP will be exposed to solid surfaces such as stainless steel and also the stresses imparted by pumping operations. The large-scale pumping imparts high shear to the solution resulting in the generation of stainless steel microparticles (Biddlecombe et al., 2007; Bee, Davis, Freund, Carpenter, & Randolph, 2010; Tyagi et al., 2009). Protein adsorption to the surfaces of these particle results in aggregates that are generated by surface-mediated processes since exposure to supernatant from centrifuged suspensions of stainless steel particles did not result in formation of protein aggregates (Bee et al., 2010).

The type of pumps and nozzles used for filling can have a huge impact on formation of mAb aggregates. In a rotary filling pump the protein solution actually lubricates the piston barrel and, due to the interaction with the piston hydrophobic surface and friction, the protein may adsorb and unfold. The unfolded protein may accumulate and eventually slough off the piston into the solution generating visible particulates (Figure 3.21). In one study two types of pumps were used, a rolling diaphragm pump and a radial piston pump (Cromwell et al., 2006). The mAb used in this study was known to be sensitive to frictional shear forces, and since the mAb solution would essentially lubricate the moving piston in the radial piston pump there was concern that this type of pump might generate aggregates. To ascertain if this was a problem ~1 L of the mAb solution was transferred 13 times between

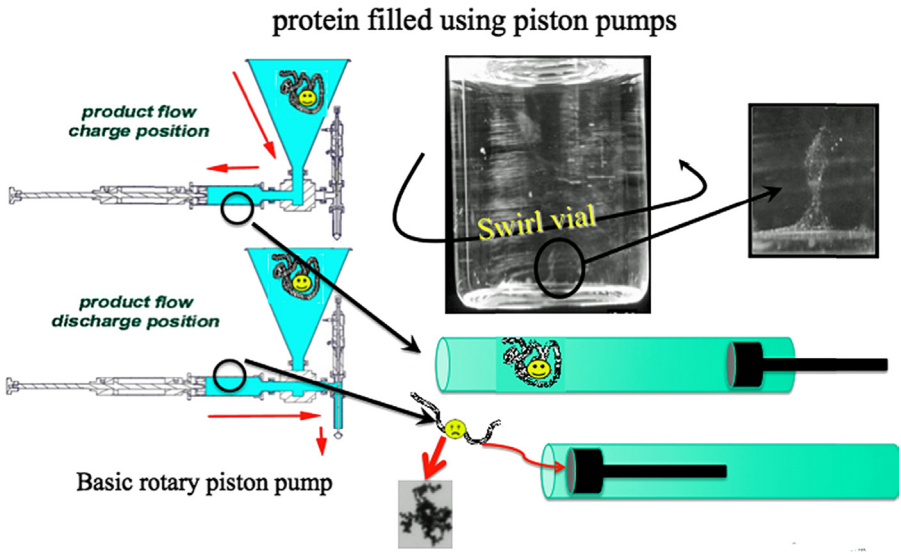

Figure 3.21 Particulate formation in protein solutions filled using rotary piston pumps when filled into vials.

two containers at low and high speeds that represented the typical and fastest filling speeds. After each transfer an aliquot was analyzed by turbidity measurements at 350 nm or by light obscuration using a Hiac particle counter. As the number of transfers increased, the turbidity and number of particles >2 mM increased (see Figure 2 in Cromwell et al., 2006). This was not observed using the rolling diaphragm pump.

Adsorption to surfaces

On adsorption to hydrophobic air–water interfaces solid particles such as stainless steel microparticles will generate aggregates as discussed previously. In addition to this type of adsorption, proteins are also capable of adsorption on solid surfaces that make up typical container closures. Generally the amount of protein that adsorbs to such surfaces is small, on the order of micrograms. Thus, proteins that are delivered at low doses may undergo substantial percentage loss due to surface adsorption. This often can be handled by adding a surface-active excipient such as a surfactant or protein to coat the container closure as is done by the addition of human serum albumin to formulations of erythropoietin (Shimoda & Kawaguchi, 1986). mAbs are high-dose drugs and when formulated at higher concentrations the percentage of mAb lost due to surface adsorption is not significant. One report discusses the loss of a murine mAb during secretion from transgenic plant tissue cultures, which was attributed to adsorption to container surfaces (Doran, 2006). However, these experiments were done in glass shake flasks at low mAb concentrations (2 μg/mL), and thus this result is not surprising.

References

Adam, W., Ahrweiler, M., Sauter, M., & Schmiedeskamp, B. (1993). Oxidation of indoles by singlet oxygen and dimethyldioxirane – isolation of indole dioxetanes and epoxides by stabilization through nitrogen acylation. *Tetrahedron Letters*, *34*(33), 5247–5250.

Aeschbach, R., Amado, R., & Neukom, H. (1976). Formation of dityrosine cross-links in proteins by oxidation of tyrosine residues. *Biochimica et Biophysica Acta*, *439*(2), 292–301.

Alexander, A. J., & Hughes, D. E. (1995). Monitoring of IgG antibody thermal-stability by micellar electrokinetic capillary chromatography and matrix-assisted laser desorption/ionization mass-spectrometry. *Analytical Chemistry*, *67*(20), 3626–3632.

Andrade, J. D., Hilady, V., Wei, A.-P., Ho, C.-H., Leas, A. S., Jeon, S. I., et al. (1992). Proteins at interfaces: principles, multivariate aspects, protein resistant surfaces, and direct imaging and manipulation of adsorbed proteins. *Clinical Materials*, *11*, 66–74.

Andya, J. D., Hsu, C. C., & Shire, S. J. (2003). Mechanisms of aggregate formation and carbohydrate excipient stabilization of lyophilized humanized monoclonal antibody formulations. *AAPS PharmSciTech*, *5*(2), 32–38.

Andya, J. D., Maa, Y. F., Costantino, H. R., Nguyen, P. A., Dasovich, N., Sweeney, T. D., et al. (1999). The effect of formulation excipients on protein stability and aerosol performance of spray-dried powders of a recombinant humanized anti-IgE monoclonal antibody. *Pharmaceutical Research*, *16*(3), 350–358.

Anfinsen, C. B. (1973). Principles that govern the folding of protein chains. *Science*, *181*, 223–230.

Antosiewicz, J., McCammon, J. A., & Gilson, M. K. (1996). The determinants of pKas in proteins. *Biochemistry*, *35*(24), 7819–7833.

Barron, E. S. G., Miller, Z. B., & Kalnitsky, G. (1947). The oxidation of dithiols. *Biochemisty Journal*, *41*, 62.

Bee, J. S., Davis, M., Freund, E., Carpenter, J. F., & Randolph, T. W. (2010). Aggregation of a monoclonal antibody induced by adsorption to stainless steel. *Biotechnology and Bioengineering*, *105*(1), 121–129.

Bee, J. S., Stevenson, J. L., Mehta, B., Svitel, J., Pollastrini, J., Platz, R., et al. (2009). Response of a concentrated monoclonal antibody formulation to high shear. *Biotechnology and Bioengineering*, *103*(5), 936–943.

Berges, J., Trouillas, P., & Houee-Levin, C. (2011). Oxidation of protein tyrosine or methionine residues: from the amino acid to the peptide. In *Cost chemistry Cm0603-melusyn joint meeting: Damages induced in biomolecules by low and high energy radiations* (Vol. 261).

Bertolotti-Ciarlet, A., Wang, W. R., Lownes, R., Pristatsky, P., Fang, Y. L., McKelvey, T., et al. (2009). Impact of methionine oxidation on the binding of human IgG1 to FcRn and Fc gamma receptors. *Molecular Immunology*, *46*(8–9), 1878–1882.

Bhatt, N. P., Patel, K., & Borchardt, R. T. (1990). Chemical pathways of peptide degradation.1. Deamidation of adrenocorticotropic hormone. *Pharmaceutical Research*, *7*(6), 593–599.

Biddlecombe, J. G., Craig, A. V., Zhang, H., Uddin, S., Mulot, S., Fish, B. C., et al. (2007). Determining antibody stability: creation of solid-liquid interfacial effects within a high shear environment. *Biotechnology Progress*, *23*(5), 1218–1222.

Brennan, T. V., & Clarke, S. (1993). Spontaneous degradation of polypeptides at aspartyl and asparaginyl residues: effects of the solvent dielectric. *Protein Science*, *2*(3), 331–338.

Burkitt, W., Domann, P., & O'Connor, G. (2010). Conformational changes in oxidatively stressed monoclonal antibodies studied by hydrogen exchange mass spectrometry. *Protein Science*, *19*(4), 826–835.

Cacia, J., Keck, R., Presta, L. G., & Frenz, J. (1996). Isomerization of an aspartic acid residue in the complementarity-determining regions of a recombinant antibody to human IgE: identification and effect on binding affinity. *Biochemistry*, *35*(6), 1897–1903.

Canovadavis, E., Baldonado, I. P., & Teshima, G. M. (1990). Characterization of chemically synthesized human relaxin by high-performance liquid-chromatography. *Journal of Chromatography*, *508*(1), 81–96.

Capasso, S., Mazzarella, L., Sica, F., & Zagari, A. (1989). Deamidation via cyclic imide in asparaginyl peptides. *Peptide Research*, *2*(2), 195–200.

Capasso, S., Mazzerella, L., Sica, F., Zagari, A., & Salvadori, S. (1993). Kinetics and mechanism of succinimide ring formation in the deamidation process of asparagine residues. *Journal of the Chemical Society Perkin Transactions I*, *2*, 679–682.

Capasso, S., & Salvadori, S. (1999). Effect of the three-dimensional structure on the deamidation reaction of ribonuclease A. *Journal of Peptide Research*, *54*(5), 377–382.

Carpenter, J. F., Randolph, T. W., Jiskoot, W., Crommelin, D. J. A., Middaugh, C. R., Winter, G., et al. (2009). Overlooking subvisible particles in therapeutic protein products: gaps that may compromise product quality. *Journal of Pharmaceutical Sciences*, *98*(4), 1201–1205.

Catak, S., Monard, G., Aviyente, V., & Ruiz-Lopez, M. F. (2008). Computational study on nonenzymatic peptide bond cleavage at asparagine and aspartic acid. *Journal of Physical Chemistry A*, *112*(37), 8752–8761.

Chan, H. S., & Dill, K. A. (1993). The protein folding problem. *Physics Today*, *46*(2), 24–32.

Chang, S. H., Teshima, G. M., Milby, T., GilleceCastro, B., & CanovaDavis, E. (1997). Metal-catalyzed photooxidation of histidine in human growth hormone. *Analytical Biochemistry*, *244*(2), 221–227.

Chelius, D., Rehder, D. S., & Bondarenko, P. V. (2005). Identification and characterization of deamidation sites in the conserved regions of human immunoglobulin gamma antibodies. *Analytical Chemistry*, *77*(18), 6004–6011.

Chu, J. W., Yin, J., Brooks, B. R., Wang, D. I. C., Ricci, M. S., Brems, D. N., et al. (2004). A comprehensive picture of non-site specific oxidation of methionine residues by peroxides in protein pharmaceuticals. *Journal of Pharmaceutical Sciences*, *93*(12), 3096–3102.

Cipolla, D. C., & Shire, S. J. (1991). Analysis of oxidized human relaxin by reverse phase Hplc, mass-spectrometry and bioassays. In *Techniques in protein chemistry II* (pp. 543–555).

Clarke, S. (1987). Propensity for spontaneous succinimide formation from Asparaginyl residues in cellular proteins. *International Journal of Peptide and Protein Research*, *30*, 808–821.

Cleland, J. L. (Ed.). (1993). *Protein folding: In vivo and in vitro*. Washington, D.C.: American Chemical Society.

Cleland, J. L., Powell, M. F., & Shire, S. J. (1993). The development of stable protein formulations: a close look at protein aggregation, deamidation, and oxidation. erratum appears in Crit Rev Ther Drug Carrier Syst 1994;11(1):60 *Critical Reviews in Therapeutic Drug Carrier Systems*, *10*(4), 307–377.

Cordoba, A. J., Shyong, B. J., Breen, D., & Harris, R. J. (2005). Non-enzymatic hinge region fragmentation of antibodies in solution. *Journal of Chromatography. B, Analytical Technologies in the Biomedical and Life Sciences*, *818*(2), 115–121.

Creed, D. (1984). The photophysics and photochemistry of the near-uv absorbing amino-acids. 2. Tyrosine and its simple derivatives. *Photochemistry and Photobiology*, *39*(4), 563–575.

Cromwell, M. E. M., Hilario, E., & Jacobson, F. (2006). Protein aggregation and bioprocessing. *AAPS Journal*, *8*(3), E572–E579.

Daugherty, A. L., & Mrsny, R. J. (2006). Formulation and delivery issues for monoclonal antibody therapeutics. *Advanced Drug Delivery Reviews*, *58*(5–6), 686–706.

Demeule, B., Gurny, R., & Arvinte, T. (2006). Where disease pathogenesis meets protein formulation: renal deposition of immunoglobulin aggregates. *European Journal of Pharmaceutics and Biopharmaceutics*, *62*(2), 121–130.

Dill, K. A., Chan, H. S., & Yue, K. (1995). The protein-folding problem – searching conformations of compact chain molecule. *Macromolecular Symposia*, *98*, 615–617.

Dill, K. A., & MacCallum, J. L. (2012). The protein-folding problem, 50 years on. *Science*, *338*(6110), 1042–1046.

Dillon, T. M., Ricci, M. S., Vezina, C., Flynn, G. C., Liu, Y. D., Rehder, D. S., et al. (2008). Structural and functional characterization of disulfide isoforms of the human IgG2 subclass. *Journal of Biological Chemistry*, *283*(23), 16206–16215.

Dill, K. A., Ozkan, S. B., Shell, M. S., & Weikl, T. R. (2008). The protein folding problem. *Annual Review of Biophysics*, *37*, 289–316.

Dill, K. A., Ozkan, S. B., Weikl, T. R., Chodera, J. D., & Voelz, V. A. (2007). The protein folding problem: when will it be solved? *Current Opinion in Structural Biology*, *17*(3), 342–346.

Doran, P. M. (2006). Loss of secreted antibody from transgenic plant tissue cultures due to surface adsorption. *Journal of Biotechnology*, *122*(1), 39–54.

Dubinina, E. E., Gavrovskaya, S. V., Kuzmich, E. V., Leonova, N. V., Morozova, M. G., Kovrugina, S. V., et al. (2002). Oxidative modification of proteins: oxidation of tryptophan and production of dityrosine in purified proteins using Fenton's system. *Biochemistry-Moscow*, *67*(3), 343–350.

Dyer, J. M., Bringans, S. D., & Bryson, W. G. (2006). Characterisation of photo-oxidation products within photoyellowed wool proteins: tryptophan and tyrosine derived chromophores. *Photochemical & Photobiological Sciences*, *5*(7), 698–706.

Edelman, G. M., Cunningham, B. A., Gall, W. E., Gottlieb, P. D., Rutishauser, U., & Waxdal, M. J. (1969). The covalent structure of an entire gammaG immunoglobulin molecule. *Proceedings of the National Academy of Sciences of the United States of America*, *63*(1), 78–85.

Engleka, K. A., & Maciag, T. (1992). Inactivation of human fibroblast growth factor-I (Fgf-1) activity by interaction with copper ions involves Fgf-1 dimer formation induced by copper-catalyzed oxidation. *Journal of Biological Chemistry*, *267*(16), 11307–11315.

Esfandiary, R., Hayes, D. B., Parupudi, A., Casas-Finet, J., Bai, S. F., Samra, H. S., et al. (2013). A systematic multitechnique approach for detection and characterization of reversible self-association during formulation development of therapeutic antibodies. *Journal of Pharmaceutical Sciences*, *102*(9), 3089–3099.

Fesinmeyer, R. M., Hogan, S., Saluja, A., Brych, S. R., Kras, E., Narhi, L. O., et al. (2009). Effect of ions on agitation- and temperature-induced aggregation reactions of antibodies. *Pharmaceutical Research*, *26*(4), 903–913.

Finley, E. L., Dillon, J., Crouch, R. K., & Schey, K. L. (1998). Identification of tryptophan oxidation products in bovine alpha-crystallin. *Protein Science*, *7*(11), 2391–2397.

Florence, T. M. (1980). Degradation of protein disulfide bonds in dilute alkali. *Biochemical Journal*, *189*(3), 507–520.

Franks, F. (1985). *Biochemistry and biophysics at low temperatures*. London: Cambridge University Press.

Galande, A. K., Trent, J. O., & Spatola, A. F. (2003). Understanding base-assisted desulfurization using a variety of disulfide-bridged peptides. *Biopolymers*, *71*(5), 534–551.

Gaza-Bulseco, G., Faldu, S., Hurkmans, K., Chumsae, C., & Liu, H. (2008). Effect of methionine oxidation of a recombinant monoclonal antibody on the binding affinity to protein A and protein G. *Journal of Chromatography. B, Analytical Technologies in the Biomedical and Life Sciences*, *870*(1), 55–62.

Gaza-Bulseco, G., Li, B. Q., Bulseco, A., & Liu, H. C. (2008). Method to differentiate asn deamidation that occurred prior to and during sample preparation of a monoclonal antibody. *Analytical Chemistry*, *80*(24), 9491–9498.

Geiger, T., & Clarke, S. (1987). Deamidation, isomerization, and racemization at asparaginyl and aspartyl residues in peptides. Succinimide-linked reactions that contribute to protein degradation. *Journal of Biological Chemistry*, *262*(2), 785–794.

Griffiths, S. W., King, J., & Cooney, C. L. (2002). The reactivity and oxidation pathway of cysteine 232 in recombinant human alpha 1-antitrypsin. *Journal of Biological Chemistry*, *277*(28), 25486–25492.

Gross, A. J., & Sizer, I. W. (1959). The oxidation of tyramine, tyrosine, and related compounds by peroxidase. *Journal of Biological Chemistry*, *234*(6), 1611–1614.

Harris, R. J. (1995). Processing of c-terminal lysine and arginine residues of proteins isolated from mammalian-cell culture. *Journal of Chromatography A*, *705*(1), 129–134.

Harris, R. J., Kabakoff, B., Macchi, F. D., Shen, F. J., Kwong, M., Andya, J. D., et al. (2001). Identification of multiple sources of charge heterogeneity in a recombinant antibody. *Journal of Chromatography B*, *752*(2), 233–245.

Hensel, M., Steurer, R., Fichtl, J., Elger, C., Wedekind, F., Petzold, A., et al. (2011). Identification of potential sites for tryptophan oxidation in recombinant antibodies using tert-butylhydroperoxide and quantitative LC-MS. *Plos One*, *6*(3), e17708.

Hiller, K. O., Masloch, B., Gobl, M., & Asmus, K. D. (1981). Mechanism of the OH. Radical induced oxidation of methionine in aqueous-solution. *Journal of the American Chemical Society*, *103*(10), 2734–2743.

Houghten, R. A., Glaser, C. B., & Li, C. H. (1977). Human somatotropin – reaction with hydrogen-peroxide. *Archives of Biochemistry and Biophysics*, *178*(2), 350–355.

Huang, L. H., Li, J. R., Wroblewski, V. J., Beals, J. M., & Riggin, R. M. (2005). In vivo deamidation characterization of monoclonal antibody by LC/MS/MS. *Analytical Chemistry*, *77*(5), 1432–1439.

Inglis, A. S. (1983). Cleavage at aspartic acid. *Methods in Enzymology*, *91*, 324–332.

Jaenicke, R. (2000). Stability and stabilization of globular proteins in solution. *Journal of Biotechnology*, *79*(3), 193–203.

Jefferis, R., & Lund, J. (2002). Interaction sites on human IgG-Fc for FcgammaR: current models. *Immunology Letters*, *82*(1–2), 57–65.

Jiskoot, W., Beuvery, E. C., Dekoning, A. A. M., Herron, J. N., & Crommelin, D. J. A. (1990). Analytical approaches to the study of monoclonal-antibody stability. *Pharmaceutical Research*, *7*(12), 1234–1241.

Ji, J. A., Zhang, B., Cheng, W., & Wang, Y. J. (2009). Methionine, tryptophan, and histidine oxidation in a model protein, PTH: mechanisms and stabilization. *Journal of Pharmaceutical Sciences*, *98*(12), 4485–4500.

Johnson, O. L., Cleland, J. L., Lee, H. J., Charnis, M., Duenas, E., Jaworowicz, W., et al. (1996). A month-long effect from a single injection of microencapsulated human growth hormone. *Nature Medicine*, *2*(7), 795–799.

Joubert, M. K., Luo, Q., Nashed-Samuel, Y., Wypych, J., & Narhi, L. O. (2011). Classification and characterization of therapeutic antibody aggregates. *Journal of Biological Chemistry*, *286*(28), 25118–25133.

Kamat, M. S., Tolman, G. L., & Brown, J. M. (1996). Formulation development of an antifibrin monoclonal antibody radiopharmaceutical. *Pharmaceutical Biotechnology*, *9*, 343–364.

Kaneko, R., & Kitabatake, N. (1999). Heat-induced formation of intermolecular disulfide linkages between thaumatin molecules that do not contain cysteine residues. *Journal of Agricultural and Food Chemistry*, *47*, 4950–4955.

Kasson, T. M. D., & Barry, B. A. (2012). Reactive oxygen and oxidative stress: *N*-formyl kynurenine in photosystem II and non-photosynthetic proteins. *Photosynthesis Research*, *114*(2), 97–110.

Khossravi, M., Shire, S. J., & Borchardt, R. T. (2000). Evidence for the involvement of histidine A(12) in the aggregation and precipitation of human relaxin induced by metal-catalyzed oxidation. *Biochemistry*, *39*(19), 5876–5885.

Kiese, S., Papppenberger, A., Friess, W., & Mahler, H. C. (2008). Shaken, not stirred: mechanical stress testing of an IgG1 antibody. *Journal of Pharmaceutical Sciences*, *97*(10), 4347–4366.

Kim, K. J., Fane, A. G., Fell, C. J. D., & Joy, D. C. (1992). Fouling mechanisms of membranes during protein ultrafiltration. *Journal of Membrane Science*, *68*(1–2), 79–91.

Klotz, A. V., & Thomas, B. A. (1993). N5-Methylasparagine and asparagine as nucleophiles in peptides – main-chain vs side-chain amide cleavage. *Journal of Organic Chemistry*, *58*(25), 6985–6989.

Kolhe, P., Amend, E., & Singh, S. K. (2010). Impact of freezing on pH of buffered solutions and consequences for monoclonal antibody aggregation. *Biotechnology Progress*, *26*(3), 727–733.

Kolhe, P., Holding, E., Lary, A., Chico, S., & Singh, S. K. (2010). Large-scale freezing of biologics: understanding protein and solute concentration changes in a cryovessel-part 2. *Biopharm International*, *23*(7), 40–49.

Kossiakoff, A. A. (1988). Tertiary structure is a principal determinant to protein deamidation. *Science*, *240*(4849), 191–194.

Kroon, D. J., Baldwinferro, A., & Lalan, P. (1992). Identification of sites of degradation in a therapeutic monoclonal-antibody by peptide-mapping. *Pharmaceutical Research*, *9*(11), 1386–1393.

Kueltzo, L. A., Wang, W., Randolph, T. W., & Carpenter, J. F. (2008). Effects of solution conditions, processing parameters, and container materials on aggregation of a monoclonal antibody during freeze-thawing. *Journal of Pharmaceutical Sciences*, *97*(5), 1801–1812.

Lam, X. M., Costantino, H. R., Overcashier, D. E., Nguyen, T. H., & Hsu, C. C. (1996). Replacing succinate with glycolate buffer improves the stability of lyophilized interferon-gamma. *International Journal of Pharmaceutics*, *142*(1), 85–95.

Lam, X. M., Lai, W. G., Chan, E. K., Ling, V., & Hsu, C. C. (2011). Site-specific tryptophan oxidation induced by autocatalytic reaction of polysorbate 20 in protein formulation. *Pharmaceutical Research*, *28*(10), 2543–2555.

Lam, X. M., Yang, J. Y., & Cleland, J. L. (1997). Antioxidants for prevention of methionine oxidation in recombinant monoclonal antibody HER2. *Journal of Pharmaceutical Sciences*, *86*(11), 1250–1255.

Levine, R. L. (1983). Oxidative modification of glutamine-synthetase.1. Inactivation is due to loss of one histidine residue. *Journal of Biological Chemistry*, *258*(19), 11823–11827.

Lewisch, S. A., & Levine, R. L. (1995). Determination of 2-oxohistidine by amino-acid-analysis. *Analytical Biochemistry*, *231*(2), 440–446.

Li, S., Nguyen, T. H., Schoneich, C., & Borchardt, R. T. (1995). Aggregation and precipitation of human relaxin induced by metal-catalyzed oxidation. *Biochemistry*, *34*(17), 5762–5772.

Li, S. H., Schoneich, C., & Borchardt, R. T. (1995a). Chemical-instability of protein pharmaceuticals – mechanisms of oxidation and strategies for stabilization. *Biotechnology and Bioengineering*, *48*(5), 490–500.

Li, S. H., Schoneich, C., & Borchardt, R. T. (1995b). Chemical pathways of peptide degradation. 8. Oxidation of methionine in small model peptides by prooxidant transition-metal ion systems – influence of selective scavengers for reactive oxygen intermediates. *Pharmaceutical Research*, *12*(3), 348–355.

Liu, H. C., Gaza-Bulseco, G., & Chumsae, C. (2009). Analysis of reduced monoclonal antibodies using size exclusion chromatography coupled with mass spectrometry. *Journal of the American Society for Mass Spectrometry*, *20*(12), 2258–2264.

Liu, H. C., Gaza-Bulseco, G., Faldu, D., Chumsae, C., & Sun, J. (2008). Heterogeneity of monoclonal antibodies. *Journal of Pharmaceutical Sciences*, *97*(7), 2426–2447.

Liu, H. C., & May, K. (2012). Disulfide bond structures of IgG molecules structural variations, chemical modifications and possible impacts to stability and biological function. *mAbs*, *4*(1), 17–23.

Lo Bello, M., Parker, M. W., Desideri, A., Polticelli, F., Falconi, M., Boccio, Del, et al. (1993). Peculiar spectroscopic and kinetic properties of Cys-47 in human placental glutathione transferase. Evidence for an atypical thiolate ion pair near the active site. *Journal of Biological Chemistry*, *268*(25), 19033–19038.

Lumry, R., & Biltonen, R. (1966). Validity of the "two-state" hypothesis for conformational transitions of proteins. *Biopolymers*, *4*(8), 917–944.

Luo, Q., Joubert, M. K., Stevenson, R., Ketchem, R. R., Narhi, L. O., & Wypych, J. (2011). Chemical modifications in therapeutic protein aggregates generated under different stress conditions. *Journal of Biological Chemistry*, *286*(28), 25134–25144.

Lura, R., & Schirch, V. (1988). Role of peptide conformation in the rate and mechanism of deamidation of asparaginyl residues. *Biochemistry*, *27*(20), 7671–7677.

Maggio, E. T. (2010). Use of excipients to control aggregation in peptide and protein formulations. *Journal of Excipients and Food Chemistry*, *1*(2), 40–49.

Mahler, H.-C., & Jiskoot, W. (Eds.). (2012). *Analysis of aggregates and particles in protein pharmaceuticals*. Hoboken, NJ: John Wiley & Sons.

Mahler, H. C., Muller, R., Friess, W., Delille, A., & Matheus, S. (2005). Induction and analysis of aggregates in a liquid IgG1-antibody formulation. *European Journal of Pharmaceutics and Biopharmaceutics*, *59*(3), 407–417.

Manning, M. C., Chou, D. K., Murphy, B. M., Payne, R. W., & Katayama, D. S. (2010). Stability of protein pharmaceuticals: an update. *Pharm Res*, *27*(4), 544–575.

Manning, M. C., Patel, K., & Borchardt, R. T. (1989). Stability of protein pharmaceuticals. *Pharmaceutical Research*, *6*(11), 903–918.

Matheson, I. B. C., & Lee, J. (1979). Chemical-reaction rates of amino-acids with singlet oxygen. *Photochemistry and Photobiology*, *29*(5), 879–881.

McDermott, M., Chiesa, R., Roberts, J. E., & Dillon, J. (1991). Photooxidation of specific residues in alpha-crystallin polypeptides. *Biochemistry*, *30*(35), 8653–8660.

McKerrow, J. H., & Robinson, A. B. (1971). Deamidation of asparaginyl residues as a hazard in experimental protein and peptide procedures. *Analytical Biochemistry*, *42*(2), 565–568.

Meinwald, C. Y., Stimson, E. R., & Scheraga, H. A. (1986). Deamidation of the asparaginyl-glycyl sequence. *International Journal of Peptide and Protein Research*, *28*(1), 79–84.

Mellor, G. W., Thomas, E. W., Topham, C. M., & Brocklehurst, K. (1993). Ionization Characteristics of the Cys-25/His-159 Interactive System and of the Modulatory Group of Papain – Resolution of Ambiguity by Electronic Perturbation of the Quasi-2-Mercaptopyridine Leaving Group in a New Pyrimidyl Disulfide Reactivity Probe. *Biochemical Journal*, *290*, 289–296.

Moore, W. V., & Leppert, P. (1980). Role of aggregated human growth hormone (hGH) in development of antibodies to hGH. *Journal of Clinical Endocrinology and Metabolism*, *51*(4), 691–697.

Nguyen, T. H., Burnier, J., & Meng, W. (1993). The kinetics of relaxin oxidation by hydrogen-peroxide. *Pharmaceutical Research*, *10*(11), 1563–1571.

Oda, M. (2004). Antibody flexibility observed in antigen binding and its subsequent signaling. *Journal of Biological Macromolecules*, *4*(2), 45–56.

Oliyai, C., & Borchardt, R. T. (1993). Chemical pathways of peptide degradation. 4. Pathways, kinetics, and mechanism of degradation of an aspartyl residue in a model hexapeptide. *Pharmaceutical Research*, *10*(1), 95–102.

Oliyai, C., Schoneich, C., Wilson, G. S., & Borchart, R. T. (1992). Chemical and physical stability of protein pharmaceuticals. In D. J. A. Crommelin, & K. K. Midha (Eds.), *Topics in pharmaceutical sciences*. Stuttgart, Germany: Med Pharm Scientific.

Overberger, C. G., & Ferraro, J. J. (1962). Oxidation of monomeric and polymeric sulfhydryl compounds. *Journal of Organic Chemistry*, *27*, 3539–3545.

Paborji, M., Pochopin, N. L., Coppola, W. P., & Bogardus, J. B. (1994). Chemical and physical stability of chimeric L6, a mouse-human monoclonal-antibody. *Pharmaceutical Research*, *11*(5), 764–771.

Pace, A. L., Wong, R. L., Zhang, Y. T., Kao, Y. H., & Wang, Y. J. (2013). Asparagine deamidation dependence on buffer type, pH, and temperature. *Journal of Pharmaceutical Sciences*, *102*(6), 1712–1723.

Patel, K., & Borchardt, R. T. (1990). Chemical pathways of peptide degradation. 2. Kinetics of deamidation of an asparaginyl residue in a model hexapeptide. *Pharmaceutical Research*, *7*(7), 703–711.

Patel, K., & Borchardt, R. T. (1990). Chemical pathways of peptide degradation. 3. Effect of primary sequence on the pathways of deamidation of asparaginyl residues in hexapeptides. *Pharmaceutical Research*, *7*(8), 787–793.

Pattison, D. I., Rahmanto, A. S., & Davies, M. J. (2012). Photo-oxidation of proteins. *Photochemical & Photobiological Sciences*, *11*(1), 38–53.

Perico, N., Purtell, J., Dillon, T. M., & Ricci, M. S. (2009). Conformational implications of an inversed pH-dependent antibody aggregation. *Journal of Pharmaceutical Sciences*, *98*(9), 3031–3042.

Pirie, A. (1971). Formation of N'-formylkynurenine in proteins from lens and other sources by exposure to sunlight. *Biochemical Journal*, *125*(1), 203–208.

Plou, F. J., Kowlessur, D., Malthouse, J. P. G., Mellor, G. W., Hartshorn, M. J., Pinitglang, S., et al. (1996). Characterization of the electrostatic perturbation of a catalytic site (Cys)-S-/(His)-Im(+)H ion-pair in one type of serine proteinase architecture by kinetic and computational studies on chemically mutated subtilisin variants. *Journal of Molecular Biology*, *257*(5), 1088–1111.

Powell, M. F. (1996). A compendium and hydropathy/flexibility analysis of common reactive sites in proteins: reactivity at Asn, Asp, Gln, and Met motifs in neutral pH solutions. In R. Pearlman, & Y. J. Wang (Eds.), *Formulation, stability and characterization of protein drugs* (pp. 1–140). New York: Plenum.

Privalov, P. L., & Khechinashvili, N. N. (1974). A thermodynamic approach to the problem of stabilization of globular protein structure: a calorimetric study. *Journal of Molecular Biology*, *86*(3), 665–684.

Qi, P., Volkin, D. B., Zhao, H., Nedved, M. L., Hughes, R., Bass, R., et al. (2009). Characterization of the photodegradation of a human IgG1 monoclonal antibody formulated as a high-concentration liquid dosage form. *Journal of Pharmaceutical Sciences*, *98*(9), 3117–3130.

Radkiewicz, J. L., Zipse, H., Clarke, S., & Houk, K. N. (1996). Accelerated racemization of aspartic acid and asparagine residues via succinimide intermediates: an ab initio theoretical exploration of mechanism. *Journal of the American Chemical Society*, *118*(38), 9148–9155.

Rao, P. E., & Kroon, D. J. (1993). Orthoclone OKT3 chemical mechanisms and functional effects of degradation of a therapeutic monoclonal antibody. In R. Pearlman, & Y. J. Wang (Eds.), *Stability and characterization of protein and peptide drugs – Case histories* (Vol. 5) (pp. 135–158). New York: Plenum.

Ratner, R. E., Phillips, T. M., & Steiner, M. (1990). Persistent cutaneous insulin allergy resulting from high-molecular-weight insulin aggregates. *Diabetes*, *39*(6), 728–733.

Ring, J., Stephan, W., & Brendel, W. (1979). Anaphylactoid reactions to infusions of plasma-protein and human-serum albumin – role of aggregated proteins and of stabilizers added during production. *Clinical Allergy*, *9*(1), 89–97.

Rippa, M., & Pontremoli, S. (1968). Evidence of a critical histidine residue in 6-phosphogluconate dehydrogenase from Candida utilis. *Biochemistry*, *7*(4), 1514–1518.

Robinson, A. B., McKerrow, J. H., & Legaz, M. (1974). Sequence dependent deamidation rates for model peptides of cytochrome C. *International Journal of Peptide & Protein Research*, *6*(1), 31–35.

Robinson, N. E., & Robinson, A. B. (2001a). Molecular clocks. *Proceedings of the National Academy of Sciences of the United States of America*, *98*(3), 944–949.

Robinson, N. E., & Robinson, A. B. (2001b). Prediction of protein deamidation rates from primary and three-dimensional structure. *Proceedings of the National Academy of Sciences of the United States of America*, *98*(8), 4367–4372.

Robinson, N. E., & Robinson, A. B. (2004). *Molecular clocks: Deamidation of asparaginyl and gltaminyl residues in peptides and proteins*. Cave Junction, OR: Althouse Press.

Robinson, A. B., Scotchler, J. W., & McKerrow, J. H. (1973). Rates of nonenzymatic deamidation of glutaminyl and asparaginyl residues in pentapeptides. *Journal of the American Chemical Society*, *95*, 8156–8159.

Ryan, M. E., Webster, M. L., & Statler, J. D. (1996). Adverse effects of intravenous immunoglobulin therapy. *Clinical Pediatrics (Philadelphia)*, *35*(1), 23–31.

Schoneich, C. (2000). Mechanisms of metal-catalyzed oxidation of histidine to 2-oxo-histidine in peptides and proteins. *Journal of Pharmaceutical and Biomedical Analysis*, *21*(6), 1093–1097.

Schreiber, G. (2002). Kinetic studies of protein-protein interactions. *Current Opinion in Structural Biology*, *12*(1), 41–47.

Schultz, J. (1967). Cleavage at aspartic acids. *Methods in Enzymology*, *11*, 255–263.

Scochler, J. W., & Robinson, A. B. (1974). Deamidation of glutaminyl residues: dependence on pH, temperature and ionic strength. *Analytical Biochemistry*, *59*.

Sen, A. C., Ueno, N., & Chakrabarti, B. (1992). Studies on human lens: I. Origin and development of fluorescent pigments. *Photochemistry and Photobiology*, *55*(5), 753–764.

Shaked, Z., Szajewski, R. P., & Whitesides, G. M. (1980). Rates of thiol-disulfide interchange reactions involving proteins and kinetic measurements of thiol pka values. *Biochemistry*, *19*(18), 4156–4166.

Shao, Z. Z., Li, Y. P., Krishnamoorthy, R., Chermak, T., & Mitra, A. K. (1993). Differential-effects of anionic, cationic, nonionic, and physiological surfactants on the dissociation, alpha-chymotryptic degradation, and enteral absorption of insulin hexamers. *Pharmaceutical Research*, *10*(2), 243–251.

Sharma, V. K. (2013). *Oxidation of amino acids, peptides and proteins*. Hoboken, NJ: John Wiley & Sons.

Sharma, V. K., & Graham, N. J. D. (2010). Oxidation of amino acids, peptides and proteins by ozone: a review. *Ozone Science & Engineering*, *32*(2), 81–90.

Shimoda, N., & Kawaguchi, T. (1986). *Method and composition for preventing the adsorption of a medicine*. C. S. K. Kaisha. EP0178576 A1.

Shire, S. J. (1996). Stability characterization and formulation development of recombinant human deoxyribonuclease I [Pulmozyme, (dornase alpha)]. In R. Pearlman, & J. Wang (Eds.), *Formulation, characterization and stability of protein drugs* (pp. 393–426). New York: Plenum.

Shire, S. J., Holladay, L. A., & Rinderknecht, E. (1991). Self-association of human and porcine relaxin as assessed by analytical ultracentrifugation and circular-dichroism. *Biochemistry*, *30*(31), 7703–7711.

Singh, S. K., Afonina, N., Awwad, M., Bechtold-Peters, K., Blue, J. T., Chou, D., et al. (2010). An industry perspective on the monitoring of subvisible particles as a quality attribute for protein therapeutics. *Journal of Pharmaceutical Sciences*, *99*(8), 3302–3321.

Singh, S. K., Kolhe, P., Mehta, A. P., Chico, S. C., Lary, A. L., & Huang, M. (2011). Frozen state storage instability of a monoclonal antibody: aggregation as a consequence of trehalose crystallization and protein unfolding. *Pharmaceutical Research*, *28*(4), 873–885.

Sluzky, V., Tamada, J. A., Klibanov, A. M., & Langer, R. (1991). Kinetics of Insulin Aggregation in Aqueous-Solutions Upon Agitation in the Presence of Hydrophobic Surfaces. *Proceedings of the National Academy of Sciences of the United States of America*, *88*(21), 9377–9381.

Snyder, G. H., Cennerazzo, M. J., Karalis, A. J., & Field, D. (1981). Electrostatic influence of local cysteine environments on disulfide exchange kinetics. *Biochemistry*, *20*(23), 6509–6519.

Sreedhara, A., Cordoba, A., Zhu, Q., Kwong, J., & Liu, J. (2012). Characterization of the isomerization products of aspartate residues at two different sites in a monoclonal antibody. *Pharmaceutical Research*, *29*(1), 187–197.

Sreedhara, A., Lau, K., Li, C., Hosken, B., Macchi, F., Zhan, D. J., et al. (2013). Role of surface exposed tryptophan as substrate generators for the antibody catalyzed water oxidation pathway. *Molecular Pharmaceutics*, *10*(1), 278–288.

Stadtman, E. R. (1990). Metal ion-catalyzed oxidation of proteins – biochemical-mechanism and biological consequences. *Free Radical Biology and Medicine*, *9*(4), 315–325.

Stadtman, E. R. (1993). Oxidation of free amino-acids and amino-acid-residues in proteins by radiolysis and by metal-catalyzed reactions. *Annual Review of Biochemistry*, *62*, 797–821.

Stadtman, E. R., & Berlett, B. S. (1998). Reactive oxygen-mediated protein oxidation in aging and disease. *Drug Metabolism Reviews*, *30*(2), 225–243.

Stadtman, E. R., & Levine, R. L. (2000). Protein oxidation. *Reactive Oxygen Species: From Radiation to Molecular Biology*, *899*, 191–208.

Strambini, G. B., & Gabellieri, E. (1996). Proteins in frozen solutions: evidence of ice-induced partial unfolding. *Biophysical Journal*, *70*(2), 971–976.

Swallow, A. J. (1960). Effect of ionizing radiation on proteins, RCO groups, peptide bond cleavage, inactivation – SH oxidation. In A. J. Swallow (Ed.), *Radiation chemistry of organic compounds* (p. 211). New York: Pergamon Press.

Sysak, P. K., Foote, C. S., & Ching, T. Y. (1977). Chemistry of singlet oxygen. 25. Photooxygenation of methionine. *Photochemistry and Photobiology*, *26*(1), 19–27.

Tanford, C. (1968). Protein denaturation. In C. Anfinsen, A. ML, J. Edsall, & F. M. Richards (Eds.), *Advances in protein chemistry* (Vol. 23) (pp. 121–282). New York: Academic Press.

Taschner, N., Muller, S. A., Alumella, V. R., Goldie, K. N., Drake, A. F., Aebi, U., et al. (2001). Modulation of antigenicity related to changes in antibody flexibility upon lyophilization. *Journal of Molecular Biology*, *310*(1), 169–179.

Teh, L. C., Murphy, L. J., Huq, N. L., Surus, A. S., Friesen, H. G., Lazarus, L., et al. (1987). Methionine oxidation in human growth-hormone and human chorionic somatomammotropin – effects on receptor-binding and biological-activities. *Journal of Biological Chemistry*, *262*(14), 6472–6477.

Teshima, G., Stults, J. T., Ling, V., & Canovadavis, E. (1991). Isolation and characterization of a succinimide variant of methionyl human growth-hormone. *Journal of Biological Chemistry*, *266*(21), 13544–13547.

Thakkar, S. V., Joshi, S. B., Jones, M. E., Sathish, H. A., Bishop, S. M., Volkin, D. B., et al. (2012). Excipients differentially influence the conformational stability and pretransition dynamics of two IgG1 monoclonal antibodies. *Journal of Pharmaceutical Sciences*, *101*(9), 3062–3077.

Tian, F., Middaugh, C. R., Offerdahl, T., Munson, E., Sane, S., & Rytting, J. H. (2007). Spectroscopic evaluation of the stabilization of humanized monoclonal antibodies in amino acid formulations. *International Journal of Pharmaceutics*, *335*(1–2), 20–31.

Timm, V., Gruber, P., Wasiliu, M., Lindhofer, H., & Chelius, D. (2010). Identification and characterization of oxidation and deamidation sites in monoclonal rat/mouse hybrid antibodies. *Journal of Chromatography. B, Analytical Technologies in the Biomedical and Life Sciences*, *878*(9–10), 777–784.

Tomita, M., Irie, M., & Ukita, T. (1969). Sensitized photooxidation of histidine and its derivatives. Products and mechanism of the reaction. *Biochemistry*, *8*(12), 5149–5160.

Tomizawa, H., Yamada, H., Ueda, T., & Imoto, T. (1994). Isolation and characterization of 101-Succinimide lysozyme that possesses the cyclic imide at Asp101-Gly102. *Biochemistry*, *33*(29), 8770–8774.

Torosantucci, R., Sharov, V. S., van Beers, M., Brinks, V., Schoneich, C., & Jiskoot, W. (2013). Identification of oxidation sites and covalent cross-links in metal catalyzed oxidized interferon Beta-1a: potential implications for protein aggregation and immunogenicity. *Molecular Pharmaceutics*, *10*(6), 2311–2322.

Tous, G. I., Wei, Z. P., Feng, J. H., Bilbulian, S., Bowen, S., Smith, J., et al. (2005). Characterization of a novel modification to monoclonal antibodies: thioether cross-link of heavy and light chains. *Analytical Chemistry*, *77*(9), 2675–2682.

Treuheit, M. J., Kosky, A. A., & Brems, D. N. (2002). Inverse relationship of protein concentration and aggregation. *Pharmaceutical Research*, *19*(4), 511–516.

Tsong, T. Y., Baldwin, R. L., & Elson, E. L. (1971). The sequential unfolding of ribonuclease A: detection of a fast initial phase in the kinetics of unfolding. *Proceedings of the National Academy of Sciences of the United States of America*, *68*(11), 2712–2715.

Tyagi, A. K., Randolph, T. W., Dong, A., Maloney, K. M., Hitscherich, C., Jr., & Carpenter, J. F. (2009). IgG particle formation during filling pump operation: a case study of heterogeneous nucleation on stainless steel nanoparticles. *Journal of Pharmaceutical Sciences*, *98*(1), 94–104.

Tyler-Cross, R., & Schirch, V. (1991). Effects of amino acid sequence, buffers, and ionic strength on the rate and mechanism of deamidation of asparagine residues in small peptides. *Journal of Biological Chemistry*, *266*(33), 22549–22556.

Uchida, K. (2003). Histidine and lysine as targets of oxidative modification. *Amino Acids*, *25* (3–4), 249–257.

Uchida, K., & Kawakishi, S. (1990). Site-specific oxidation of angiotensin-I by copper(II) and L-ascorbate – conversion of histidine-residues to 2-imidazolones. *Archives of Biochemistry and Biophysics*, *283*(1), 20–26.

Underwood, L. E., Voina, S. J., & Van Wyk, J. J. (1974). Restoration of growth by human growth hormone (Roos) in hypopituitary dwarfs immunized by other human growth hormone preparations: clinical and immunological studies. *Journal of Clinical Endocrinology and Metabolism*, *38*(2), 288–297.

Usami, A., Ohtsu, A., Takahama, S., & Fujii, T. (1996). Effect of pH, hydrogen peroxide and temperature on the stability of human monoclonal antibody. *Journal of Pharmaceutical and Biomedical Analysis*, *14*(8–10), 1133–1140.

Vermeer, A. W. P., Bremer, M. G. E. G., & Norde, W. (1998). Structural changes of IgG induced by heat treatment and by adsorption onto a hydrophobic Teflon surface studied by circular dichroism spectroscopy. *Biochimica Et Biophysica Acta-General Subjects*, *1425*(1), 1–12.

Vermeer, A. W. P., Giacomelli, C. E., & Norde, W. (2001). Adsorption of IgG onto hydrophobic teflon. Differences between the F-ab and F-c domains. *Biochimica Et Biophysica Acta-General Subjects*, *1526*(1), 61–69.

Violand, B. N., Schlittler, M. R., Kolodziej, E. W., Toren, P. C., Cabonce, M. A., Siegel, N. R., et al. (1992). Isolation and characterization of porcine somatotropin containing a succinimide residue in place of Aspartate-129. *Protein Science*, *1*(12), 1634–1641.

Vlasak, J., & Ionescu, R. (2008). Heterogeneity of monoclonal antibodies revealed by charge-sensitive methods. *Current Pharmaceutical Biotechnology*, *9*(6), 468–481.

Voorter, C. E. M., Dehaardhoekman, W. A., Vandenoetelaar, P. J. M., Bloemendal, H., & Dejong, W. W. (1988). Spontaneous peptide-bond cleavage in aging alpha-crystallin through a succinimide intermediate. *Journal of Biological Chemistry*, *263*(35), 19020–19023.

Wakankar, A. A., Borchardt, R. T., Eigenbrot, C., Shia, S., Wang, Y. J., Shire, S. J., et al. (2007). Aspartate isomerization in the complementarity-determining regions of two closely related monoclonal antibodies. *Biochemistry*, *46*(6), 1534–1544.

Wang, Y.-C. J., & Hanson, M. A. (1988). Parenteral formulations of proteins and peptides: stability and stabilizers. *Journal of Parenteral Science and Technology*, *42*(Suppl.), S3–S26.

Wang, W., & Roberts, C. J. (Eds.). (2010). *Aggregation of therapeutic proteins*. Hoboken, NJ: John Wiley & Sons.

Wang, W., Singh, S., Zeng, D. L., King, K., & Nema, S. (2007). Antibody structure, instability, and formulation. *Journal of Pharmaceutical Sciences*, *96*(1), 1–26.

Wang, W. R., Vlasak, J., Li, Y. S., Pristatsky, P., Fang, Y. L., Pittman, T., et al. (2011). Impact of methionine oxidation in human IgG1 Fc on serum half-life of monoclonal antibodies. *Molecular Immunology*, *48*(6–7), 860–866.

Wei, Z. P., Feng, J. H., Lin, H. Y., Mullapudi, S., Bishop, E., Tous, G. I., et al. (2007). Identification of a single tryptophan residue as critical for binding activity in a humanized monoclonal antibody against respiratory syncytial virus. *Analytical Chemistry*, *79*(7), 2797–2805.

Wentworth, P., Jones, L. H., Wentworth, A. D., Zhu, X. Y., Larsen, N. A., Wilson, I. A., et al. (2001). Antibody catalysis of the oxidation of water. *Science*, *293*(5536), 1806–1811.

Wisniewski, R., & Wu, V. L. (1996). Large-scale freezing and thawing of biopharmaceutical products. In K. E. Avis (Ed.), *Biotechnology and biopharmaceutical manufacturing, processing, and preservation* (Vol. 2) (pp. 7–50). USA: Interpharm/CRC Press.

Wong, C., Strachan-Mills, C., & Burman, S. (2012). Facile method of quantification for oxidized tryptophan degradants of monoclonal antibody by mixed mode ultra performance liquid chromatography. *Journal of Chromatography A*, *1270*, 153–161.

Wright, H. T. (1991a). Nonenzymatic deamidation of asparaginyl and glutaminyl residues in proteins. *Critical Reviews in Biochemistry and Molecular Biology*, *26*(1), 1–52.

Wright, H. T. (1991b). Sequence and structure determinants of the nonenzymatic deamidation of asparagine and glutamine residues in proteins. *Protein Engineering*, *4*(3), 283–294.

Wypych, J., Li, M., Guo, A., Zhang, Z. Q., Martinez, T., Allen, M. J., et al. (2008). Human IgG2 antibodies display disulfide-mediated structural isoforms. *Journal of Biological Chemistry*, *283*(23), 16194–16205.

Yamagata, S., Takahashi, K., & Egami, F. (1962). The structure and function of ribonuclease T1. IV. Photooxidation of ribonuclease T1. *Journal of Biochemistry*, *52*, 261–266.

Yang, T. H., Cleland, J. L., Lam, X., Meyer, J. D., Jones, L. S., Randolph, T. W., et al. (2000). Effect of zinc binding and precipitation on structures of recombinant human growth hormone and nerve growth factor. *Journal of Pharmaceutical Sciences*, *89*(11), 1480–1485.

Yang, T. H., Dong, A. C., Meyer, J., Johnson, O. L., Cleland, J. L., & Carpenter, J. F. (1999). Use of infrared spectroscopy to assess secondary structure of human growth hormone within biodegradable microspheres. *Journal of Pharmaceutical Sciences*, *88*(2), 161–165.

Yang, A. S., Gunner, M. R., Sampogna, R., Sharp, K., & Honig, B. (1993). On the calculation of Pk(a)s in Proteins. *Proteins Structure Function and Genetics*, *15*(3), 252–265.

Zhang, W., & Czupryn, M. J. (2002). Free sulfhydryl in recombinant monoclonal antibodies. *Biotechnology Progress*, *18*(3), 509–513.

Zhang, J., Yip, H., & Katta, V. (2011). Identification of isomerization and racemization of aspartate in the Asp-Asp motifs of a therapeutic protein. *Analytical Biochemistry*, *410*(2), 234–243.

Zhang, T., Zhang, J., Hewitt, D., Tran, B., Gao, X. Y., Qiu, Z. J., et al. (2012). Identification and characterization of buried unpaired cysteines in a recombinant monoclonal IgG1 antibody. *Analytical Chemistry*, *84*(16), 7112–7123.

Zhao, F., Ghezzo-Schoneich, E., Aced, G. I., Hong, J., Milby, T., & Schoneich, C. (1997). Metal-catalyzed oxidation of histidine in human growth hormone. Mechanism, isotope effects, and inhibition by a mild denaturing alcohol. *Journal of Biological Chemistry*, *272*(14), 9019–9029.

Zheng, J. Y., & Janis, L. J. (2006). Influence of pH, buffer species, and storage temperature on physicochemical stability of a humanized monoclonal antibody LA298. *International Journal of Pharmaceutics*, *308*(1–2), 46–51.

Formulation of proteins and monoclonal antibodies (mAbs)

4

As discussed previously in Chapter 1, formulation to attain stability is only one area for successful pharmaceutical development. It is not necessary to provide a formulation that provides the best stability, but rather only one that meets the overall requirements for the target product profile. In this chapter, we will discuss the overall approaches used for development of formulations for protein therapeutics as well as the challenges and issues that occur during development. Previously the different degradation routes that proteins undergo were reviewed. Essentially the diversity of chemistry due to the differences in the 20 common amino acids that make up a protein results in challenges in determining the optimal conditions whereby the different degradation routes are all minimized. In addition to the chemical degradations, physical degradation routes involving conformational changes and aggregation also need to be addressed. This greater complexity of instability differentiates protein drugs from the more traditional small-molecule drugs.

Formulation of monoclonal antibodies

As discussed previously in Chapter 3, a majority of monoclonal antibodies (mAbs) have been formulated for IV administration. A summary of formulations of 46 mAbs, Fc fusion, and Fab conjugates approved in the US is shown in Table 4.1. More than half of the formulations (29) are liquids and the remaining (19) solid dosage forms prepared by lyophilization.

Dosage form assessment—solid versus liquid dosage forms

The choice between a liquid and solid dosage form requires a careful assessment of the TPP, which uses several sources including marketing research, formulation, and process development. Liquid products are more convenient for the end user, and can ensure better patient compliance since reconstitution of the product is not required. In addition, dosing accuracy may be better than for a reconstituted solid dosage form since considerable error may occur on measurement of volume added for reconstitution. However, since many of the chemical degradation routes are hydrolytically driven, the liquid formulations are usually less stable than solid dosage forms, which may limit their shelf life and require special handling during manufacture, shipping, storage, and use. Although it may be possible to minimize those reactions that reduce activity or quality of the final product, it usually is more difficult to control the physical stability of liquid protein products since proteins and mAbs are inherently sensitive to exposure to surfaces in the liquid state and may denature or aggregate if not adequately protected or appropriately handled. Exposure to final manufacturing

Monoclonal Antibodies. http://dx.doi.org/10.1016/B978-0-08-100296-4.00004-X

Table 4.1 Formulations for antibodies, Fc fusion, and Fab conjugates approved in the US

Brand name	Molecule	Dosage form	Administration route	Formulation
Abthrax	Raxibacumab	50 mg/mL, 35 mL per vial	IV infusion	Citric acid 0.13 mg/mL, sodium citrate 2.8 mg/mL, glycine 18 mg/mL, polysorbate 80, 0.2 mg/mL, sucrose 10 mg/mL, with a pH of 6.5
Actemera	Tocilizumab	Liquid: 80 mg/4 mL single-dose vial, 200 mg/10 mL single-dose vial, 400 mg/20 mL single-dose vial	IV infusion: 20 mg/mL solution in all vials (pH 6.5)	80 mg/4 mL (2.21 mg sodium) 200 mg/10 mL (4.43 mg sodium) and 400 mg/20 mL (8.85 mg sodium) vials: disodium phosphate dodecahydrate and sodium dihydrogen phosphate dehydrate (as a 15 mmol per L phosphate buffer), 0.5 mg/mL polysorbate 80, 50 mg/mL sucrose, water for injection SC approved October 2013
Adecetris	Brentuximab vedotin	Lyophilized: 50 mg single-dose vial	IV infusion: reconstituted with 10.5 mL of preservative-free sterile water for injection (pH 6.6)	5 mg/mL brentuximab vedotin single-dose vials: 70 mg/mL trehalose dihydrate, 5.6 mg/mL sodium citrate dihydrate, 0.21 mg/mL citric acid monohydrate, 0.20 mg/mL polysorbate 80, water for injection
Amevive	**Alefacept**	Lyophilized: 7.5 and 15 mg single-dose vial	IV infusion or intramuscular injection: 7.5 and 15 mg vials to be reconstituted with 0.5 mL of water for injection (pH 6.9)	0.5 mL reconstituted vials: 12.5 mg sucrose; 5 mg glycine; 3.6 mg sodium citrate dehydrate; 0.06 mg citric acid monohydrate
Arcalyst	Rilonacept	Lyophilized: 20 mL single-dose vial with 160 mg rilonacept	SC injection: reconstitute with 2.3 mL of sterile water for injection 80 mg/mL rilonacept (pH 6.2–6.8)	160 mg vial: 40 mM histidine; 50 mM arginine; 3.0% (w/v) polyethylene glycol 3350; 2.0% (w/v) sucrose; 1.0% (w/v) glycine
Azerra	Ofatumumab	Liquid: 100 mg/5 mL single-use vial; 1000 mg/50 mL single-use vial	IV infusion: 20 mg/mL solution in all vials (pH 5.5)	100 and 1000 mg vials: 10 mg/mL arginine, diluted hydrochloric acid, 0.019 mg/mL edentate disodium, 0.2 mg/mL polysorbate 80, 6.8 mg/mL sodium acetate, 2.98 mg/mL sodium chloride, water for injection

Avastin	Bevacizumab	Liquid: 100 mg/4 mL single-use vial; 400 mg/16 mL single-use vial	IV infusion: 25 mg/mL solution (pH 6.2)	100 mg vial: 240 mg α,α-trehalose dehydrate; 23.3 mg sodium phosphate (monobasic, monohydrate); 4.8 mg sodium phosphate (dibasic, anhydrous); 1.6 mg polysorbate 20; water for injection 400 mg vial: 960 mg α,α-trehalose dehydrate; 92.8 mg sodium phosphate (monobasic, monohydrate); 19.2 mg sodium phosphate (dibasic, anhydrous); 6.4 mg polysorbate 20; water for injection
Benlysta	Belimumab	Lyophilized: 120 mg/5 mL single-dose vial; 400 mg/20 mL single-dose vial	IV infusion: 80 mg/mL reconstituted with free sterile water for injection (pH 6.5)	120 mg/5mL and 400 mg/20 mL vials: 0.16 mg/mL citric acid, 0.4 mg/mL polysorbate 80, 2.7 mg/mL sodium citrate, 80 mg/mL sucrose
Blincyto	**Blinatumomab**	Lyophilized single-use vials	IV infusion: IV solution stabilizer is added to IV bags and lyophilized vial reconstituted with SWFI added. Note that IV solution stabilizer is not to be used to reconstitute the vials	Each single-use vial of Blincyto contains 35 mcg blinatumomab, citric acid monohydrate (3.35 mg), lysine hydrochloride (23.23 mg), polysorbate 80 (0.64 mg), trehalose dihydrate (95.5 mg), and sodium hydroxide to adjust pH to 7.0. After reconstitution with 3 mL of preservative-free Sterile Water for Injection, USP, the resulting concentration is 12.5 mcg/mL blinatumomab IV Solution Stabilizer is supplied in a single-use vial as a sterile, preservative-free, colorless to slightly yellow, clear solution. Each single-use vial of IV Solution Stabilizer contains citric acid monohydrate (52.5 mg), lysine hydrochloride (2283.8 mg), polysorbate 80 (10 mg), sodium hydroxide to adjust pH to 7.0, and water for injection

Continued

Table 4.1 Formulations for antibodies, Fc fusion, and Fab conjugates approved in the US—cont'd

Brand name	Molecule	Dosage form	Administration route	Formulation
Bexxar	Tositumomab and I-131 Tositumomab	Liquid: 35 and 225 mg single-use vial	Intravenous infusion: 2.5 mL for 35 mg vial; 16.1 mL for 225 mg vial; 14 mg/mL solution (pH 7.2)	35 and 225 mg vials: 10% maltose; 145 mM sodium chloride; 10 mM phosphate; water for injection
Campath	Alemtuzumab	Liquid: 30 mg/mL single-use vial	IV: 1 mL (pH 6.8–7.4)	40 mg vial: 8.0 mg sodium chloride; 1.44 mg dibasic sodium phosphate; 0.2 mg potassium chloride; 0.2 mg monobasic sodium phosphate; 0.1 mg polysorbate 80; 0.0187 mg disodium edetate dehydrate
Cimzia	Certolizumab pegol	Lyophilized: 200 mg single-dose vial Liquid: single-use prefilled 1 mL syringe	SC injection: reconstitute with 1 mL of sterile water for injection (pH 5.2)	200 mg vial: 100 mg sucrose; 0.9 mg lactic acid; 0.1 mg polysorbate
Enbrel	TNFR-Fc	Lyophilized: 25 mg multidose vial Liquid: 25 mg single-use prefilled syringe; 50 mg single-use autoinjector	SC: reconstituted lyo product with sterile water for injection (SWFI) (pH 7.2); all solutions are 50 mg/mL concentration (liquid formulation: pH 6.1–6.5; lyophilized pH 7.1–7.7	25 mg lyophilized vial: 40 mg mannitol; 10 mg sucrose; 1.2 mg tromethamine Liquid solutions: 1% sucrose; 100 mM sodium chloride; 25 mM L-arginine hydrochloride; 25 mM sodium phosphate
Entyvio	**Vedolizumab**	Lyophilized 300 mg per vial	IV infusion	Each single-use vial contains 300 mg vedolizumab, 23 mg L-histidine, 21.4 mg L-histidine monohydrochloride, 131.7 mg L-arginine hydrochloride, 500 mg sucrose and 3 mg polysorbate 80, pH 6.3 upon reconstitution

Erbitux	Centuximab	Liquid: 100 mg/50 mL single-use vial; 200 mg/100 mL single-use vial	IV infusion: 2 mg/mL solution in all vials (pH 7.0–7.4)	100 and 200 mg vials: 8.48 mg/mL sodium chloride; 1.88 mg/mL sodium phosphate dibasic heptahydrate; 0.41 mg/mL sodium phosphate monobasic monohydrate; water for injection
Eylea	Aflibercept	Liquid: 2 mg/0.05 mL single-dose vial	Ophthalmic intravenous injection: 40 mg/mL solution in all vials (pH 6.2)	2 mg/0.05 mL vial: 10 mM sodium phosphate, 40 mM sodium chloride, 0.03% polysorbate 20, 5% sucrose
Gazyva	**Obinutuzumab**	25 mg/mL; 1000 mg per vial	IV infusion	20 mM histidine chloride, 240 mM trehalose, 0.02% poloxamer 188, with a pH of 6.0
Herceptin	Trastuzumab	Lyophilized 440 mg multidose vial	IV: reconstitute with 20 mL bacteriostatic water for injection or SWFI (for single-use vial (pH 6.0)	440 mg vial: 400 mg α,α-trehalose dihydrate; 9.9 mg L-histidine HCl; 6.4 mg L-histidine; 1.8 mg polysorbate 20
Humira	Adalimumab	Liquid: 1 mL PFS	SC: 40 mg/0.8 mL solution (pH 5.2)	0.8 mL solution in PFS: 4.93 mg sodium chloride; 0.69 mg monobasic sodium phosphate dehydrate; 1.22 mg dibasic sodium phosphate dehydrate; 0.24 mg sodium citrate; 1.04 mg citric acid monohydrate; 9.6 mg mannitol; 0.8 mg polysorbate 80; water for injection
Ilaris	Canakinumab	Lyophilized: 180 mg single-dose vial	SC injection: reconstituted with 1 mL of preservative-free SWFI	180 mg vial: sucrose; L-histidine; L-histidine HCl monohydrate; polysorbate 80
Kadcyla	Ado-trastuzumab emtansine	Lyophilized 100 or 160 mg per vial	IV infusion	Upon reconstitution, it contains 20 mg/mL Ado-trastuzumab emtansine with 0.02% polysorbate 20, 10 mM sodium succinate, 6% sucrose, with a pH of 5.0
Keytruda	**Pembrolizuma**	Lyophilized 50 mg vial	IV infusion	Upon reconstitution each 2 mL solution contains L-histidine (3.1 mg), polysorbate 80 (0.4 mg), sucrose (140 mg), and small amounts of HCl/NaOH to adjust pH to 5.5

Continued

Table 4.1 Formulations for antibodies, Fc fusion, and Fab conjugates approved in the US—cont'd

Brand name	Molecule	Dosage form	Administration route	Formulation
Lucentis	Ranibizumab	Liquid: 0.5 mg single-use vial	Intravitreal injection: 0.05 mL (pH 5.5)	10 mg/mL vial: 10 mM histidine HCl; 10% α,α-trehalose dihydrate, 0.01% polysorbate 20
Mylotarg	**Gemtuzumab ozogamicin**	Lyophilized: 5 mg single-dose vial	IV: reconstitute with 5 mL of SWFI	5 mg vial: dextran 40; sucrose; sodium chloride; monobasic and dibasic sodium phosphate
Opdivo	**Nivolumab**	Liquid single-use formulation, 4 and 10 mL vials at 10 mg/mL nivolumab	The required volume of OPDIVO is transferred into an intravenous container, and diluted with either 0.9% sodium chloride injection, USP or 5% dextrose injection, USP, to prepare an infusion with a final concentration ranging from 1 to 10 mg/mL	Each mL of OPDIVO solution contains nivolumab 10 mg, mannitol (30 mg), pentetic acid (0.008 mg), polysorbate 80 (0.2 mg), sodium chloride (2.92 mg), sodium citrate dihydrate (5.88 mg), and water for injection, USP. May contain hydrochloric acid and/or sodium hydroxide to adjust pH to 6
Orencia	**Abatacept**	Lyophilized: 250 mg single-use vial	IV infusion: reconstitute with 10 mL SWFI (pH 7.2–7.8)	250 mg vial: 500 mg maltose; 17.2 mg monobasic sodium phosphate; 14.6 mg sodium chloride
Orthoclone OKT-3	Muromab-CD3	Liquid: 5 mg ampoule	IV	5 mg ampoule: 2.25 mg monobasic sodium phosphate; 9.0 mg dibasic sodium phosphate; 43 mg sodium chloride; 1.0 mg polysorbate 80
Perjeta	Pertuzumab	Liquid: 420 mg/14 mL single-use vial	IV infusion: 30 mg/mL solution in all vials (pH 6.0)	420 mg/14 mL (30 mg/mL) vials: 20 mM L-histidine acetate, 120 mM sucrose and 0.02% polysorbate 20
Prolia	Denosumab	Liquid: 60 mg/1 mL single-dose vial; 60 mg/1 mL single-dose prefilled syringe	SC injection: 60 mg/mL solution (pH 5.2)	Single-dose vial: 4.7% sorbitol, 17 mM acetate, sodium hydroxide, water for injection Single-dose prefilled syringe: 4.7% sorbitol, 17 mM acetate, 0.01% polysorbate 20, sodium hydroxide, water for injection

Raptiva	Efalizumab	Lyophilized: 150 mg single-use vial	SC injection: reconstitute with 1.3 mL water for injection (pH 6.2)	150 mg vial: 123.2 mg sucrose; 6.8 mg L-histidine hydrochloride monohydrate; 4.3 mg L-histidine; 3 mg polysorbate 20
Remicade	Infliximab	Lyophilized: 100 mg single-use vial	IV: reconstitute with SWFI (pH 7.2)	100 mg vial: 500 mg sucrose; 0.5 mg polysorbate 80; 2.2 mg monobasic sodium phosphate monohydrate; 6.1 mg dibasic sodium phosphate dihydrate
Removab	Catumaxomab	Liquid: prefilled syringe 10 mg in 0.1 mL solution or 50 mg in 0.5 mL solution	Intraperitoneal infusion: 0.1 mg/mL solution in prefilled syringe	First of other ingredients: sodium citrate, citric acid monohydrate, polysorbate 80, and water for injection
Reopro	Abciximab	Liquid: 10 mg single-use vial	IV: 5 mL (pH 7.2)	10 mg vial: 0.01 M sodium phosphate; 0.15 M sodium chloride; 0.001% polysorbate 80; water for injection
Rituxan	Rituximab	Liquid: 100 and 500 mg single-use vial	IV: 10 mg/mL, solution (pH 6.5)	100 mg (10 mL) and 500 mg (50 mL) vials: 9 mg/mL sodium chloride; 7.35 mg/mL sodium citrate dihydrate; 0.7 mg/mL polysorbate 80; water for injection
Scintimun	Besilesomab	Lyophilized powder: 1 mg single-use vial	Intravenous injection: reconstitution with 6 mL solution of propane tetraphosphonic acid (PTP) (tranchelator agent), tin (II) chloride (or stannous chloride) (reducing agent), sodium hydroxide, and hydrochloric acid (pH adjustment)	1 mg vial: sodium dihydrogen phosphate and disodium hydrogen phosphate and sorbitol
Simponi	Golimumab	Liquid: 50 mg single-dose PFS; single-dose prefilled autoinjector	SC injection: 0.5 mL (pH 5.5)	0.5 mL solution: 50 mg golimumab antibody; 0.44 mg L-histidine and L-histidine monohydrochloride monohydrate; 20.5 mg sorbitol; 0.08 mg polysorbate 80; water for injection

Continued

Table 4.1 Formulations for antibodies, Fc fusion, and Fab conjugates approved in the US—cont'd

Brand name	Molecule	Dosage form	Administration route	Formulation
Simulect	Basiliximab	Lyophilized: 10 and 20 mg single-use vials	Central or peripheral IV	10 mg vial: 3.61 mg monobasic potassium phosphate; 0.50 mg disodium hydrogen phosphate (anhydrous); 0.80 mg sodium chloride; 10 mg sucrose; 40 mg mannitol; 20 mg glycine 20 mg vial: 7.211 mg monobasic potassium phosphate; 0.99 mg disodium hydrogen phosphate (anhydrous); 1.61 mg sodium chloride; 20 mg sucrose; 80 mg mannitol; 40 mg glycine
Soliris	Eculizumab	Liquid: 300 mg single-use vial	IV infusion: 30 mL (pH 7.0)	300 mg vial: 13.8 mg sodium phosphate monobasic; 53.4 mg sodium phosphate dibasic; 263.1 sodium chloride; 6.6 mg polysorbate 80 (vegetable origin); water for injection
Stelara	Ustekinumab	Liquid: 45 mg/0.5 mL and 90 mg/1 mL single-dose prefilled syringe; 45 mg/0.5 mL and 90 mg/1 mL single-dose vials	SC injection: 90 mg/mL solution in all vials and prefilled syringes (pH = 5.7–6.3)	Single-dose vial and single-dose prefilled syringe: 1 mg/mL L-histidine and L-histidine monohydrochloride monohydrate, 0.04 mg/mL polysorbate 80, 76 mg/mL sucrose
Sylvant	Siltuximab	Lyophilized: 100 and 400 mg single-use vial	IV infusion: add 5.2 mL to 100 mg vial and 20 mL to 400 mg vial. Final concentration at 20 mg/mL siltuximab. Administration over 1 h IV after dilution into 250 mL 5% dextrose	Each Sylvant 100 mg single-use vial contains 100 mg siltuximab, 3.7 mg L-histidine (from L-histidine and L-histidine monohydrochloride monohydrate), 0.8 mg polysorbate 80, and 169 mg sucrose Each Sylvant 400 mg single-use vial contains 400 mg siltuximab, 14.9 mg L-histidine (from L-histidine and L-histidine monohydrochloride monohydrate), 3.2 mg polysorbate 80, and 677 mg sucrose

Synagis	Pavlizumab	Liquid: 50 and 100 mg single-dose vial	IM: 1 mL of 100 mg/mL or 2 mL of 50 mg/mL solution (pH 6.0)	50 mg vial: 1.9 mg histidine; 0.06 mg glycine; 0.2 mg chloride 100 mg vial: 3.9 mg histidine; 0.1 mg glycine; 0.5 mg chloride
Tysabri	Natalizumab	Liquid: 300 mg single-use vial	IV infusion: 15 mL (pH 6.1)	300 mg vial: 123 mg sodium chloride; 17.0 mg sodium phosphate, monobasic, monohydrate; 7.24 mg sodium phosphate, dibasic, heptahydrate; 3.0 mg polysorbate 80; water for injection
Vectibix	Panitumumab	Liquid: 100 mg/50 mL single-use vial; 200 mg/100 mL single-use vial; 400 mg/200 mL single-use vial	IV infusion: 2 mg/mL solution in all vials (pH 5.6–6.0)	100 mg vial: 29 mg sodium chloride; 34 mg sodium acetate; water for injection 200 and 400 mg vials contain the same excipients at the same ratio to panitumumab as the 100 mg vial
Xgeva	Denosumab	Liquid: 120 mg/1.7 mL single-dose vial	SC injection: 70 mg/mL solution in all vials (pH 5.2)	Single-dose vial: 4.6% sorbitol, 18 mM acetate, sodium hydroxide, water for injection
Xolair	Omalizumab	Lyophilized: 202.5 mg single-use vial	SC injection: reconstitute with 1.4 mL SWFI	202.5 mg vial: 145.5 mg sucrose; 2.8 mg L-histidine hydrochloride monohydrate; 1.8 mg L-histidine; 0.5 mg polysorbate 20
Yervoy	Ipilimumab	Liquid: 500 mg/10 mL single-dose vial; 200 mg/40 mL single-dose vial (pH 7)	Intravenous infusion: 5 mg/mL solution in all vials	500 mg/10 mL and 200 mg/40 mL vials: 0.04 mg/mL pentetic acid, 10 mg/mL mannitol, 0.1 mg/mL polysorbate 80, 5.85 mg/mL sodium chloride, 3.15 mg/mL tromethamine hydrochloride, water for injection
Zenapax	Dacilizumab	Liquid: 25 mg single-dose vial	IV: 5 mL (pH 6.9)	25 mg vial: 3.6 mg sodium phosphate monobasic monohydrate; 11 mg sodium phosphate dibasic heptahydrate; 4.6 mg sodium chloride; 0.2 mg polysorbate 80
Zevalin	**Britumomab**	Liquid: 3.2 mg single-dose vial	IV infusion 2 mL vial kit: 3.2 mg active ingredient vial, 0.9% saline	Vial: 750 mg human albumin; 76 mg sodium chloride

Created by S.J. Shire with the assistance of John Wang.

operations (filling and finishing), long-term storage, extremes in temperature (including freeze/thaw), severe agitation, and moderate to intense light may have considerable impact on the physical appearance of a liquid protein product. When adequate stability is not possible in the liquid state or when a longer shelf life is desired, solid dosage forms may be preferred. Although the chemical degradation routes generally are slower in solids since water has been removed, physical degradation routes may predominate, i.e., degradation routes are different in solid versus liquid dosage forms.

The most common technique for drying proteins is lyophilization (freeze-drying) and there are several excellent reviews on this technology (Carpenter, 2004; Carpenter, Pikal, Chang, & Randolph, 1997; Gatlin & Nail, 1994). Spray drying of protein pharmaceuticals (Broadhead, Rouan, Hau, & Rhodes, 1994; Chan, Clark, Gonda, Mumenthaler, & Hsu, 1997; Mumenthaler, Hsu, & Pearlman, 1994) has also been used to generate solid dosage forms, although mainly for preparing dry powders for the inhalation route, since spray drying can produce appropriately sized particles for pulmonary deposition (Chan et al., 1997).

An advantage of lyophilized products is that dose concentration and injection volume can be easily altered during reconstitution of the product. However, formulation design coupled with lyophilization cycle development can add to the overall development time of such products. In the case of lyophilization, the freezing and drying process can sometimes cause degradation of proteins in the solid state and thus analytical tools, such as Fourier transform infrared spectroscopy, to probe protein conformation in the solid state have been successfully used to determine which excipients protect proteins from freezing stresses and those excipients that protect during the drying phase of the process (Carpenter, Prestrelski, & Arakawa, 1993; Prestrelski, Arakawa, & Carpenter, 1993). The physical state of these excipients can be probed using differential scanning calorimetry (Hancock, Dalton, Pikal, & Shamblin, 1998; Clas, Dalton, & Hancock, 1999) and X-ray diffraction (Young, 2012). Another disadvantage of a lyophilized product is that it can be more expensive and time-consuming to couple a solid dosage form with a delivery device. Dual-chamber syringes for direct reconstitution of the product followed by administration have been developed but are more expensive to develop than a vial or single-chambered syringe (Michaels, 1988). If a dual-chambered syringe is to be used with an autoinjector, this becomes even more difficult since the injector will need to aid in reconstitution as well as delivery.

One advantage of lyophilized formulations is in the development of multiuse formulations. Weight-based or surface area-based dosing can result in significant product waste for a single-use vial configuration, which is undesirable for expensive protein drugs. This problem can be addressed by providing several different dosing vials to accommodate patients different dose requirements. If the range of patient doses is not large (i.e., when only two vial sizes are needed), this will usually suffice. However, for wider dosing ranges, increasing the number of vial configurations to three or more adds development and quality control costs for the manufacturer. Thus, the development of one multiuse vial configuration is a more cost-effective approach. Each multiuse vial must have sufficient amount of drug for the highest dose patient to withdraw at least one full dose, while allowing lower dose patients to withdraw several doses from each vial. These formulations require inclusion of a preservative to allow for multiple entries into a vial. Although several preservatives are approved for parenteral use (including compounds

such as *m*-cresol, chlorocresol, phenol, benzyl alcohol, methyl paraben, propyl paraben, benzethonium chloride, benzylalkonium chloride, thimerosal, and chlorobutanol), the chemical and physical properties of these preservatives may make formulation of proteins a challenging task. Potential interaction of preservatives with the protein can diminish the effectiveness of the preservative, and degradation of preservatives can also produce compounds that interact with proteins. As an example, the commonly used preservative benzyl alcohol undergoes oxidation to benzaldehyde (Hewala, 1994) that can react with the primary amines of proteins (Roberts & Caserio, 1967). This problem can be mitigated by development of a lyophilized formulation that is reconstituted with a preservative-containing diluent, hence shortening the time of exposure of the protein to the preservative.

Approaches for formulation development

The most common strategy used for development of protein drug formulations is to set up a study that screens different excipients and solution conditions. However, these screens can be very large, labor intensive, and time-consuming. Often experiments are designed to obtain quickly an understanding of the critical properties of the protein drug. These preformulation studies investigate the response of the protein to a variety of stresses induced by different solution conditions. The studies include a general characterization of the protein that may reveal potential stability issues (Chang & Hershenson, 2002). Preformulation studies can also be simplified by using information on the response of the protein to the solution conditions during upstream process development. During cell culture and recovery and purification process development, observations regarding stability at different temperatures, ionic strength, and pH may help in narrowing the range of conditions that need to be explored.

Development of stability-indicating assays

During the preformulation step assays are also developed that can monitor changes that may impact potency and safety of the product. These so-called "stability-indicating" assays are then used in a full development screening program. Often one assay such as reversed phase HPLC is sufficient to monitor the stability of a small-molecule drug, but for proteins it is necessary to use several assays to monitor stability. An example of this is for a mAb where size exclusion chromatography (SEC) showed small changes in the chromatogram after 1 year of storage at −70, 5, 30, and 40 °C (Figure 4.1(a)). However, analysis by hydrophobic interaction chromatography (HIC) after papain digestion (generating Fabs) after 1 year of storage at the same temperatures showed significant changes in the chromatogram (Figure 4.1(b)). Essentially different assays explore different properties of a complex molecule such as a protein, and thus several assays are required to adequately monitor the stability of a protein. Thus, a SEC assay that is sensitive to changes in the aggregation and fragmentation of a protein may not pick up degradation that results from changes in Asp isomerization as detected by the HIC assay. Using only one assay may explore only one of many degradation routes. This is akin to the famous parable about different blind men touching different parts of an elephant and coming to very different conclusions regarding the animal's appearance (Figure 4.2).

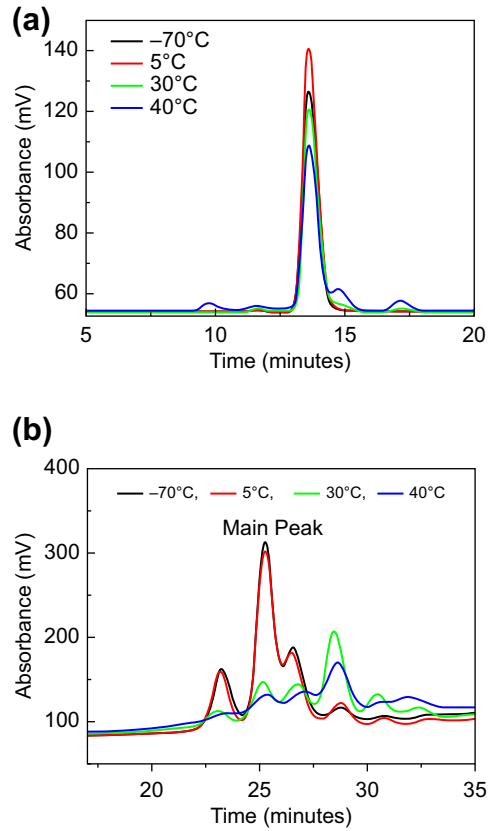

Figure 4.1 Stability of a mAb after 1 year of storage at −70, 5, 30, and 40 °C as assessed by (a) size exclusion chromatography and (b) hydrophobic interaction chromatography after papain digestion. Figure provided by Jun Liu, Genentech.

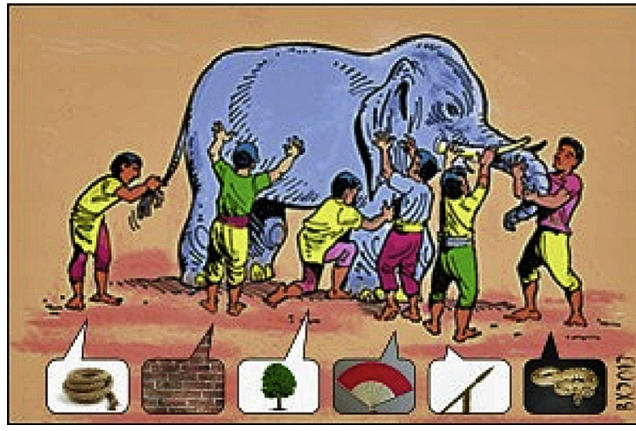

Figure 4.2 Blind men investigating the appearance of an elephant.

Given the great variety of techniques for analyzing and characterizing proteins (Chapter 2), it is a challenge to assess which of the assays are relevant to developing a stable formulation and delivery system, i.e., stability-indicating assays. Since many of the chemical degradations in proteins are fairly well understood, particularly in regard to how conformation and primary structure impact degradation routes, it is often possible to determine which degradation routes may be prevalent for a particular protein under development. These assessments can then lead to a more rational and directed approach for formulation development. Examples of such assessments are now discussed.

In silico methods to assess protein degradation routes

Deamidation and isomerization reactions as previously discussed are highly dependent on amino acids adjacent to the potential deamidation/isomerization site. Identification of such hot spots suggests whether this may be a major degradation route and also enable careful peptide mapping around the potential sites to determine how susceptible those sites are to alteration. If there is information on the conformation from either X-ray crystallography or nuclear magnetic resonance studies the accuracy of the predictions of these "hot spots" can be increased (Robinson & Robinson, 2001).

Computational methods to assess propensity to aggregate have also been developed. Many of the computer algorithms based on aggregation of proteins in neurodegenerative diseases have been recently reviewed (Kumar, Wang, & Singh, 2010). The specific aggregation-prone regions (APRs) in these proteins appear to be involved with association of β-strand motifs. Many of these algorithms can predict correctly >80% of the sequences involved. An important principle that comes out of these analyses is that not all regions of a protein contribute equally to aggregation, but rather short peptide sequences within the protein may predominate in the aggregation process. It was suggested that since mAbs have a great deal of β-structure, these algorithms could be useful in predicting APRs in mAbs. The computations have shown that APRs are mainly found in the CDR loops and adjoining β-strands of mAbs (Kumar et al., 2010; Wang, Das, Singh, & Kumar, 2009; Wang, Hu, et al., 2009).

Complexity of stability determinations during formulation development: real time versus accelerated stability

Generally during development of formulations for small molecules high temperatures are used to assess changes since the kinetics of various reactions increase with temperature. The temperature dependence of the kinetic rate constants generally follows Arrhenius kinetics and can be used to determine shelf life at the lower temperature storage conditions. Thus, this approach greatly speeds up the development process and precludes the need for real-time stability analysis (Fagain, Sheehan, & O'Kennedy, 1991). This approach can work with small-molecule drugs since usually only one

reaction mechanism is being investigated. However, since there are many potential degradation routes in proteins due to the increased number of functional groups the Arrhenius plots may not be linear. In addition, a protein and mAb are susceptible to conformational changes at higher temperatures possibly resulting in greater solvent exposure of amino acid residues that undergo degradation. Thus, the degradation kinetics at the higher temperatures may be significantly different than at the lower recommended storage conditions requiring very different formulations. For these reasons regulatory agencies currently require real-time stability assessment for determination of product shelf life (Werner & Langlouis-Gau, 1989).

Although Arrhenius kinetics are not useful for setting shelf life of proteins this kinetic approach has been used successfully to evaluate enzymatic activity of proteases with appropriate modeling using more than one pathway. This approach may work well for proteases since the enzymatic activity is intimately related to the protein conformation, and essentially only one reaction is being monitored: the unfolding of the proteins prior to any chemical modification. Although there may be several different unfolded forms, these different forms will all be inactive and not distinguishable from each other by activity assays. In the case of the enzyme α-glucosidase isolated from the bacterial thermophile *Bacillus thermoglucosidius*, the incorporation of a reversible and irreversible pathway into the kinetic model resulted in linear Arrhenius plots for the rate constants for each process (Suzuki, Nakamura, Kishigami, & Abe, 1980; Yoshioka, Izutsu, Aso, & Takeda, 1991).

Accelerated rate studies become more complicated when a number of analytical assays are used rather than just final activity loss. As an example, for interleukin 1b it was shown that at or below 30 °C, the primary degradation pathway was deamidation, whereas at or above 39 °C, it was aggregation and precipitation (Gu et al., 1991). Thus, the different degradation routes of this protein precluded shelf life prediction from accelerated studies. As was discussed earlier, it was possible to use accelerated studies as a predictive tool if the degradation is monitored for one specific route over a temperature range where the protein conformation is unchanged (Shire, 1996).

Liquid formulation development

Many of the degradation routes that were discussed are highly dependent on solution pH and ionic strength as well as temperature of storage. Although it is virtually impossible to prevent all the degradations from occurring, minimizing the rates of all the reactions, hence optimizing the stability, can be used to develop a successful liquid formulation of a protein or mAb. An example of this is the pH dependence of the pseudo first-order rate constant for deamidation and Asp isomerization in an IgG_1 mAb (Figure 4.3). From these data it is clear that formulation at ~pH 6 would be optimum for both reactions, and generally many liquid mAb formulations are formulated between pH 6 and 7 (Table 4.1).

Development of stable liquid formulations requires screening of different excipients, and each excipient has a specific purpose. The development of a liquid formulation that uses excipients already present in marketed products may require less safety testing than an excipient that has never been used. However, potential interactions with other excipients as well as the protein drug do not guarantee a fast and

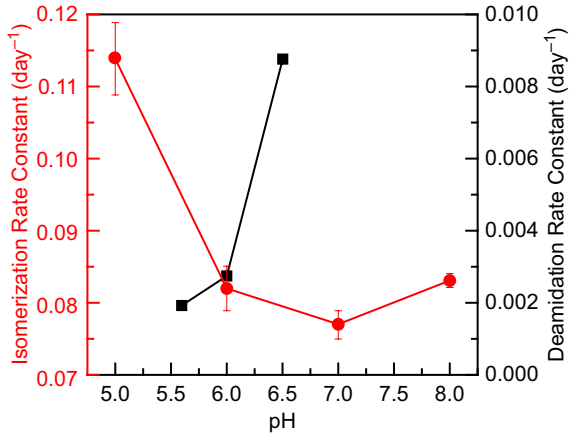

Figure 4.3 The pseudo first-order rate constants for deamidation and isomerization in an IgG1 mAb as a function of pH.
From Shire, Liu, Fries, Matheus, and Mahler (2010).

easy development process. Reviews of common excipients and their function in a formulation are available (Nema, Washkuhn, & Brendel, 1997; Pramanick, Singodia, & Chandel, 2013; Wang & Kowal, 1980). A brief summary of excipients and function in a liquid protein, mAb formulation are now discussed.

Buffers for pH control

Many of the degradation pathways such as deamidation and Asp isomerization are pH dependent (Figure 4.4), and thus excipients need to be added that control the pH. Some of the most commonly used buffers for pH control include acetate, citrate, succinate (pH 3–6), phosphate, histidine (pH 6–8), Tris, and carbonate (>pH 8). The buffer concentration is usually kept low (10–30 mM) to provide enough buffering capacity for control of pH while allowing the solution pH to change rapidly upon administration. Buffer salts such as Tris have fairly large temperature dependence of the pKa ($\Delta pKa/\Delta T°C = -0.028$) and this needs to be taken into account when preparing formulations. Thus, if a Tris buffer system is prepared at 25 °C, the pH of the solution during a recommended storage of 5 °C will be different. Some buffer salts such as disodium phosphate are prone to crystallization upon freezing, and this impacted the stability of a protein during freezing and thawing (Pikal-Cleland, Rodriguez-Hornedo, Amidon, & Carpenter, 2000). The impact of buffer ion on stability of a protein has also been observed. The aggregation of an IgG_1 mAb without the presence of any other stabilizers showed that histidine provides additional stability when compared to other buffering ions (Figure 4.4). The pH does not appear to be a major contributor when considering different buffer species since buffer systems with the same pH (formulations B, C, and D in Figure 4.4) still show significant differences in stabilization.

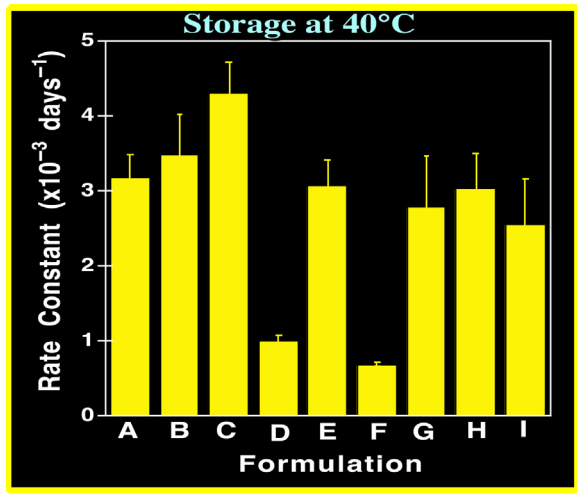

Figure 4.4 The pseudo first-order aggregation rate constant for an IgG1 mAb stored at 40 °C as a function of buffer species. A, no excipients; B, potassium phosphate, pH 7; C, sodium phosphate, pH 7; D, histidine, pH 7; E, sodium succinate, pH 6.5; F, histidine, pH 6; G, sodium succinate, pH 6; H, sodium succinate, pH 5.5; I, sodium succinate, pH 5.
Figure provided by Jim Andya or Jun Liu. 21st Interphex Japan, Tokyo, Japan 2008.

Ionic strength and tonicity modifiers

Ionic strength can impact the behavior of proteins resulting in salting in (increased solubility) or salting out (decreased solubility). The decrease in solubility with an increase in ionic strength is usually attributed to the colloidal stability of a protein. In this framework a protein at any given pH has a specific net charge. Thus the protein molecules repel each other and predominate over any attractive interactions. As the ionic strength is increased the net charge repulsion is decreased, resulting in potential attractive protein–protein interactions, resulting in decrease of solubility and increase in protein aggregation. It has been reported that the turbidity of an IgG_1 mAb solution increased with an increase in ionic strength of the formulation and that the T_m for unfolding as determined by DSC decreased with an increase in NaCl concentration (Wang, Hu, et al., 2009). It was also observed that the viscosity of these more turbid mAb solutions increased with an increase in ionic strength. In another example, an IgG_1 mAb showed increased turbidity with an increase in ionic strength, and appeared to correlate nicely with determination of the B22 and the DSC interaction parameter, k_D (discussed in greater detail in Chapter 9) (Figure 4.5), i.e., positive B22 and k_D at 15 mM NaCl where net interactions are repulsive, and negative B22 and k_D at 150 mM NaCl where net interactions are attractive.

The tonicity of a protein formulation is related to the osmotic pressure gradient across a semipermeable membrane. This pressure gradient is generated due to the concentration of solutes outside the membrane compartment versus inside the membrane compartment. The traditional discussion of tonicity as it relates to biological systems is usually assessed on the effect of the solution tonicity on red blood cells. When the concentration of solute is

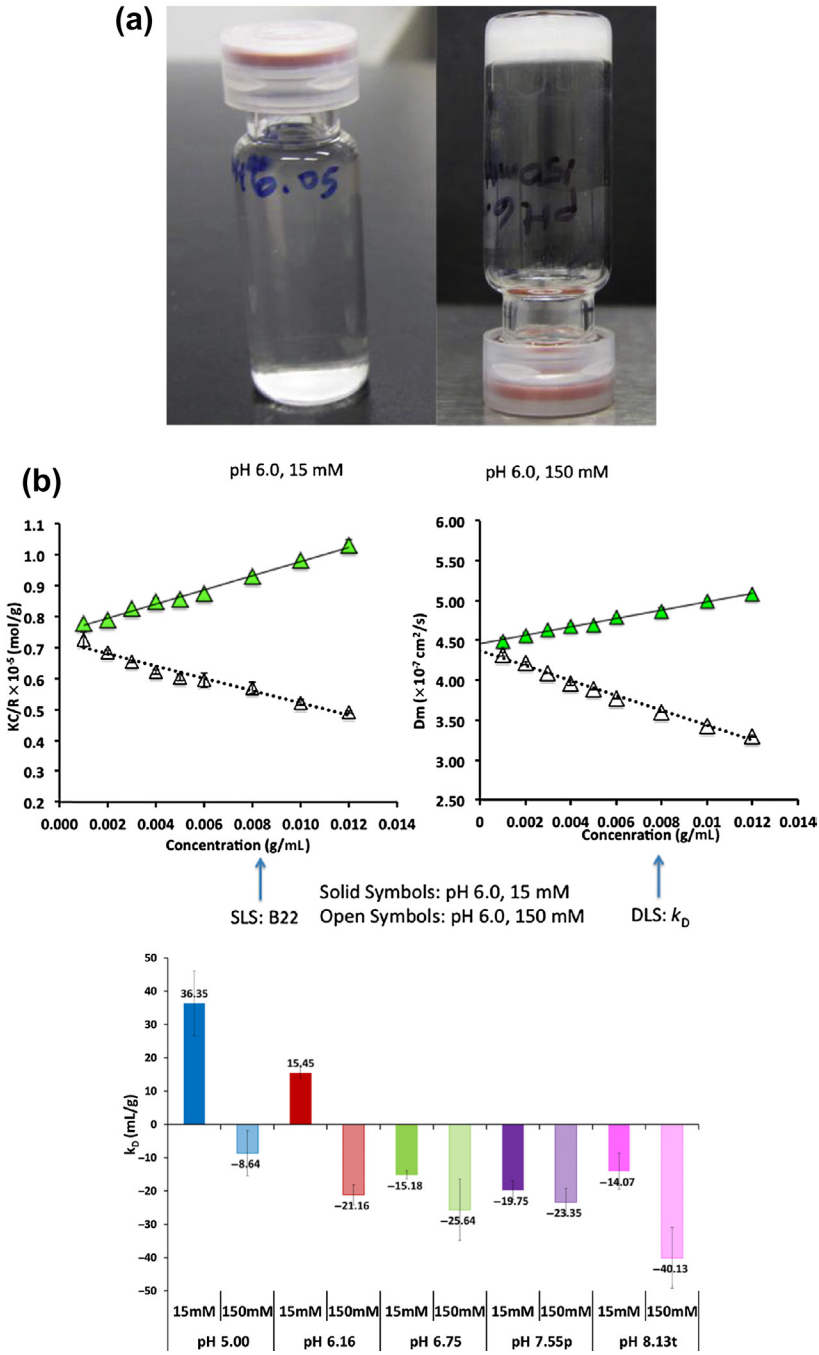

Figure 4.5 (a) IgG1 mAb solubility/gel formation at pH 6 at 15 and 150 mM NaCl. (b) B22 determined by SLS and k_D determined by DLS at pH 6 at 15 and 150 mM NaCl. Figures provided by M. Pindrus, University of Connecticut, 2014.

higher in solution than within the red blood cell water will flow out through the cell membrane in order to balance the concentration of solutes across the membrane. The solution is hypotonic when the concentration of solutes within the red cell is greater than the solution outside the cell. This results in an influx of water often resulting in the bursting of the cell. The solution is termed isotonic when the fluid within the cell has a similar concentration of solutes as outside the cell. Usually an IV injection or infusion requires an isotonic preparation, whereas an IM or SC injection may be able to handle hypertonic and hypotonic conditions since the protein drug is not administered directly into the blood. Nonetheless, there has been concern related to disruption of tissue and possible pain on injection. In a study in rabbits, NaCl solutions ranging from 0.9% (300 mOsm) to 10% (3300 mOsm) were administered by IM and SC injections (Zietkiewicz, Kostrzewska, & Gregor, 1971). Tissue damage, as evidenced by necrosis, occurred between 3.9% (1300 mOsm) and 5.1% (1670 mOsm). In this study, 69 drugs were also evaluated for tonicity and 22 were isotonic, 23 hypertonic, and 24 hypotonic. The final conclusion from this study was that solutions up to 1300 mOsm do not cause necrosis of SC and muscle tissue. Most importantly it was concluded that for SC and IM injections the solutions do not need to be isotonic, but should avoid the critical limits of hypertonicity. It should be emphasized that this study only investigated tissue damage and did not address what the limits were for pain on injection. In another study, factors associated with muscle pain in humans were assessed using NaCl solutions of different tonicities (Brazeau, Cooper, Svetic, Smith, & Gupta, 1998). It was shown that muscle pain on IM injection only occurred for hypertonic solutions.

The tonicity of a protein formulation is modulated by inclusion of solutes, and the ionic strength of the formulation is dictated by the presence of charged solutes. One of the most used excipients for adjusting tonicity and ionic strength is NaCl. However, NaCl can hasten the corrosion of stainless steel, especially the 316L grade used in the bioprocessing of protein drugs (Ryan, Williams, Chater, Hutton, & McPhail, 2002). Thus, alternative excipients should be used for adjustment of ionic strength and/or tonicity. Sugars, which are added as stabilizers, can also be used to adjust the tonicity. If it is not possible to use less corrosive excipients such as NaCl another strategy is to use a higher grade of stainless steel alloy, which contains very little iron. Hastelloy has been used and although more expensive, the rate of corrosion of this stainless steel alloy is decreased compared to the common 316L stainless steel, which has a higher iron content (Davis, 1994; Srindhar, 1992).

Surfactants and surface-active agents

Liquid formulations of proteins and mAbs are susceptible to denaturation at air–water interfaces, which are easily generated during swirling, stirring, and agitation of the solution. The stresses on the protein due to agitation by shaking are different from those by stirring and result in different size distribution of particulates and aggregates (Luo et al., 2011). Generally, surfactants and surface-active agents are added to minimize the aggregate formation at hydrophobic air–water interfacial surfaces. The most commonly used surfactants are polysorbate 20 and 80. These surfactants may contain peroxides, which can oxidize amino acid residues that are prone to oxidation (Kishore, Kiese, et al., 2011; Kishore, Pappenberger, et al., 2011). Commercial sources of peroxide-free polysorbates

are available, but need to be handled and stored properly (Ha, Wang, & Wang, 2002). In particular, incubation of polysorbate 80 in air at high temperatures promotes peroxide formation, and removal of oxygen is recommended for long-term storage. The oxidation induced by peroxides as a result of polysorbate 20 degradation can be inhibited by antioxidants as shown in a study using an IgG_1 mAb Fab (Lam, Lai, Chan, Ling, & Hsu, 2011). In this study, it was shown that a Trp residue was oxidized as a result of the presence of increased levels of peroxide in polysorbate 20, and the decomposition of the polysorbate-involved free radicals. Addition of ethylenediaminetetraacetic acid (EDTA), catalase, and free Trp prevented oxidation. In addition to the generation of peroxides, degradation of polysorbates can also result in the generation of poorly soluble molecules such as fatty acids, and polyoxyethylene esters of fatty acids. The generation of these compounds appeared to slightly increase the subvisible particle counts in four different mAb formulations. However, overall these degradation products did not appear to impact the stability of the mAbs. A greater concern would be the decrease in effective concentration of surfactant that is needed to prevent aggregation as a result of exposure to air–water interfaces created by agitation of the liquid formulation (Kishore, Kiese, et al., 2011). It has also been shown that polysorbate 80 had several degradation products even after several months of storage, at 4 °C, whereas polysorbate 20 contained fewer degradation products than found in polysorbate 80 (Gilardi-Lorenz, 2006). Many of these impurities found in polysorbate 80 were not found in polysorbate 20, and thus polysorbate 20 may be the preferred surfactant for protein formulations. These studies prompted the recommendation that polysorbate 80 solutions should be stored at 4 °C with protection from light and air.

Antioxidants

Antioxidants have been widely used in pharmaceutical products to inhibit the oxidation process. A review and summary of antioxidants that have been used in pharmaceutical dosage forms is available (Akers, 1982). Although many of these antioxidants have been used successfully in small-molecule formulations, the unknown toxicity and potential incompatibility with protein drugs have resulted in limited use of the antioxidants in protein formulations. Several antioxidants for inhibiting Met oxidation in proteins have been used, and these include chelating agents, reducing agents, oxygen scavengers, and chain terminators. As shown previously, many oxidation degradations of proteins are catalyzed by metals, and thus chelating agents such as EDTA that bind to metals may be effective in controlling oxidation in proteins. Reducing agents such as glutathione can reverse the oxidation by reducing the oxidized product, whereas oxygen scavengers are added molecules that more readily oxidize than the residues in a protein. The latter strategy was used successfully to inhibit oxidation of Met residues in an IgG1 mAb formulation by adding the free amino acid Met (Lam, Yang, & Cleland, 1997), and Trp oxidation in a mAb Fab fragment by adding the free amino acid Trp (Lam et al., 2011). Although the addition of Trp in the case of the mAb Fab fragment was effective, a study by Wang et al. (Ji, Zhang, Cheng, & Wang, 2009) showed that the route of the Trp oxidation could govern the effectiveness of addition of Trp. Specifically Trp oxidation in a model compound, parathyroid hormone (PTH), was done using either 2,2′-azobis(2-amidinopropane) dihydrochloride

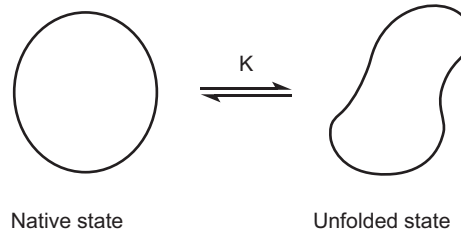

Figure 4.6 Schematic of protein stabilization due to increased surface area of the denatured state and ensuing preferential hydration.
From Arakawa and Timasheff (1982).

(AAPH) or H_2O_2+Fe(II). The addition of free Trp only protected the oxidation of Trp in PTH by AAPH.

Protein Stabilizers

In a series of classic papers, Timasheff and colleagues discuss how compounds that are excluded from the protein surface are able to stabilize the protein in aqueous formulations (Arakawa & Timasheff, 1982; Lee & Timasheff, 1981; Timasheff, 2002; Xie & Timasheff, 1997). Sugars, in particular, are excellent stabilizers. The basic mechanism for stabilization of the protein conformation is that when stabilizers are preferentially excluded from the protein surface this results in a preferential hydration of the protein. As discussed previously this in turn can lead to more structured water around the protein, which increases the chemical potential mainly due to a decrease in system entropy. In order to assess the impact of preferential hydration on protein conformation it is instructive to compare the native state of a protein, which is in equilibrium with the denatured state. Since the surface area of the denatured state is greater than in the native state (Figure 4.6) (Arakawa & Timasheff, 1982), and since the addition of sugars results in a positive free-energy change, and it is assumed that this change increases with an increase in surface area, the unfolded state of the protein will have a greater increase in chemical potential than the folded state when sugar is added resulting in a shift of the equilibrium that favors the native state of the protein.

Recently an excipient that has been used frequently in protein formulations is Arg (Arakawa, Ejima, et al., 2007; Arakawa, Tsumoto, Kita, Chang, & Ejima, 2007). This excipient is able to increase protein solubility, reduce aggregation, and decrease viscosity of mAb formulations. The latter property of Arg will be discussed in the chapter dealing with development of high-concentration mAb formulations for SC delivery. It has been suggested that arginine stabilization of proteins occurs by affecting solvent properties such as surface tension as well as by interacting with protein amino acid side chains and peptide bonds (Arakawa, Ejima, et al., 2007; Baynes, Wang, & Trout, 2005).

Lyophilization Formulation Development

The freeze-drying process consists of a freezing step followed by a drying step whereby water is removed by sublimation from the frozen state. Excipients that stabilize the protein during freezing may not be acceptable for stabilization during drying. As an example, it was shown that solutions of 1–10% (wt/vol) of polyethylene

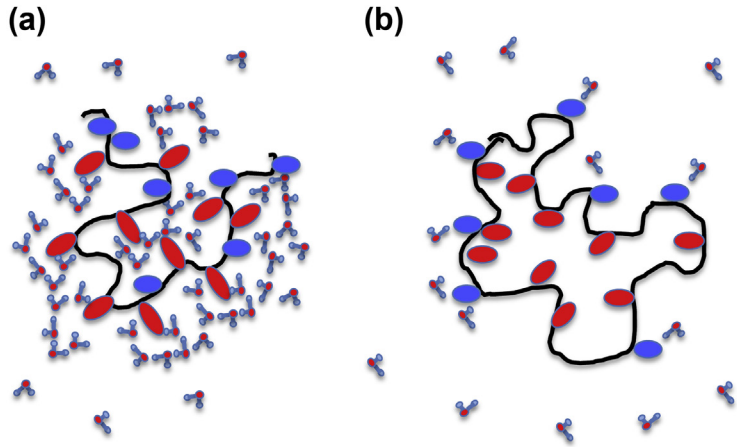

Figure 4.7 (a) Depiction of an unfolded protein with hydrogen-bonded clathrate water structure surrounding hydrophobic residues (as red ellipses red). (b) Depiction of a folded protein with exposed hydrophilic residues (as blue ellipses blue) hydrogen bonding to specific water molecules. For simplicity the normal hydrogen bonding of the bulk water has been omitted.

glycol (PEG) could protect proteins such as lactate dehydrogenase and phosphofructokinase during freezing and thawing, but not during the drying process (Prestrelski, Arakawa, & Carpenter, 1993). The main mechanism of PEG for stabilization during freezing is due to the preferential exclusion of PEGs from the protein surface. It was shown that this mechanism, first proposed by Timasheff and colleagues to explain stabilization in nonfrozen aqueous systems, also protects proteins during the freezing and thawing process. Essentially, the chemical potential of a protein and the solute are increased when the solute is excluded from the surface of the protein. This destabilization is greater for the unfolded protein since there is a greater surface area exposed to solvent upon unfolding. Thus, in the presence of a preferentially excluded solute, such as PEG, the native structure with less exposed surface area is favored. The PEG is excluded mainly due to steric hindrance and this effect appears to be maintained during freezing. However, during the drying step the preferential exclusion mechanism is no longer valid since the hydration layer around the protein has been removed. It has been proposed that effective solutes for protection during drying are due to the direct interaction of the solute with protein resulting in replacement of hydrogen bonds that were lost during the removal of the hydration layer, and has been termed the water-replacement hypothesis. The unique properties of water are believed to promote the folding of a protein into a compact structure. Exposure of hydrophobic residues that are in the inside core of a folded protein results in an ordering of water molecules around the hydrophobic residue which in turn lowers the total entropy of the system. Thus the folding of a protein is driven by release of bound water into the bulk phase during the folding process, resulting in an overall increase in the system entropy (Figure 4.7(a)). Removal of the "clathrate" water from the protein surface by the drying process then removes this entropically driven mechanism and a folded protein may unfold when much of the bound water is removed. The

protein in the folded state has exposed hydrophilic residues which may be hydrogen bonded to specific water molecules (Figure 4.7(b)). Removal of all the water in the system can destabilize the protein conformation by removal of the specific water molecules which hydrogen bond to the polar groups on the protein surface. Thus, over-drying exposes polar groups that can cause opalescence upon reconstitution, while under-drying increases the rates of the hydrolytic reactions, which can cause degradation and potential losses in activity (see Figure 7 in Hsu et al., 1991). An alternative mechanism is that of formation of an amorphous glassy state whereby protein mobility is restricted, rendering a protein more stable because it is less susceptible to degradation mechanisms that require protein flexibility and moisture (Belton & Gil, 1994; Levine & Slade, 1992). To ensure a glassy state, the freeze-dried preparation must be stored at a temperature below the characteristic glass transition temperature, Tg. The Tg value is dependent on the mass percent of each component including water. Water has a very low Tg value (−135 °C), and thus increasing the water content of a freeze-dried formulation will greatly reduce Tg. As an example, increasing the water content of a freeze-dried preparation from 1% to 3–4% (g H_2O/100 g dried powder) results in a Tg value below room temperature. Thus, development of a lyophilization cycle that results in sufficiently dried powder is extremely important to ensure a Tg value that easily accommodates lower storage temperatures. In fact, Tg values above room temperature are advantageous since the product need not necessarily be stored at refrigerated temperatures. However, even if the cycle produces a high Tg value at low moisture content, residual moisture in the vial stoppers can increase water content of the formulation during storage resulting in a decrease of the Tg value. This problem can be mitigated by thoroughly drying the stoppers before use, or using a stopper with a coating, which serves as a barrier for moisture transfer.

It is likely that both the water replacement and glassy state mechanisms are important to ensure a good drying protectant. It has been shown that the glassy state itself is not sufficient to stabilize a protein after freeze-drying (Prestrelski, Arakawa, & Carpenter, 1993; Zhang, Prestralski, Arakawa, & Carpenter, 1993). In particular, it has been shown that storage of a freeze-dried preparation below the Tg does not always result in a stable product, i.e., stabilization of the protein conformation is also required. Thus, dextran has a high Tg value >75 °C, but is unable to conserve protein structure during freeze-drying. Proteins freeze-dried in dextran degrade more rapidly than when formulated with either sucrose or trehalose, which can contribute hydrogen bonding to the protein during removal of water. Generally, disaccharides such as both sucrose and trehalose can function as promoters of the glassy state due to their relatively high Tg values as well as stabilizers of protein structure via their ability to contribute replacement hydrogen bonding. Sucrose and trehalose are also excellent lyoprotectants since they do not crystallize easily during the lyophilization process. If the lyoprotectant were to phase separate due to crystallization, it would not be able to interact with the protein resulting in little drying protection. Such was the case during development of an anti-IgE mAb freeze-dried formulation where stability was assessed at 2–8 °C storage in a 10 mM sodium succinate buffer at pH 5 in the presence of several sugars (Figure 4.8). Of all the sugars tested, mannitol was by far the worst lyoprotectant, mainly due to the ease of crystallization of mannitol during the freezing process.

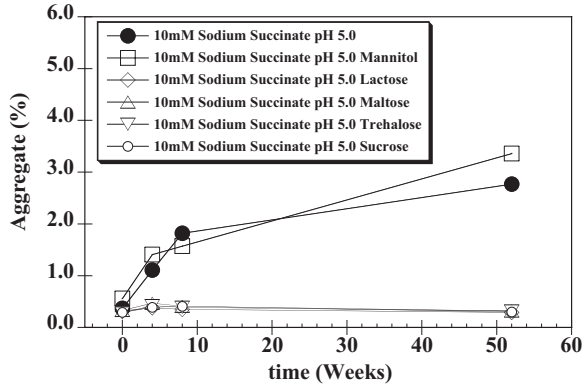

Figure 4.8 Generation of aggregate as determined by size exclusion chromatography for an IgG1 anti-IgE mAb formulated in 10 mM succinate buffer at pH 5 with different sugars at 275 mM.

Caveats when using sugars as lyoprotectants

It is well known that reducing sugars, such as glucose, can form adducts with free amino acid groups in a protein which may result in lysine–lysine covalent aggregates (Nagaraj, Shipanova, & Faust, 1996). This reaction, known as the Maillard reaction, proceeds during storage in the dried state resulting in a "browning" of the lyophilized cake. The modified protein also may be unstable and thus reducing sugars should be avoided (Carpenter, Chang, Garzon-Rodriques, & Randolph, 2002; Carpenter et al., 1997). Nonreducing disaccharides such as sucrose are susceptible to hydrolysis at low pH, and thus the solution conditions could result in generation of reducing sugars (Chambre, Iditoiu, & Szabo, 2007). As an example, an IgG_1 mAb was formulated at pH 5 with mannitol, lactose, trehalose, and sucrose and after lyophilization stored at 40 °C for 1 year. A substantial amount of aggregate formed when no lyoprotectant was added, as expected, and as noted previously, mannitol provided no protection because of its propensity to crystallize (Figure 4.9(a)). Good protection from aggregate formation was provided by lactose, maltose, and trehalose. Although lactose and maltose are reducing sugars, they did not impact formation of aggregate under these conditions. However, sucrose, a nonreducing disaccharide, can hydrolyze into the component reducing monosaccharides fructose and glucose under mildly acidic conditions (Edye & Clarke, 1998). Thus, at pH 5 and at 40 °C the IgG_1 lyophilized cakes shrunk and turned brown with a concomitant increase in aggregate. Although the presence of glucose was not ascertained in this study, it is likely that the hydrolysis of sucrose to glucose and fructose at pH 5 was responsible for the degradation. Interestingly, an increase of pH from 5 to 6 resulted in no aggregate formation after storage for 24 weeks at 40 °C, demonstrating the pH sensitivity of the hydrolysis reaction (Figure 4.9(b)). Even when formulating at pH >6 it is important to consider the buffer species that is chosen. As discussed previously, buffer salts such as sodium dibasic phosphate can easily crystallize on freezing resulting in a pH shift. A great example of this was a study by Deluca and colleagues where ribonuclease A was formulated in a 0.1 M sodium phosphate buffer system with sucrose as a lyoprotectant

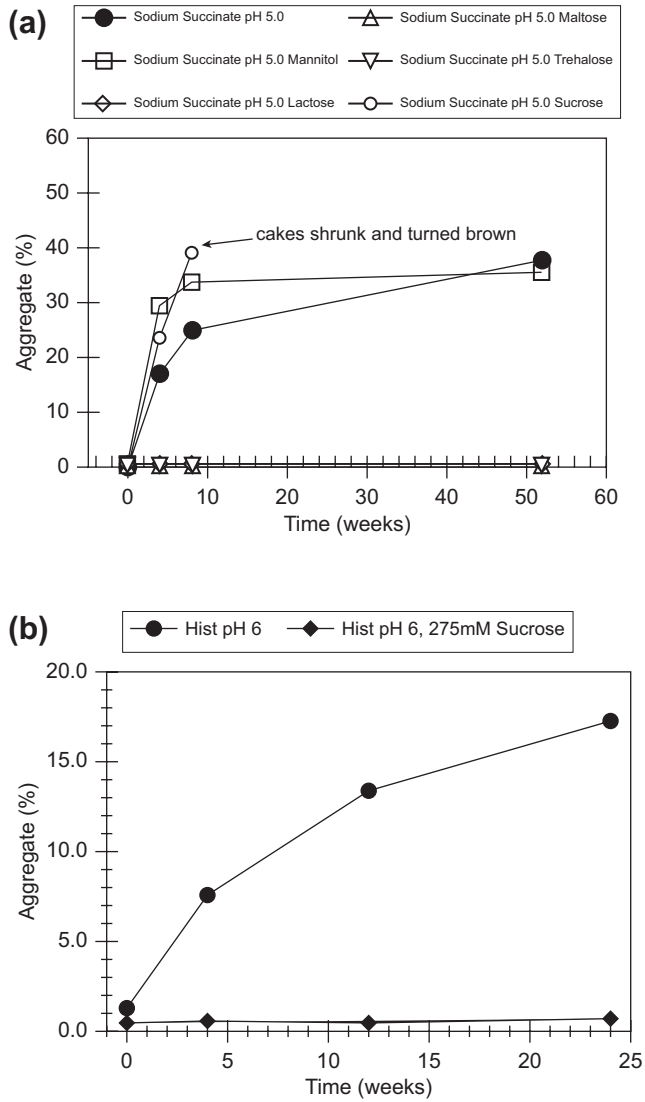

Figure 4.9 (a) Effect of sugars at 275 mM on aggregate formation of a lyophilized IgG1 mAb at 5 mg/mL in 5 mM sodium succinate, pH 5.0 during 1 year storage at 40 °C. (b) Effect of increased pH to 6.0 on prevention of aggregate formation of a lyophilized IgG1 mAb at 5 mg/mL in 5 mM His-HCl during 24 weeks storage at 40 °C.

at pH 3, 6.4, and 10 (Townsend & Deluca, 1988). After freeze-drying, the samples were stored at 45 °C and the specific activities for the enzyme were determined. A control sample freeze-dried in distilled water showed little decrease in activity over 30 days of storage, whereas at pH 10 the decrease was ~25%, pH 3 at ~75%, pH 6.4 at ~25%, and pH 10 at ~75%. The large decrease at pH 3 is not surprising since sucrose may have hydrolyzed under those conditions and at pH 10 the decrease may have resulted

from conformational changes at extremes of pH. However, at pH 6.4, there should have been little hydrolysis and yet the activity loss was significant. It was hypothesized that the crystallization of the dibasic sodium phosphate salt led to a large decrease in pH resulting in generation of glucose. Accompanying the large loss in activity for the pH 6.4 sample was a large increase in the amount of aggregate as determined by SEC and SDS PAGE. The latter assay demonstrated the covalent nature of the linked aggregates. Thin layer chromatography conclusively showed the generation of glucose in samples freeze-dried from a sodium phosphate buffer system at pH 6.4 (Townsend & Deluca, 1988). Thus, selection of pH with an appropriate buffer system that does not result in a decrease in pH upon freezing is crucial for successful freeze-drying.

References

Akers, M. J. (1982). Antioxidants in pharmaceutical products. *Journal of Parenteral Science and Technology*, *36*(5), 222–228.

Arakawa, T., Ejima, D., Tsumoto, K., Obeyama, N., Tanaka, Y., Kita, Y., et al. (2007). Suppression of protein interactions by arginine: a proposed mechanism of the arginine effects. *Biophysical Chemistry*, *127*(1–2), 1–8.

Arakawa, T., & Timasheff, S. N. (1982). Stabilization of protein-structure by sugars. *Biochemistry*, *21*(25), 6536–6544.

Arakawa, T., Tsumoto, K., Kita, Y., Chang, B., & Ejima, D. (2007). Biotechnology applications of amino acids in protein purification and formulations. *Amino Acids*, *33*(4), 587–605.

Baynes, B. M., Wang, D. I. C., & Trout, B. L. (2005). Role of arginine in the stabilization of proteins against aggregation. *Biochemistry (Moscow)*, *44*, 4919–4925.

Belton, P. S., & Gil, A. M. (1994). Ir and Raman-spectroscopic studies of the interaction of trehalose with hen egg-white lysozyme. *Biopolymers*, *34*(7), 957–961.

Brazeau, G. A., Cooper, B., Svetic, K. A., Smith, C. L., & Gupta, P. (1998). Current perspectives on pain upon injection of drugs. *Journal of Pharmaceutical Sciences*, *87*(6), 667–677.

Broadhead, J., Rouan, S. K. E., Hau, I., & Rhodes, C. T. (1994). The effect of process and formulation variables on the properties of Spray-Dried beta-galactosidase. *Journal of Pharmacy and Pharmacology*, *46*(6), 458–467.

Carpenter, J. (2004). Rational design of stable lyophilized protein formulations. *Protein Science*, *13*, 54.

Carpenter, J. F., Chang, B. S., Garzon-Rodriques, W., & Randolph, T. W. (2002). Rational design of stable lyophilized protein formulations-theory and practice. In J. F. Carpenter, & M. C. Manning (Eds.), *Rational design of stable lyophilized protein formulations-theory and practice* (pp. 109–133). New York: Kluwer Academic/Plenum Publishers.

Carpenter, J. F., Pikal, M. J., Chang, B. S., & Randolph, T. W. (1997). Rational design of stable lyophilized protein formulations: some practical advice. *Pharmaceutical Research*, *14*(8), 969–975.

Carpenter, J. F., Prestrelski, S. J., & Arakawa, T. (1993). Separation of freezing-induced and drying-induced denaturation of lyophilized proteins using stress-specific stabilization. 1. Enzyme-activity and calorimetric studies. *Archives of Biochemistry and Biophysics*, *303*(2), 456–464.

Chambre, D., Iditoiu, C., & Szabo, M. R. (2007). The reaction conditions influence on sucrose acid hydrolysis studied by means of DSC method. *Journal of Thermal Analysis and Calorimetry*, *88*(3), 681–686.

Chan, H. K., Clark, A., Gonda, I., Mumenthaler, M., & Hsu, C. (1997). Spray dried powders and powder blends of recombinant human deoxyribonuclease (rhDNase) for aerosol delivery. *Pharmaceutical Research*, *14*(4), 431–437.

Chang, B. S., & Hershenson, S. (2002). Practical approaches to protein formulation development. *Pharmaceutical Biotechnology*, *13*, 1–25.

Clas, S. D., Dalton, C. R., & Hancock, B. C. (1999). Differential scanning calorimetry: applications in drug development. *Pharmaceutical Science & Technology Today*, *2*(8), 311–320.

Davis, J. R. (1994). In *ASM specialty handbook®*. Ohio: ASM International.

Edye, L. A., & Clarke, M. A. (1998). Sucrose loss and color formation in sugar manufacture. *Advances in Experimental Medicine and Biology*, *434*, 123–133.

Fagain, C. O., Sheehan, H., & O'Kennedy, R. (1991). Accelerated degradation testing. *American Biotechnology Laboratory*, *9*(9), 31–32.

Gatlin, L., & Nail, S. L. (1994). Freeze-drying. In R. G. Harriison (Ed.), *A practical overview. Pharmaceutical process validation* (pp. 445–477). New York: Marcel Dekker.

Gilardi-Lorenz, F. I. (2006). *Analytical characterisation of the excipient polysorbate 80*. Swiss Federal Institute of Technology.

Gu, L. C., Erdos, E. A., Chiang, H. S., Calderwood, T., Tsai, K., Visor, G. C., et al. (1991). Stability of interleukin-1-beta (Il-1-Gamma) in aqueous-solution–analytical methods, kinetics, products, and solution formulation implications. *Pharmaceutical Research*, *8*(4), 485–490.

Ha, E., Wang, W., & Wang, Y. J. (2002). Peroxide formation in polysorbate 80 and protein stability. *Journal of Pharmaceutical Sciences*, *91*(10), 2252–2264.

Hancock, B. C., Dalton, C. R., Pikal, M. J., & Shamblin, S. L. (1998). A pragmatic test of a simple calorimetric method for determining the fragility of some amorphous pharmaceutical materials. *Pharmaceutical Research*, *15*(5), 762–767.

Hewala, I. I. (1994). Gas-liquid-chromatographic and difference spectrophotometric techniques for the determination of benzaldehyde in benzyl alcohol. *Journal of Pharmaceutical and Biomedical Analysis*, *12*(1), 73–79.

Hsu, C. C., Ward, C. A., Pearlman, R., Nguyen, H. M., Yeung, D. A., et al. (1991). Determining the optimum residual moisture in lyophilized protein pharmaceuticals. *Developments in Biological Standardization*, *74*, 255–271.

Ji, J. A., Zhang, B., Cheng, W., & Wang, Y. J. (2009). Methionine, tryptophan, and histidine oxidation in a model protein, PTH: mechanisms and stabilization. *Journal of Pharmaceutical Science*, *98*(12), 4485–4500.

Kishore, R. S. K., Kiese, S., Fischer, S., Pappenberger, A., Grauschopf, U., & Mahler, H. C. (2011). The degradation of polysorbates 20 and 80 and its potential impact on the stability of biotherapeutics. *Pharmaceutical Research*, *28*(5), 1194–1210.

Kishore, R. S., Pappenberger, A., Dauphin, I. B., Ross, A., Buergi, B., Staempfli, A., et al. (2011). Degradation of polysorbates 20 and 80: studies on thermal autoxidation and hydrolysis. *Journal of Pharmaceutical Science*, *100*(2), 721–731.

Kumar, S., Wang, X., & Singh, S. K. (2010). Identification and impact of aggregation–prone regions in proteins and therapeutic monoclonal antibodies. In W. Wang, & C. J. Roberts (Eds.), *Aggregation of therapeutic proteins* (pp. 103–118). Hoboken, NJ: John Wiley & Sons.

Lam, X. M., Lai, W. G., Chan, E. K., Ling, V., & Hsu, C. C. (2011). Site-specific tryptophan oxidation induced by autocatalytic reaction of polysorbate 20 in protein formulation. *Pharmaceutical Research*, *28*(10), 2543–2555.

Lam, X. M., Yang, J. Y., & Cleland, J. L. (1997). Antioxidants for prevention of methionine oxidation in recombinant monoclonal antibody HER2. *Journal of Pharmaceutical Sciences*, *86*(11), 1250–1255.

Lee, J. C., & Timasheff, S. N. (1981). The stabilization of proteins by sucrose. *Journal of Biological Chemistry*, *256*(14), 7193–7201.

Levine, H., & Slade, L. (1992). Another view of trehalose for drying and stabilizing biological materials. *Biopharm International*, *5*, 36–40.

Luo, Q., Joubert, M. K., Stevenson, R., Ketchem, R. R., Narhi, L. O., & Wypych, J. (2011). Chemical modifications in therapeutic protein aggregates generated under different stress conditions. *Journal of Biological Chemistry*, *286*(28), 25134–25144.

Michaels, T. M., Jr. (1988). Dual chamber prefill syringes. *Journal of Parenteral Science and Technology*, *42*(6), 199–202.

Mumenthaler, M., Hsu, C. C., & Pearlman, R. (1994). Feasibility study on spray-drying protein pharmaceuticals–recombinant human growth-hormone and tissue-type plasminogen-activator. *Pharmaceutical Research*, *11*(1), 12–20.

Nagaraj, R. H., Shipanova, I. N., & Faust, F. M. (1996). Protein cross-linking by the Maillard reaction. Isolation, characterization, and in vivo detection of a lysine-lysine cross-link derived from methylglyoxal. *Journal of Biological Chemistry*, *271*(32), 19338–19345.

Nema, S., Washkuhn, R. J., & Brendel, R. J. (1997). Excipients and their use in injectable products. *PDA Journal of Pharmaceutical Science and Technology*, *51*(4), 166–171.

Pikal-Cleland, K. A., Rodriguez-Hornedo, N., Amidon, G. L., & Carpenter, J. F. (2000). Protein denaturation during freezing and thawing in phosphate buffer systems: monomeric and tetrameric beta-galactosidase. *Archives of Biochemistry and Biophysics*, *384*(2), 398–406.

Pramanick, S., Singodia, D., & Chandel, V. (2013). Excipient selection in parenteral formulation development. *Pharma Times*, *45*(3), 65–77.

Prestrelski, S. J., Arakawa, T., & Carpenter, J. F. (1993). Separation of freezing-induced and drying-induced denaturation of lyophilized proteins using stress-specific stabilization. 2. Structural studies using infrared-spectroscopy. *Archives of Biochemistry and Biophysics*, *303*(2), 465–473.

Roberts, J. D., & Caserio, M. C. (1967). *Aldehydes and ketones: Reactions at the carbonyl group. Modern organic chemistry* (pp. 309–333). New York: W. A. Benjamin, Inc.

Robinson, N. E., & Robinson, A. B. (2001). Prediction of protein deamidation rates from primary and three-dimensional structure. *Proceedings of the National Academy of Sciences of the United States of America*, *98*(8), 4367–4372.

Ryan, M. P., Williams, D. E., Chater, R. J., Hutton, B. M., & McPhail, D. S. (2002). Why stainless steel corrodes. *Nature*, *415*(6873), 770–774.

Shire, S. J. (1996). Stability characterization and formulation development of recombinant human deoxyribonuclease I [Pulmozyme, (dornase alpha)]. In R. Pearlman, & J. Wang (Eds.), *Formulation, characterization and stability of protein drugs* (pp. 393–426). New York: Plenum.

Shire, S. J., Liu, J., Friess, W., Matheus, S., & Mahler, H.-C. (2010). *High concentration antibody formulations in formulation and process development strategies for manufacturing of a biopharmaceutical* (pp. 349–379). Hoboken, NJ: Wiley & Sons.

Srindhar, N. (1992). In J. R. Davis (Ed.), *Corrosion* (Vol. 13) (pp. 643–647). Ohio: ASM International.

Suzuki, Y., Nakamura, N., Kishigami, T., & Abe, S. (1980). Bacillus-thermoglucosidius alpha-glucosidase—temperature-dependence of activity and stability. *Journal of Biochemistry*, *87*(3), 745–751.

Timasheff, S. N. (2002). Protein-solvent preferential interactions, protein hydration, and the modulation of biochemical reactions by solvent components. *Proceedings of the National Academy of Sciences of the United States of America*, *99*(15), 9721–9726.

Townsend, M. W., & Deluca, P. P. (1988). Use of lyoprotectants in the freeze-drying of a model protein, ribonuclease A. *Journal of Parenteral Science and Technology*, *42*(6), 190–199.

Wang, X. L., Das, T. K., Singh, S. K., & Kumar, S. (2009). Potential aggregation prone regions in biotherapeutics a survey of commercial monoclonal antibodies. *mAbs*, *1*(3), 254–267.

Wang, N., Hu, B., Ionescu, R., Mach, H., Sweeney, J., Hamm, C., et al. (April 2009). Opalescence of an IgG1 monoclonal antibody formulation is mediated by ionic strength and excipients. *Biopharm International*, 36–47.

Wang, Y. C., & Kowal, R. R. (1980). Review of excipients and pH's for parenteral products used in the United States. *Journal of the Parenteral Drug Association*, *34*(6), 452–462.

Werner, R. G., & Langlouis-Gau, H. (1989). Meeting the regulatory requirements for pharmaceutical production of recombinant DNA derived products. *Arzneimittelforschung*, *39*(1), 108–111.

Xie, G. F., & Timasheff, S. N. (1997). The thermodynamic mechanism of protein stabilization by trehalose. *Biophysical Chemistry*, *64*(1–3), 25–43.

Yoshioka, S., Izutsu, K., Aso, Y., & Takeda, Y. (1991). Inactivation kinetics of enzyme pharmaceuticals in aqueous-solution. *Pharmaceutical Research*, *8*(4), 480–484.

Young, A. L. (2012). Powder X-ray Diffraction and its Application to Biotherapeutic Formulation Development. *American Pharmaceutical Review*, *15*(1).

Zhang, M. Z., Prestralski, S. J., Arakawa, T., & Carpenter, J. F. (1993). Glass formation is necessary but not sufficient for stabilization of proteins during freeze-drying. *Biophysical Journal*, *64*, A268.

Zietkiewicz, W., Kostrzewska, E., & Gregor, A. (1971). In vivo studies on the action of the osmolality of parenterally administered drugs. *Grzyby Drozdzopodobne*, *23*, 869–870.

Challenges in the intravenous (IV) administration of monoclonal antibodies (mAbs)

5

A majority of mAbs have been formulated for intravenous (IV) administration delivery, especially for treatment of cancer where the drug is usually administered in the hospital or an infusion center (Tables1.1 and 4.1). The IV administration is usually given as an infusion rather than a bolus, and thus requires dilution of the mAb formulation, including excipients into appropriate fluids suitable for IV administration. The resulting dilution of the excipients, especially surfactants, which may decrease below the concentration required for prevention of aggregation during agitation, may be an issue and will be discussed later in this chapter. In addition, compounds from the plastic used to manufacture IV bags may impact the stability of the mAb or pose a safety risk.

Extractables and leachables from IV bags and impact on protein/mAb stability

Extractables are compounds released from product contact surfaces after exposure to aggressive solvent conditions that exceed what the drug product normally encounters during normal storage and use, that is, extremes in pH, ionic strength, and temperature. Leachates are a subset of the extractables, which may elute from the product container contact surfaces during normal use and storage conditions (Wakankar et al., 2010). Since there is a potential for exposure of these compounds after dilution of the mAb therapeutic into IV bags, it is important to evaluate the compatibility and safety of the mAb in the IV infusion bags and sets. This can be a daunting process since there is a large selection of IV bag types available, which are made from different plastic materials. Some of the bags may also have stopper components at the filling ports and these may also need to be evaluated. A further complication, especially in Europe, is the recent practice of using a centralized IV additive service where drug is diluted into bags in advance, often requiring freezing and storage prior to shipment to the site for IV administration (Needle, 2008). Thus, assessment of the impact of longer-term storage and freezing–thawing of the drug product in the bags may be required.

The materials and manufacturing processes used by manufacturers are often considered to be proprietary. This makes leachate studies difficult, especially since additives such as plasticizers, polymerization initiators, and stabilizers that are usually used in the manufacture of the IV bags may differ in different plastic materials or even in the same type of plastic materials from each manufacturer (Quackenbos, 1954; Till et al., 1982). The leachates can include organics, metals, and volatile sulfur-containing compounds, which end up as contaminants in the drug product IV solution (Gallelli & Groves, 1993; Jenke, 2002, 2003, 2005; Jenke et al., 2005). The variability of the

Monoclonal Antibodies. http://dx.doi.org/10.1016/B978-0-08-100296-4.00005-1

levels of these leachables within or between batches, even for the same manufacturer, can be significant (Desai et al., 2007; Nuijen et al., 2001). An extensive review on the compatibility, especially as to safety, has been published (Jenke, 2007). Zinc compounds that leach from plastic surfaces can generate particulates or precipitates of drug products (Ambados, 1996; Desai et al., 2007; Gallelli & Groves, 1993). Carcinogens, such as di-2-ethylhexyl-phthalate (DEHP), have also been identified as leachable compounds from the plastic used in IV bags (Nuijen et al., 2001). The two most widely used plastics in IV bags in the US are polyvinyl chloride (PVC) and polyolefin (PO). There are several reports documenting the presence of metals, cyclohexanone, DEHP, and other organic and acidic compounds due to leaching from PVC IV bag surfaces (Arbin, Jacobson, Hanniene, Hagman, & Ostelius, 1986; Borchert et al., 1986; Cheung, Hallock, Vishnuvajjala, Nguyenle, & Wang, 1998; Demore, Vigneron, Perrin, Hoffman, & Hoffman, 2002; Pearson & Trissel, 1993; Ulsaker & Korsnes, 1977). Manufacturers have claimed that PO bags and infusion sets are free of DEHP and other plasticizers, but other leachates such as organic acids and antioxidants have been reported (Jenke, 2005, 2007; Jenke et al., 2005; Labo, Tocchi, & Rock, 1984; Labow, Tocchi, & Rock, 1986). It has been shown in several cases that drugs diluted into PO bags are more stable than when diluted into PVC bags (Jenke, 2005; Jenke et al., 2005; Nuijen et al., 2001; Thiesen & Kramer, 1999).

As mentioned there can be variation of leachable levels between lot and within the same lot from the same manufacturer. This can complicate leachable IV bag studies requiring the testing of several bags from the same or different lots. Recently it was also shown that IV bags made from a particular polymer by the same manufacturer may contain components or methods of manufacture, which result in a different product that may have an impact on the quality of the pharmaceutical being prepared for IV administration (Chang et al., 2010). In this study, it was first shown that saline in PVC and PO bags from the same manufacturer had UV absorption spectra with a maximum absorption at ~320 nm which was not present in saline that never was in an IV bag (Figure 5.1(a)). Most strikingly, PO bags of different size (250 vs 100 mL) had different intensity of absorption where it was greater in the 100 mL size. It was also found that the absorbance increased with time of exposure in the 100 mL PO bags stored at 60 °C. A protein, dulanermin, normally a homotrimer, was found to dissociate after storage in 100 mL PO bags followed by freezing and thawing, but not in PVC bags (Figure 5.1(b)). Mass spectroscopy analysis identified the compound responsible as 2-mercaptobenzothiazole, and addition of pure 2-mercaptobenzothiazole to a solution of dulanermin after freeze–thaw resulted in the same degradation as what occurred in IV bags. At first glance, all of this was surprising since the 100 and 250 mL IV bags were made from the same plastic, PO, by the same manufacturer. Disassembly of the bags revealed that a rubber stopper was used at the entry port for the 100 mL size but not the 250 mL size (Figure 5.2). Incubation of this stopper with saline showed the presence of zinc as well as absorption spectra with a maximum at 320 nM. Thus, the source of the leachate was not from the PO resin but rather an additional rubber component at the entry port. This example illustrates the complexity and difficulty of performing leachate studies on IV bags used for IV administration and most importantly shows that leachates can impact the stability of the protein. In this example, a single Zn ion

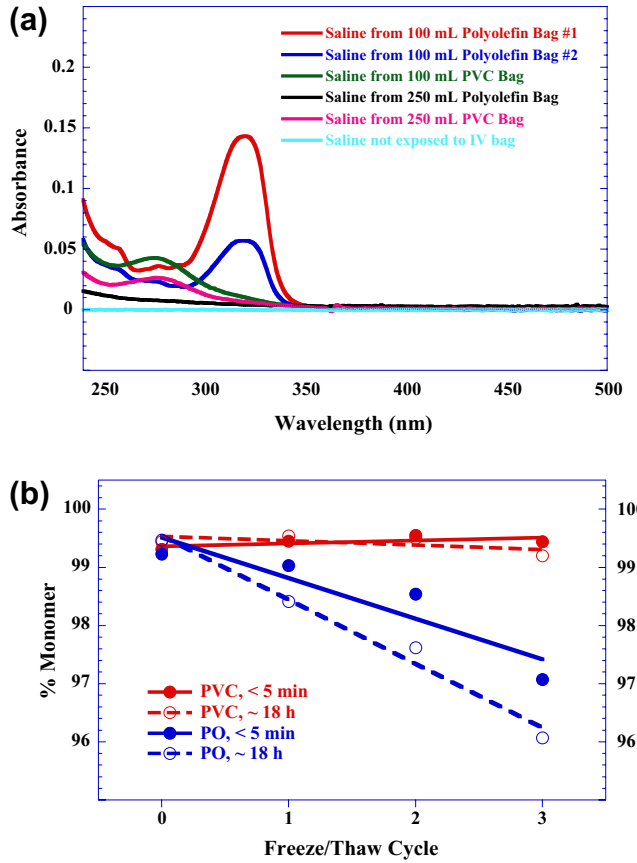

Figure 5.1 (a) Comparison of the absorbance of saline solutions from different intravenous (IV) administration infusion bags. (b) Stability of dulanermin in 100 mL IV infusion bags and the effect of freezing and thawing. Dulanermin was diluted into 100 mL IV bags to a final concentration of 0.08 mg/mL and then removed for analysis immediately or after 16 h.
From Chang et al. (2010).

holds the homotrimer together (referred to as the monomer) and when incubated with a compound capable of removing the zinc resulted in an instability when the protein was subjected to the stress of freezing and thawing.

The degradation of a mAb stored in IV bags due to exposure of leachates has not been well documented in the literature. However, metal ion leaching from IV bags can occur, and it has been shown that IgG2 mAb not stored in IV bags can undergo subtle changes in tertiary structure when exposed to Fe (III) ions (Zhou et al., 2010). The ions may promote oxidation reactions, which in turn impacts the physical stability of the antibody. In particular it was shown that potential aggregation-prone regions and hydrophobic patches in the IgG2 mAb are in close proximity to amino acid residues whose binding with metal ions leads to oxidation and aggregation (Kumar, Zhou, & Singh, 2014). In addition, two studies have been published purporting to show that

Figure 5.2 Comparison of disassembled components of 100 and 250 mL polyolefin (PO) bags from the same manufacturer.
Adapted from Chang et al. (2010).

there was no stability impact to the mAbs tested after dilution into PVC bags (Ikesue, Vermeulen, Hoke, & Kolesar, 2010; Parti & Mankarious, 1997).

mAb aggregation and particulate formation during IV administration

Although leachates from IV bags can impact the stability as well as safety of a mAb prepared for IV administration, the simple process of dilution into a bag with suitable IV administration fluid can have serious consequences. The excipients used to create a robust and stable formulation in a vial are diluted, as is the mAb. Surfactants that have been added to prevent adsorption to surfaces and generation of aggregates of mAb at the air–water interfaces may decrease below the necessary concentration for effectiveness. Often when proteins adsorb to solid surfaces they undergo an unfolding on the surface, and after release into the solution, contribute to aggregate and particulate formation

(Andrade et al., 1992). However, not all proteins unfold on hydrophobic surfaces. It has been suggested that adsorption of mAbs to hydrophobic surfaces may not necessarily lead to an unfolding (Wiseman & Frank, 2012; Xu et al., 2006). This behavior is likely related to the type of surface and the conformational stability of a particular mAb. In situations where dilution of a mAb into an IV bag results in adsorption onto an IV bag surface without unfolding, there still is the possibility of under-dosing the patient due to loss of mAb.

Surfactants are added not just to prevent adsorption to solid surfaces but also to prevent interaction of the protein with the hydrophobic surface found at the air–water interface. As an example, for an IgG4 mAb formulated with suboptimal levels of the surfactant, polysorbate 20 (PS20) aggregates and subvisible particles were generated following gentle agitation after dilution into PVC and PO IV bags containing 0.9% saline (Kumru et al., 2012). The soluble aggregates and particulates were also characterized using HIAC particle counting, SEC, SDS PAGE, nanoparticle tracking analysis with a NanoSight LM-14 instrument, microflow digital imaging, and turbidity measurements. This study also showed that with sufficient PS20 particle formation was minimized. It was also shown that PVC IV bags caused more particle formation than the PO bags.

Clinical in-use studies as a strategy to address problems during IV administration of mAbs

Sreedhara et al. discussed the need for clinical in-use studies of IV bag preparations (Sreedhara et al., 2012). The pharmacist has the responsibility to ensure product stability in the final administered form and the setting of a "beyond-use" date based on the United States Pharmacopeia 797 where the "beyond-use" date is defined as the time the compounded sterile preparation must be used to avoid loss of potency, contamination, and safety risks. Since the manufacturer of the drug is most familiar with the drug products and has several assays used to support lot release and formulation development, it makes sense for the manufacturer to assess the "beyond-use" dating. In the published study by Sreedhara et al. four IgG1 mAbs were tested after dilution into IV bags (summarized in Table 5.1(a)). The impact of final PS20 concentration after dilution of mAb1 and mAb2 into PO IV bags with and without a 60 mL headspace showed that dilution of the PS20 resulted in aggregate formation for both mAbs after agitation in the presence of a headspace. The minimum level for protection was different for the two mAbs and no aggregate formed if the headspace was removed (Tables 5.1(b) and (c)). These results showed that dilution of the protective surfactant can lead to noticeable degradation of the product and that the generation of an air–water interface on agitation was responsible for the aggregate formation. This study shows the need for the manufacturer to conduct thorough "beyond-use" dating assessment, especially in regard to duration of storage, and impact of agitation and lowered surfactant levels due to dilution. There are several ways this problem can be mitigated. The choice of IV bag volume and levels of surfactant in the formulation can be adjusted so that there is a protective surfactant concentration after dilution into the IV bag. Also minimizing the headspace should work but it may be a less practical approach.

Table 5.1a Summary of four mAb preparations used in intravenous (IV) administration bag dilution study

Sample	mAb concentration in glass vials (mg/mL)	PS20 concentration in glass vials (w/v%)	Expected mAb concentration after dilution in IV bags (mg/mL)	Expected PS20 concentration after dilution in IV bags (w/v%)	IV bag size used in current study (mL)[a]
mAb1	30	0.02	1.7	0.001	250
mAb2	60	0.02	2.4	0.0008	250
mAb2	60	0.02	1.0	0.0003	250
mAb3	50	0.04	5.0	0.004	100

[a]Overage not included.
Reproduced from Sreedhara et al. (2012).

Table 5.1b Summary of percentage of aggregates for mAb1 over time after agitation in 250 mL polyolefin intravenous (IV) administration bags with controlled 60 mL headspace and headspace removed

Expected PS20 level (w/v%)	% aggregate after 4 h of agitation at 30 °C			
	Controlled 60 cm^3 headspace		Headspace removed	
	Average % aggregates ($n = 2$)[a]	% difference[b]	Average % aggregates ($n = 2$)[a]	% difference[b]
Control (no agitation)	0.3	0	0.3	0
0%	0.45[c]	22.2[c]	0.3	0
0.0001%	0.7	0	0.3	0
0.0003%	0.5	0	0.3	0
0.001%	0.3	0	0.3	0
0.003%	0.3	0	0.3	0

[a]Two separate IV bags were analyzed.
[b]% difference $= [(x_1 - x_2)/(x_1 + x_2)/2] \times 100$.
[c]Bag 1 showed 0.5% aggregate, whereas bag 2 showed 0.4% aggregate.
Reproduced from Sreedhara et al. (2012).

Another concern during preparation of a mAb for IV dosing is the choice of diluent. Saline is often used and is available in IV bags of different sizes, but 5% dextrose solutions have also been used for dilution of drugs for IV administration. However, it has been shown that prolonged exposure of diluted mAb in a dextrose solution can lead to glycation of the mAb as detected by boronate affinity chromatography

Table 5.1c Summary of percentage of aggregates for mAb2 over time after agitation in 250 mL PO IV bags with controlled 60 mL headspace and headspace removed

Expected PS20 level (w/v%)	% aggregate after 4 h of agitation at 30 °C			
	Controlled 60 cm^3 headspace		Headspace removed	
	Average % aggregates ($n = 2$)[a]	% difference[b]	Average % aggregates ($n = 2$)[a]	% difference[b]
Control (no agitation)	0.7	7.8	0.7	0.1
0%	1.7	16.8	0.7	0.8
0.0001%	1.6	7.6	0.7	0
0.0003%	1.4	14.9	0.7	0.5
0.001%	1.5	27.5	0.7	0.6
0.003%	0.9	2.1	0.6	0.1

[a]Two separate IV bags were evaluated.
[b]% difference = $[(x_1 - x_2)/(x_1 + x_2)/2] \times 100$ where x_1 and x_2 are measurements from each bag.
Reproduced from Sreedhara et al. (2012).

(Fischer, Hoernschemeyer, & Mahler, 2008), and thus the use of such a diluent probably should be avoided.

Recently admixtures of two monoclonal antibodies for IV administration have been developed (Glover et al., 2013). The physical and chemical stabilities resulting from dilution of Herceptin® and Perjeta® into IV bags with 0.9% saline were evaluated. This can be challenging since the two antibodies may have different requirements for stabilization. These admixtures were compared to the individual dose preparation for each antibody. The color, appearance and clarity, concentration, and turbidity by ultraviolet spectroscopy, particulate analysis by HIAC Royco light obscuration, size exclusion chromatography, non-gel sieving capillary sodium dodecyl sulfate electrophoresis, analytical ultracentrifugation, and ion exchange chromatography did not show any observable differences between the controls, that is, Perjeta® and Herceptin® each alone in an IV bag, and the admixtures stored at either 5 or 30 °C for up to 24 h. The biophysical assays did not show any interactions between the two mAbs. These studies support the dilution of these two mAbs for storage for up to 24 h at 5 and 30 °C.

References

Ambados, F. (1996). Incompatibility between aminophylline and element zinc injections. *Australian Journal of Hospital Pharmacy*, *26*, 370–371.

Andrade, J. D., Hilady, V., Wei, A.-P., Ho, C.-H., Leas, A. S., Jeon, S. I., et al. (1992). Proteins at interfaces: principles, multivariate aspects, protein resistant surfaces, and direct imaging and manipulation of adsorbed proteins. *Clinical Materials*, *11*, 66–74.

Arbin, A., Jacobson, S., Hanniene, K., Hagman, A., & Ostelius, J. (1986). Studies on contamination of intravenous solution from PVC bags with dynamic headspace GC-MS and LC-diode array techniques. *International Journal of Pharmaceutics*, *28*, 211–218.

Borchert, S. J., Abe, A., Aldrich, D. S., Fox, L. E., Freeman, J. E., & White, R. D. (1986). Particulate matter in parenteral products: a review. *Journal of Parenteral Science and Technology*, *40*(5), 212–241.

Chang, J. Y., Xiao, N. J., Zhu, M., Zhang, J., Hoff, E., Russell, S. J., et al. (2010). Leachables from saline-containing IV bags can alter therapeutic protein properties. *Pharmaceutical Research*, *27*(11), 2402–2413.

Cheung, A. P., Hallock, Y. F., Vishnuvajjala, B. R., Nguyenle, T., & Wang, E. (1998). Compatibility and stability of bryostatin 1 in infusion devices. *Investigational New Drugs*, *16*(3), 227–236.

Demore, B., Vigneron, J., Perrin, A., Hoffman, M. A., & Hoffman, M. (2002). Leaching of diethylhexyl phthalate from polyvinyl chloride bags into intravenous etoposide solution. *Journal of Clinical Pharmacy and Therapeutics*, *27*(2), 139–142.

Desai, N. R., Shah, S. M., Koczone, J., Venci-Joncie, M., Sistoo, C., & Ludwig, S. A. (2007). Zinc content of commercial diluents widely used in drug admixtures prepared for intravenous infusion. *International Journal of Pharmaceutical Compounding*, *11*(5), 426–432.

Fischer, S., Hoernschemeyer, J., & Mahler, H. C. (2008). Glycation during storage and administration of monoclonal antibody formulations. *European Journal of Pharmaceutics and Biopharmaceutics*, *70*(1), 42–50.

Gallelli, J. F., & Groves, M. J. (1993). Usp perspectives on particle contamination of injectable products. *Journal of Parenteral Science and Technology*, *47*(6), 289–292.

Glover, Z. W. K., Gennaro, L., Yadav, S., Demeule, B., Wong, P. Y., & Sreedhara, A. (2013). Compatibility and stability of pertuzumab and trastuzumab admixtures in i.v. infusion bags for coadministration. *Journal of Pharmaceutical Sciences*, *102*(3), 794–812.

Ikesue, H., Vermeulen, L. C., Hoke, R., & Kolesar, J. M. (2010). Stability of cetuximab and panitumumab in glass vials and polyvinyl chloride bags. *American Journal of Health-System Pharmacy*, *67*(3), 223–226.

Jenke, D. (2002). Extractable/leachable substances from plastic materials used as pharmaceutical product containers/devices. *PDA Journal of Pharmaceutical Science and Technology*, *56*(6), 332–371.

Jenke, D. (2003). Extractable/leachable substances from plastic materials used as pharmaceutical product containers/devices (vol 56, pg 365, 2002). *PDA Journal of Pharmaceutical Science and Technology*, *57*(2), 141–147.

Jenke, D. R. (2005). Linking extractables and leachables in container/closure applications. *PDA Journal of Pharmaceutical Science and Technology*, *59*(4), 265–281.

Jenke, D. (2007). Evaluation of the chemical compatibility of plastic contact materials and pharmaceutical products; safety considerations related to extractables and leachables. *Journal of Pharmaceutical Sciences*, *96*(10), 2566–2581.

Jenke, D. R., Jene, J. M., Poss, M., Story, J., Tsilipetros, T., Odufu, A., et al. (2005). Accumulation of extractables in buffer solutions from a polyolefin plastic container. *International Journal of Pharmaceutics*, *297*(1–2), 120–133.

Kumar, S., Zhou, S. X., & Singh, S. K. (2014). Metal ion leachates and the physico-chemical stability of biotherapeutic drug products. *Current Pharmaceutical Design*, *20*(8), 1173–1181.

Kumru, O. S., Liu, J., Ji, J. Y. A., Cheng, W., Wang, Y. J., Wang, T. T., et al. (2012). Compatibility, physical stability, and characterization of an IgG4 monoclonal antibody after dilution into different intravenous administration bags. *Journal of Pharmaceutical Sciences*, *101*(10), 3636–3650.

Labo, R. S., Tocchi, M., & Rock, G. (1984). *A leachable material from polyolefin bags*. Munich, Germany: 20th International Society Blood Transfusion.

Labow, R. S., Tocchi, M., & Rock, G. (1986). Contamination of platelet storage bags by phthalate esters. *Journal of Toxicology and Environmental Health*, *19*(4), 591–598.

Needle, R. (2008). *The CIVAS handbook: Centralised intravenous additive services reference*. London: Pharmaceutical Press.

Nuijen, B., Bouma, M., Manada, C., Jimeno, J. M., Lazaro, L. L., Bult, A., et al. (2001). Compatibility and stability of the investigational polypeptide marine anticancer agent kahalalide F in infusion devices. *Investigational New Drugs*, *19*(4), 273–281.

Parti, R., & Mankarious, S. (1997). Stability assessment of lyophilized intravenous immunoglobulin after reconstitution in glass containers and poly(vinyl chloride) bags. *Biotechnology and Applied Biochemistry*, *25*, 13–18.

Pearson, S. D., & Trissel, L. A. (1993). Leaching of diethylhexyl phthalate from polyvinylchloride containers by selected drugs and formulation components. *American Journal of Hospital Pharmacy*, *50*(7), 1405–1409.

Quackenbos, H. M. (1954). Plasticizers in vinyl chloride resins. *Industrial and Engineering Chemistry*, *46*, 1355.

Sreedhara, A., Glover, Z. K., Piros, N., Xiao, N. N., Patel, A., & Kabakoff, B. (2012). Stability of IgG1 monoclonal antibodies in intravenous infusion bags under clinical in-use conditions. *Journal of Pharmaceutical Sciences*, *101*(1), 21–30.

Thiesen, J., & Kramer, I. (1999). Physico-chemical stability of docetaxel premix solution and docetaxel infusion solutions in PVC bags and polyolefine containers. *Pharmacy World & Science*, *21*(3), 137–141.

Till, D. E., Reid, R. C., Schwartz, P. S., Sidman, K. R., Valentine, J. R., & Whelan, R. H. (1982). Plasticizer migration from polyvinyl-chloride film to solvents and foods. *Food and Chemical Toxicology*, *20*(1), 95–104.

Ulsaker, G. A., & Korsnes, R. M. (1977). Determination of cyclohexanone in intravenous solutions stored in PVC bags by gas-chromatography. *The Analyst*, *102*(1220), 882–883.

Wakankar, A. A., Wang, Y. J., Canova-Davis, E., Ma, S., Schmalzing, D., Grieco, J., et al. (2010). On developing a process for conducting extractable-leachable assessment of components used for storage of biopharmaceuticals. *Journal of Pharmaceutical Science*, *99*(5), 2209–2218.

Wiseman, M. E., & Frank, C. W. (2012). Antibody adsorption and orientation on hydrophobic surfaces. *Langmuir*, *28*(3), 1765–1774.

Xu, H., Zhao, X. B., Grant, C., Lu, J. R., Williams, D. E., & Penfold, J. (2006). Orientation of a monoclonal antibody adsorbed at the solid/solution interface: a combined study using atomic force microscopy and neutron reflectivity. *Langmuir*, *22*(14), 6313–6320.

Zhou, S. X., Zhang, B., Sturm, E., Teagarden, D. L., Schoneich, C., Kolhe, P., et al. (2010). Comparative evaluation of disodium edetate and diethylenetriaminepentaacetic acid as iron chelators to prevent metal-catalyzed destabilization of a therapeutic monoclonal antibody. *Journal of Pharmaceutical Sciences*, *99*(10), 4239–4250.

This page intentionally left blank

Challenges in the subcutaneous (SC) administration of monoclonal antibodies (mAbs)

6

Many of the formulations developed for monoclonal antibodies (mAbs) have been for intravenous (IV) administration since drugs for indications such as cancer therapy could be easily administered in a hospital, often in an infusion center. This conventional route of administration usually was developed because of poor bioavailability by most other routes, greater control during administration, that is, if there are immediate adverse events the IV can be stopped, and faster pharmaceutical development. For clinical indications where treatment may be more convenient in a physician's office, clinic, or at home, the subcutaneous (SC) route of delivery is more appealing. In particular, the coupling of an SC formulation with a syringe and autoinjector increases the convenience and ease of use for the patient and ensures better compliance. IV administration of mAbs requires frequent dosing regimens and relatively high clinical doses, usually in the range of 5–700 mg per patient. The doses are often administered as a fixed dose (Campath 3–30 mg) or on the basis of body weight (Herceptin at 2–4 mg/kg) or body surface area (Erbitux 250–400 mg/m^2) of the patient. The frequency of IV administration is dictated by the requirement of maintaining a pharmacodynamically effective concentration and is linked to the circulatory half-life, typically 12–48 h for a murine mAb and 3–21 days for a chimeric, humanized, or human IgG1 mAb (Mould & Sweeney, 2007).

SC dosing is generally restricted to small volumes that do not exceed 1.5 mL, due to the tissue backpressure, resulting in loss of drug due to seepage, and injection pain (Jorgensen et al., 1996). Thus, the high doses required for effective mAb therapy necessitate the development of a high-concentration mAb formulation, often greater than 100 mg/mL. Prior to 2000, there was only one mAb formulation for SC delivery, and it was at 50 mg/mL (Enbrel). One mAb was developed for intramuscular (IM) injection and was formulated at 100 mg/mL (Syngis). Since then, 11 mAb formulations were approved for SC delivery, 5 greater than 100 mg/mL and one as high as 200 mg/mL (Table 4.1). The road to development of these high concentrations has not been easy, since aggregation and particulate formation are highly concentration dependent, and may become the dominant degradation pathway at high concentration.

The challenge of formulating at high concentration

Most of the chemical degradations of proteins are concentration independent, and thus designing stable formulations to minimize chemical degradations at high concentrations are very similar to those for more standard lower concentration formulations. On the other hand, protein aggregation is expected to be a predominant degradation pathway at high concentrations since bi- or multimolecular collisions can lead to aggregate formation.

Monoclonal Antibodies. http://dx.doi.org/10.1016/B978-0-08-100296-4.00006-3

The relationship of concentration to aggregate and particulate formation will depend on the size of the aggregates as well as the mechanism for protein association (Glatz, 1992; Manning, Chou, Murphy, Payne, & Katayama, 2010; Manning, Patel, & Borchardt, 1989). It has been suggested that irreversible noncovalent aggregation may proceed via interaction of hydrophobic groups which is rate limiting, resulting in pseudo first-order reaction kinetics (Chi, Krishnan, Randolph, & Carpenter, 2003), rather than the expected higher order concentration dependency. However, at high concentrations, protein flexibility, alteration of volume required for a conformational change, and excluded volume effects may have considerable impact on the aggregation mechanism. Thus, even if there is a rate-limiting step that is concentration independent at lower concentrations, subsequent concentration-dependent steps may lead to more rapid kinetics at higher concentration. Although in general the rate of aggregation may increase with protein concentration there are exceptions such as aggregate formation at air–water interfaces, which as previously discussed has an inverse concentration dependency (Treuheit, Kosky, & Brems, 2002).

The reduced rate of commercial success in developing high-concentration SC formulations can put a severe strain on time and resources, and thus formulation scientists try to avoid huge developmental efforts leading to phase I clinical trials. Thus, many companies have used a platform approach, which may be successful if there is a large amount of experience in developing one class of molecule such as an IgG_1 mAb. This overall approach has been recently reviewed and may lead to faster development (Warne, 2011). However, one danger is that if the platform formulation does not work, valuable time will be lost when other formulations could have been explored.

Impact on delivery due to high viscosity at high mAb concentrations

In addition to the challenges in formulation, there are challenges in other areas required for successful pharmaceutical development of a high-concentration mAb formulation (Figure 1.1) such as the impact on delivery and ability to manufacture on a large scale. Macromolecules such as mAbs can be expected to have high viscosities at high concentration due to their size. Early studies on the concentration dependence of viscosity for an IgG_1 mAb showed a strong correlation with the time required to draw 1 mL through a syringe with a 27 gauge needle (Figure 6.1). The force required to inject a Newtonian fluid with viscosity η (Pa s) with a syringe of inner radius R_s equipped with a needle of length (l) and inner radius R_n at a volumetric flow rate Q (mL/s) is given by the Hagen–Poiseuille equation (Allmendinger et al., 2014; Sutera & Skalak, 1993):

$$F = (8QlR_s^2\eta)/R_n^4 + F_{friction} \tag{6.1}$$

The first term is the "glide" force required to push the fluid through the syringe and the added term is the frictional force that occurs from contact of the movable plunger with the inner barrel of the syringe. The frictional force can be determined by using glycerol–water solutions of known viscosity using (6.1) the Hagen–Poiseuille equation. Essentially a linear regression of a plot of the measured glide force as a function of viscosity gives the needle diameter, R_n if R_s is known, from the slope and the frictional force as the intercept.

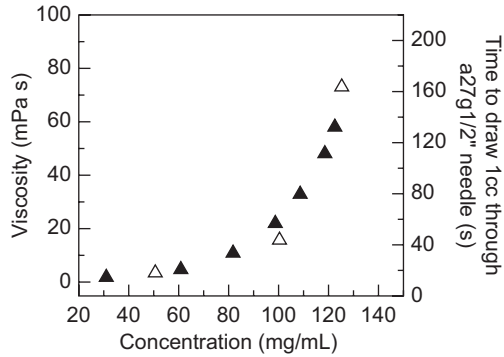

Figure 6.1 The effect of protein concentration on viscosity (closed triangles) and time to draw 1 cc through a syringe with a ½″ 27 g needle (open triangles). The IgG1 mAb was formulated in 16 mM His, 266 mM sucrose, 0.03% polysorbate 20 at pH 6. Viscosity was determined using a MCR300 rheometer (Anton Paar) using a CP50-1 cone/plate measuring system at 25 °C and a shear rate of 200/s.
From Liu et al. (2005).

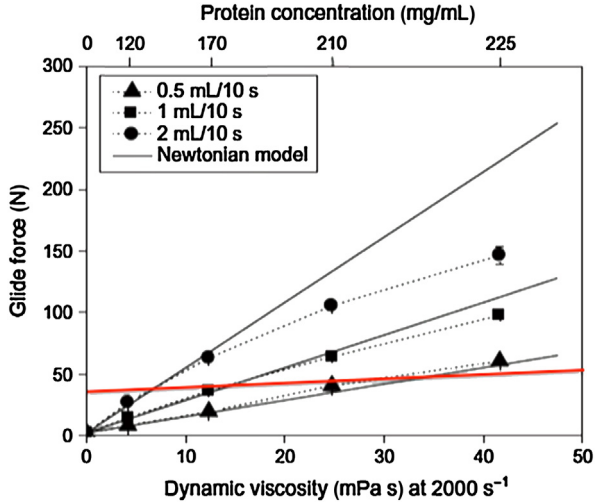

Figure 6.2 Glide forces as a function of viscosity determined at 2×10^3/s (25 °C) compared to glide forces calculated based on the Hagen–Poiseuille equation (solid lines). The glide forces were measured at a volumetric flow of 0.5 mL/10 s (triangle), 1 mL/10 s (square), and 2 mL/10 s (circle). Mean values and standard deviation are reported ($N=3$). The dotted lines are presented to guide the eye and the red line shows the generally acceptable 30 N glide force for syringes.
Adapted from Allmendinger et al. (2014).

A typical 27 gauge needle has an inner diameter of 0.21 mm. Simulations that determine glide force as a function of viscosity for a 27 gauge needle show that delivery of <1 mL in 10 s using the equation for Newtonian fluids gives very good results when compared to actual measurements of a mAb. At 2 mL/10 s there is considerable deviation from the Newtonian model (Figure 6.2) since high-concentration mAb solutions are non-Newtonian resulting in a decrease of viscosity

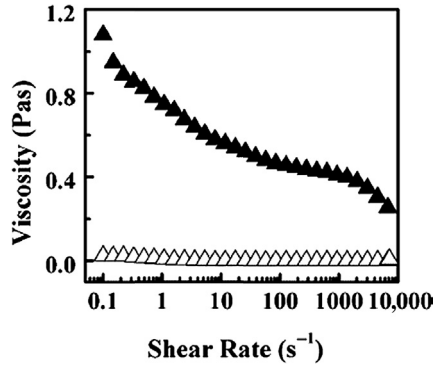

Figure 6.3 The non-Newtonian behavior of an IgG1 mAb as shown by dependence of viscosity on shear rate at 10 mg/mL (open triangles) and 200 mg/mL (solid triangles). All solutions were at 425 mM sucrose, 25 mM His, and 0.05% polysorbate 20 at pH 6. Viscosity was measured using an MCR300 rheometer (Anton PARR) equipped with a CP50-1 cone/plate measuring system at 25 °C. From Liu et al. (2005).

at higher shear (Figure 6.3) (Liu, Nguyen, Andya, & Shire, 2005) that yields a lower glide force. A model has been created for non-Newtonian fluids and used resulting in an excellent agreement with measured values for a Carbopol gel (Allmendinger et al., 2014). It has been suggested that the maximum force for manual injection with a syringe is about 30 N (Burckbuchler et al., 2010). Thus, injections for 1 mL in about 10 s become more difficult to handle at viscosity greater than 12 mPa s (Figure 6.2).

Impact on manufacturing of high-concentration SC formulations due to high viscosity

Creating a robust high-concentration formulation poses several challenges as discussed, but even if this is done successfully on a small scale a big challenge is to manufacture the formulation economically and in a reasonable time scale. The most commonly used unit operation in the pharmaceutical industry for concentration and exchange of the DS into the formulation is tangential flow filtration (Genovesi, 1983; van Reis & Zydney, 2001; Shiloach, Martin, & Moes, 1988). In this process, protein is circulated by pumping through a series of permeable hollow fiber tubes that allow for transport of water and small molecules, but not large macromolecules. Achieving a high concentration can be difficult because higher concentration than the target concentration can occur at the membrane interface, and depending on the mAbs propensity to interact with the solid surfaces of the fibers may result in adsorption and unfolding at the surface that leads to decreased transport and membrane fouling. Proteins can also be shear sensitive, and the continuous circulation through the pumps and tubing can result in shear or cavitation that results in protein denaturation and potential fouling of the tangential flow filtration (TFF) membranes. High viscosity of the protein solutions may result in high backpressures that may exceed the capacity

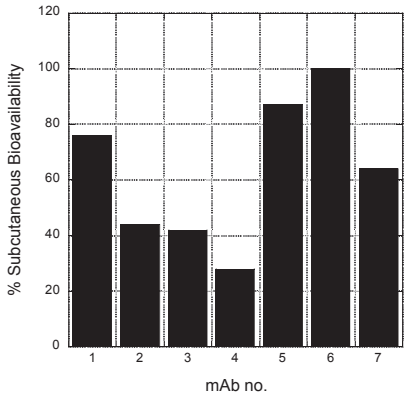

Figure 6.4 Bioavailability of seven different mAbs after subcutaneous delivery.
Used with permission from Robert Kelley, Genentech, 2014.

of the pumps resulting in a decrease of membrane flux requiring very long times to reach the targeted concentration. Higher viscosity of mAb solutions also may make it difficult to recover the concentrated solution resulting in economically unacceptable losses (Shire, 2009; Shire, Shahrokh, & Liu, 2004).

Bioavailability of a high-concentration mAb formulation for SC delivery

The bioavailability of mAbs given by the SC route of administration can vary widely. In a study using a minipig model, it was shown that the bioavailability of seven mAbs ranges from 24% to 100% (Figure 6.4). Several factors have been cited that govern the bioavailability of proteins administered SC and include the role of the lymph and blood capillaries in systemic absorption: the site of the SC injection, variability between patients related to the SC layer morphology, the depth of the injections, molecular properties of the mAbs, stability of the mAbs, and mAb formulation. The major focus for pharmaceutical development is stability and formulation of the mAbs. Recent studies suggest that positively charged mAbs may bind to SC tissue depending on the ionic strength and pH of the mAb formulation (Mach et al., 2011). The impact of this binding can be modulated by increasing formulation ionic strength or by increasing the mAb concentration resulting in a saturation of the binding to the tissue. The effect of increasing the formulation ionic strength was demonstrated using an ex vivo rat model. Specifically, two mAbs were incubated with rat SC tissue using formulations with different ionic strengths and the amount of mAb not absorbed to tissue was determined using size exclusion chromatography (SEC) of the supernatant after centrifugation to remove cell debris. An increase in the formulation ionic strength resulted in a decrease of mAb bound to SC tissue suggesting an electrostatic mechanism. The impact of multiple charged buffer species was also investigated and it was shown that specific binding of these charged species may alter the electrostatic

interactions that affect the binding of the mAbs to the SC tissue. Thus, appropriate choice of buffer components and alteration of ionic strength may be used to modulate adsorption to SC tissue that could impact the bioavailability of the mAb.

Development of analytical tools for high-concentration formulation development

Many of the analytical methods that are currently used to investigate covalent (chemical) and conformational alterations in proteins are easily adapted to the study of proteins at high concentration (Jones, 1993; Pearlman & Nguyen, 1991). Analytical techniques such as differential scanning calorimetry (DSC), modulated DSC (Breen, Curley, Overcashier, Hsu, & Shire, 2001; McPhillips, Craig, Royall, & Hill, 1999), Fourier transform infrared spectroscopy (Costantino, Chen, Griebenow, Hsu, & Shire, 1998; Prestrelski, Tedeschi, Arakawa, & Carpenter, 1993), Raman (Tuma, 2005), and fluorescence (Sharma & Kalonia, 2003) spectroscopy have been used to characterize solid-state formulations, and can be useful in developing alternatives to TFF for creating concentrated DP subsequent to reconstitution (discussed in more detail in the next chapter). Unfortunately many of the analytical technologies used to characterize proteins require dilution of the protein to lower concentrations or the use of solvents that differ from the initial formulation composition. This may have considerable impact on the results since changes in solvent composition or concentration may change the behavior of the protein that occurs at the higher concentration.

It is especially important to analyze for molecular weight and size in the high-concentration formulation. As discussed previously, SEC has several disadvantages including potential interaction with the chromatographic resin, and impact of hydrodynamic volume on molecular weight determination. The first issue is usually mitigated using organic solvents or salts to minimize the column interactions, but there is then the uncertainty regarding whether there is a perturbation of the protein–protein interactions that results in aggregate formation. The impact of hydrodynamic volume and shape can be addressed using an online static light scattering (SLS) detector to determine molecular weights directly across the chromatographic peaks. However, due to the dilution during the chromatography any reversible self-association that is concentration dependent may not be detected due to the shifting of the equilibrium toward monomer at the lower concentration. As an example, the rapid dissociation of a monoclonal antibody upon dilution yielded varying aggregate levels by SEC, depending on the time and temperature of analysis after sample dilution (Moore, Patapoff, & Cromwell, 1999).

Thus, the characterization and study of protein–protein interactions at high concentration are difficult to assess with those methodologies. Having said that, determinations using DLS at low concentration have proven to be useful in predicting the viscosity behavior and solubility of mAbs. However, in order to investigate the properties of concentrated mAbs requires development of analytics that can be used at high concentrations. Some of the methods, including the DLS technology, will be discussed further in the next chapter.

References

Allmendinger, A., Fischer, S., Huwyler, B., Mahler, H. C., Schwarb, E., Zarraga, I. E., et al. (2014). Rheological characterization and injection forces of concentrated protein formulations: an alternative predictive model for non-Newtonian solutions. *European Journal of Pharmaceutics and Biopharmaceutics*, *87*(2), 318–328.

Breen, E. D., Curley, J. G., Overcashier, D. E., Hsu, C. C., & Shire, S. J. (2001). Effect of moisture on the stability of a lyophilized humanized monoclonal antibody formulation. *Pharmaceutical Research*, *18*(9), 1345–1353.

Burckbuchler, V., Mekhloufi, G., Giteau, A. P., Grossiord, J. L., Huille, S., & Agnely, F. (2010). Rheological and syringeability properties of highly concentrated human polyclonal immunoglobulin solutions. *European Journal of Pharmaceutics and Biopharmaceutics*, *76*(3), 351–356.

Chi, E. Y., Krishnan, S., Randolph, T. W., & Carpenter, J. F. (2003). Physical stability of proteins in aqueous solution: mechanism and driving forces in nonnative protein aggregation. *Pharmaceutical Research*, *20*(9), 1325–1336.

Costantino, H. R., Chen, B., Griebenow, K., Hsu, C. C., & Shire, S. J. (1998). Fourier-transform infrared spectroscopic investigation of the secondary structure of aqueous and dried recombinant human deoxyribonuclease I. *Pharmacy and Pharmacology Communications*, *4*, 391–395.

Genovesi, C. S. (1983). Several uses for tangential-flow filtration in the pharmaceutical industry. *J. Parenteral Science and Technology*, *37*(3), 81–86.

Glatz, C. E. (1992). In T. J. Ahern & M. C. Manning (Eds.), *Modeling of aggregation-precipitation phenomena. Stability of protein pharmaceuticals*. New York: Plenum Press.

Jones, A. J. S. (1993). Analysis of polypeptides and proteins. *Advanced Drug Delivery Reviews*, *10*(1), 29–90.

Jorgensen, J. T., Romsing, J., Rasmussen, M., MollerSonnergaard, J., Vang, L., & Musaeus, L. (1996). Pain assessment of subcutaneous injections. *Annals of Pharmacotherapy*, *30*(7–8), 729–732.

Liu, J., Nguyen, M. D. H., Andya, J. D., & Shire, S. J. (2005). Reversible self-association increases the viscosity of a concentrated monoclonal antibody in aqueous solution. *Journal of Pharmaceutical Sciences*, *94*(9), 1928–1940.

Mach, H., Gregory, S. M., Mackiewicz, A., Mittal, S., Lalloo, A., Kirchmeier, M., et al. (2011). Electrostatic interactions of monoclonal antibodies with subcutaneous tissue. *Therapeutic Delivery*, *2*(6), 727–736.

Manning, M. C., Chou, D. K., Murphy, B. M., Payne, R. W., & Katayama, D. S. (2010). Stability of protein pharmaceuticals: an update. *Pharmaceutical Research*, *27*(4), 544–575.

Manning, M. C., Patel, K., & Borchardt, R. T. (1989). Stability of protein pharmaceuticals. *Pharmaceutical Research*, *6*(11), 903–918.

McPhillips, H., Craig, D. Q. M., Royall, P. G., & Hill, V. L. (1999). Characterisation of the glass transition of HPMC using modulated temperature differential scanning calorimetry. *International Journal of Pharmaceutics*, *180*(1), 83–90.

Moore, J. M. R., Patapoff, T. W., & Cromwell, M. E. M. (1999). Kinetics and thermodynamics of dimer formation and dissociation for a recombinant humanized monoclonal antibody to vascular endothelial growth factor. *Biochemistry*, *38*(42), 13960–13967.

Mould, D. R. & Sweeney, K. R. D. (2007). The pharmacokinetics and pharmacodynamics of monoclonal antibodies – mechanistic modeling applied to drug development. *Current Opinion in Drug Discovery & Development, 10*(1), 84–96.

Pearlman, R., & Nguyen, T. H. (1991). New York. In V. H. L. Lee (Ed.), *Analysis of protein drugs. Peptide and protein drug delivery* (pp. 247–301). Marcel Dekker.

Prestrelski, S. J., Tedeschi, N., Arakawa, T., & Carpenter, J. F. (1993). Dehydration-induced conformational transitions in proteins and their inhibition by stabilizers. *Biophysical Journal*, *65*(2), 661–671.

Sharma, V. K., & Kalonia, D. S. (2003). Steady-state tryptophan fluorescence spectroscopy study to probe tertiary structure of proteins in solid powders. *Journal of Pharmaceutical Sciences*, *92*(4), 890–899.

Shiloach, J., Martin, N., & Moes, H. (1988). Tangential flow filtration. *Advances in Biotechnological Processes*, *8*, 97–125.

Shire, S. J. (2009). Formulation and manufacturability of biologics. *Current Opinion in Biotechnology*, *20*(6), 708–714.

Shire, S. J., Shahrokh, Z., & Liu, J. (2004). Challenges in the development of high protein concentration formulations. *Journal of Pharmaceutical Sciences*, *93*(6), 1390–1402.

Sutera, S. P., & Skalak, R. (1993). The history of Poiseuille's law. *Annual Review of Fluid Mechanics*, *25*, 1–19.

Treuheit, M. J., Kosky, A. A., & Brems, D. N. (2002). Inverse relationship of protein concentration and aggregation. *Pharmaceutical Research*, *19*(4), 511–516.

Tuma, R. (2005). Raman spectroscopy of proteins: from peptides to large assemblies. *Journal of Raman Spectroscopy*, *36*(4), 307–319.

van Reis, R., & Zydney, A. (2001). Membrane separations in biotechnology. *Current Opinion in Biotechnology*, *12*(2), 208–211.

Warne, N. W. (2011). Development of high concentration protein biopharmaceuticals: the use of platform approaches in formulation development. *European Journal of Pharmaceutics and Biopharmaceutics*, *78*(2), 208–212.

7 Strategies to deal with challenges of developing high-concentration subcutaneous (SC) formulations for monoclonal antibodies (mAbs)

The major degradation that occurs at high concentrations of proteins and monoclonal antibodies (mAbs) is aggregation and insolubility. Insolubility of a protein at high concentration can manifest itself as formation of particulates or phase separations including formation of gels. In addition to this, as previously discussed, is the increase of viscosity at higher concentrations which pose challenges for administration and manufacturing. All of these phenomena are linked to protein–protein interactions (PPI) that increase at higher concentration because of the closer proximity of the protein. The role of PPI and impact on properties such as viscosity will be discussed in more detail in the next chapter. Here we will discuss strategies that can be used to mitigate the challenges, in particular, the issue of the impact of viscosity on pharmaceutical development of mAbs.

Using existing manufacturing technologies through redesign of equipment or modification of process variables to produce high-concentration formulations

The most common process unit operation for concentration of proteins and mAbs is tangential flow filtration (TFF). As previously discussed, increases in viscosity and also decreases in diffusion could result in sufficient backpressure, which decreases the efficiency of the process because of exceeding the capacity of the pumps. In addition, interactions with the TFF membranes could result in unfolding of the proteins leading to insolubility issues. Recovery of the concentrated protein from the TFF system may also be problematic because of the higher viscosity, which decreases flow and results in loss of the concentrated drug product (DP). The performance and recovery from TFF systems has been reviewed and involves the design of the TFF properties such as hold-up volumes and tank-working volumes, as well as operational parameters such as system pressure and pump flow rates, which are limited by the viscosity of the solution (Rao, Gefroh, & Kaltenbrunner, 2012). Essentially, the TFF process involves four steps. In the first step, the formulated DS is concentrated to an intermediate concentration lower than the final target, and in the second step, it is diafiltered into the formulation buffer system. In the third step, the solution is concentrated to a level beyond the final targeted concentration. The overconcentration is required since there is a considerable volume of final DP held in piping outside the TFF processing tank, which is often recovered with a formulation buffer flush in the final step resulting in

Monoclonal Antibodies. http://dx.doi.org/10.1016/B978-0-08-100296-4.00007-5

dilution of the product. Some of this dilution can be minimized by using a N_2 gas purge but still may be limited by how much of the product can easily flow out of the system at the higher viscosity at final targeted DP concentration. A strategy that has been used successfully to concentrate mAbs and increase yield is to use high temperature to lower viscosity during the TFF unit operation. The pressure drop for the TFF system can be decreased at higher temperatures (Figure 7.1(a)) as the viscosity of the solution decreases (Figure 7.1(b)), resulting in increased flux ($L/m^2/h$) at a given pressure drop (Figure 7.1(c)). Such a strategy has been used successfully for a mAb where the process temperature was increased from 23 to 46 °C, resulting in a twofold decrease in viscosity and a twofold increase in the filtration flux (Winter, 2008; Liu, Ma, Winter, & Bayer, 2010). As much as 600 g of mAb has been processed to 150 mg/mL with a 96.2% yield using such a modified TFF unit operation. Implementation of this strategy does require extensive study of the stability of the mAb at the elevated temperature. Thus, the choice of a formulation that minimizes degradation at elevated temperature goes hand in hand with the TFF process design. Also investigation of impact of higher temperature on bioburden may require addition of microorganisms at different temperatures to ensure there is sufficient control of growth during the elevated temperature process.

Development of alternative processes/formulations for manufacturing of high-concentration dosage forms

Although TFF is the most commonly used unit operation to manufacture a high-concentration protein/mAb final DP, any drying technique that can be scaled up for manufacturing can be used. An example of this is the use of freeze-drying to produce a solid dosage form, which can be reconstituted using a lower volume than that loaded into the vials before freeze-drying (Figure 7.2). One of the drawbacks for such a process is that not only is the mAb concentrated upon reconstitution but also are all the excipients. This raises a level of concern regarding the final tonicity of the reconstituted product since preparations that greatly exceed isotonicity may result in impacting adsorption of the drug at the injection site as well as result in increased pain and tissue damage (Chapter 6). Lowering the concentration of excipients may circumvent this problem, but there needs to be a sufficient amount of stabilizer to ensure minimization of degradation during the freeze-drying process. As an example, the tonicity of a freeze-dried formulation for subcutaneous (SC) delivery of an IgG1 mAb at high concentration was dependent on the loading concentration of the mAb. The final concentration after reconstitution is given below:

$$C_F = C_L V_L / (V_R + V_S) \tag{7.1}$$

where C_F is the final concentration after reconstitution, C_L is the loading concentration of mAb, V_L is the loading volume V_R is the volume of diluent added for reconstitution, and V_S is the volume contributed from the remaining solids. The expected final concentration

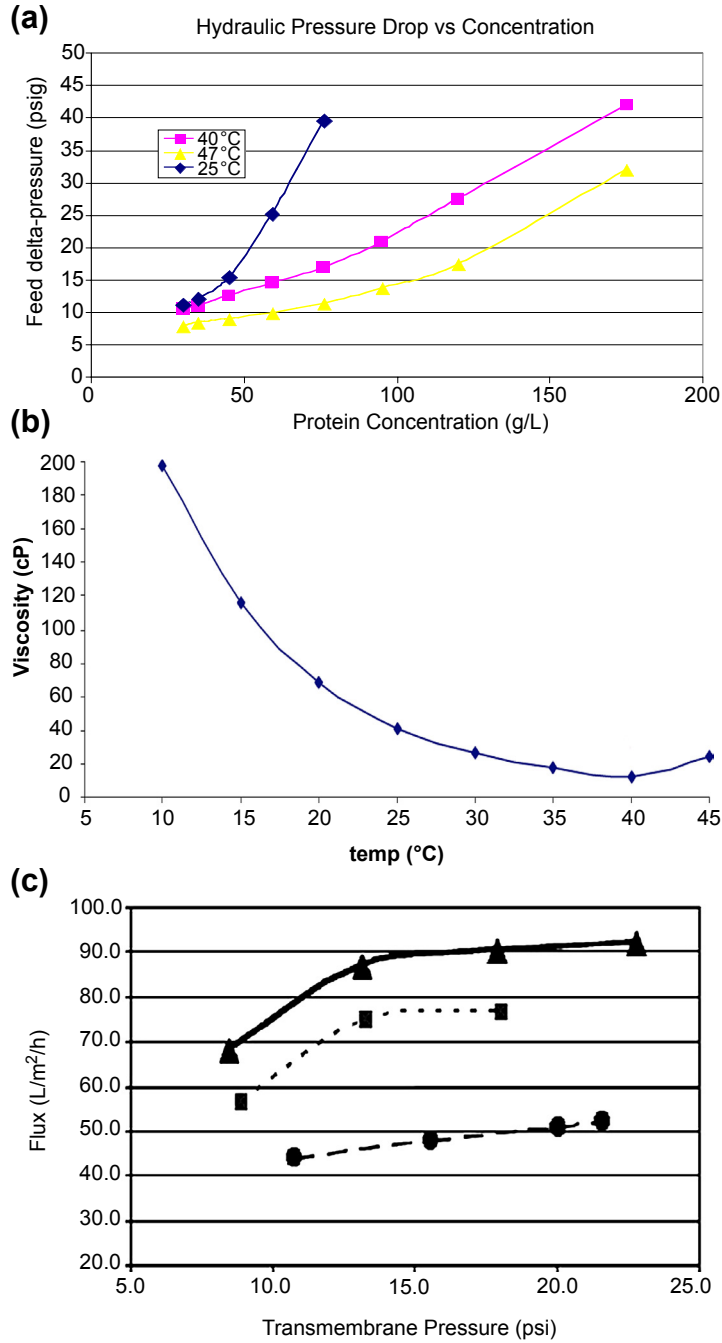

Figure 7.1 (a) Pressure drop in a tangential flow filtration (TFF) system as a function of temperature, (b) viscosity of an IgG1 mAb at 150 mg/mL as a function of temperature, and (c) the TFF flux ($L/m^2/h$) versus transmembrane pressure (psi) at different temperatures for an IgG1mAb1, initially at 30 mg/mL and at 23 (solid circles), 40 (solid squares), and 46 °C (solid triangles).
Figures kindly provided by Charles Winter.

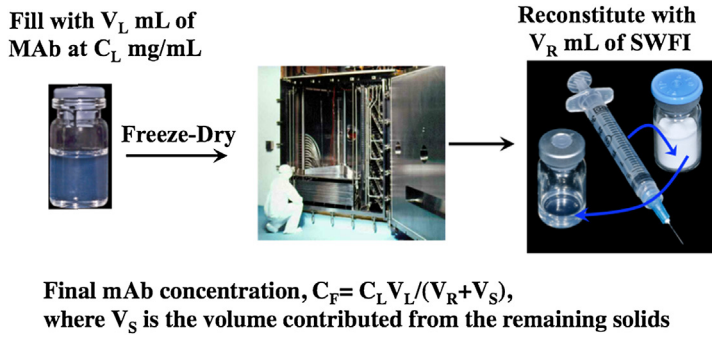

Figure 7.2 Using lyophilization to manufacture a high-concentration subcutaneous (SC) formulation. SWFI, sterile water for injection.

will be higher than the actual value if the contribution of volume from the solids is not included. This contribution can be estimated by

$$V_S = C_L V_{pro} + \sum_{i}^{n} C_{si}\, V_{si} \tag{7.2}$$

where V_{pro} and V_{si} are the partial specific volumes for protein and the ith solute at concentration C_{si}, respectively.

The molar ratio of lyoprotectant to the mAb will determine the amount of aggregate that forms during freeze-drying, and this ratio as well as the loading concentration of protein and excipients will dictate the tonicity of the final reconstituted product (Figure 7.3) (Shire, 2009). Thus, if the targeted final concentration of mAb after reconstitution is 200 mg/mL, then a lyoprotectant to mAb ratio of 250:1 and 500:1 will result in tonicities of 333 and 666 mM, respectively. Although a ratio of 500:1 can provide better stability than a ratio of 250:1, there might be some concern regarding the hypertonicity of the reconstituted formulation. The effect of lyoprotectant:mAb molar ratio on stability of an IgG_1 mAb at 2–8 and 30 °C is shown in Figure 7.4. As can be seen, a molar ratio of 500:1 can provide good stability at 30 °C when compared to a 250:1 ratio. However, because of the concern of impact on bioavailability and injection pain, it may make more sense to use the lower molar ratio. Thus, since the lyophilized DP can be stored and refrigerated in a clinic, and the stability at 2–8 °C is similar for both molar ratios, the lower molar ratio could be used. This example shows that choosing the most stable formulation is not necessarily the best path and should be dictated by the overall target product profile.

Although the viscosity of the mAb at the lower-loading concentration may be low, the viscosity of the reconstituted DP can be quite high and can impact delivery by injection (Chapter 6). Another issue is that the increased viscosity may also affect the time for reconstitution as shown in Figure 7.5. In addition to the viscosity, the loading concentration can also lead to significant increases in reconstitution time (Shire, Liu, Friess, Matheus, & Mahler, 2010; Shire, Shahrokh, & Liu, 2004). It was shown that as the protein-loading concentration decreased, reconstitution times also decreased. Investigation of the morphology of the lyophilized solid by scanning electron microscopy showed a gradual transition

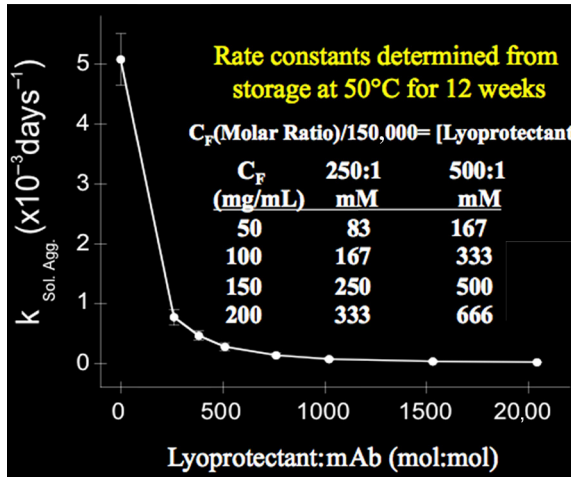

Figure 7.3 Stability and final tonicity after reconstitution as a function of lyoprotectant:mAb molar ratio.

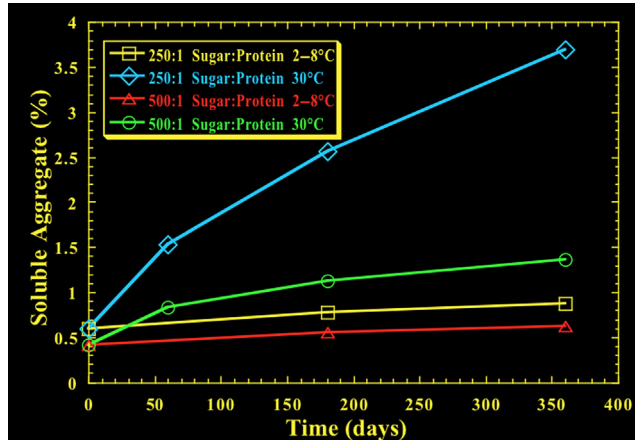

Figure 7.4 Stability of an IgG1 mAb as a function of lyoprotectant:mAb molar ratio and temperature of storage.

from a dense solid to a more loosely packed structure as protein-loading concentration was decreased (Figure 7.6). Thus, the ease of wetting of the cake and the impact on reconstitution time are very likely related to the differences in this morphology.

In the example discussed, the high-concentration formulation is created when adding sterile water for injection into the vial. Thus, the end user actually prepares the high concentration for SC delivery by reconstituting the lyophilized cake with a lower volume than used for the loading of the mAb prior to freeze-drying. This method can also be scaled up using bulk freeze-drying in trays, which after reconstitution and filtration can be filled into vials.

Different drying technologies can also be used to manufacture suspensions of mAbs at high concentrations, where the dried solute is added to a suspension vehicle that

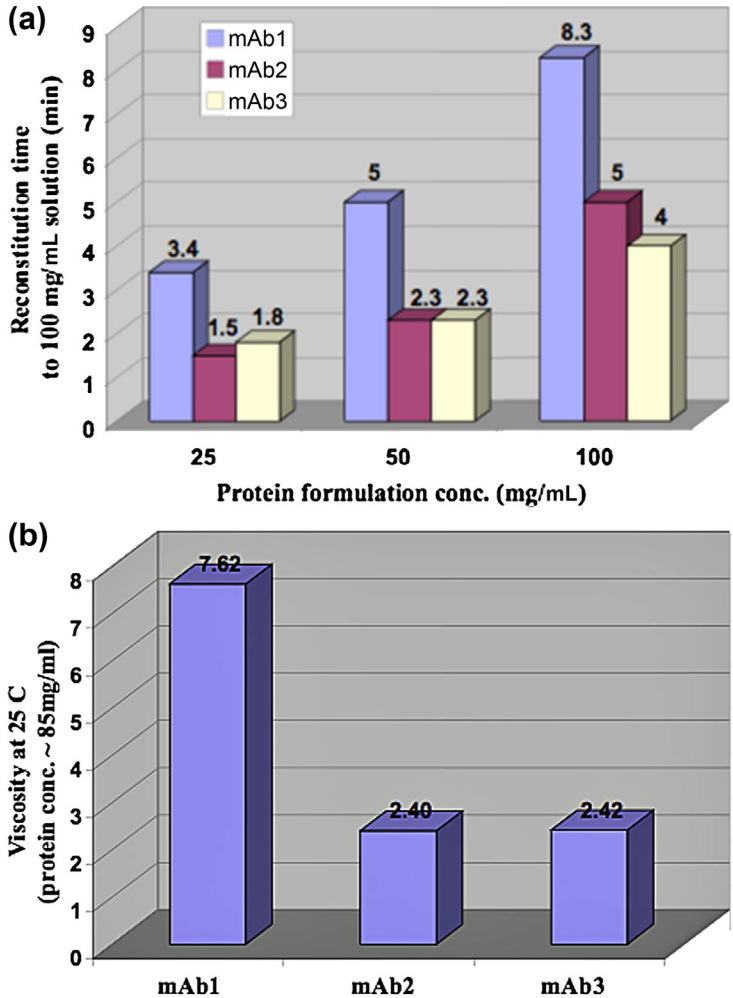

Figure 7.5 Three humanized IgG1 mAbs with the same IgG1 human Fc construct but different complementarity determining regions (CDRs) formulated identically and lyophilized using the same lyophilization process. (a) Time to reconstitute the lyophilized cake resulting in a final mAb concentration of 100 mg/mL. (b) Viscosity at 25 °C after reconstitution to a final mAb concentration of 85 mg/mL.
From Shire et al. (2010).

does not result in solubilization of the solute. The viscosity of the suspension vehicle should be low since the vehicle viscosity would contribute to the suspension viscosity as suggested by Einstein's equation for the viscosity of solutions (Einstein, 1911):

$$\eta = \eta_0 (1 + 2.5\varphi) \tag{7.3}$$

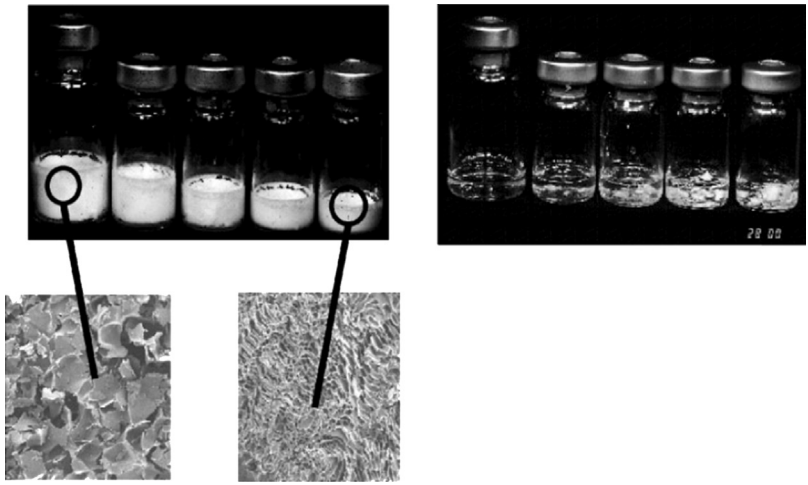

Figure 7.6 Lyophilization of a mAb as a function of loading concentration. Upper left panel: Loading concentrations from left to right were 40, 60, 80, 100, and110 mg/mL, respectively, while maintaining the same total mass of mAb and excipients. Lower left panels: Scanning electron microscopy of lyophilized solid for the 40 and 110 mg/mL mAb loading concentrations. Right panel: 10 min after reconstitution of vials in the upper left panel to 125 mg/mL with sterile water for injection.
From Shire et al. (2004).

where η is the suspension viscosity, η_0 the viscosity of the suspension vehicle, and φ the volume fraction of solute (volume of solute/volume of solution).

Suspension of proteins should have viscosities that approach that of the diluent used for the suspension if the volume fraction of dispersed solute is low. As an example, crystallization of mAbs has been used to generate high-concentration suspensions, which generally have lower viscosity than the equivalent aqueous formulation (Figure 7.7) (although as will be discussed, appropriate selection of excipients can generate aqueous high concentration at low viscosity) (Yang et al., 2003). Suspensions have also been created using milled lyophilized powder (Chen et al., 2005), amorphous precipitates (Matheus, Friess, Schwartz, & Mahler, 2009), generation of excipient-free protein microspheres (Brown et al., 2006), and powders from spray drying (Bowen, Armstrong, & Maa, 2012; Dani, Platz, & Tzannis, 2007). In the recent study by Bowen et al., it was shown that suspensions of three mAbs in a low-viscosity oil, Miglyol® 840 (η_0 = ~9 mPa s), generally outperformed liquid formulations for injectability as assessed by glide force measurements despite higher viscosities when compared to equivalent mAb concentrations for liquid formulations. It was also emphasized that Einstein's equation (7.3) is valid only for dilute suspensions. An empirical equation relating suspension viscosity to powder concentration was derived and compared to a modified form of the Einstein equation. The latter was found to underestimate the empirical data. Another important finding was that the suspension viscosity was similar for all the mAbs studied although the liquid viscosity was very dependent on the mAb that was formulated.

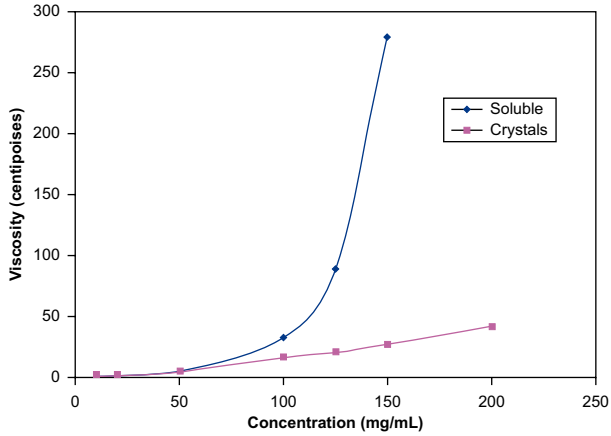

Figure 7.7 Viscosity measurements of infliximab. Infliximab (100 mg/vial containing 500 mg of sucrose, 0.5 mg of polysorbate 80, 2.2 mg of monobasic sodium phosphate (monohydrate), and 6.1 mg of dibasic sodium phosphate (dihydrate)) was reconstituted in water to concentrations of 10, 25, 50, 100, 125, and 150 mg/mL and compared with various concentrations of crystalline suspensions. For crystalline suspensions of infliximab, a 200 mg/mL solution (which was in formulation buffer containing 10% ethanol, 10% PEG 3350, 0.1% Tween 80, and 50 mM trehalose in 50 mM sodium phosphate buffer, pH 7.0) was tested for viscosity in addition to the concentrations mentioned above for soluble infliximab.
Reproduced from Yang et al. (2003).

Using formulation excipients to reduce viscosity

As discussed, formulation development is important in designs of new manufacturing processes. Much of the alternate process development used lyophilization and spray drying, which require appropriate excipients to stabilize the protein/mAb from the stresses that occur during the alternative drying processing. On another tact, it would be highly desirable to create a liquid formulation that can be easily manufactured using TFF. High viscosity at high concentrations is clearly one of the challenges that need to be overcome, and thus it is imperative to use excipients that can lower viscosity in a liquid formulation. In later chapters the role of PPI will be discussed, particularly attractive interactions, which appear to be a major contributor to the high viscosities that have been observed for some mAbs. The nature of these interactions will dictate what excipients are most effective in disrupting these interactions. In early studies by Liu et al. (Liu, Nguyen, Andya, & Shire, 2005) it was shown that attractive electrostatic interactions predominate at the high concentration of an IgG_1 mAb, and that addition of NaCl was effective in lowering viscosity (this will be discussed in more detail in Chapter 9). In subsequent studies by Kanai et al., it was shown that addition of cations appears to reduce the viscosity of this mAb by screening of interactions whereas binding of anions to the mAb is involved in the viscosity reduction (Kanai, Liu,

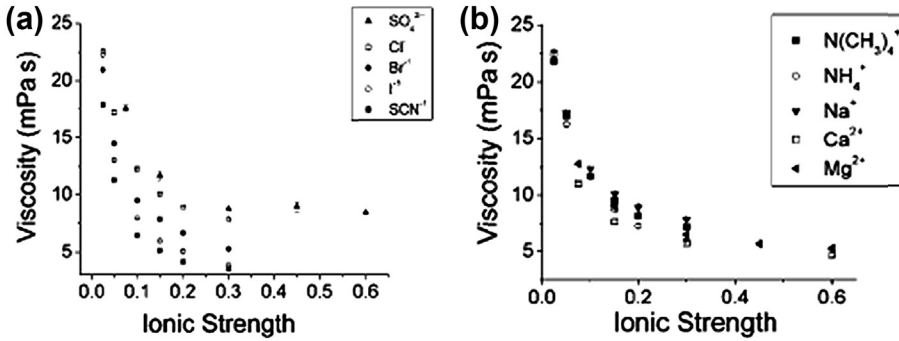

Figure 7.8 Solution viscosity of 125 mg/mL IgG1 mAbmAb1 in 30 mM histidine buffer at pH 6.0 with different addition of salts as a function of ionic strength. (a) Series of sodium salts. (b) Series of chloride salts.
Adapted from Kanai et al. (2008).

Patapoff, & Shire, 2008). What was most notable is that the effectiveness of the anion appeared to be related to the Hofmeister series, where the more chaotropic salts were more effective in the reduction of viscosity (Figure 7.8). On the other hand, it was shown that the use of hydrophobic salts could significantly reduce the viscosity of concentrated bovine serum albumin and γ-globulin (300–400 mg/mL) (Du & Klibanov, 2011). It was shown that the more hydrophobic the excipient, the more effective it was in reducing viscosity to levels below 50 mPa s. As an example, addition of the hydrophobic salt trimethylphenyl ammonium iodide was more effective than NaI in reduction of the viscosity of 300 mg/mL γ-globulin (Figure 7.9). It was proposed that the hydrophobic salts compete with hydrophobic attractions that result in protein network formation at the high concentration. The conclusion that this is in general the case has yet to be substantiated since this study involved only two, albeit very different, proteins.

Another excipient that has been used to effectively reduce viscosity of mAbs is ArgHCl (Bowen, Liu, & Patel, 2011; Connolly et al., 2012; Inoue, Takai, Arakawa, & Shiraki, 2014; Kanai et al., 2008). In the recent work by Inoue et al., it was shown that Arg decreased the viscosity of three antibody solutions (bovine γ-globulin, human γ-globulin, and human IgG), but not that of globular proteins such as α-amylase and α-chymotrypsin. It was suggested that at least two interaction mechanisms could explain the effect of ArgHCl on viscosities of high antibody concentrations. Specifically it was proposed that at concentrations of ArgHCl below 200 mM along with other excipients such as LysHCl, GdnHCl, and NaCl reduction of viscosity occurred primarily by ion screening and suppression of electrostatic interactions. On the other hand at higher excipient concentrations (500–1000 mM), the effectiveness of ArgHCl on viscosity reduction was significantly greater than for GdnHCl, LysHCl, and NaCl suggesting that the reduction of viscosity by ArgHCl was not simply due to suppression of electrostatic interactions, but also other interactions such as cation–π interactions between the guanidinium group of Arg and the aromatic groups of protein

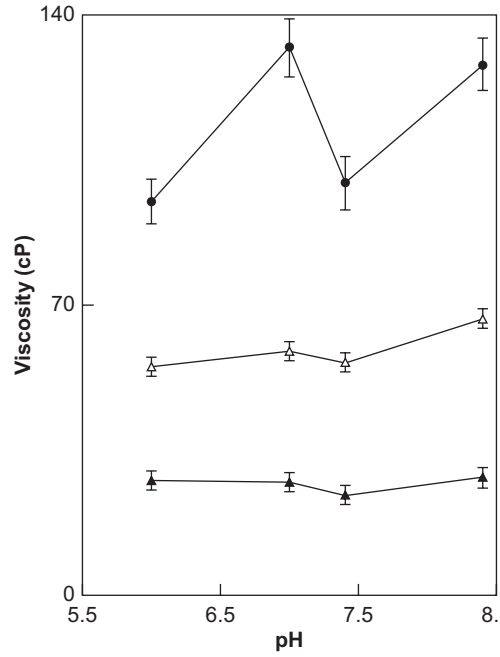

Figure 7.9 The pH-dependence of the viscosity of a 300 mg/mL γ-globulin solution with no excipient added (solid circles) or in the presence of 0.5 M NaI (open triangles) or 0.5 M trimethylphenylammonium iodide (solid triangles). From Du and Klibanov (2011).

(Arakawa et al., 2007; Inoue et al., 2014). An important use of ArgHCl in reducing viscosity is for an IgG1 mAb where the ideal pH of the liquid formulation was 6.0 where the rates of Asp isomerization and deamidation are minimized as discussed previously (Figure 4.3). However, at pH 6 the viscosity of this IgG1 mAb at 130 mg/mL is at a maximum (Figure 7.10). Thus, a formulation that stabilizes chemical degradations also results in a maximum viscosity. Using an ArgHCl histidine buffer system at pH 6 effectively reduced the viscosity from about 80 to 13 mPa s while maintaining the optimization of the chemical degradations (Figure 7.10). Although ArgHCl appears to have wide applicability for dealing with PPI and viscosity, it does not always work effectively. An IgG_4 mAb (with a mutation at the hinge region that makes it more like an IgG_1 mAb preventing the half molecule formation often seen with IgG4) was formulated with and without arginine salts. The rate of aggregation was substantially greater in the presence of arginine succinate at pH 5.5 and the viscosity was essentially unaltered when formulated with arginine acetate at pH 5.5 (Figure 7.11). Since these studies were not conducted with ArgHCl, it leaves open the question of the role of the counterion, but certainly shows that arginine may not always be effective in reducing viscosity of a mAb.

Another approach to lowering viscosity is to formulate mAbs at lower concentrations since the viscosity varies exponentially with concentration (Figure 6.1). However, such an approach requires the SC administration of large volumes to attain similar dosing at the higher concentrations. Until now excipients have been chosen based on their ability to reduce attractive interactions and lower viscosity of the

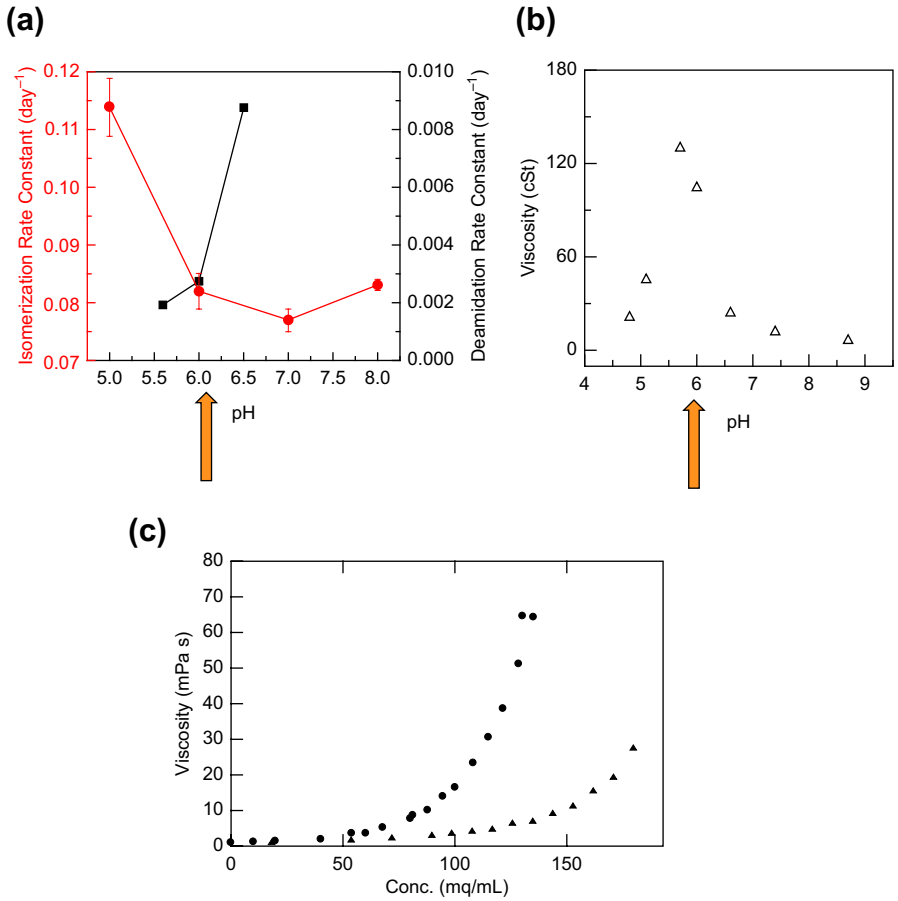

Figure 7.10 (a) The pseudo first-order rate constants for deamidation and isomerization in an IgG1 mAb as a function of pH. (b) The kinematic viscosity as a function of pH at 125 mg/mL IgG1 mAb. (c) Viscosity of the IgG1 mAb with no excipients (solid circles) and addition of 200 mM ArgHCl (solid triangles).
Figure 7.10(a) and (b) adapted from Shire et al. (2010).

high-concentration mAb formulation. An excipient has also been developed that alters the SC environment allowing for administration of volumes greater than 1.5 mL for SC dosing. The SC space matrix is composed of several materials including hyaluronan, which creates the viscoelastic component of the SC interstitial matrix. An enzyme, human hyaluronidase (rhuPH-20), that depolymerizes the hyaluronan results in the ability to inject large volumes by the SC route of administration (Bookbinder et al., 2006; Narasimhan, Mach, & Shameem, 2012). The interstitial matrix is reconstructed rapidly after the injection and clearance of the enzyme. This technology referred to as Enhanze™ by the company Halozyme has been successfully used in SC delivery of large volumes of two mAbs, Herceptin® and Mab Thera® (Shpilberg & Jackisch, 2013). In addition to enabling large SC volume injections, it has been

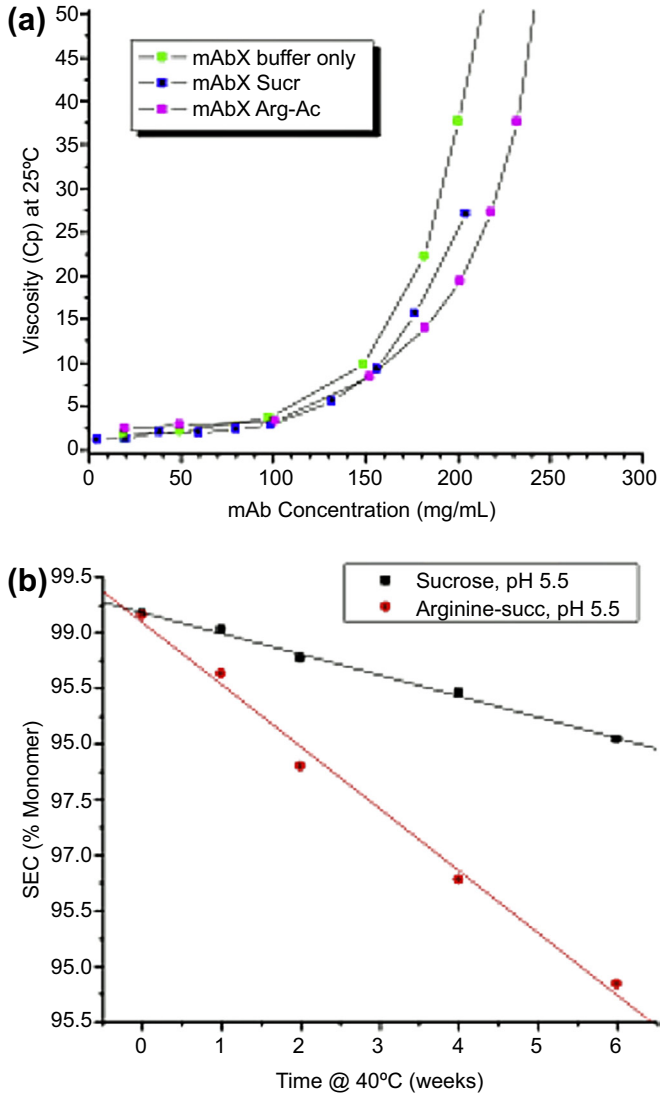

Figure 7.11 Effect of arginine compounds on (a) viscosity and (b) aggregation as measured by decrease in monomer by SEC for an IgG_4 mAb. SEC, size-exclusion chromatography. From Tom Scherer (unpublished observations).

shown that the Halozyme technology can result in significant improvements in pharmacokinetics and bioavailability (Bookbinder et al., 2006).

Another way to administer large volumes by the SC route is to use injection delivery devices. The next chapter will discuss some of those options as well as the technical challenges for development of such devices coupled with the protein drug, especially the interplay between device and formulation design.

References

Arakawa, T., Ejima, D., Tsumoto, K., Obeyama, N., Tanaka, Y., Kita, Y., et al. (2007). Suppression of protein interactions by arginine: a proposed mechanism of the arginine effects. *Biophysical Chemistry*, *127*(1–2), 1–8.

Bookbinder, L. H., Hofer, A., Haller, M. F., Zepeda, M. L., Keller, A., Lim, J. E., et al. (2006). A recombinant human enzyme for enhanced interstitial transport of therapeutics. *Journal of Controlled Release*, *114*(2), 230–241.

Bowen, M., Armstrong, N., & Maa, Y. F. (2012). Investigating high-concentration monoclonal antibody powder suspension in nonaqueous suspension vehicles for subcutaneous injection. *Journal of Pharmaceutical Sciences*, *101*(12), 4433–4443.

Bowen, M. N., Liu, J., & Patel, A. (2011). *Compositions and methods useful for reducing the viscosity of protein-containing formulations*. U. P. Office. USA. 130058958 A1.

Brown, L. R., Yang, M., O'Connell, E., Lafreniere, D., Knubovets, T., & Piran, U. (2006). High concentration monoclonal antibody suspensions for subcutaneous injection. *The AAPS Journal*, *8*(S2). Abstract W4141.

Chen, G., Luk, A., Houston, P., Li, L., Sharon, M., Garley, M., et al. (2005). Injectable nonaqueous suspension of highly concentrated proteins for non-IV administration. *The AAPS Journal*, *7*(S2). Abstract W4141.

Connolly, B. D., Petry, C., Yadav, S., Demeule, B., Ciaccio, N., Moore, J. M. R., et al. (2012). Weak interactions govern the viscosity of concentrated antibody solutions: high-throughput analysis using the diffusion interaction parameter. *Biophysical Journal*, *103*(1), 69–78.

Dani, B., Platz, R., & Tzannis, S. T. (2007). High concentration formulation feasibility of human immunoglobulin G for subcutaneous administration. *Journal of Pharmaceutical Sciences*, *96*(6), 1504–1517.

Du, W., & Klibanov, A. M. (2011). Hydrophobic salts markedly diminish viscosity of concentrated protein solutions. *Biotechnology and Bioengineering*, *108*(3), 632–636.

Einstein, A. (1911). 1911. A new determination of molecular dimensions. *Annalen der Physik*, *34*, 591–592.

Inoue, N., Takai, E., Arakawa, T., & Shiraki, K. (2014). Specific decrease in solution viscosity of antibodies by arginine for therapeutic formulations. *Molecular Pharmaceutics*, *11*(6), 1889–1896.

Kanai, S., Liu, J., Patapoff, T. W., & Shire, S. J. (2008). Reversible self-association of a concentrated monoclonal antibody solution mediated by Fab–Fab interaction that impacts solution viscosity. *Journal of Pharmaceutical Sciences*, *97*(10), 4219–4227.

Liu, H. F., Ma, J. F., Winter, C., & Bayer, R. (2010). Recovery and purification process development for monoclonal antibody production. *Mabs*, *2*(5), 480–499.

Liu, J., Nguyen, M. D. H., Andya, J. D., & Shire, S. J. (2005). Reversible self-association increases the viscosity of a concentrated monoclonal antibody in aqueous solution. *Journal of Pharmaceutical Sciences*, *94*(9), 1928–1940.

Matheus, S., Friess, W., Schwartz, D., & Mahler, H. C. (2009). Liquid high concentration IgG1 antibody formulations by precipitation. *Journal of Pharmaceutical Sciences*, *98*(9), 3043–3057.

Narasimhan, C., Mach, H., & Shameem, M. (2012). High-dose monoclonal antibodies via the subcutaneous route: challenges and technical solutions, an industry perspective. *Therapeutic Delivery*, *3*(7), 889–900.

Rao, S., Gefroh, E., & Kaltenbrunner, O. (2012). Recovery modeling of tangential flow systems. *Biotechnology and Bioengineering*, *109*(12), 3084–3092.

Shire, S. J. (2009). Formulation and manufacturability of biologics. *Current Opinion in Biotechnology*, *20*(6), 708–714.

Shire, S. J., Liu, J., Friess, W., Matheus, S., & Mahler, H.-C. (2010). High-concentration antibody formulations. In F. Jameel & S. Hershenson (Eds.), *Formulation and process development strategies for manufacturing of a biopharmaceutical* (pp. 349–379). Hoboken, NJ: Wiley & Sons.

Shire, S. J., Shahrokh, Z., & Liu, J. (2004). Challenges in the development of high protein concentration formulations. *Journal of Pharmaceutical Sciences*, *93*(6), 1390–1402.

Shpilberg, O., & Jackisch, C. (2013). Subcutaneous administration of rituximab (MabThera) and trastuzumab (Herceptin) using hyaluronidase. *British Journal of Cancer*, *109*(6), 1556–1561.

Winter, C. (2008). Formulation strategy and high temperature UF to achieve high concentration rhuMAbs. In *Recovery of biologics conference XIII.* Quebec city, Quebec, Canada.

Yang, M. X., Shenoy, B., Disttler, M., Patel, R., McGrath, M., Pechenov, S., et al. (2003). Crystalline monoclonal antibodies for subcutaneous delivery. *Proceedings of the National Academy of Sciences of the United States of America*, *100*(12), 6934–6939.

Development of delivery device technology to deal with the challenges of highly viscous mAb formulations at high concentration

8

Using delivery devices to deliver large volume mAb formulations by the subcutaneous route

Large volumes of high concentration mAbs can potentially be delivered subcutaneously (SC) by using delivery device injection technology. Currently most commercially available autoinjectors, although simple to use, are limited to ~1 mL injection with solution viscosities <20 mPas. Autoinjectors are under development that can handle greater volumes and higher viscosities, but from a practical size limitation probably will not be much larger than 3 mL injectors. The rapid injection, usually less than 10 s for this larger volume, may require the use of rhuPH-20. A short review of the issues in development of such injectors and discussion of a particular technology are available (White & Harvey, 2014). Another technology that is very promising is the development of SC infusion patch devices, which can deliver large volumes (at least 5 mL) and high viscosity solutions over a period of time, usually 15–30 min. These devices are worn directly attached at the infusion site (not unlike a transdermal patch) and may have a separate wireless control device such as used in the OmniPod® pump patch system. This is relatively new technology and several companies are developing such technology. There is little in the peer-reviewed literature that discusses or reviews this technology for applications of mAb delivery. Some of the published literature discusses long-term SC infusion of insulin (Pickup, Keen, Parsons, & Alberti, 1978), development of pump patch systems that can deliver 2 mL of insulin (Schaepelynck et al., 2011), and some of the technical challenges that must be met to develop such systems (Skladany, Miller, Guthermann, & Ludwig, 2008). There are trade commercial publications with several articles, many focused on a particular company′s technology (see the recent issue 51 on bolus wearable injectors by ONdrugDelivery, July 23, 2014 as well as the introduction by Jansen, 2014).

Delivery of viscous solutions using a prefilled syringe

In some cases, it is desirable to deliver ~1 mL of a viscous mAb formulation using either a prefilled syringe or an autoinjector. Most autoinjectors commercially available can handle between 10 and 20 mPas viscous solution, but a more viscous solution may

Monoclonal Antibodies. http://dx.doi.org/10.1016/B978-0-08-100296-4.00008-7

lead to incomplete injection since the forces applied are not high enough to deliver the entire dose volume. The mAb Cimzia® is formulated at 200 mg/mL and is available in a prefilled syringe. A syringe using a 25 g needle with large flanges was developed and apparently can be used by arthritis patients to deliver the full 1-mL dose. The development of this syringe led to several design awards and was recognized by the Arthritis Foundation for ease of use. Needle technology has also been developed to handle highly viscous solutions. Examples include thin wall needles that have larger internal diameters than standard needles, and specially designed needles such as Imprint's DepotOne® that uses a needle that does not have uniform diameter (Maynard, 2003). Essentially, the needle narrows at the tip for easy insertion but is wider at the top to handle viscous solutions. In addition, the aperture for drug delivery is located on the side rather than at the tip used in conventional needles.

The technical challenges for device and formulation development

The development of a delivery device begins with an understanding of the requirements of the device for ease of use for a clinical indication. Ergonomic studies, especially using field studies with models and actual patients, help to define the size, shape, and actuation mechanism for the device (French, 2013; Reynolds, 2012). When the drug is coupled with the device, it is termed a combination product, and even though the device may be designed and manufactured by a separate device company, the pharmaceutical company is responsible for the fully integrated system. Thus, not only must the drug be compatible with the device and remain stable but also the functionality of the device must not deteriorate over the shelf life of the product. Some of the important considerations are the choice of the primary container/closure system in the device, the compatibility of the formulated drug with all surfaces, and the assurance that the correct dose is delivered. Here, we will not discuss further the ergonomic studies that are needed for device development since this is beyond the scope of this book. The choice of container/closure impact on functionality, and compatibility of the formulated drug product with the device will be discussed.

Primary container/closure systems for devices to be used with mAbs

The most common injector systems commercially available are pen injectors that are designed for multiple doses, prefilled syringes, and autoinjectors (Figure 8.1). The pen injectors typically use a cartridge system coupled with a multiuse formulation. The need for large doses of mAbs usually precludes such a device, and a bolus autoinjector is usually the device of choice. The choice of the primary container/closure can still be a cartridge, but a better choice would be a prefilled syringe since if the device cannot be ready at time of entry into the market place, a prefilled syringe can still be used as

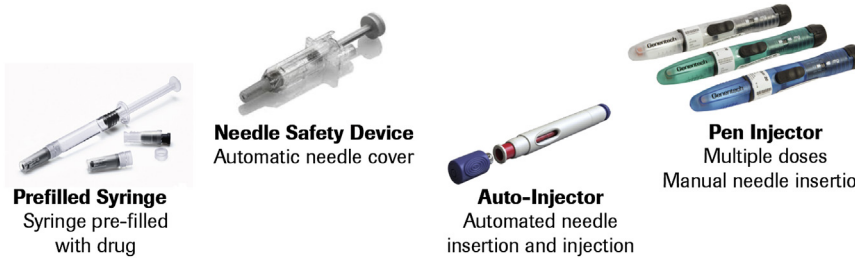

Figure 8.1 Injectors used for subcutaneous (SC) delivery.
From French (2013).

a product. Current regulations require the use of a needle safety device for prefilled syringes to prevent accidental needle sticks for the end user, and there are several commercial systems available (Hyman, 2002; Trim, 2004).

Silicone oil interactions with proteins and mAbs in prefilled syringes

Prefilled syringes have been traditionally manufactured from glass, which require silicone oil coating to avoid high glide forces. Silicone oil has been implicated in the generation of aggregates and particulates of mAbs (Britt et al., 2012; Thirumangalathu et al., 2009). Both of these studies investigated the impact of formulation excipients on the interaction of mAbs with silicone oil emulsions. The key findings were that formulations buffered with 10 mM L-histidine at pH 6 with addition of 140 mM NaCl resulted in increased absorption of the mAb to the silicone oil. The addition of surfactants such as polysorbate 20 resulted in a decrease in the absorption. Although intrinsic tryptophan fluorescence quenching using acrylamide suggested that the tertiary structure of the mAbs was significantly changed, there was not any observed precipitation of the mAbs. However, in a separate study, the tertiary structure of a mAb was perturbed at lower ionic strength, but not at higher ionic strength after absorption to silicone oil droplets (Gerhardt, Bonam, Bee, Carpenter, & Randolph, 2013). It was also shown that the secondary structure of the mAb was unaltered after adsorption to the silicone oil–water interface suggesting that the adsorbed mAb has a molten globule-like conformation. This partially unfolded mAb was prone to aggregation, especially during agitation. In another study, mAb formulated without surfactant was filled into prefilled syringes where the mAb was exposed directly to silicone oil/glass surfaces, air–water interfaces, and agitation (Gerhardt et al., 2014). Flow microscopy was used to detect the presence of particles $\geq 2\,\mu m$ in diameter. The greatest particle concentrations were found in agitated syringes containing an air bubble, which contributed to the generation of air–water interfacial surfaces. A mechanism was proposed that involved the overall impact of silicone oil–water interfaces, air–water interfaces, and agitation on the generation of particulates. Essentially, protein/mAbs without surfactant are adsorbed to the silicone oil–water interface that can result in formation of a

gel. The air bubble during agitation creates sufficient shear to dislodge this surface gel into the bulk of the solution. Although silicone oil droplets confound the determination of subvisible particulates, flow microscopy can discriminate between the irregular shaped protein particulates and round silicone oil droplets. In this study, both types of images were detected, as well as agglomerates of aggregated proteins and silicone oil droplets. It was suggested that additional refinements of the flow microscopy technology are needed in order to fully characterize the observed particulates. Recent studies have shown that it is possible to distinguish silicone oil droplets from protein particles and dust particles using enhanced flow microscopy technology (Sharma, King, Oma, & Merchant, 2010; Vandesteeg & Kilbert, 2013).

To avoid the issue of silicone oil, companies have developed plastic syringes that are now available and used commercially (Kiang, 2011; Markarian, 2013). Another approach has been to use baked-on silicone oil on glass syringes, but this has been difficult to do with glued-in staked needle syringes because of the high temperatures required for the process. It was shown that a baked-on silicone oil surface resulted in less particulate formation for an IgG_2 mAb compared to a standard siliconized glass syringe (see Figure 5 in Badkar, Wolf, Bohack, & Kolhe, 2011). Alternative technologies using cross-linked silicone oil to minimize sloughing from the surface have also been developed (Depaz, Chevolleau, Jouffray, Narwal, & Dimitrova, 2014). A comparison of submicron particulate counts in polysorbate 80 solutions in phosphate-buffered saline shows a reduction in counts for a baked-on silicone oil layer and a chemically cross-linked silicone oil surface compared to a standard sprayed-on process for prefilled syringes (Figure 8.2(a)) using different instruments (Figure 8.2(b)). The cross-linked silicone oil surfaces in the prefilled syringe resulted in the lowest amount of particulate counts and enhanced durability of the silicone layer in the presence of two mAbs.

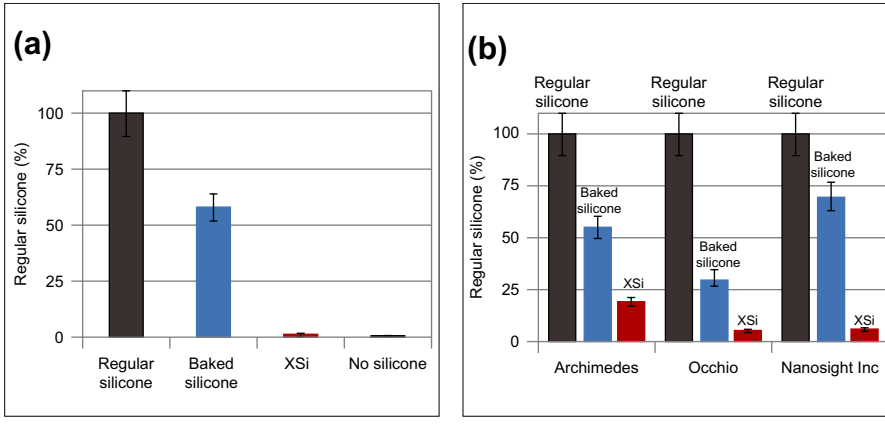

Figure 8.2 Particle released for polysorbate 80 solutions in phosphate-buffered saline for (a) sprayed-on silicone (regular), baked silicone, and cross-linked silicone on glass (XSi) and (b) submicron counts measured by Archimedes, Occhio, and Nanosight instruments.
From Depaz et al. (2014).

Impact of leachables from prefilled syringe components

Leachates and their impact on protein drugs, especially when filled into prefillable syringes, have become a major concern for regulatory agencies (Nashed-Samuel, Liu, Fujimori, Perez, & Lee, 2011). Some of this stems from the lessons learned from erythropoietin (EPO), specifically Eprex®, that was initially in vials and then filled into prefilled syringes. In addition, the route of administration was changed from IV to SC, and a formulation change was made from human serum albumin to polysorbate 80. These changes resulted in an increase in pure red cell aplasia (PRCA) whereby an immunogenic response not just from the drug, but also to the patient's endogenous EPO resulting in an inability to make red blood cells (Casadevall et al., 2002). It has been suggested that leachables eluting from the stopper in the prefilled syringe are adjuvants that stimulate the immune system (Boven et al., 2005). This conclusion has been questioned since the leachates had an adjuvant effect when administering ovalbumin, but not for Eprex® (Schellekens & Jiskoot, 2006). An alternative explanation was proposed where micelles from the polysorbate 80 generated aggregated EPO. However, the final conclusion was that many things were changed at the same time, and thus it is difficult to determine what was the single cause for the increased PRCA (Locatelli, Del Vecchio, & Pozzoni, 2007). Although the exact cause for the increased PRCA is not known, the observation that leachates were extracted from the uncoated stoppers in prefilled syringes (Pang et al., 2007) has made leachates a major concern. Although plastic syringes appear to be a good alternative to glass syringes since silicone oil is not needed, there are concerns regarding potential leachates from the plastic surfaces (Jenke, 2007).

Potential interactions with stainless steel needles

The stainless steel in needles is usually constructed from 304 stainless steel. The 300 series are prone to pitting corrosion in the presence of chloride ion, and this may be a long-term concern for mAbs that are in contact with the needle surface for extended periods of time. Although this has been a concern, there are several products in prefilled staked needle syringes that have significant amounts of chloride ion (Table 8.1).

A study was conducted using an IgG_1 mAb to determine whether or not the corrosion of a stainless steel needle in the presence of a mAb formulated with chloride ion was an issue. Prefilled mAb syringes were stored at 2–8 °C for ~7 months. The wetting of the needles was assessed by inserting a stainless steel wire into the needle and sealed with silicone glue (Dow Corning 3140). Since the mAb formulation is conductive, any liquid contacting both the syringe needle and the end of the stainless steel wire could be measured by using an external electrical excitation. A Radiometer Analytical Voltalab 30 potentiostat configured for impedance measurement was used to determine the wetted state of the wired syringes and the degree of wetting of the stainless steel needle surface. In order to determine if silicone oil could protect against potential pitting, 316L stainless steel coupons with and without silicone oil coatings were assessed for potential electrochemical pitting. Also the extraction of metal from

Table 8.1 Some drugs formulated in chloride-based formulations and filled into staked needle syringes

Drug	Manufacturer	pH	(NaCl)	Other	Needle	Volume	Storage (°C)
Fragmin (LMW heparin)	Pharmacia & Upjohn	5–7.5	"Isotonic" (~130 mM)	8 or 16% drug (MW 5000)	27 gauge × 0.5″	0.2 mL	20–25
Infergen (Interferon-α)	Amgen	7.0	100 mM	Sodium phosphate 25 mM	26 gauge × 5/8″	0.5	2–8
Kineret (IL-1Ra)	Amgen	6.5	140 mM	Sodium citrate 0.19%, 0.018% EDTA	27 gauge	0.67	2–8
Orgaran (antithrombotic)	Organon	7	"Isotonic" (~130 mM)	Sodium sulfite 0.15%; drug MW 5500	25 gauge × 5/8″	0.6	2–8
Vaqta (Hep. A vaccine)	Merck		150 mM	Alum; sodium borate 0.007%	1″	1.0	2–8

From David Overcashier, Genentech (private communication, 2002).

the needle was assessed by pushing a small amount of liquid out of each needle and resealing the assemblies prior to storage. Small volumes (5–20 µL) were withdrawn from each syringe and assayed for trace metal analysis using inductively coupled plasma mass spectrometry (ICP-MS). In addition, stability of the mAb was compared after storage in vials and prefilled syringes. The main conclusions from these studies were that silicone oil could not lower the potential for corrosion, but the stainless steel needle did not cause significant changes in stability of the mAb in the prefilled syringe (Liu et al., unpublished observations).

Potential problems with tungsten in prefilled syringes

Tungsten pins are used to create the hole for placement of the needle in staked needle prefilled syringes. During the processing with these tungsten pins, tungsten oxide vapor deposits in the narrow volume of the syringe where the needle is attached, and tungsten particles can shed during the storage of the prefilled syringes. Proteins can interact with the tungsten particles and oxides resulting in protein aggregation (Swift, Nashed-Samuel, Liu, Narhi, & Davis, 2007). It has been reported that the aggregation of Epoetin® (EPO) in prefilled syringes is linked to the interaction of tungsten and is a likely cause of immunogenicity (Seidl et al., 2012). Investigations were also carried out to determine the root cause of the interaction of tungsten with proteins (Jiang et al., 2009; Liu et al., 2010). The study by Jiang et al. investigated the relationship between tungsten, visible particles, and protein aggregation. Two different model proteins were incubated with extracts from tungsten pins used in the manufacturing of the prefilled syringes and compared to the proteins incubated with different tungsten solutions which included tungstic acid (H_2WO_4), tungsten trioxide (WO_3), sodium tungstate dihydrate ($Na_2WO_4{\cdot}2H_2O$), and sodium polytungstate ($Na_6O_{39}W_{12}$). The extracts from the tungsten pins were more effective in generating soluble protein aggregates than the tungsten solutions. It was also shown that the effect of tungsten on aggregation was greater at pH below 4 and dependent on tungsten species and concentration. One of the model proteins had a large helical content and it was suggested that electrostatic interactions were mainly responsible for the tungsten–protein interactions. Spectroscopic studies using FTIR and CD showed that the protein aggregates were composed of essentially natively folded proteins, which may explain the highly immunogenic response of these aggregates. Aggregates of natively folded protein often mimic the replicative coat protein surface of a virus (termed "virus-like particles") and generate an immune response that results in effective neutralization of properly folded proteins (Rosenberg, 2006).

Studies using a mAb have also shown an interaction with tungsten resulting in precipitation (Bee, Nelson, Freund, Carpenter, & Randolph, 2009). Specifically, tungsten poly anions below pH 6 precipitated the mAb rapidly within seconds. At pH 5 tungsten levels at about 3 ppm were sufficient to precipitate a mAb at low concentration (0.02 mg/mL). It was also shown as for previous model proteins that the native secondary structure of the mAb was retained in the precipitated mAb. Most importantly, it was concluded that a small number of tungsten particles were sufficient to precipitate the mAb at pH 5.

Filling of highly concentrated mAbs into prefilled syringes

A recent study using mAb formulated at 180 mg/mL investigated the key parameters for successful filling of the mAb into a prefilled syringe (Shieu et al., 2014). The key parameters investigated were solution viscosity, concentration, and surface tension. A benchtop filling unit driven with a peristaltic pump and glass nozzles to visualize the liquid flow with a high speed camera was used to determine optimal filling parameters. The key objectives were to create a filling process with no splashes, bubble, and foaming coupled with a process that minimized risk of fill nozzle clogging during nozzle idle time due to formulation drying at or near the nozzle tip. The nozzle size, airflow around the nozzle tip, pump suck-back, fluid viscosity, and protein concentration were key variables, whereas pump velocity, acceleration, and fluid/nozzle interphase properties were shown to have smaller impact.

At this point, several strategies for dealing with highly viscous mAb solutions for SC delivery and processing have been discussed. These include process, formulation, and delivery device design. Another approach is to explore the root causes of high viscosity, and the protein–protein interactions that govern such properties. A basic understanding of the rheological behavior of highly concentrated mAb solutions should enable better design of the mAbs as well as more rational formulation approaches, and this will be discussed in the next chapter.

References

Badkar, A., Wolf, A., Bohack, L., & Kolhe, P. (2011). Development of biotechnology products in prefilled syringes: technical considerations and approaches. *AAPS PharmSciTech*, *12*(2), 564–572.

Bee, J. S., Nelson, S. A., Freund, E., Carpenter, J. F., & Randolph, T. W. (2009). Precipitation of a monoclonal antibody by soluble tungsten. *Journal of Pharmaceutical Sciences*, *98*(9), 3290–3301.

Boven, K., Stryker, S., Knight, J., Thomas, A., van Regenmortel, M., Kemeny, D. M., et al. (2005). The increased incidence of pure red cell aplasia with an Eprex formulation in uncoated rubber stopper syringes. *Kidney International*, *67*(6), 2346–2353.

Britt, K. A., Schwartz, D. K., Wurth, C., Mahler, H. C., Carpenter, J. F., & Randolph, T. W. (2012). Excipient effects on humanized monoclonal antibody interactions with silicone oil emulsions. *Journal of Pharmaceutical Sciences*, *101*(12), 4419–4432.

Casadevall, N., Nataf, J., Viron, B., Kolta, A., Kiladjian, J., Martin-Dupont, P., et al. (2002). Pure red-cell aplasia and antierythropoietin antibodies in patients treated with recombinant erythropoietin. *New England Journal of Medicine*, *346*(7), 469–475.

Depaz, R. A., Chevolleau, T., Jouffray, S., Narwal, R., & Dimitrova, M. N. (2014). Cross-linked silicone coating: a novel prefilled syringe technology that reduces subvisible particles and maintains compatibility with biologics. *Journal of Pharmaceutical Sciences*, *103*(5), 1384–1393.

French, D. (2013). *Strategies for human factors and clinical studies for combination products*. Prague: CMC Strategy Forum Europe 2013.

Gerhardt, A., Bonam, K., Bee, J. S., Carpenter, J. F., & Randolph, T. W. (2013). Ionic strength affects tertiary structure and aggregation propensity of a monoclonal antibody adsorbed to silicone oil-water interfaces. *Journal of Pharmaceutical Sciences*, *102*(2), 429–440.

Gerhardt, A., Mcgraw, N. R., Schwartz, D. K., Bee, J. S., Carpenter, J. F., & Randolph, T. W. (2014). Protein aggregation and particle formation in prefilled glass syringes. *Journal of Pharmaceutical Sciences*, *103*(6), 1601–1612.

Hyman, W. A. (2002). Human factors analysis of needle safety devices. *Journal of Clinical Engineering*, *27*(4), 280–286.

Jansen, P. (2014). Introduction: pharma perspective on injection delivery: wearable bolus injectors. *ONDrugDelivery*, *51*(7).

Jenke, D. (2007). Evaluation of the chemical compatibility of plastic contact materials and pharmaceutical products; safety considerations related to extractables and leachables. *Journal of Pharmaceutical Sciences*, *96*(10), 2566–2581.

Jiang, Y. J., Nashed-Samuel, Y., Li, C., Liu, W., Pollastrini, J., Mallard, D., et al. (2009). Tungsten-induced protein aggregation: solution behavior. *Journal of Pharmaceutical Sciences*, *98*(12), 4695–4710.

Kiang, P. H. (2011). Future materials for prefilled syringe components. *American Pharmaceutical Review*, *14*(5), 54–58.

Liu, W., Swift, R., Torraca, G., Nashed-Samuel, Y., Wen, Z. Q., Jiang, Y., et al. (2010). Root cause analysis of tungsten-induced protein aggregation in pre-filled syringes. *PDA Journal of Pharmaceutical Science and Technology*, *64*(1), 11–19.

Locatelli, F., Del Vecchio, L., & Pozzoni, P. (2007). Pure red-cell aplasia "epidemic"—mystery completely revealed? *Peritoneal Dialysis International*, *27*, S303–S307.

Markarian, J. (2013). Using plastic for parenteral containers: experts discuss trends in use of plastics for parenteral containers. *BioPharm International*, *23*, 30–33.

Maynard, K. (2003). *Imprint's DepotOne: A small needle for viscous formulations*.

Nashed-Samuel, Y., Liu, D., Fujimori, K., Perez, L., & Lee, H. (2011). Extractable and leachable implications of biological products in prefilled syringes. *American Pharmaceutical Review*, *14*(1).

Pang, J., Blanc, T., Brown, J., Labrenz, S., Villalobos, A., Depaolis, A., et al. (2007). Recognition and identification of UV-absorbing leachables in EPREX pre-filled syringes: an unexpected occurrence at a formulation-component interface. *PDA Journal of Pharmacuetical Science and Technology*, *61*(6), 423–432.

Pickup, J. C., Keen, H., Parsons, J. A., & Alberti, K. G. (1978). Continuous subcutaneous insulin infusion: an approach to achieving normoglycaemia. *British Medical Journal*, *1*(6107), 204–207.

Reynolds, G. (2012). Growth in at-home administration sparks need for integrated delivery solutions. *ONDrugDelivery*, *33*, 16–18.

Rosenberg, A. S. (2006). Effects of protein aggregates: an immunologic perspective. *AAPS Journal*, *8*(3), E501–E507.

Schaepelynck, P., Darmon, P., Molines, L., Jannot-Lamotte, M. F., Treglia, C., & Raccah, D. (2011). Advances in pump technology: insulin patch pumps, combined pumps and glucose sensors, and implanted pumps. *Diabetes & Metabolism*, *37*, S85–S93.

Schellekens, H., & Jiskoot, W. (2006). Eprex-associated pure red cell aplasia and leachates. *Nature Biotechnology*, *24*(6), 613–614.

Seidl, A., Hainzl, O., Richter, M., Fischer, R., Bohm, S., Deutel, B., et al. (2012). Tungsten-induced denaturation and aggregation of epoetin alfa during primary packaging as a cause of immunogenicity. *Pharmaceutical Research*, *29*(6), 1454–1467.

Sharma, D. K., King, D., Oma, P., & Merchant, C. (2010). Micro-flow imaging: flow microscopy applied to sub-visible particulate analysis in protein formulations. *AAPS Journal*, *12*(3), 455–464.

Shieu, W., Torhan, S. A., Chan, E., Hubbard, A., Gikanga, B., Stauch, O. B., et al. (2014). Filling of high concentration monoclonal antibody formulations into pre-filled syringes: filling

parameter investigation and optimization. *PDA Journal of Pharmacuetical Science and Technology*, *68*(2), 153–163.

Skladany, M. J., Miller, M., Guthermann, J. S., & Ludwig, C. R. (2008). Patch-pump technology to manage type 2 diabetes mellitus: hurdles to market acceptance. *Journal of Diabetes Science and Technology*, *2*(6), 1147–1150.

Swift, R., Nashed-Samuel, Y., Liu, W., Narhi, L., & Davis, J. (2007). Tungsten, prefilled syringes and protein aggregation. In *2007 National ACS meeting. Boston, MA*.

Thirumangalathu, R., Krishnan, S., Ricci, M. S., Brems, D. N., Randolph, T. W., & Carpenter, J. F. (2009). Silicone oil- and agitation-induced aggregation of a monoclonal antibody in aqueous solution. *Journal of Pharmaceutical Sciences*, *98*(9), 3167–3181.

Trim, J. C. (2004). A review of needle-protective devices to prevent sharps injuries. *British Journal of Nursing*, *13*(3), 144, 146–153.

Vandesteeg, N., & Kilbert, C. (2013). Differentiation of subvisible silicone oil droplets from irregular standard dust particles. *Journal of Pharmaceutical Sciences*, *102*(6), 1696–1700.

White, S., & Harvey, L. (2014). Oval's auto-injector platform for the delivery of high-viscosity drugs. *ONDrugDelivery*, *47*, 6–10.

The molecular basis of high viscosity of monoclonal antibodies (mAbs) at high concentration

9

What is viscosity?

Although viscosity has been discussed in previous chapters in context of how it impacts pharmaceutical development of mAbs, it was never clearly defined. In general viscosity is understood by many to be related to the flow of a liquid and its "stickiness to surfaces." Here we discuss some formal definitions for viscosity and what methodologies have been used to determine viscosity of protein solutions.

The viscosity of a liquid is essentially a measure of the resistance of fluids to flow. This can be expressed quantitatively by imagining that the fluid is broken up into several volume elements where a volume element's movement relative to another volume element is as shown in Figure 9.1. If the volume element, at a distance dx (center to center), is moving with a relative velocity du relative to the second element then the frictional force, F_f, will be proportional to this relative velocity and the contact surface area, dA, between the volume elements. The force should also be inversely proportional to the distance dx between the centers of the volume elements (Tanford, 1967, pp. 317–336). Thus,

$$F_f \sim (du/dx)\, dA \tag{9.1}$$

And the proportionality constant, η, is the viscosity, so that

$$F_f = \eta\, (du/dx)\, dA \tag{9.2}$$

From this, the viscosity has units of g/cm s. In honor of Jean Léonard Marie Poiseuille this combination of units is called 1 Poise or 1 P. Recently the convention has been to express the units of viscosity in terms of units of pressure, which is Newtons/m^2 or kg/m s and is called 1 Pa in honor of the physicist Blaise Pascal. Thus, 1 Pa s has the dimensions kg/m s or 0.1 Poise, and therefore 1 centiPoise (cP) is equivalent to 1 milli Pa sec or 1 mPa s. Fluids can vary widely in their viscosities as shown in Table 9.1, ranging from 0.02 mPa s for air to that of 1×10^6 mPa s for window putty.

Another important aspect of viscosity is the difference between a "Newtonian" and "Non-Newtonian" fluid. Essentially the viscosity as defined by Eqn (9.2) is defined as a simple proportionality constant that is independent of the velocity of flow of the fluid. This is not always the case since for some fluids the flow gives rise to an orientation of the molecules, which then alters the frictional force between the adjacent volume elements. A practical determination of whether a fluid is "non-Newtonian"

Monoclonal Antibodies. http://dx.doi.org/10.1016/B978-0-08-100296-4.00009-9

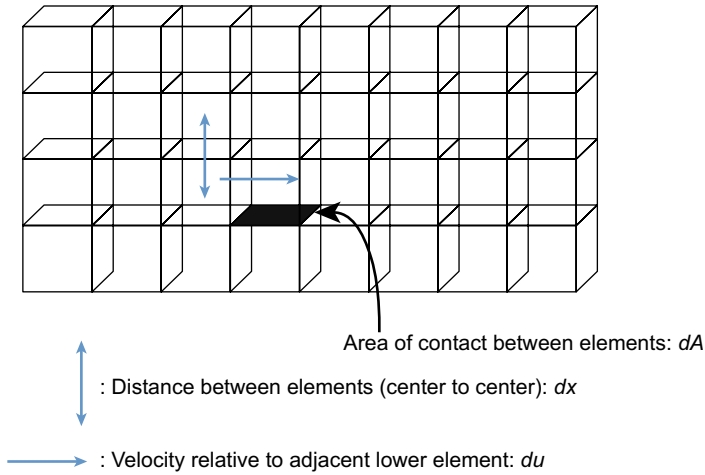

Figure 9.1 A volume element moving relative to a lower volume element with relative velocity equal to *du*.

Table 9.1 Viscosities of different fluids in mPa s

Fluid	Viscosity (mPa s)	Fluid	Viscosity (mPa s)
Air at room temperature	0.02	Motor oil SAE 10 at 20 °C	65
Acetone at 20 °C	0.33	Motor oil SAE 40 at 20 °C	319
Water at 20 °C	1.0	Castor oil at 26.9 °C	650
Ethanol at 25 °C	1.1	Dark Canadian maple syrup at 25 °C	1028
Mercury at 26.9 °C	1.5	Glycerol at 20 °C	1410
Kerosene at 26.9 °C	1.6	Honey at room temperature	10,000–20,000
Linseed oil at 26.9 °C	33	Peanut butter at room temperature	250,000
Corn oil at 25 °C	51	Window putty at room temperature	$>5\times10^{6}$
Olive oil at 25 °C	63	Pitch at 25 °C	2.3×10^{11}

is to measure the viscosity at different velocity gradients (dv/x) and determine if the viscosity changes. Orientation of the molecules at high velocity gradients will result in a decrease in frictional force and hence lower viscosity. This behavior is often referred to a shear thinning, and was observed to happen for an IgG_1 mAb (Figure 6.3) (Liu, Nguyen, Andya, & Shire, 2005).

The viscosity of a protein/mAbs solution is dependent on the temperature of the solution, concentration, shape, and molecular weight of the macromolecule as well as the interactions between the molecules. At a particular temperature the viscosity

of the protein solution, η, can be related to the solvent viscosity, η_0, and the protein concentration, c, by a power series (Cantor & Schimmel, 1980):

$$\eta = \eta_0 \left(1 + k_1 c + k_2 c^2 + \cdots\right) \tag{9.3}$$

where k_1 is related to the contribution from the individual protein molecules, and k_2 and higher order coefficients are related to interactions of two, three, or more protein molecules. The parameter k_1 has been termed the intrinsic viscosity, [η] but has units of mL/g, and can be determined experimentally by extrapolating to zero protein concentration so that

$$[\eta] = \lim_{c_{A0}} \left(\eta_{sp}/c\right) \tag{9.4}$$

where

$$\eta_{sp} \text{ is } (\eta - \eta_0)/\eta_0 \tag{9.5}$$

The intrinsic viscosity is dependent on the protein shape and size and can be related to the partial specific volume of the hydrated protein, V (size) and a parameter, ν, that is related to shape by the equation (Van Holde, 1971, pp. 141–157):

$$[\eta] = V\nu \tag{9.6}$$

Einstein determined for spherical particles $\nu = 5/2$ (Einstein, 1911), whereas for prolate (football-shaped) and oblate (disc-shaped) objects the parameter ν is related to the ratio of the minor and major axis and has been termed the Simha parameter (Mehl, Oncley, & Simha, 1940). At higher concentrations the higher order coefficients will begin to dominate and will significantly contribute to the viscosity.

How is viscosity measured experimentally?

Glass capillary viscometry

One of the oldest techniques for measuring viscosity of solutions is the glass capillary viscometer. This method involves determining the time for a fluid to move a specified distance through a capillary tube immersed in a constant-temperature water bath. The most precise and accurate measurements require times not less than 200 s and not more than 1000 s. For a Newtonian fluid the kinematic viscosity is

$$\eta_k = 10^6 \pi g D^4 Ht/(128\, VL) \tag{9.7}$$

where D is the capillary diameter, L the capillary length, H the distance the fluid with volume V travels in time t, and g is the acceleration due to gravity. The kinematic viscosity has units of cm^2/s also called Stokes so that

$$\eta = \eta_k \rho \tag{9.8}$$

where ρ is the density of the solution in g/cm^3.

Falling ball viscometer

This type of viscometer is used for measuring Newtonian fluids. In the falling ball viscometer, a spherical steel ball is allowed to fall through a tube containing the solution to be measured. Yuan and Lin have reviewed this method, which is seldom used for determination of viscosities of proteins (Yuan & Lin, 2008, p. 40) since the measurements are complicated by the necessity of using up to six balls to span the viscosity range. However, Patapoff and Esue used a falling ball viscometer to determine bulk viscosity of a mAb solution as a function of polysorbate 20 addition (Patapoff & Esue, 2009). They showed a slight, but negligible increase in viscosity with addition of polysorbate 20.

Rotational rheometers

The most common method used to determine viscosities of protein solutions is the rotational rheometer. Rheometry extends the determination of viscosity to also investigate the elastic properties of solutions, which are a determination of how energy is stored during the flow and deformation of the fluid. These rheometers investigate a fluid that is sheared between a static and rotating surface. There are several geometries used including parallel plates, concentric circles, and one of the most used geometries, a cone and plate. In this rheometer, the lower circular plate is flat and the upper plate is a truncated conical plate with a common cone angle of 1–3°. Removal of the apex of the cone that intersects the lower plate allows for precise determinations of a uniform shear rate resulting in a shear stress, σ, that is related the applied torque, M (Newtons meter) and the cone radius, R (m):

$$\sigma = 3M/2\pi R^3 \tag{9.9}$$

Then the viscosity, η, is related to M, R, the angular velocity in radians/s, ω and the cone angle in radians, α:

$$\eta = 3M\alpha/2\pi R^3\omega \tag{9.10}$$

Another type of a rotational rheometer is one that uses parallel plates, and is often used for characterization of elasticity by observing the properties of fluids placed between the two oscillating plates. The main advantage of this method is that with a small gap between plates the volume required for a measurement is greatly reduced, and that very high shear rates can be achieved with the smaller gap size. Some of the problems that can occur with this method, such as errors in gap size for small gaps, are summarized by Jezek et al. (2011).

It has been reported that using a cone and plate rheometer resulted in extensive shear thinning for an IgG_1 mAb whereby after multiple shear cycles viscosity increased due

to formation of insoluble aggregates (Patapoff & Esue, 2009). Addition of polysorbate 20 inhibited the aggregate formation and resulted in little change in viscosity after multiple cycles. It was hypothesized that the mAb formed a thin layer at the protein air–water interface that resulted in unfolding and generation of insoluble aggregate species. The addition of the surfactant, as discussed in previous chapters, prevents this aggregation by adsorption to this interface, thus preventing the mAb from exposure to the hydrophobic air–water interface. This example shows that such artifacts can occur and need to be taken into consideration when interpreting the experimental results.

Other methods for determination of viscosity

Microfluidic rheometry using pressure drops to determine viscosity

Recently a rheometer has been developed that uses pressure drop measurements to determine viscosity (Hudson, Sarangapani, Pathak, & Migler, 2014; Pipe & McKinley, 2009). This rheometer generally can meet the need to use small microliter volumes of material, has a wide dynamic range of shear rates (range of ~3 decades), and no air–sample interface, which has been shown to be a potential problem in conventional rotational viscometers (Patapoff & Esue, 2009). This instrument has an uncertainty of only a few percent and its performance was evaluated using monoclonal antibody solutions at different concentrations, pH, and temperature (Hudson et al., 2014).

Viscosity determined using travel time of a magnetic piston

A viscometer that measures viscosity by determining the travel time of a magnetically oscillating piston has been developed. The pistons were calibrated using fluids with viscosity ranges of 0.5–5, 2.5–50, and 5–100 mPa; and used to determine viscosities of monoclonal antibody solutions from 20 to 225 mg/mL (Yadav, Shire, & Kalonia, 2010).

Use of standard capillary electrophoresis instrumentation

It has been shown that using a capillary electrophoresis (CE) instrument without the applied electric field, Newtonian fluid viscosities could be determined by filling the capillary with the protein sample by applying a constant pressure (Allemendinger et al., 2014). A dye such as riboflavin is used to monitor the movement of the dye in the presence of the protein in the capillary. Using the Hagen–Poiseuille equation (Eqn (6.1), Chapter 6) the movement of the riboflavin peak is converted to a viscosity of the solution. Accuracy and precision was verified by comparing the CE determinations with cone and plate measurements. Viscosities in the range of 5–40 mPa s were reliably measured using this technique which has short measurement times (1–15 min), and small sample volume (a few microliter) when using a 20.5 cm length capillary of 50 μm diameter.

Fully automated capillary viscometer

An instrument that measures viscosity of protein solutions automatically by varying solute concentration and shear rate has been described (Grupi & Minton, 2012). By measuring the pressure difference between the two ends of the capillary filled with a protein solution flowing at a known rate, enables determination of the viscosity using the Hagen–Poiseuille equation. A volume of as little as 0.75 mL can provide the viscosity as a function of concentration and shear rate. Viscosities as high as 500 mPa s and as low as 1 mPa s at shear rates between 10 and 2×10^3/s have been determined with good accuracy and precision.

Use of dynamic light scattering

Diffusion coefficients determined by dynamic light scattering (DLS) measurements can be used to compute viscosities of protein solutions (He et al., 2010) by using the Stokes–Einstein equation:

$$D = kT/6\pi\eta R \tag{9.11}$$

where D is the diffusion coefficient, k the Boltzmann's constant, T the temperature, R the radius of a particle, and η the viscosity of the solution. Using polystyrene beads with known values of R allows for the determination of the viscosity of the protein solution that the beads are suspended in. The size of the beads is larger than that of the protein molecules, and thus the DLS signals can easily be separated. This method was used to determine viscosities of two mAb solutions and the results when compared with cone and plate measurements showed good agreement. Using a DLS instrument with plate reader allowed for rapid determination (~5 times less than cone and plate) using ~10 times less sample.

Determination of viscoelastic properties using a quartz crystal microbalance

Many of the most used methods to measure viscosities of protein solutions require fairly large volumes (3–5 mL), which may be difficult to obtain for high-concentration protein/mAb formulations during early stages of development. A technique based on the use of piezoelectric quartz crystals showed that this technique could be used to obtain viscoelastic data in 2-3 min with as little as 8–10 μL of solution. The basic theory and use of quartz impedance analysis were used to generate viscosity values at 25 °C for liquid solutions of sucrose, urea, PEG-400, glucose, and ethylene glycol, all Newtonian fluids, and found to be reproducible and consistent with literature values (Saluja & Kalonia, 2004). This initial work was extended to determine full rheological properties of protein solutions at high concentration (Saluja & Kalonia, 2005). The main properties of the vibrating quartz crystal used to compute viscoelastic properties of solutions are the measured shifts ± solution of the series resistance, R_2, and

inductance shift, L_2. The inductance shift and crystal resonance frequency, ω, are used to calculate the reactance shift, X_2, by

$$X_2 = \omega L_2 \tag{9.12}$$

For Newtonian fluids R_2 and X_2 are equal and related to the viscosity, η, by

$$\eta = 2R_2^2 / \left(A^2 \rho \omega\right) \tag{9.13}$$

where A is a crystal constant and ρ the solution density.

For a viscoelastic fluid the storage modulus, G′, related to the elasticity of the solution, and G″, related to the viscosity of the solution, are expressed as

$$G' = \left(R_2^2 - X_2^2\right) / \left(A^2 \rho\right), \; G'' = \left(2R_2 X_2\right) / \left(A^2 \rho\right) \tag{9.14}$$

Both the storage and loss modulus contribute to the complex viscosity of the solution, η*, by the relationship

$$\eta^* = \left[\left(\left(G'\right)^2 + \left(G''\right)^2\right)^{1/2}\right] / \omega \tag{9.15}$$

The storage modulus, G′, determined by ultrasonic rheology has been shown to be an important parameter for the analysis of protein–protein interactions at high protein concentrations (Saluja, Badkar, Zeng, Nema, & Kalonia, 2007). This was demonstrated by determining G′ at a frequency of 10 MHz for an IgG_2 mAb between pH 3 and 9 at 4 mM ionic strength. A comparison of the pH and ionic strength dependency of G′ with the DLS interaction parameter, k_D, shows similar trends (Figure 9.2). In this publication data were also presented for determination of B22 but was incorrectly done with the DLS instrument. This issue has been thoroughly discussed and is related to detector saturation in the DLS instrument (Yadav, Scherer, Shire, & Kalonia, 2011).

The DLS k_D parameter is determined by plotting the diffusion coefficient determined by DLS as a function of concentration. The mutual diffusion coefficient, D_m, at any given concentration depends on the diameter d_H of the protein/mAb and the interactions between the molecules (Eberstein, Georgalis, & Saenger, 1994; Mandel, 1993). At high dilution the diffusion coefficient, D_s, is the diffusion coefficient for a single molecule with a particular diameter. The concentration dependency of D_m can be determined by (Zhang & Liu, 2003)

$$D_m = D_s \left(1 + k_D c\right) \tag{9.16}$$

where c is the mass concentration of protein or mAb and the slope k_D is the interaction parameter which can be expressed as

$$k_D = 2B_{22} M_w - \zeta_1 - 2\nu_{sp} \tag{9.17}$$

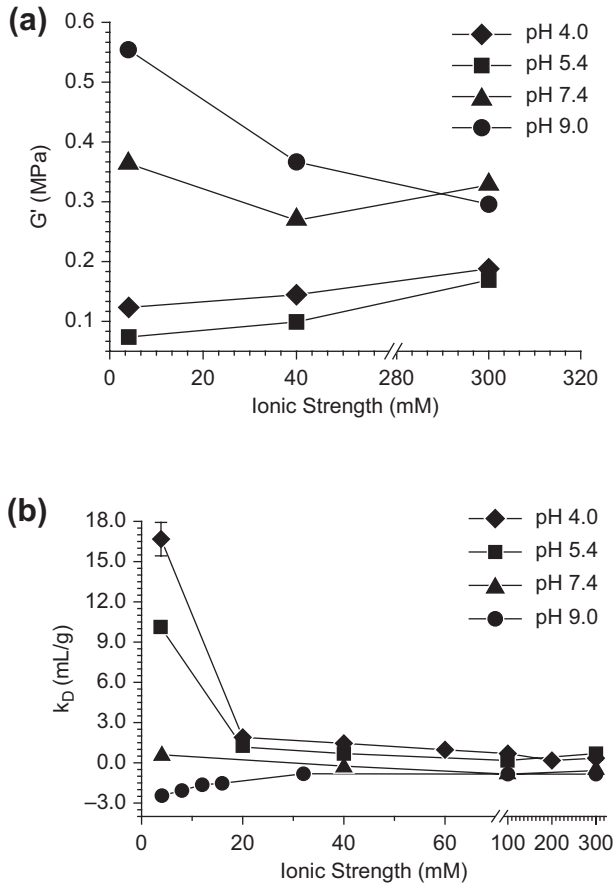

Figure 9.2 G′(a) and k_D (b) for an IgG2 mAb as a function of pH and ionic strength at 25 °C. G′ was determined at 120 mg/mL mAb. The ionic strength was adjusted for all determinations using NaCl. All lines connecting data points are hand drawn to guide the eye.
From Saluja et al. (2007).

where ζ_1 is the coefficient of the linear term in the virial expansion of the frictional coefficient as a function of protein or mAb concentration, and v_{sp} is the partial specific volume of the protein or mAb (Zhang & Liu, 2003). Thus the first term represents the thermodynamic component of k_D due to the chemical potential that drives the diffusion process whereas the last two terms are purely hydrodynamic (Harding & Johnson, 1985). A positive value for k_D is the result of an increase in D_m over D_s as concentration increases, which translates into an apparent decrease in the solute diameter suggesting a facilitation of diffusion due to net repulsive interactions. A negative value for k_D is the result of a decrease in D_m versus D_s as concentration increases, which translates into an apparent increase in the protein or mAb diameter resulting in an inhibition of diffusion due to net attractive protein–protein interactions. Theoretical considerations have been discussed that show that if the determined k_D value for a

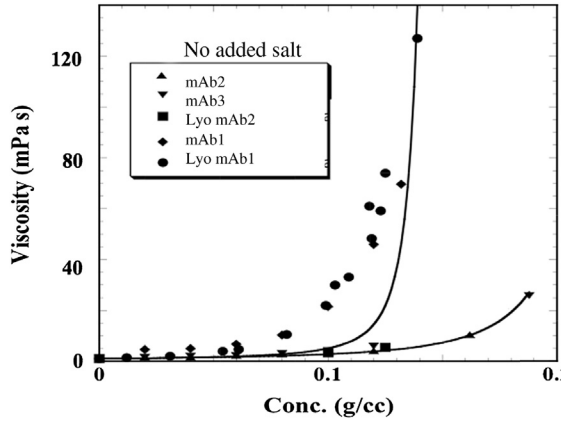

Figure 9.3 Viscosity at 25 °C as a function of protein concentration for lyophilized and TFF concentrated mAb1. The TFF nonlyophilized samples of mAb1, mAb2, and mAb3 and reconstituted mAb1 lyophilized samples are in 266 mM sucrose and 16 mM histidine at pH 6 and 0.03% polysorbate 20. The lyophilized mAb2 samples are in either 240 mM trehalose, 40 mM histidine, 0.04% polysorbate 20 at pH 6 or in 300 mM trehalose, 50 mM histidine, and 0.05% polysorbate 20 at pH 6. The solid line is the result of fitting of the data to the modified Mooney equation as described in the text.
Composite of figures from Liu et al. (2005).

molecule the size of a monoclonal antibody is less negative than −5.34 mL/g, then the net interactions are repulsive, whereas if the value is more negative than −5.34 mL/g the net interactions are attractive (Yadav, Shire, et al., 2010).

The dependence of viscosity on attractive protein–protein interactions

As shown and discussed previously in Chapter 7 the reconstitution time for a lyophilized mAb was dependent on the viscosity after addition of diluent (Figure 7.5). A viscosity–concentration profile for three IgG1 mAbs that were constructed using the same human IgG1 framework is shown in Figure 9.3. These profiles were analyzed using the modified Mooney equation for quasi-spherical particles (Ross & Minton, 1977):

$$\eta = \eta_0 \exp\left([\eta]\, c / (1 - k/\nu)\, [\eta]\, c\right) \tag{9.18}$$

where η_0 is the solvent viscosity, $[\eta]$ the intrinsic viscosity of the protein or mAb, k is a "crowding factor," and ν is the Simha parameter related to the ellipsoid of revolution used to model the protein (Mehl et al., 1940). A typical value for $[\eta]$ of 6.3 cm^3/g for an IgG_1 (Hall & Abraham, 1984; Kilar et al., 1985) (strictly speaking this will be a function of the solvent parameters) and a determined η_0 of 1.1 mPa was used for the

nonlinear regression analysis where the parameter k/v was used as a fitting parameter. This semiempirical modified Mooney equation (Equation 9.18), based on Mooney's original equation for spherical particles, involves only repulsive interactions between molecules due to molecular crowding at high concentrations (Mooney, 1951). This effect commonly termed "excluded volume" is simply the decrease in free volume to accommodate a particular large macromolecule due to its overall size (Zhou, Rivas, & Minton, 2008). Thus, viscosity increases with concentration can be predicted with this model provided there are no other interactions. Most importantly, the size and shape of the protein dictates the excluded volume that results theoretically in the lowest viscosity at a particular concentration that the protein can attain. As seen in Figure 9.3, the viscosity–concentration profile for mAb2 and mAb3 are adequately described using the modified Mooney equation, suggesting that there are no additional interactions beyond the repulsive interactions due to excluded volume for these mAbs. However, the viscosity–concentration profile for mAb1 could not be fitted using the modified Mooney equation, that is, the viscosity increases with concentration to a much greater extent than what would be expected for purely excluded volume effects. Since these three mAbs have similar size and shape, this strongly suggests that there are additional interactions between mAb1 molecules that cannot be accounted for with a simple excluded volume model. Adjustment of the ionic strength to ~150 mM NaCl results in little change to mAb2 and mAb3 viscosity profile resulting in a good fit to the modified Mooney equation, whereas the viscosity decreases dramatically for mAb1 with a viscosity–concentration profile that can be roughly fitted with the modified Mooney equation (Figure 9.4) (Liu et al., 2005; Liu, Nguyen, Andya, & Shire, 2006). These results suggest that the interactions are electrostatic in nature and that they are reversible.

Determination of the DLS interaction parameter at low concentration has proven useful as a predictor of high viscosity at high concentration (Connolly et al., 2012) as well as static light scattering (SLS) (Saluja et al., 2007; Yadav, Laue, Kalonia, Singh, & Shire, 2012) and analytical ultracentrifugation (Saito et al., 2012) for determination of the second virial coefficient, B22, again at low concentration. Although in general these determinations at low concentration are able to predict viscosity and assess protein–protein interactions at high concentration there have been discrepancies. It would be highly desirable to assess molecular weight as a function of concentration, especially at the higher concentration. This has been a formidable challenge since the most common assay to evaluate molecular size has been SEC that because of dilution during the chromatography results in reversible aggregates that dissociate to monomers (see Chapter 3 and Figure 3.18). Analytical ultracentrifugation can be a useful technology to assess these interactions at high concentrations, but because of the large refractive gradient formed during centrifugation at high concentrations the refraction of the light beam from the photoelectric scanner may result in it not being in alignment with the detecting phototube (Svensson, 1954a, 1954b). Minton and Lewis have shown that it is possible to acquire data at high protein concentration, using myoglobin at a loading concentration of about 180 mg/mL, and thin window gasket materials for the centrifuge cell centerpiece, which results in very small light paths (Minton & Lewis, 1981). Although this technique can be used, it is difficult due to wrinkling of the gasket, leaks, etc. An alternative technology using preparative

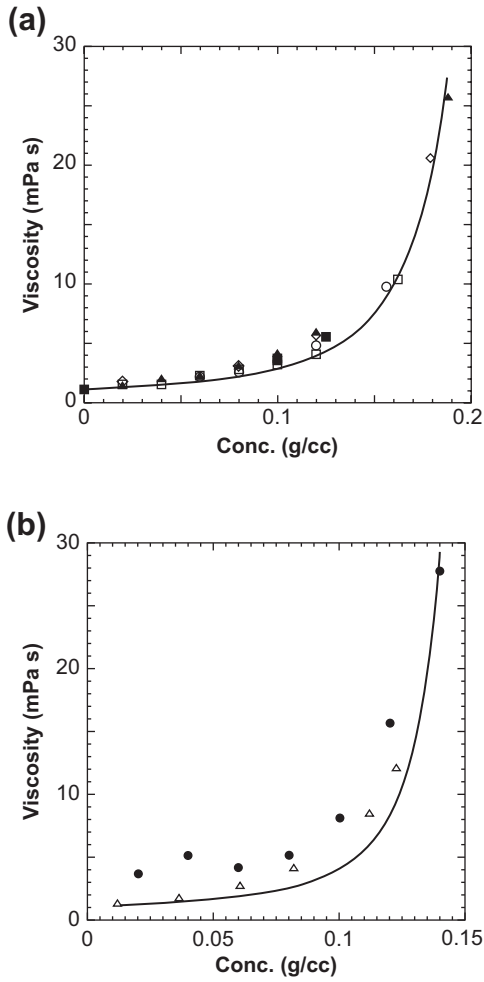

Figure 9.4 Viscosity at 25 °C as a function of protein concentration for (a) reconstituted lyophilized and nonlyophilized mAb2 (open symbols no added salt, solid symbols at 150 mM NaCl) and (b) lyophilized and reconstituted (open triangles) and nonlyophilized (solid circles) mAb1 at 150 mM NaCl. The lines are best nonlinear regression fits of the data to the extended Mooney equation as described in the text. Adapted from Liu et al. (2005).

ultracentrifuges coupled with a microfractionator (Minton, 1989) is cumbersome, but has been used successfully in our lab for analysis of mAb solutions at high concentration (Liu et al., 2005). The sedimentation equilibrium studies were conducted in a Beckman XL-I ultracentrifuge without the optical system. After layering ~300 µL of the mAb solution on top of 100 µL fluorocarbon (FC-43) in thick-walled polycarbonate centrifuge tubes, the samples were centrifuged at 15,000 rpm in a swinging bucket SW 60 Ti rotor for 36–48 h. Attainment of equilibrium was established by comparing data after 36 h versus 48 h. Immediately after centrifugation, contents of each tube were dispersed in 10 µL fractions using a commercially available microfractionator into a 96-well plate, and after dilution with phosphate-buffered saline the concentrations were determined by UV absorption spectroscopy (Figure 9.5). This method works because of the large concentration gradient that is established after attaining

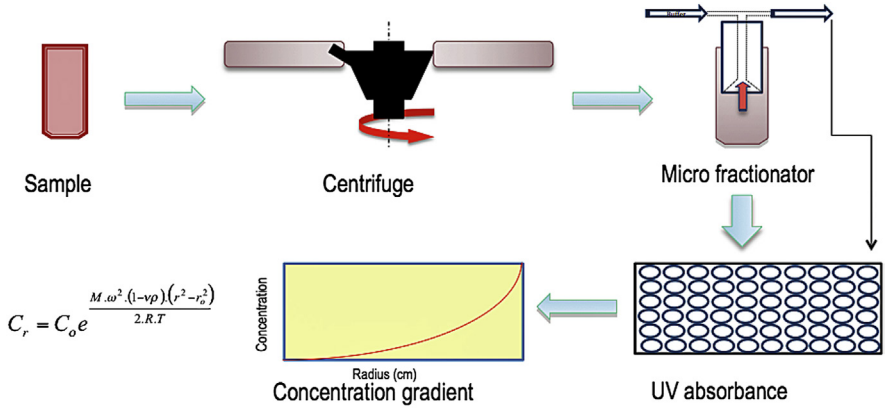

Figure 9.5 Sedimentation equilibrium measurements using preparative centrifuges. Figure created by Sandeep Yadav.

equilibrium, providing sufficient time to carefully remove the centrifuge tubes and place them into the automated microfractionator. Obviously once the individual fractions are diluted the gradient is destroyed, but a total concentration at the radial position of sampling is obtained resulting in the creation of an absorbance versus radial position plot (Figure 9.5). Generally the analysis of analytical ultracentrifugation data is done under sufficiently dilute conditions so that for an ideal sedimenting species the following equation is used (Yphantis, 1964):

$$c(r) = c_0 \exp\left[M_w (1 - \nu\rho) \omega^2 \left(r^2 - r_0^2\right) / 2RT\right] \tag{9.19}$$

where c(r) is the mass concentration at radial position r, c_0 is the initial loading mass concentration, r_0 is the radial reference position, ν is the partial specific volume for the protein, ρ is the solution density, ω is the angular velocity, R is the gas constant, and T is the absolute temperature during centrifugation. However for high-concentration protein/mAb solutions the conditions are no longer ideal due to the presence of protein–protein interactions and the determination of the actual weight average molecular weight, M_w, from the experimentally determined apparent molecular weight, M_{app}, requires the use of an activity coefficient as described by the following equation (Chatelier & Minton, 1987):

$$M_{app} = M_w [1 + c (d \ln \gamma / dc)] \tag{9.20}$$

where γ is the activity coefficient for the protein or mAb. Since mAb2 and mAb3 viscosity data could be adequately described by the excluded volume equation of Mooney it was assumed that mAb2 and mAb3 were essentially monomeric in solution. This assumption results in a multiplicative correction factor as a function of mass concentration, c, when M_w is set equal to 150 kDa. After applying this correction to the apparent molecular weight data for mAb1, a corrected weight average molecular weight was obtained. These corrections are estimates that may not account for complete correction,

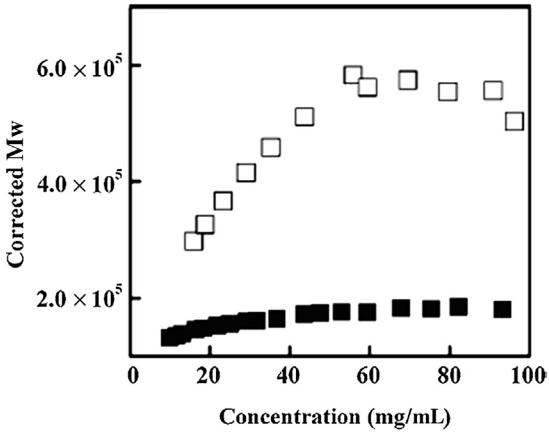

Figure 9.6 The corrected weight average molecular weight as a function of concentration for mAb1 at a loading concentration of 100 mg/mL in 240 mM trehalose, 40 mM histidine, 0.04% polysorbate 20 at pH 6 with no added salt (open squares) and with 150 mM NaCl (solid squares).
From Liu et al. (2005).

but the results clearly show that mAb1 self-associates as a function of concentration, that is, reversible, and after adjustment of ionic strength to ~150 mM with NaCl these interactions as reflected by the determined M_w are greatly reduced (Figure 9.6). Moreover, this nicely correlated with the reduction in mAb1 viscosity strongly suggesting that the attractive interactions are linked to the increased viscosity. Additional verification of these results was obtained by using SLS to determine molecular weight as a function of concentration for protein or mAb solutions at high concentrations (Scherer, Liu, Shire, & Minton, 2010). Analysis of the data using adhesive hard sphere models showed that at lower ionic strength (40 mM) the mAb1 data could best be described using a monomer–n-mer equilibrium association where the best-fit parameter for n was 6. Interestingly this is similar to the sedimentation equilibrium analysis that shows the Mw at higher concentration leveling off at ~4x the monomer molecular weight of 150 kDa (Figure 9.6). It was also shown that mAb2 does weakly self-associate to a dimer so that the initial assumption that there were no interactions beyond those of an excluded volume model was not correct, and this may account for the difference in highest molecular weight attained by self-associating mAb1 molecules as determined by AUC and SEC analysis.

Specific interactions in mAb1 that result in increase of viscosity

The reversible self-association of mAb1 and mAb2 was further studied by Kanai et al. (Kanai, Liu, Patapoff, & Shire, 2008) using full-length mAbs as well as Fab and $F(ab')_2$ fragments. It was proposed that a "network" or clustering of mAbs at high concentration was a primary determinant for the observed high viscosities. The concept of protein network formation as a function of concentration has been proposed previously (Porcar et al., 2010; Stradner et al., 2004) and is not without controversy (Shukla et al., 2008a, 2008b). Recently, additional studies using small angle neutron scattering of hemoglobin solutions have provided additional support for the

"networking" concept (Stadler, Schweins, Zaccai, & Lindner, 2010). The main idea is that if the protein or mAbs are interacting in a long-range network, then displacement of a single mAb requires movement of the other network-associated mAbs resulting in a larger viscous drag. The formation of a network would require involvement of multiple binding sites on a mAb and such interactions could occur through Fab–Fc, Fab–Fab or both interactions. Fc–Fc interactions were ruled out since both mAb1 and mAb2 have the same Fc amino acid sequence, and yet mAb2 does not have aberrantly high viscosity at the high concentration.

In order to determine which regions of the mAb are involved, the viscosity of the $F(ab')_2$ fragments (Figure 9.7(a)) of mAb_1 and mAb_2 was determined. Overall

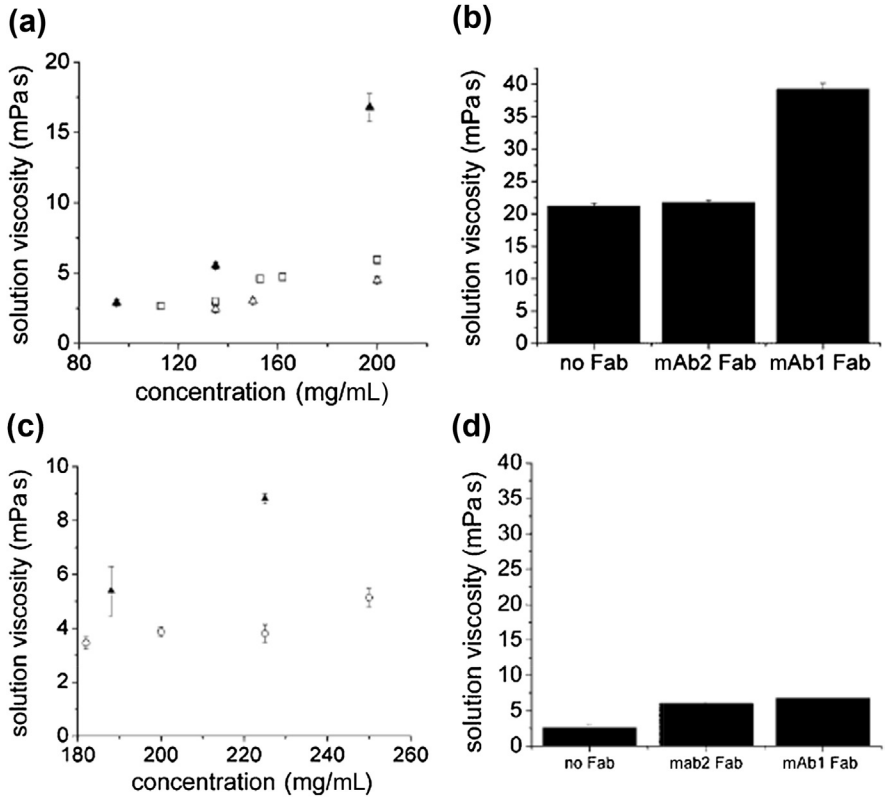

Figure 9.7 (a) Viscosity of mAb1 and mAb2 $F(ab')_2$ fragments in 30 mM histidine buffer at pH 6.0, mAb1 $F(ab')_2$ (solid triangles) and mAb2 $F(ab')_2$ (open squares) and mAb1 $F(ab')_2$ in buffer with 200 mM NaSCN (open triangles). (b) Viscosity of full-length mAb1 mixed with Fab fragments as indicated. The full-length mAb1 concentration is 110 mg/mL and Fab concentration is 100 mg/mL in 30 mM histidine buffer at pH 6.0. (c) Viscosity of mAb1 (solid triangles) and mAb2 Fab (open circles) fragments in 30 mM histidine, pH 6.0. (d) Viscosity of full-length mAb2 mixed with Fab fragments as indicated. The full-length mAb2 concentration is 100 mg/mL and Fab concentration is 100 mg/mL in 30 mM histidine buffer at pH 6.0.
From Kanai et al. (2008).

there was a similar trend in the viscosity–concentration profile of the fragments to that observed for the full-length mAbs, that is, viscosity increased dramatically for mAb1 $F(ab')_2$ with increased concentration and slightly for mAb2 $F(ab')_2$. Moreover the addition of NaSCN, which dramatically lowered viscosity of full-length mAb1, also reduced the viscosity of the mAb1 fragment to that of the mAb2 fragment (Figure 9.7(a)). This study showed that for mAb1 the Fab–Fab attractive interactions play an important role in determining the viscosity at high concentrations. From this result it was reasoned that if mAb1 Fab were added to full-length mAb1, there would be a reduction in viscosity due to the inhibition of network formation by binding of the monovalent Fab fragment. The surprising result was that although addition of mAb2 Fab to full-length mAb had no impact on viscosity, as expected, the addition of mAb1 Fab resulted in a twofold increase (Figure 9.7(b)). This strongly suggested that the Fab fragment itself has multiple interaction sites allowing for network formation. This was further substantiated by the difference in viscosity–concentration profile for mAb1 Fab versus mAb2 Fab (Figure 9.7(c)).

Since mAb1 and mAb2 have the same Fc it was expected that if there is significant interaction between Fab and Fc regions, and that since the Fab fragment has multiple interaction sites that the addition of mAb1 Fab to full-length mAb2 should result in a large increase in viscosity. The addition of mAb1 Fab to full-length mAb2 resulted in a small increase suggesting that mAb1 Fab alone does not form a significant interaction with the Fc region (Figure 9.7(d)).

The reversible self-association of mAb1 as a function of pH, ionic strength, and mAb concentration was further studied by Yadav et al. using the DSL-determined k_D interaction parameter, and the storage modulus, G′ determined with ultrasonic rheology (Yadav, Liu, Shire, & Kalonia, 2010). The G′ measurements as a function of pH and ionic strength showed similar trends observed for the kinematic viscosity–pH profile shown previously (Liu et al., 2005). It was also noted that the measured k_D values at the low concentration for DLS measurements at pH 5, 6, and 7 were not significantly different whereas the G′ value increased dramatically at ~ pH 6 for measurements >80 mg/mL. These results suggest that the magnitude of the existing attractive interactions at low concentration are greatly increased with increasing mAb concentration, and therefore the results of the dilute solution measurements do not necessarily reflect the extent and magnitude of these interactions at the higher concentrations. It was also observed that the pI for mAb1 determined by isoelectric focusing is about 7.8, and therefore the net charge on the mAb should be zero at pH 7.8. Thus, at pH values above 7.8 the mAb has a net negative charge and below 7.8 a positive charge, and under both conditions the mAbs should repel each other and have maximum attraction at ~ pH 7.8 since they theoretically could approach each other at close distance. This does not appear to be the case at high concentration where the pH of maximum attraction is ~6.7 as shown by the G′ and kinematic viscosity measurements. In particular, the different behavior at pH 6 versus pH 7 needed to be explained and Yadav et al. proposed a charge fluctuation model between histidine residues in close proximity to each other with pK_a at ~6 (Yadav, Liu, et al., 2010).

Impact of net charge versus localized surface charge distribution on protein–protein interactions and viscosity as a function of mAb concentration

Proteins and mAbs with a net charge are expected to contribute to repulsive interactions and although many solution properties such as solubility and viscosity at low concentrations can be interpreted with this colloidal view, the work of Yadav et al. (Yadav, Shire, et al., 2010; Yadav, Shire, & Kalonia, 2011; Yadav, Shire, & Kalonia, 2012) and recently Sarangapani et al. (Sarangapani, Hudson, Migler, & Pathak, 2013) have discussed the limitations of the colloidal model when applied to high concentration mAb solutions. At low concentrations at a given pH the mAb molecules behave as particles with a net charge and essentially can be treated as point charges. It has been shown that dilute protein solutions exhibit a minimum viscosity at the pI and increasing viscosity at pH values away from the pI (Buzzell & Tanford, 1956; Cofrades, Careche, Carballo, & Colmenero, 1993; Komatsubara, Suzuki, Nakajima, & Wada, 1973; Tanford & Buzzell, 1956). This has been attributed to electroviscous effects (Rubio-Hernandez, Carrique, & Ruiz-Reina, 2004). The primary effect is due to the diffuse double layer of counterions surrounding the molecule which increases the "drag" of the molecule due to the additional counterion layer whereby near the pI where the net charge is zero there would be significant reduction of this double layer leading to a minimum in the viscosity. Viscosity measurements of bovine serum albumin at higher concentrations show an opposite effect where the viscosity is a maximum at the pI. This phenomenon can be ascribed to the fact that at low concentrations the molecules sense a net charge repulsion, whereas at high concentration the surface distribution of charges can lead to large attractions via charge–dipole interactions. This was further demonstrated by determining the effective charge at 5 mg/mL mAb and viscosity at different concentrations for four different mAbs (Yadav, Shire, et al., 2010). The viscosity at concentrations >50 mg/mL did not correlate with the net effective charge of the mAbs. Whereas the viscosity differences at pH 6 and 15 mM ionic strength were mAb4>mAb1>mAb 5>mAb3, the effective net charge differences were mAb5> mAb3>mAb4>mAb1 (Figure 9.8). Thus, the net charge does not correctly predict the rank order of viscosity for the monoclonal antibodies, whereas the surface charge distribution does account for the different viscoelastic behaviors of the different mAbs (Yadav, Laue, et al., 2012).

Aggregation and viscosity of mAbs

As discussed, reversible attractive interactions that result in clustering of mAbs appears to be a driving force for the high viscosities observed at high concentration. A general schematic view of the role of aggregates in the generation of highly viscous solutions has been presented (Figure 9.9) (Yadav, Laue, et al., 2012). It was suggested that irreversible close contact mAbs aggregates would result in decreased viscosity where in the extreme these aggregates are suspensions. This simplistic model has been criticized since it has been shown that closely associated aggregates can indeed generate higher

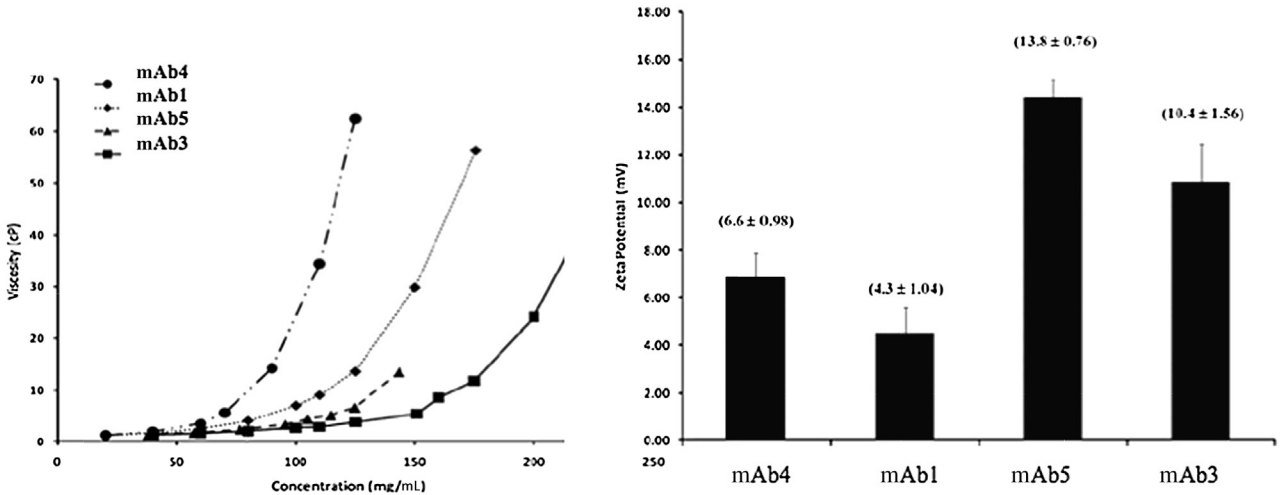

Figure 9.8 Viscosity and net charge for four mAbs at pH 6, 15 mM ionic strength.
From Yadav, Laue et al. (2012).

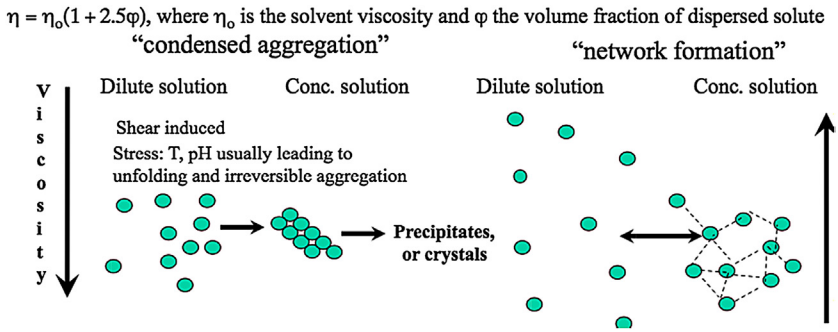

Figure 9.9 Schematic differentiating the effect on solution viscosity of long-range network formation versus soluble irreversible aggregate and suspension formation.
From Yadav, Laue et al. (2012).

viscosity (Pathak, Sologuren, & Narwal, 2013). A good example of this is the polymerization of hemoglobin S (HbS) that is responsible for the pathology of sickle cell anemia. Upon polymerization the viscosity of hemoglobin solutions increases dramatically (Kowalczykowski & Steinhardt, 1977). On the other hand, it has been shown that the viscosity values of ordered suspensions are significantly smaller than the values corresponding to the disordered suspensions (Gondret & Petit, 1996). Many of the models are based on spherical particles and there can be a significant difference in behavior for elongated particles, especially if aligned during the fluid flow as shown for studies using the rod-like particles of tobacco mosaic virus coat protein (TMVP) (Lauffer, 1938). It has been suggested that the notion that irreversible clustering results in a phase separation leading to a decrease in viscosity is incorrect since there is a trade-off between viscosity decrease due to monomer loss from solution and a viscosity increase due to formation of suspended protein clusters with increased cluster volume fraction (Pathak et al., 2013). The authors cite examples where bovine serum IgG clusters generated by unfolding at high temperatures result in an increase in viscosity, and conclude that irreversible aggregates or clusters always result in higher viscosities. On the other hand, Liu et al. showed that nondissociable soluble aggregates in solution do not increase the viscosity (Liu et al., 2005). In their study freeze-dried mAb1 was reconstituted with either sterile water for injection (SWFI) or 0.9% saline and soluble aggregate measured by SEC and AUC as well as viscosity by cone and plate rheometry at low shear. Freeze-dried mAb1 was also stored at 60 °C for 1 week and reconstituted with SWFI and soluble aggregate and viscosity was measured. As seen in Table 9.2, the heated sample has as much as 11% soluble aggregate and yet the measured viscosity was significantly less than that measured for mAb1 after reconstitution with SWFI that contained <1% soluble aggregate. The mAb1 sample reconstituted with saline showed the lowest viscosity although it has similar levels <1% of irreversible aggregate. These studies strongly suggested that the reversible formation of network-associated molecules dominates the viscosity properties and that solutions that contain irreversible condensed aggregates have decreased viscosity. Many of these observations show the complexity of soluble aggregate formation impact on viscosity as opposed to suspensions of aggregates. At any rate, an important consideration is what is the nature of the interactions that result in mAb clustering at

Table 9.2 Summary of nondissociable soluble aggregates of mAb1 in different formulations

	Soluble aggregates by SEC	Soluble aggregates by AUC	Viscosity (mPa s)
mAb1 reconstituted with SWFI[a]	0.2%	0.5%	60
mAb1 reconstituted with saline[b]	0.3%	0.6%	12
Lyophilized mAb1 stored at 60 °C, and reconstituted with SWFI[c]	11%	11%	41

SWFI, sterile water for injection.
[a]Lyophilized mAbl was reconstituted with 1.4 mL SWFI to final concentration of 125 mg/mL protein, 16 mM histidine, 266 mM sucrose, 0.03% polysorbate 20, at pH 6.0.
[b]Lyophilized mAbl was reconstituted with 0.9% saline to final concentration of 125 mg/mL protein, 16 mM histidine. 266 mM sucrose, 0.03% polysorbate 20, 128 mM NaCl, at pH 6.0.
[c]Lyophilized mAbl was stored at 60 °C for 1 week and then reconstituted with 1.4 mL SWFI to final concentration of 125 mg/mL protein, 16 mM histidine, 266 mM sucrose, 0.03% polysorbate 20, at pH 6.0.
From Liu et al. (2005).

high concentration. It can be expected that hydrophobic and electrostatic interactions are both present at high concentration and the domination of one versus the other would dictate formulation strategies to decrease viscosity. Thus, for some mAbs it has been shown that "hydrophobic" salts can disrupt interactions resulting in viscosity decrease (Du & Klibanov, 2011), whereas addition of ionic salts can decrease viscosity for other mAbs (Kanai et al., 2008; Liu et al., 2005). In the case of several mAbs it has been shown that the main attractive interactions are electrostatic in nature and that measured average dipole moments for mAb1 and mAb2 as a function of pH correlate with the DLS interaction parameter, k_D and G′ and viscosity measurements (Figure 9.10) (Singh, Yadav, Shire, & Kalonia, 2014). In particular, the magnitude of the mAb1 dipole moment increased from pH 4 to 6.5 and fell off sharply from pH 7 to 9.0, whereas the dipole moment for mAb2 with the same IgG_1 human Fc framework as mAb1 has its largest magnitude somewhere between pH 7 to 9, and is significantly lower at pH 6.5. Previously it was shown that the G′ storage modulus for mAb1was at a maximum at ~pH 6 at low ionic strength (Yadav, Shire, et al., 2012). The strength of the attractive interactions is reflected in the G′ value and this was corroborated by the negative values for k_D for mAb1 at pH 6 and low ionic strength (Yadav, Shire, et al., 2012). The measured dipole moments for mAb2 as a function of pH are also consistent with previously determined G′ and k_D values, which are maximum at pH 8. Finally, these observed pH trends for dipole moment, G′ and k_D for mAb1 and mAb2 correlate with the pH dependency of viscosity (Liu et al., 2005; Yadav, Shire, et al., 2012), suggesting that for mAb1 and mAb2, dipole interactions contribute significantly to the rheological properties of these mAbs at high concentration.

Computation of the electrostatic potential surfaces for mAb1 versus mAb2 showed that the Fab region of mAb1 had a substantially more negative potential surface than that of mAb2 (Figure 9.11) (Yadav, Laue, et al., 2012), which undoubtedly contributes to the presence of dipole–dipole interaction. The molecular basis for these differences will now be discussed.

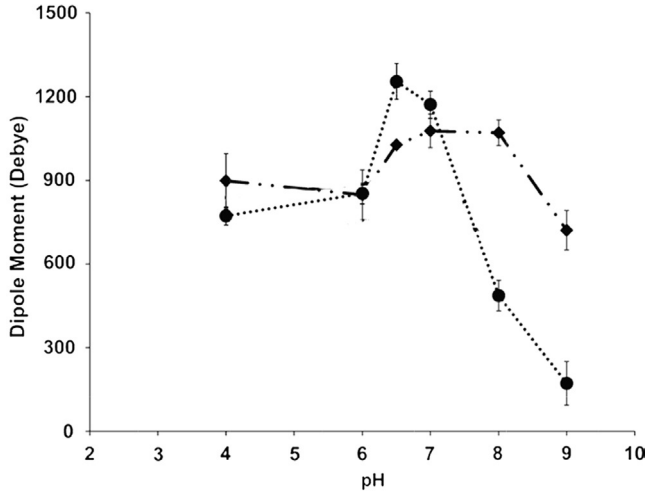

Figure 9.10 Measured overall dipole moment for mAb1 (solid circles) versus mAb2 (solid triangles) as a function of pH.
Adapted from Singh et al. (2014).

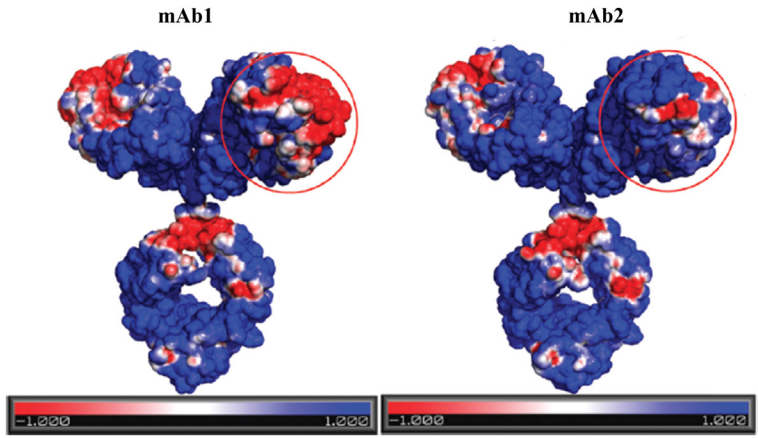

Figure 9.11 Computed electrostatic potential surfaces for mAb1 and mAb2.
Adapted from Yadav et al. (2012).

Linking amino acid sequence to self-association and viscoelastic behavior of mAb1 and mAb2

The viscosity and self-association of mAb1 and mAb2 have been thoroughly explored. These two mAbs bind to very different targets but were constructed using essentially the same human IgG_1 Fc construct. Thus, the main differences between these mAbs resides is their complementary determining region (CDR), and therefore provides an opportunity to make changes in the CDR to assess impact on self-association and

viscoelastic properties (Yadav, Sreedhara, et al., 2011). In addition to the specific amino acid sequence differences there also was a four-amino-acid sequence insert in the CDR1 light chain of mAb1. There can also be some heterogeneity (Chapter 1) contributed by differences in the carbohydrate chain between mAb1 and mAb2. In order to determine if the amino acid sequence insert might contribute to observed differences in viscoelastic behavior between mAb1 and mAb2 a mutant, M1, was created where the four-amino-acid insert was removed. Another mutant of mAb1, M11, was expressed in *Escherichia coli* resulting in an aglycosylated molecule (Simmons et al., 2002). A close examination of the CDRs for mAb1 and mAb2 showed that a number of charged residues are present in the variable light (VL) and variable heavy (VH) chain of mAb1, which are not present in mAb2 at the same positions in the sequence. The main differences in the VL are some aspartates, glutamates, and histididyl residues. In order to assess which of these charged residues are responsible for the differences in viscosity between mAb1 and mAb2 a number of "charge-swap" mutants were created by swapping residues from mAb2 into their respective mAb1 sequence positions. Mutants M5 and M6 are mAb1 with noncharged residues from mAb2 in the VL and VH chains, respectively. The mutant M7 is mAb1 with the noncharged residues from mAb2 in both the VL and VH chains. The mutant, M10, is a mAb2 molecule with the charged residues from mAb1 substituted in both the VL and VH chains (Table 9.3) (Yadav, Sreedhara, et al., 2011). The results of the viscosity measurements as a function of concentration for mAb1, mAb2, and the different mutants are shown in Figure 9.12 along with schematics of the mutants showing the amino acid substitutions. The M1 mutant that has the deletion of the four amino-acid sequence has the same viscosity–concentration profile as mAb1 showing that this specific insert in the sequence of mAb1 does not impact the viscosity. In addition the aglycosylated mutant, M11, also shows the same profile as mAb1 showing that the carbohydrate chain does not impact the viscosity of mAb1. A partial decrease of the viscosity was observed for mutants with changes in either the VL chain (M5) or in the VH chain (M6), but the viscosity values are still greater than that observed for mAb2, and are independent of ionic strength. When the charged residues were swapped out in both the VL and VH chains of mAb1 the viscosity–concentration profile was the same as for mAb2. The increase in ionic strength greatly reduced the corrected molecular weight for mAb1, which is consistent with previous determinations that showed decrease in molecular weight and viscosity at higher ionic strength. This once again shows the linkage of reversible self-association to viscosity and the fact that the prominent attractive interactions are electrostatic in nature. The M10 mutant was expected to increase in viscosity since the charged residues from mAb1 were substituted into the mAb2 structure. However, the viscosity did not increase and was similar to that observed for mAb2. Previously a linkage between reversible self-association at high concentration with increased viscosity was established using the preparative analytical ultracentrifugation technique (Liu et al., 2005). The corrected weight average molecular weights (corrected as described previously using mAb2 data) for mAb1, the M7, and the M10 mutants were determined by the preparative AUC technique at low (15 mM) and high ionic strength (150 mM) (Figure 9.13). The corrected molecular weight for mAb1 at 15 mM ionic strength is greater than M7 and M10 showing that mAb1

Table 9.3 Summary of mutants as a result of performing mutations in the complementary determining region (CDR) sequence of mAb1 and mAb2. Bold amino acid residues are charged residues in the CDR sequences of the mAbs

CDR	Light chain 1[a]	Light chain 3[a]	Heavy chain 3[b]	The rest of the CDR	Description
mAb1	QSV**D**Y**D**G**D**SYMN	**HED**PYT	GS**H**YFG**H**W**H**FAVW	mAb1 LC and HC	mAb1 WT
mAb2	Q—**D**V**N**TAVA	**YTT**PPT	WG**GD**GF**Y**A**MD**YW	mAb2 LC and HC	mAb2 WT
M1	Q—**DGD**SYMN	**HED**PYT	GS**H**YFG**H**W**H**FAVW	mAb1 LC and HC	mAb1 with SVDY deletion in LC1
M5	QSV**D**Y**AGN**SYMN	**YTT**PYT	GS**H**YFG**H**W**H**FAVW	mAb1 LC and HC	mAb1 with substitution in LC1 and LC3
M6	QSV**D**Y**D**G**D**SYMN	**HED**PYT	GS**G**YFG**Y**W**M**FAVW	mAb1 LC and HC	mAb1 with substitution in HC3
M7	QSV**D**Y**AGN**SYMN	**YTT**PYT	GS**G**YFG**Y**W**M**FAVW	mAb1 LC and HC	mAb1 with substitution in LC1, LC3, and HC3
M10	**E**—**D**V**D**TAVA	**HED**PPT	WG**HD**GF**H**A**HD**YW	mAb2 LC and HC	mAb2 with substitution in LC1, LC3, and HC3
M11	QSV**D**Y**D**G**D**SYMN	**HED**PYT	GS**H**YFG**H**W**H**FAVW	mAb1 LC and HC; made in *Escherichia coli*	Aglycosylated mAb1

Numbers 1 and 3 correspond to the different loops *of* the variable regions (LC light chain; HC heavy chain) in the CDR.
[a]Mutations performed in the variable light (VL) chain sequence.
[b]Mutations performed in the variable heavy (VH) chain sequence.
From Yadav, Sreedhara et al. (2011).

self-associates to a greater extent than M7 and M10 under these conditions. Replacement of the mAb1 charged residues in both the VL and VH chain resulted in a lower molecular weight, and was similar to the M10 mutant. Thus, the self-association behavior of mutant M10 where residues were substituted into the mAb2 structure is consistent with the observed low viscosity–concentration profile. The question, however, still remains as to why the charged residue substitutions into mAb2 did not result in increased self-association and increased viscosity.

Coarse-grained molecular dynamics computations

Molecular dynamics simulations have been done on a full-length mAb and proven useful in understanding how the Fc and Fab domains move and interact with each other (Brandt, Patapoff, & Aragon, 2010). Although with increases in computational power where it is possible to simulate the motion of all the atoms in a single molecule the size of an IgG_1 mAb, it remains a formidable problem to do the simulations for a large number of mAbs in solution. Given the interest in understanding how the mAbs are self-associating to form clusters or networks over relatively long time and trajectories requires an alternative approach. Coarse-grained (CG) modeling, where sites are constructed with appropriate physical parameters allow for the simulation with many molecules (Izvekov & Voth, 2005; Voth, 2009). Representative CG models were generated to specifically investigate the formation of clusters in mAb1 and mAb2 (Chaudhri et al., 2012). The model used included two with a compact configuration (Fab–Fab angle of 36°) and an extended configuration (Fab–Fab angle of 130°) to evaluate the

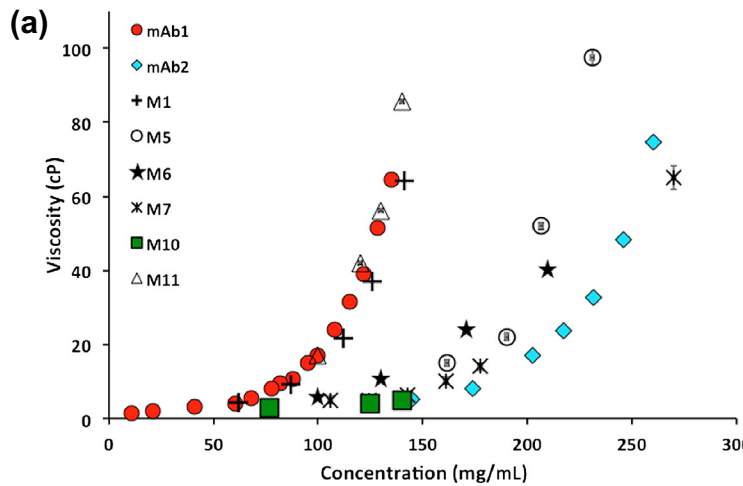

Figure 9.12 (a) Viscosity as a function of mAb concentration of mAb1 and mAb2 mutants with (b) schematics showing amino acid substitutions. All mAbs and mutants are at pH 6 and 15 mM ionic strength. Viscosity determined using a cone-plate rheometer at a shear rate of 1000/s at 25 °C. Adapted from figures created by Sandeep Yadav.

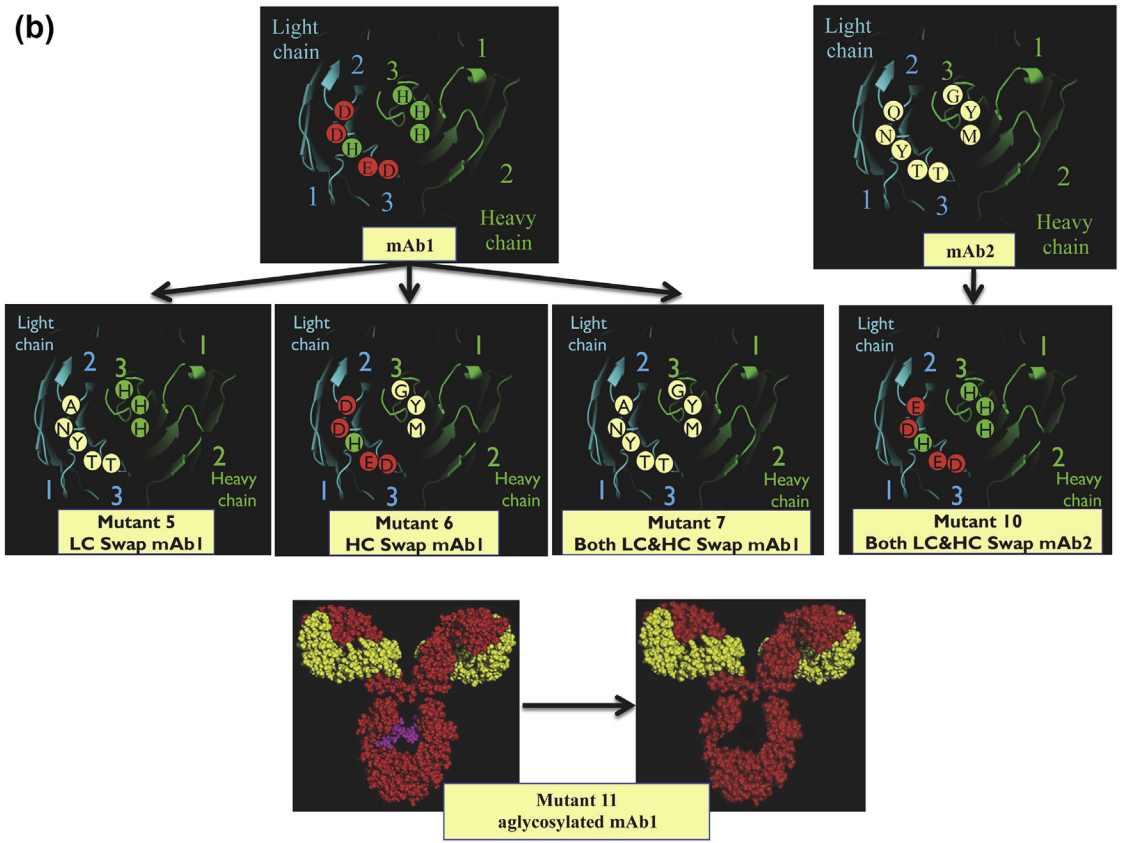

Figure 9.12 Continued.

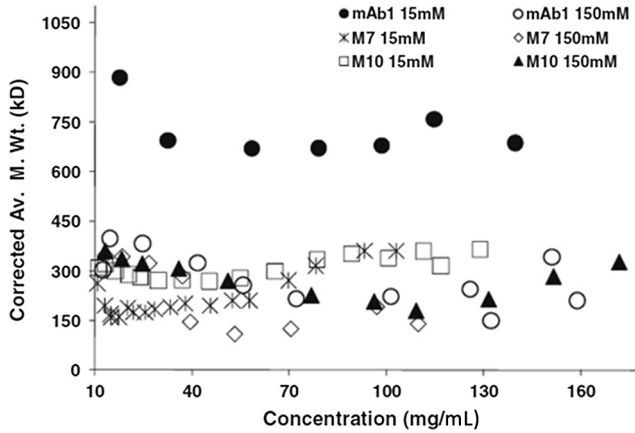

Figure 9.13 The corrected weight average molecular weights for mAb1 and mutants, using the non-ideality corrections for mAb2 (Eqn (9.19)). The measurement was conducted at pH 6.0, histidine hydrochloride buffer in 15 and 150 mM ionic strength (made up by addition of NaCl) at 12,000 rpm at 20 °C.

impact of hinge flexibility on the intermolecular interactions. Also two models were developed with 12 sites and another with 26 sites. Each site was assigned a center of mass for placement of the corresponding CG site, which are connected through an elastic network. The mass and charge of each CG site was computed by summing up the masses and partial charges respectively that represent the amino acid residues that make up the site. The interactions between the CG sites are chosen to represent an averaged large-scale protein motion. Local fluctuation of individual atoms is averaged and effective interactions considered. Then the total effective potential is described as a sum of the intraprotein and interprotein interactions by

$$U_{total} = U_{intra} + U_{inter} \tag{9.21}$$

The intraprotein interactions were computed on the basis of bond strengths, angles, and spring constants for the interconnections. The intermolecular interactions were computed as a sum of a long-range electrostatic potential, U_{colomb} and dispersion and repulsive forces used a Lennard Jones potential, U_{LJ}, with smoothing forces. The computations were done at concentrations ranging from 20 to 120 mg/mL at pH 6. The computed results for the 12-site model were similar to the 26-site model as well as for the compact versus extended structure. The essential results showed that mAb1 formed three-dimensional heterogeneous structures with dense regions or clusters compared to mAb2 (Figure 9.14(a)). The computations also showed that strong Fab–Fab interactions were responsible for the differences between mAb1 and mAb2, but Fab–Fc interactions could also contribute. The distribution of clusters at 120 mg/mL was also shown where it was clear that mAb1 generated a more extensive self-association network than mAb2 (Figure 9.14(b)). These simulations corroborate the previous molecular weight data obtained by preparative AUC and SLS. The CG model was

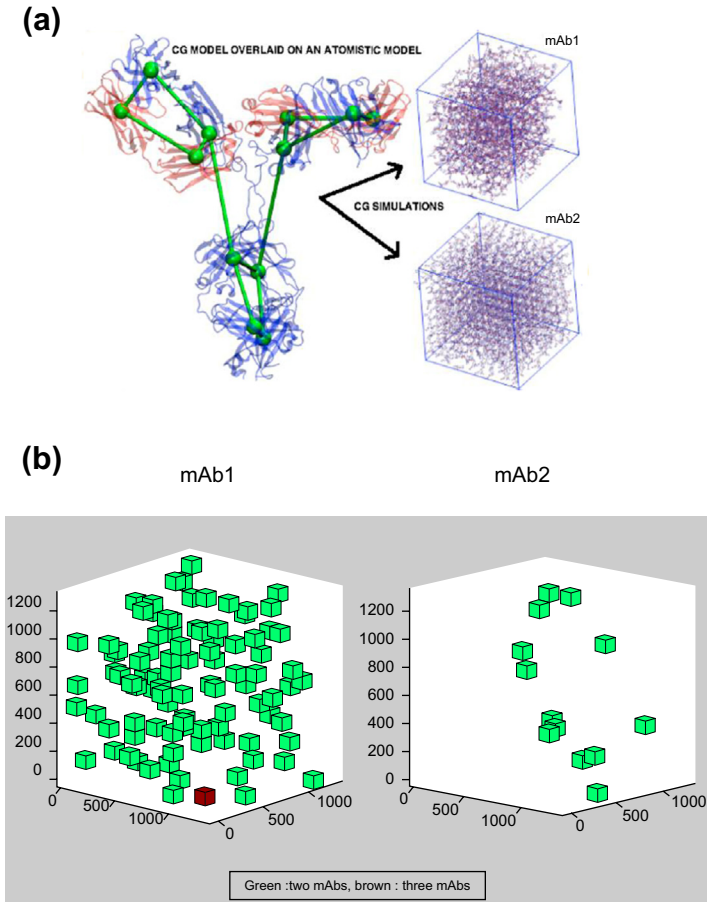

Figure 9.14 CG computations for mAb1 versus mAb2 using a 12 site compact configuration model at 125 mg/mL and pH 6. (a) The 12 site model overlaid on the atomistic model (ribbon diagram) and structures formed of mAb1 versus mAb2 (b) Distribution of equilibrated structures obtained by dividing the domain into cubic boxes of 106 Å3 (100 Å per side) and counting the number of mAbs in each box. The boxes are color coded where boxes with two mAbs are green and with three are brown.
Adapted from Chaudhri et al. (2012).

also used to evaluate the behavior of mutants M5, M6, M7, and M10 (Chaudhri et al., 2013). The 12-site model again gave similar results compared to the 26-site model. To further understand the behavior of all these mAbs at higher concentrations a density based clustering algorithm was used. Clusters were defined using the criteria that a minimum of four clusters are found within a neighboring radial radius of 100Å. The average cluster size for mAb1 ranges from 5 to 45, whereas the algorithm gave no evidence of clusters in mAb2, M1, M5, M7, and M10. An important conclusion from this study is that the simulations successfully predict that the mutant M10 does not form an extensive network at higher concentration compared to mAb1 and thus the

viscosity would be lower. This shows the utility of CG simulations and helped explain the behavior of M10. It is also noteworthy that M6 appeared to have the largest amount of dimer clusters showing that although there are sufficient attractive interactions to form clusters overall they are not large in size. This is especially interesting since M6 has a lower viscosity than observed for mAb1, mainly due to the lack of formation of larger clusters/network organization during self-association at higher concentrations.

The in-depth analysis and strategies used to understand the differences in mAb1 and mAb2 viscosities should be applicable to studies of other mAbs. The genetic engineering approach that was used to swap charges between CDRs has limited utility for creating a mAb with better pharmaceutical properties, since the activity of the mAb is decreased due to the manipulations in the CDR. However, it should be possible to change residues in the flanking CDR frame, thus retaining activity while improving solution properties.

References

Allemendinger, A., Dieu, L.-H., Fischer, S., Mueller, R., Mahler, H.-C., & Huwyler, J. (2014). High-throughput viscosity measurement using capillary electrophoresis instrumentation and its application to protein formulation. *Journal of Pharmaceutical and Biomedical Analysis*, *90*, 51–58.

Brandt, J. P., Patapoff, T. W., & Aragon, S. R. (2010). Construction, MD simulation, and hydrodynamic validation of an all-atom model of a monoclonal IgG antibody. *Biophysical Journal*, *99*(3), 905–913.

Buzzell, J. G., & Tanford, C. (1956). The effect of charge and ionic strength on the viscosity of ribonuclease. *Journal of Physical Chemistry*, *60*, 1204–1207.

Cantor, C. R., & Schimmel, P. R. (1980). Viscometry. In L. W. McCombs (Ed.), *Biophysical chemistry, part II: Techniques for the study of biological structure and function* (pp. 643–659). San Francisco: W. H. Freeman and Co.

Chatelier, R. C., & Minton, A. P. (1987). Sedimentation equilibrium in macromolecular solutions of arbitrary concentration. I. Self-associating proteins. *Biopolymers*, *26*(4), 507–524.

Chaudhri, A., Zarraga, I. E., Kamerzell, T. J., Brandt, J. P., Patapoff, T. W., Shire, S. J., et al. (2012). Coarse-grained modeling of the self-association of therapeutic monoclonal antibodies. *Journal of Physical Chemistry B*, *116*(28), 8045–8057.

Chaudhri, A., Zarraga, I. E., Yadav, S., Patapoff, T. W., Shire, S. J., & Voth, G. A. (2013). The role of amino acid sequence in the self-association of therapeutic monoclonal antibodies: insights from coarse-grained modeling. *Journal of Physical Chemistry B*, *117*(5), 1269–1279.

Cofrades, S., Careche, M., Carballo, J., & Colmenero, F. J. (1993). Protein-concentration, Ph and ionic-strength affect apparent viscosity of actomyosin. *Journal of Food Science*, *58*(6), 1269–1272.

Connolly, B. D., Petry, C., Yadav, S., Demeule, B., Ciaccio, N., Moore, J. M. R., et al. (2012). Weak interactions govern the viscosity of concentrated antibody solutions: high-throughput analysis using the diffusion interaction parameter. *Biophysical Journal*, *103*(1), 69–78.

Du, W., & Klibanov, A. M. (2011). Hydrophobic salts Markedly Diminish viscosity of concentrated protein solutions. *Biotechnology and Bioengineering*, *108*(3), 632–636.

Eberstein, W., Georgalis, Y., & Saenger, W. (1994). Molecular-interactions in crystallizing lysozyme solutions studied by photon-correlation spectroscopy. *Journal of Crystal Growth*, *143*(1–2), 71–78.

Einstein, A. (1911). A new determination of molecular dimensions. *Annalen der Physik*, *34*, 591–592.

Gondret, P., & Petit, L. (1996). Viscosity of periodic suspensions. *Physics of Fluids*, *8*(9), 2284–2290.

Grupi, A., & Minton, A. P. (2012). Capillary viscometer for fully automated measurement of the concentration and shear dependence of the viscosity of macromolecular solutions. *Analytical Chemistry*, *84*(24), 10732–10736.

Hall, C. G., & Abraham, G. N. (1984). Size, shape, and hydration of a self-associating human-IgG myeloma protein – axial asymmetry as a contributing factor in serum hyperviscosity. *Archives of Biochemistry and Biophysics*, *233*(2), 330–337.

Harding, S. E., & Johnson, P. (1985). The concentration-dependence of macromolecular parameters. *Biochemical Journal*, *231*(3), 543–547.

He, F., Becker, G. W., Litowski, J. R., Narhi, L. O., Brems, D. N., & Razinkov, V. I. (2010). High-throughput dynamic light scattering method for measuring viscosity of concentrated protein solutions. *Analytical Biochemistry*, *399*(1), 141–143.

Hudson, S. D., Sarangapani, P., Pathak, J. A., & Migler, K. B. (2014). A microliter capillary rheometer for characterization of protein solutions. *Journal of Pharmaceutical Sciences*.

Izvekov, S., & Voth, G. A. (2005). A multiscale coarse-graining method for biomolecular systems. *Journal of Physical Chemistry B*, *109*(7), 2469–2473.

Jezek, J., Rides, M., Derham, B., Moore, J., Cerasoli, E., Simler, R., et al. (2011). Viscosity of concentrated therapeutic protein compositions. *Advanced Drug Delivery Reviews*, *63*(13), 1107–1117.

Kanai, S., Liu, J., Patapoff, T. W., & Shire, S. J. (2008). Reversible self-association of a concentrated monoclonal antibody solution mediated by Fab-Fab interaction that impacts solution viscosity. *Journal of Pharmaceutical Sciences*, *97*(10), 4219–4227.

Kilar, F., Simon, I., Lakatos, S., Vonderviszt, F., Medgyesi, G. A., & Zavodszky, P. (1985). Conformation of human-IgG subclasses in solution – small-angle x-ray-scattering and hydrodynamic studies. *European Journal of Biochemistry*, *147*(1), 17–25.

Komatsubara, M., Suzuki, K., Nakajima, H., & Wada, Y. (1973). Electroviscous effect of lysozyme in aqueous solutions. *Biopolymers*, *12*(8), 1741–1746.

Kowalczykowski, S., & Steinhardt, J. (1977). Kinetics of hemoglobin-s gelation followed by continuously sensitive low-shear viscosity – changes in viscosity and volume on aggregation. *Journal of Molecular Biology*, *115*(2), 201–213.

Lauffer, M. A. (1938). The viscosity of tobacco mosaic virus protein solutions. *Journal of Biological Chemistry*, *126*, 443–453.

Liu, J., Nguyen, M. D. H., Andya, J. D., & Shire, S. J. (2005). Reversible self-association increases the viscosity of a concentrated monoclonal antibody in aqueous solution. *Journal of Pharmaceutical Sciences*, *94*(9), 1928–1940.

Liu, J., Nguyen, M. D. H., Andya, J., & Shire, S. J. (2006). Erratum- reversible self association increases the viscosity of a concentrated monoclonal antibody in aqueous solution. *Journal of Pharmaceutical Sciences*, *95*(1), 234–235.

Mandel, M. (1993). Applications of dynamic light scattering to polyelectrolytes in solution. In W. Brown (Ed.), *Dynamic light scattering: The method and some applications* (pp. 319–371). New York: Oxford University Press.

Mehl, J. W., Oncley, J. L., & Simha, R. (1940). Viscosity and the shape of protein molecules. *Science*, *92*(2380), 132–133.

Minton, A. P. (1989). Analytical centrifugation with preparative ultracentrifuges. *Analytical Biochemistry*, *176*(2), 209–216.

Minton, A. P., & Lewis, M. S. (1981). Self-Association in highly concentrated solutions of myoglobin: a novel analysis of sedimentation equilibrium of highly non-ideal solutions. *Biophysical Chemistry*, *14*, 317–324.

Mooney, M. (1951). The viscosity of a concentrated suspension of spherical particles. *Journal of Colloid Science*, *6*(2), 162–170.

Patapoff, T. W., & Esue, O. (2009). Polysorbate 20 prevents the precipitation of a monoclonal antibody during shear. *Pharmaceutical Development and Technology*, *14*(6), 659–664.

Pathak, J. A., Sologuren, R. R., & Narwal, R. (2013). Do clustering monoclonal antibody solutions really have a concentration dependence of viscosity? *Biophysical Journal*, *104*(4), 913–923.

Pipe, C. J., & McKinley, G. H. (2009). Microfluidic rheometry. *Mechanics Research Communications*, *36*(1), 110–120.

Porcar, L., Falus, P., Chen, W. R., Faraone, A., Fratini, E., Hong, K. L., et al. (2010). Formation of the dynamic clusters in concentrated lysozyme protein solutions. *Journal of Physical Chemistry Letters*, *1*(1), 126–129.

Ross, P. D., & Minton, A. P. (1977). Hard quasispherical model for the viscosity of hemoglobin solutions. *Biochemical and Biophysical Research Communications*, *76*(4), 971–976.

Rubio-Hernandez, F. J., Carrique, F., & Ruiz-Reina, E. (2004). The primary electroviscous effect in colloidal suspensions. *Advances in Colloid and Interface Science*, *107*(1), 51–60.

Saito, S., Hasegawa, J., Kobayashi, N., Kishi, N., Uchiyama, S., & Fukui, K. (2012). Behavior of monoclonal antibodies: relation between the second virial coefficient (B2) at low concentrations and aggregation propensity and viscosity at high concentrations. *Pharmaceutical Research*, *29*(2), 397–410.

Saluja, A., Badkar, A. V., Zeng, D. L., Nema, S., & Kalonia, D. S. (2007). Ultrasonic storage modulus as a novel parameter for analyzing protein-protein interactions in high protein concentration solutions: correlation with static and dynamic light scattering measurements. *Biophysical Journal*, *92*(1), 234–244.

Saluja, A., & Kalonia, D. S. (2004). Measurement of fluid viscosity at microliter volumes using quartz impedance analysis. *AAPS PharmSciTech*, *5*(3) Article 47.

Saluja, A., & Kalonia, D. S. (2005). Application of ultrasonic shear rheometer to characterize rheological properties of high protein concentration solutions at microliter volume. *Journal of Pharmaceutical Sciences*, *94*(6), 1161–1168.

Sarangapani, P. S., Hudson, S. D., Migler, K. B., & Pathak, J. A. (2013). The limitations of an exclusively colloidal view of protein solution hydrodynamics and rheology. *Biophysical Journal*, *105*(10), 2418–2426.

Scherer, T. M., Liu, J., Shire, S. J., & Minton, A. I. (2010). Intermolecular interactions of IgG1 monoclonal antibodies at high concentrations characterized by light scattering. *Journal of Physical Chemistry B*, *114*(40), 12948–12957.

Shukla, A., Mylonas, E., Di Cola, E., Finet, S., Timmins, P., Narayanan, T., et al. (2008a). Absence of equilibrium cluster phase in concentrated lysozyme solutions. *Proceedings of the National Academy of Sciences of the United States of America*, *105*(13), 5075–5080.

Shukla, A., Mylonas, E., Di Cola, E., Finet, S., Timmins, P., Narayanan, T., et al. (2008b). Reply to Stradner et al.: equilibrium clusters are absent in concentrated lysozyme solutions. In *Proceedings of the national academy of sciences of the United States of America* (Vol. 105(44)) (p. E76).

Simmons, L. C., Reilly, D., Klimowski, L., Raju, T. S., Meng, G., Sims, P., et al. (2002). Expression of full-length immunoglobulins in *Escherichia coli*: rapid and efficient production of aglycosylated antibodies. *Journal of Immunological Methods*, *263*(1–2), 133–147.

Singh, S. N., Yadav, S., Shire, S. J., & Kalonia, D. S. (2014). Dipole-dipole interaction in antibody solutions: correlation with viscosity behavior at high concentration. *Pharmaceutical Research*.

Stadler, A. M., Schweins, R., Zaccai, G., & Lindner, P. (2010). Observation of a large-scale superstructure in concentrated hemoglobin solutions by using small angle neutron scattering. *Journal of Physical Chemistry Letters*, *1*(12), 1805–1808.

Stradner, A., Sedgwick, H., Cardinaux, F., Poon, W. C. K., Egelhaaf, S. U., & Schurtenberger, P. (2004). Equilibrium cluster formation in concentrated protein solutions and colloids. *Nature*, *432*(7016), 492–495.

Svensson, H. (1954a). The second-order aberrations in the interferometric measurement of concentration gradients. *Optica Acta*, *1*, 25–32.

Svensson, H. (1954b). The second-order aberrations in the interferometric measurement of concentration gradients. II. Experimental verification of theory. *Optica Acta*, *1*, 90–93.

Tanford, C. (1967). *Flow processes in viscous fluids. Physical chemistry of macromolecules*. USA: John Wiley & Sons.

Tanford, C., & Buzzell, J. G. (1956). The viscosity of aqueous solutions of bovine serum albumin between pH 4.3 and 10.5. *The Journal of Physical Chemistry*, *60*, 225–231.

Van Holde, K. E. (1971). *Viscosity. Physical biochemistry*. Englewood Cliffs, NJ: Prentice-Hall, Inc.

Voth, G. A. (Ed.). (2009). *Coarse-graining of condensed phase and biomolecular systems*. Boca Raton: CRC Press.

Yadav, S., Laue, T. M., Kalonia, D. S., Singh, S. N., & Shire, S. J. (2012). The influence of charge distribution on self-association and viscosity behavior of monoclonal antibody solutions. *Molecular Pharmaceutics*, *9*(4), 791–802.

Yadav, S., Liu, J., Shire, S. J., & Kalonia, D. S. (2010). Specific interactions in high concentration antibody solutions resulting in high viscosity. *Journal of Pharmaceutical Sciences*, *99*(3), 1152–1168.

Yadav, S., Scherer, T. M., Shire, S. J., & Kalonia, D. S. (2011). Use of dynamic light scattering to determine second virial coefficient in a semidilute concentration regime. *Analytical Biochemistry*, *411*(2), 292–296.

Yadav, S., Shire, S. J., & Kalonia, D. S. (2010). Factors affecting the viscosity in high concentration solutions of different monoclonal antibodies. *Journal of Pharmaceutical Sciences*, *99*(12), 4812–4829.

Yadav, S., Shire, S. J., & Kalonia, D. S. (2011). Viscosity analysis of high concentration bovine serum albumin aqueous solutions. *Pharmaceutical Research*, *28*(8), 1973–1983.

Yadav, S., Shire, S. J., & Kalonia, D. S. (2012). Viscosity behavior of high-concentration monoclonal antibody solutions: correlation with interaction parameter and electroviscous effects. *Journal of Pharmaceutical Sciences*, *101*(3), 998–1011.

Yadav, S., Sreedhara, A., Kanai, S., Liu, J., Lien, S., Lowman, H., et al. (2011). Establishing a link between amino acid sequences and self-associating and viscoelastic behavior of two closely related monoclonal antibodies. *Pharmaceutical Research*, *28*(7), 1750–1764.

Yphantis, D. A. (1964). Equilibrium ultracentrifugation of dilute solutions. *Biochemistry*, *3*, 297–317.

Yuan, P., & Lin, B.-Y. (Oct. 27, 2008). *Measurement of viscosity in a vertical falling ball viscometer*. American Laboratory.

Zhang, J., & Liu, X. Y. (2003). Effect of protein-protein interactions on protein aggregation kinetics. *Journal of Chemical Physics*, *119*(20), 10972–10976.

Zhou, H. X., Rivas, G. N., & Minton, A. P. (2008). Macromolecular crowding and confinement: biochemical, biophysical, and potential physiological consequences. *Annual Review of Biophysics*, *37*, 375–397.

The future of monoclonal antibodies (mAbs) as therapeutics and concluding remarks

10

Although monoclonal antibodies (mAbs) have had considerable success as therapeutics, the initial development of mAbs as therapeutics had several problems (Ezzell, 2001; Oldham & Dilman, 2008; Reichert, Rosensweig, Faden, & Dewitz, 2005). The original production of mAbs used fused mouse lymphocyte and myeloma cells resulting in the generation of murine mAbs (Kohler & Milstein, 2005; Milstein, 1999). When these murine mAbs were introduced into clinical studies in the early 1980s, there generally was a lack of efficacy and rapid clearance mainly due to the patients generating human anti-mouse antibodies. These problems were solved with the introduction of chimera mAbs where the fragment antigen-binding (Fab) region was murine with a human Fc construct (Boulianne, Hozumi, & Shulman, 1984; Morrison, Johnson, Herzenberg, & Oi, 1984). Eventually techniques were developed to produce humanized mAbs where the complementarity determining regions (CDRs) were still made up of murine residues but the rest of the mAb was a human sequence (Jones, Dear, Foote, Neuberger, & Winter, 1986). The production of humanized mAbs also required computer modeling to alter flanking sequences around the CDRs to maintain full activity (Presta et al., 1993). Fully human antibodies have also been produced using immortalization and hybridoma techniques to human cells (Cole, Campling, Atlaw, Kozbor, & Roder, 1984; Lakow, Valentine, Vaughan, Tsoukas, & Carson, 1984). Another problem with early development of mAbs was limitations on the amount of mAb that could be manufactured and processed. Many of the mAb doses were found to be quite high, thus requiring new technologies to meet the manufacturing requirements. Fortunately, the design of an efficient cell culture system with high titers, rapid and economical recovery, and purification steps has enabled manufacturing of large batches of mAbs. Thus, the generation of human and humanized versions of the mAbs, and improvements in process and manufacturing, have contributed largely to the success of these important biotherapeutics.

Recently, a major advance in mAb design is the creation of so-called "antibody drug conjugates" (ADCs) (Casi & Neri, 2012; Wakankar, 2010). The ADC approach uses mAbs as delivery systems that can deliver therapeutic agents directly to targeted cells. This has become an important new class of molecule for the treatment of cancer since standard chemotherapy results in toxic levels in the blood inhibiting the ability to achieve greater and more effective doses. Currently there are only two commercialized ADCs, Adcetris and Kadcyla (Mylotarg was the first ADC approved for market in 2001, but was withdrawn from the market in June 2010 due to safety issues and lack of efficacy). Nonetheless, there are now ~45 ADCs in clinical trials as summarized in a report from Roots Analysis Private Ltd. (Market-report, 2014). This class of molecule presents a new set of challenges for pharmaceutical development, but the details of the

Monoclonal Antibodies. http://dx.doi.org/10.1016/B978-0-08-100296-4.00010-5

development process for ADCs are not currently in the scope of this book. As a brief summary, the mAb that will be conjugated with drug is no longer the final drug product, but rather an intermediate. The drug conjugates are linked to the mAb usually through a cysteine or lysine residue. There are several different linker chemistries that have been used or proposed (Casi & Neri, 2012), and an important consideration is that the linker needs to be stable during systemic circulation to ensure low levels of free drug, whereas it needs to be cleavable after insertion of the ADC into cells so that sufficiently high doses of free drug can be released into the targeted cell. Thus, stability assessments of the linker as well as of the conjugated mAb are critical for successful pharmaceutical development. The final drug product is the conjugated mAb and since many of the drugs are hydrophobic the physicochemical stability of the conjugated mAb will be dependent on the drug–antibody ratio (DAR) as well as the process used to conjugate the mAb (Wakankar et al., 2010). The process of linking the drug results in a heterogeneous population of mAbs with different DAR. Thus, an important part of the development process requires full characterization as a function of DAR and a consistent manufacturing whereby produced lots have similar distribution of species and essentially the same average value for the DAR.

Other developments for the next wave of mAb therapeutics are development of bispecifics that have two different Fabs that bind to different cellular targets (Rouet & Christ, 2014; Thakur & Lum, 2010). Single-chain mAbs have also been developed (Sheets et al., 1998) that may require different strategies than that used for full-length mAbs and mAb fragments. Again these new mAb agents have not been covered in this book, and undoubtedly as they become an important source of new therapies, will need to be discussed in more detail.

The development of mAbs as therapeutic agents has come a long way from the early failures, and it is clear from the huge number of mAb therapies in development and clinical trials that this class of protein biotherapeutics will continue to be a prominent weapon for many diseases, especially in the treatment of cancers.

References

Boulianne, G. L., Hozumi, N., & Shulman, M. J. (1984). Production of functional chimaeric mouse human-antibody. *Nature*, *312*(5995), 643–646.

Casi, G., & Neri, D. (2012). Antibody-drug conjugates: basic concepts, examples and future perspectives. *Journal of Controlled Release*, *161*(2), 422–428.

Cole, S. P. C., Campling, B. G., Atlaw, T., Kozbor, D., & Roder, J. C. (1984). Human monoclonal-antibodies. *Molecular and Cellular Biochemistry*, *62*(2), 109–120.

Ezzell, C. (October 2001). Magic bullets fly again. *Scientific American*, 35–41.

Jones, P. T., Dear, P. H., Foote, J., Neuberger, M. S., & Winter, G. (1986). Replacing the complementarity-determining regions in a human-antibody with those from a mouse. *Nature*, *321*(6069), 522–525.

Kohler, G., & Milstein, C. (2005). Continuous cultures of fused cells secreting antibody of predefined specificity (Reprinted from Nature, 256, 1975). *Journal of Immunology*, *174*(5), 2453–2455.

Lakow, E. S., Valentine, M. A., Vaughan, J. H., Tsoukas, C. D., & Carson, D. A. (1984). Effects of monoclonal-antibodies against lymphocyte surface-antigens on interleukin-2 excretion by Epstein-Barr virus-specific human T-cell hybridomas. *Cellular Immunology*, *85*(1), 67–74.

Market-report. (2014). *Antibody drug conjugates market* (2nd ed.). 2014–2024.

Milstein, C. (1999). The hybridoma revolution: an offshoot of basic research. *Bioessays*, *21*(11), 966–973.

Morrison, S. L., Johnson, M. J., Herzenberg, L. A., & Oi, V. T. (1984). Chimeric human-antibody molecules – mouse antigen-binding domains with human constant region domains. *Proceedings of the National Academy of Sciences of the United States of America-Biological Sciences*, *81*(21), 6851–6855.

Oldham, R. K., & Dilman, R. O. (2008). Monoclonal antibodies in cancer therapy: 25 years of progress. *Journal of Clinical Oncology*, *26*(11), 1774–1777.

Presta, L. G., Lahr, S. J., Shields, R. L., Porter, J. P., Gorman, C. M., Fendly, B. M., et al. (1993). Humanization of an antibody-directed against IgE. *Journal of Immunology*, *151*(5), 2623–2632.

Reichert, J. M., Rosensweig, C. J., Faden, L. B., & Dewitz, M. C. (2005). Monoclonal antibody successes in the clinic. *Nature Biotechnology*, *23*(9), 1073–1078.

Rouet, R., & Christ, D. (2014). Bispecific antibodies with native chain structure. *Nature Biotechnology*, *32*(2), 136–138.

Sheets, M. D., Amersdorfer, P., Finnern, R., Sargent, P., Lindqvist, E., Schier, R., et al. (1998). Efficient construction of a large nonimmune phage antibody library: the production of high-affinity human single-chain antibodies to protein antigens. *Proceedings of the National Academy of Sciences of the United States of America*, *95*(11), 6157–6162.

Thakur, A., & Lum, L. G. (2010). Cancer therapy with bispecific antibodies: clinical experience. *Current Opinion in Molecular Therapeutics*, *12*(3), 340–349.

Wakankar, A. A. (2010). *Antibody drug conjugates: The next wave of monoclonal antibody-mediated chemotherapeutics*. AAPS Newsmagazine, May, AAPS Press. pp. 15–21.

Wakankar, A. A., Feeney, M. B., Rivera, J., Chen, Y., Kim, M., Sharma, V. K., et al. (2010). Physicochemical stability of the antibody-drug conjugate Trastuzumab-DM1: changes due to modification and conjugation processes. *Bioconjugate Chemistry*, *21*(9), 1588–1595.

This page intentionally left blank

Index

Note: Page numbers followed by "f" and "t" indicate figures and tables respectively.

This page intentionally left blank